Measurement and analysis of the protective effects of anti-sickling hemoglobins in sickle cell disease : application to gene therapy strategies

Nicolas Hebert

UNIVERSITÉ PARIS-EST

UNIVERSITÉ PARIS-EST

Ecole doctorale : SVS - Sciences de la Vie et de la Santé

Laboratoire : Transfusion et Maladies du Globule Rouge (INSERM U955 – IMRB – EFS)

Thèse de doctorat

Spécialité : Biologie Cellulaire et Moléculaire

Nicolas HEBERT

Measurement and analysis of the protective effects of anti-sickling hemoglobins in sickle cell disease: application to gene therapy strategies

Thèse dirigée par le **Pr. Pablo BARTOLUCCI**

Soutenue publiquement le 16 novembre 2020

Composition du jury :

Pr. France PIRENNE	Président du jury
Pr. Anne GALY	Rapporteur
Pr. Guillaume LETTRE	Rapporteur
Pr. Marina CAVAZZANA	Examinateur
Pr. Carlo BRUGNARA	Examinateur
Pr. Philippe CONNES	Examinateur

Travaux réalisés au sein de

L'INSTITUT MONDOR DE RECHERCHE BIOMEDICALE

Laboratoire : Transfusion et Maladies du Globule Rouge

Dirigé par le Pr. France PIRENNE

UNIVERSITE PARIS-EST CRETEIL

INSERM UMR955

ETABLISSEMENT FRANÇAIS DU SANG

Centre Félix REYES – 2ième étage

5, rue Gustave EIFFEL

94000 CRETEIL

Mesure et analyse des effets protecteurs des hémoglobines anti-polymérisantes dans la drépanocytose : application aux stratégies de thérapie génique

Mots clés : drépanocytose, hémoglobine, thérapie génique, chimérisme érythrocytaire

Résumé :

La drépanocytose est une maladie héréditaire dans laquelle les globules rouges (GR) ont un variant de l'hémoglobine (Hb), appelée HbS. Elle est causée par la substitution d'un seul acide aminé de la sous-unité β-globine : une valine au lieu d'un acide glutamique en sixième position. Cette mutation confère à l'HbS la capacité de polymériser sous l'effet de la désoxygénation, entraînant la formation de longues fibres. Les GR normaux sont élastiques, circulent librement et vivent généralement entre 90 et 120 jours. Les GR drépanocytaires sont rigides, déshydratés, très sensibles à l'hémolyse, ont une durée de vie de 10 à 20 jours et ont tendance à rester coincés en raison de la polymérisation de l'HbS, ce qui entraîne un blocage de la circulation sanguine. Les progrès de la biologie cellulaire et moléculaire ont conduit au développement de la transplantation de cellules souches hématopoïétiques (CSH) allogéniques, la seule option curative disponible pour les patients. Cependant, la transplantation de CSH est confrontée à des problèmes tels que le manque relatif de donneurs compatibles et les risques de maladie du greffon contre l'hôte ou de rejet du greffon. C'est pourquoi la thérapie génique est une alternative prometteuse. Elle consiste en une modification génétique des CSH autologues pour exprimer de l'Hb anti-polymérisante comme l'Hb foetale (HbF) ou des Hb génétiquement modifiées pour inhiber la polymérisation de l'HbS. Pour cela, l'Hb anti-polymérisante doit être exprimée en quantité suffisante par GR. Il est donc indispensable de disposer d'outils capables d'évaluer à la fois la teneur en Hb des GR et leurs propriétés fonctionnelles. Nous décrivons ici le développement d'une nouvelle méthode permettant la quantification précise de l'HbF dans des GR individualisés. Nous montrons que ce test est suffisamment précis pour mesurer des seuils d'HbF avec une pertinence clinique. Comme preuve de concept, nous avons déterminé des seuils de protection de l'HbF chez des patients atteints de drépanocytose et traités avec de l'hydroxyurée, un inducteur d'HbF. Nous montrons également que cette méthode est intéressante pour évaluer l'efficacité de la thérapie génique. Enfin, nous rapportons que l'analyse des propriétés des GR peut démontrer la correction fonctionnelle induite par l'expression d'Hb anti-polymérisante. Dans l'ensemble, nous démontrons le potentiel et la pertinence de ces analyses pour mieux caractériser l'efficacité des stratégies de thérapie génique visant à guérir la drépanocytose.

Measurement and analysis of the protective effects of anti-sickling hemoglobins in sickle cell disease: application to gene therapy strategies

Key words: sickle cell disease, hemoglobin, gene therapy, erythrocyte chimerism

Summary:

Sickle cell disease (SCD) is an inherited disorders in which red blood cells (RBCs) have a variant of the hemoglobin (Hb), named HbS. It is caused by the substitution of a single amino acid in the β-globin subunit: a valine instead of a glutamate in the sixth position. This mutation results in the capability of HbS to polymerize under deoxygenation, leading to the formation of long fibers. Normal RBCs are elastic, flow freely through circulation and typically live between 90-120 days. Sickle RBCs are rigid, dehydrated, highly sensitive to hemolysis, have a 10-20 days lifespan, and tend to get stuck because of HbS polymerization, resulting in blood flow blockage. Advances in cellular and molecular biology have led to the development of allogenic hematopoietic stem cell (HSC) transplantation, the only available curative option for patients. However, HSC transplantation faces issues such as relative lack of sibling donors, risks of graft versus host disease or graft rejection. Therefore, gene therapy is a promising alternative. It consists in genetical modification of autologous HSC to express anti-sickling Hb such as fetal Hb (HbF) or HbF-based engineered Hb inhibiting HbS polymerization. To be successful, anti-sickling Hb must be expressed in enough quantity per RBC. Therefore, disposing of tools able to assess both Hb content in RBCs and functional properties of RBCs are mandatory. Herein we describe the development of a new method allowing precise HbF quantification in individual RBCs. We show that this assay is precise enough to measure thresholds of HbF with clinical relevance. As a proof of concept, we determined protective thresholds of HbF in SCD patients treated with hydroxyurea, a well-known HbF inducer. We also showed that this method is of interest in assessing gene therapy efficacy. Lastly, we report that analyzing RBCs properties can demonstrate functional correction induced by anti-sickling Hb expression. Altogether, we demonstrate the potential and the relevance of these analyzes to better characterize gene therapy strategies efficacy aiming to cure SCD.

Table of content

List of figures

List of tables

Foreword

Sickle cell disease (SCD) results from a single amino acid substitution in the β-globin chain of the hemoglobin (Hb). This mutation confers to HbS complex capability of polymerization under deoxygenated state. Few treatments exist to treat SCD and they consist more in focusing on best supportive care than cure. They include blood transfusion and medication, all of them finally focusing on the correction of the impaired red blood cells (RBCs) properties induced by HbS polymerization. The only available curative treatment consists in hematopoietic stem cell transplantation (HSCT). While substantial improvements have been made in the last years, HSCT still faces challenges such as compatible donor availability and associated adverse risks. Therefore, gene therapy is a promising alternative strategy to treat SCD with the aim of becoming a new curative treatment. This is possible by expressing anti-sickling Hb which can inhibit HbS polymerization within RBCs. Being performed in an autologous system, gene therapy circumvents issues encountered with HSCT. Despite the undeniable progress of gene therapy in the last years, the treatment of SCD by this approach requires both clinical studies to confirm the disappearance of the SCD-related symptoms and parallel biological studies to assess its efficacy at the RBC level.

Like HCST, gene therapy induces a mixed chimerism in the receiver. It has been estimated that at least 20% of HCS donor mixed chimerism results in almost a full donor RBCs chimerism. The erythrocyte chimerism induced by gene therapy is more complex because of the site integration, of the affinity between α and β globin and of the number of transgene copy per cell. The curative response will depend not only on the number of HSC which has been corrected, i.e. transduced with the lentiviral vector, but also on the degree of correction, i.e. the level of transgene expression in each cells. Thus, at the biological level, gene therapy for SCD requirement to be successful is conditioned by two elements: the proportion of corrected cells and their level of correction. The most important is the amount of anti-polymerizing hemoglobin that each red cell contains. The primary end point for biological efficacy should be the quantitative measure of the HbS by RBC or RBC precursors Indeed, HbS polymerization is directly dependent on its intracellular concentration, and a sufficient

amount of anti-polymerizing hemoglobin must be present in the cell to completely inhibit it. In addition, the majority of these cells must contain at least this sufficient amount to totally reverse SCD phenotypes.

Therefore, new ways to appraise gene therapy efficacy for SCD are mandatory to confirm the first success and to allow much more. It is essential to dispose of tools to assess the effectiveness of gene therapy at the RBC level with clinical significance.

The aims of this study are to develop and improve analyzes able to demonstrate the protective effects of the anti-sickling hemoglobins against SCD phenotypes. The strategy is to be able to better assess the benefits of gene therapy in treated patients by determining the minimal amount of anti-sickling hemoglobin production to reach at the cellular level and the sufficient RBC percentage of the population expressing this protective threshold to correct SCD phenotypes. In this context, a new method which has been invented in our group, and which consists in the precise individual RBC fetal hemoglobin quantification has been improved for clinical purpose. As a proof of concept, this method has been used to determine protective thresholds of HbF content against the pathognomonic VOC in SCD patients on HU treatment. Moreover, as numerous physical and biological RBCs properties are impaired as a result of HbS polymerization, methods for evaluating physical and biological properties of RBCs has been used to assess the protective effect of the production of the anti-sickling β^{A-T87Q}-globin in RBCs of SCD patients treated by gene therapy in the HGB-205 study (NCT02151526).

The first part of my thesis consists in a review of the literature about selected aspects of SCD and red cell biology. The first chapter focuses on the role and function of hemoglobin as oxygen transporter and on the molecular basis of SCD, namely the HbS polymerization. It will be followed by a description of physiological RBC biology, from their synthesis to their removal. The third chapter describes the impaired RBCs properties resulting from HbS polymerization and involved in SCD pathophysiology. Lastly, an overview of available treatments for SCD, including pharmacological drugs, blood transfusions and then gene therapy strategies currently tested, will be presented. The second part focuses on the results obtained on the protective effects of the anti-sickling hemoglobins and the way to assess them in patients treated with gene therapy. It will be followed by a third part consisting in a general discussion of the results and their utility for gene therapy strategies.

Part 1: Review of the literature

Chapter 1 – Molecular basis of sickle cell disease

1. Brief history

From the first description in 1846 of symptoms now considered as characteristic of the disease, followed the first formal description of a “peculiar elongated and sickle-shaped red blood corpuscles in a case of severe anemia”, published by James Herrick, in 1910 (1). He describes a 20-years-old patient from Grenada in the Caribbean who consulted in 1904 after five weeks of coughing intensified in chills and fever two days before the examination. The patient has several scars on his legs following ulceration, difficulties in breathing and the action of a heart under strong stimulation without ingestion of any stimulants. The blood test reveals, in addition to a severe anemia, numerous erythroblasts and a polychromatophilia (observable during hemolytic anemias and dyserythropoiesis) and the presence of many red blood cells (RBCs) of irregular shape, "thin, elongated, in sickle and croissant shapes” (Figure 1). The patient was readmitted several times to hospital for "muscular rheumatism" and "bilious attacks" and died in 1916, aged 32, in Grenada, of pneumonia (2).

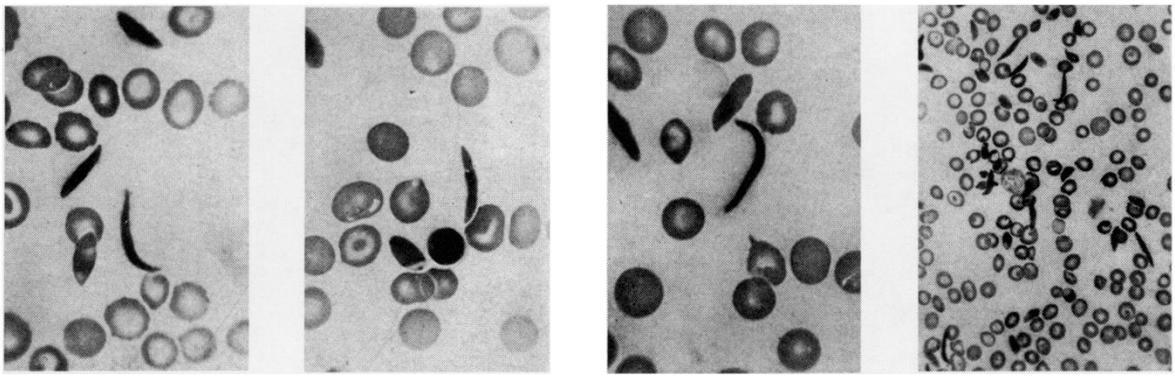

Figure 1 | Photographs of blood smears with elongated and sickle-shaped red blood cells. Figure from Savitt and Glodberg (2).

Later, in 1922, Vernon Mason was the first to use the term "sickle cell anemia", from the characteristic shape of the red cells (3). Lemuel Diggs and colleagues, in the 1930s, described the phenomena of occlusion of blood capillaries by sickle-shaped RBCs, implicated in the painful episodes commonly observed in patients. He also observed that the erythrocytes of newborn infants sickle slower than those of children or adults (4). Sickle cell disease (SCD) then received "first molecular disease status" when Pauling and his colleagues laid the groundwork in 1949 for the presence of an abnormal hemoglobin (Hb), called hemoglobin S (HbS), from sickle, in the RBCs of affected individuals (5). This work also showed that some individuals have both normal and sickle Hb within their RBCs, while individuals with SCD only have HbS. They thus demonstrate that SCD is a homozygous hereditary disease according to Mendelian laws of autosomal recessive transmission. This was followed in 1957 by the demonstration that HbS is the result of a single amino acid substitution in the 6th position of the beta-globin chain of the hemoglobin (β-globin) as compared to normal hemoglobin (6). Then in 1963, it was showed that this amino acid substitution results from a single nucleotide substitution on the corresponding gene, *HBB* (7). The resulting allele was named β^S.

2. Sickle cell disease epidemiology

2.1. β^S allele frequency distribution across the world

The β^S mutated allele is the most common Hb mutation in the world. The heterozygous status results in the sickle cell trait (HbAS). In those individuals, erythrocytes contain both HbA and HbS, with levels being approximately 60% and 40% of total Hb, respectively. This comes from the fact that β^S-globin has a lower affinity for α-globin than normal β-globin (β^A), mainly because of electrical charge. While α-globin is positively charged, β-globin is negative, thus facilitating their interaction. However, β^S-globin is less negative than β^A-globin. It results in the differential association of α-β dimers during Hb synthesis (8).

It is estimated that the number of HbAS individuals exceeds 300 million in world. The β^S geographical distribution is mainly determined by two factors: endemicity of malaria and population movements. The superposition between the geographic distribution of the β^S allele frequency and the endemicity of malaria in sub-Saharan Africa has been observed in the 1950s, leading to the hypothesis that individuals with only one β^S allele (sickle cell trait), could

be protected against *Plasmodium falciparum* malaria (9). There are now clear evidences that HbAS genotype provides protection against severe forms of *P. falciparum* malaria (10,11). These studies suggest that the β^S allele has arisen and been amplified by selection, explaining its high frequencies, whose prevalence can reach 25% in malaria-endemic areas such as Nigeria or India (12–14) (Figure 2).

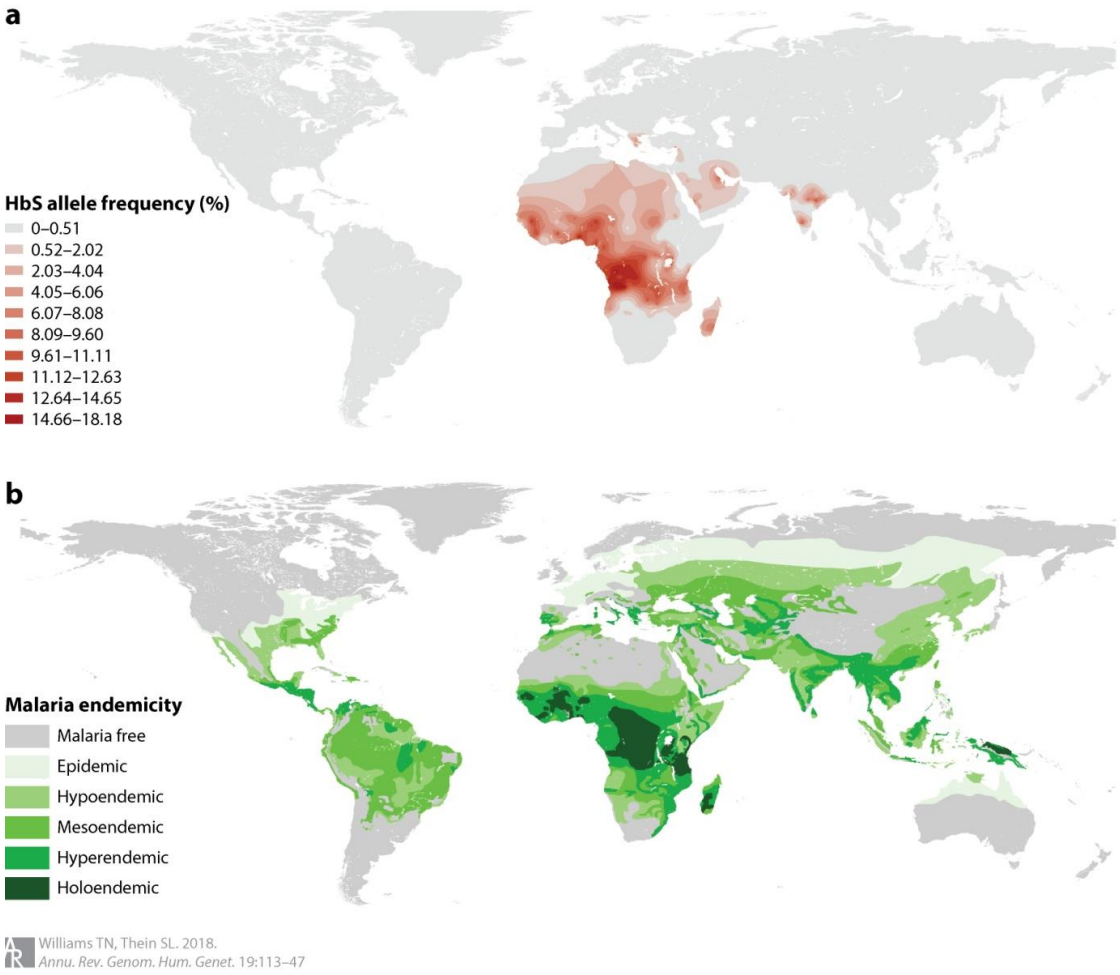

Figure 2 | Comparison between global β^S (HbS) allele frequency distribution and historical distribution of *Plasmodium falciparum* malaria. (**a**) Geospatial HbS allele frequency generated by a Bayesian model-based geostatistical framework. (**b**) Historical map of malaria endemicity digitized from data published in the 1960s. The classes are defined by parasite rates. Figure from Williams and Thein (15).

2.2. Incidence and prevalence

Population migrations, including slave trade between the 16th and 19th centuries, led to a much wider distribution of the HbS allele, particularly in North America, Western Europe, India, Brazil and West Indies, contributing to make the disease a global burden (16).

The incidence of SCD varies by country and was estimated to be around 150,000 affected babies each year in 2015. Approximatively 80% of these births are in Africa (Figure 3). A recent meta-analysis estimated that birth prevalence of homozygous sickle cell disease was 112 per 100 000 live births, with a birth prevalence in Africa of 1125 per 100 000 compared with 43 per 100 000 in Europe (17,18). It is then estimated that around twenty million people are affected by SCD worldwide. SCD new patients are predicted to increase exponentially in the next decades with associated human migration and further globalization continuing to expand SCD throughout the world.

Unfortunately, many countries cannot afford the high cost required to provide the complex care for SCD patients. While in high-income countries, the current life expectancy for individuals with SCD is estimated to be between 45-55 years of age, in low- and middle-income countries it is believed that most children die before reaching adulthood, because of poor access to appropriate care (17,19).

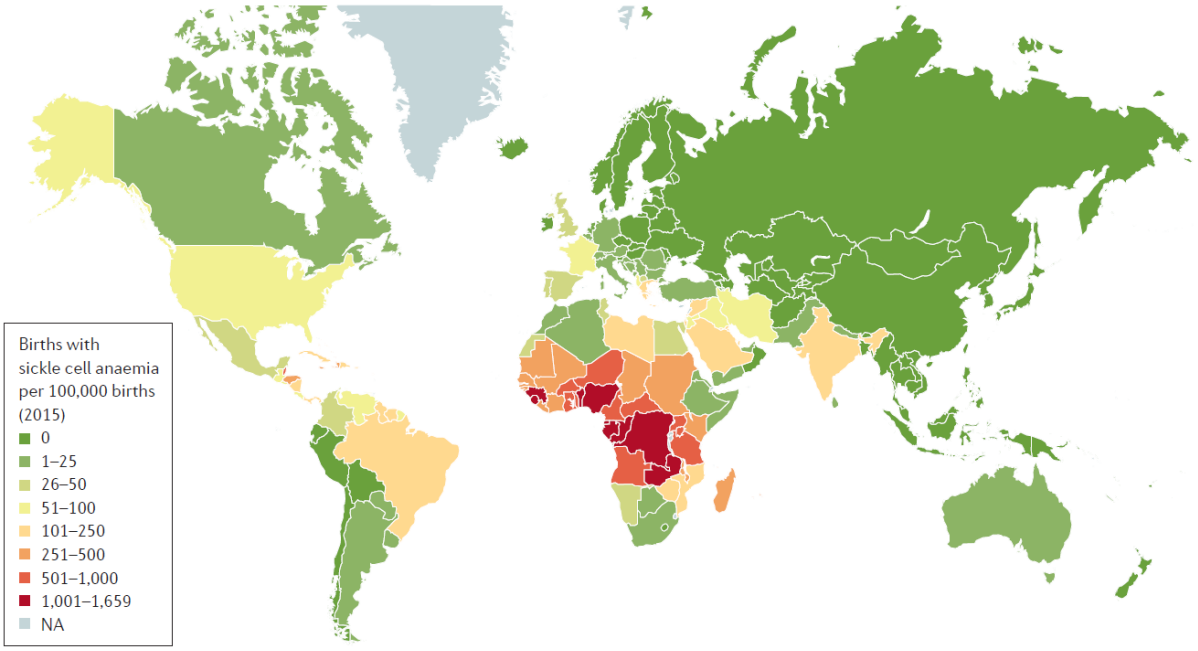

Figure 3 | Global geographic distribution of the estimated number of births with sickle cell anemia per 100,000 births per country in 2015. Figure from Kato, *et al.* (20).

3. Molecular basis of the disease: a mutation of the hemoglobin β-subunit

3.1. A genetic disease

SCD is a monogenic genetic disease caused by the mutation of the *HBB* gene located on chromosome 11 (11p15.4) which encodes for the β-globin chain. A substitution of a single nucleotide, at the level of the sixth codon (GAG replaced by GTG: c.A20T), is responsible for the substitution of the sixth amino acid in the polypeptide chain, a hydrophilic negatively charged glutamic acid replaced by a hydrophobic neutral valine (p.Glu6Val) thus leading to the production of an abnormal protein.

3.2. The human hemoglobin

3.2.1. Human hemoglobin structure

Hb is the main protein of RBCs. About 30% of the total mass of a RBC corresponds to Hb, a proportion that reaches 97% on its dry mass (21). It is a molecule formed by the assembly of three fundamental elements: iron atoms, porphyrins and proteins. It belongs to the globin protein family. With a molecular weight of around 65,000 Dalton, it is made up of 4 subunits called chains. Adult hemoglobin (HbA), is the predominant Hb within RBCs after birth, and is composed of two α-globin chains subunits and two β- globin chains subunits. The existence of this 4 polypeptide chains assembly was demonstrated in 1958 by partial hydrolysis of the protein (22). A few years later, the dissociation of each of these chains under acidic pH allowed the identification of their relative amino acid composition (23).

Each of the four globin chains is composed of α-helices, (7 helices per α-chain and 8 helices per β-chain) connected by short non-helical regions. Spatially, this organization forms an internal hydrophobic pocket in which is embedded a prosthetic group called heme (Figure 4). The latter is covalently linked to the histidine at position 87 of the α-chain and to the histidine at position 92 of the β-chain. The heme is made up of an iron atom in the center of a heterocyclic ring, called porphyrin, a plane and electron-donor molecule (Figure 5). This iron atom is in ferrous form (Fe^{2+}), which allows the fixation of dioxygen (O_2) molecules, but also other diatomic ligands such as carbon monoxide (CO). Thus, each tetrameric Hb molecule allows the fixation and the transport of 4 molecules of O_2 (24). It is of interest to note that

oxidized Hb, also named methemoglobin (metHb), whose iron atoms in heme are in ferric form (Fe^{3+}), cannot bind O_2 and is relatively unstable, tending to lose heme, and denature.

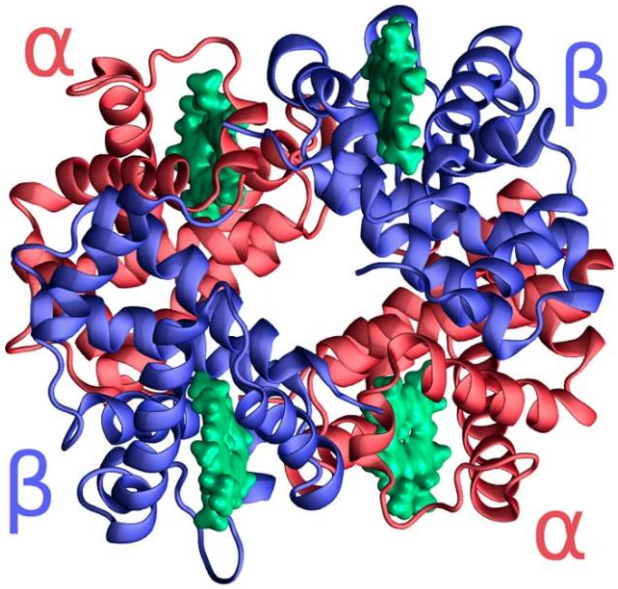

Figure 4 | 3D Structure of tetrameric hemoglobin showing the alpha helices. The α- and β-globin chains are represented in red and blue, respectively. The heme group (in green) is embedded within the hydrophobic center of each globin chain. Figure from Bringas, *et al*. (25).

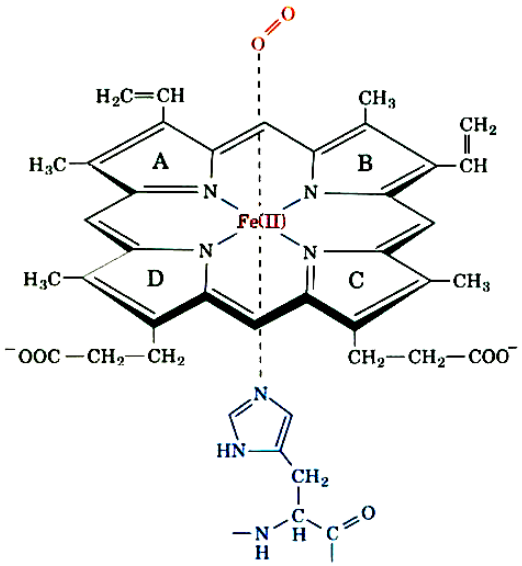

Figure 5 | Heme molecular structure. In the center of porphyrin, the iron atom is hexacoordinated (a total of six valences). Four valences are linked to the four nitrogen atoms of the porphyrin itself. A valence is linked to another nitrogen atom of a histidine in the globin chain (proximal histidine, in blue). The sixth valence allows the possibility to receive a molecule of dioxygen (O_2, in red) or any other possible ligand. Figure from Bouzhir-Sima (26).

3.2.2. Human hemoglobin function

Hb is highly adapted to its function in the body: oxygen transport. The tertiary and quaternary structures of Hb are crucial in its role as a transporter. The quaternary Monod-Wyman-Changeux model of cooperative and allosteric regulation (MWC), proposed in 1965, describes the two forms of the protein (27). They depend on the oxygenation state of the 4 subunits and on the pH. The fully oxygenated form, whose 4 subunits have an O_2 molecule each, is called the R form (for relaxed). Conversely, the T form (for tense) corresponds to a totally deoxygenated molecule. The pH and the partial oxygen pressure (pO_2) of the environment influence the balance between the two forms. At elevated pH and in the presence of oxygen, the R form is favored (and Hb therefore seeks to capture oxygen); at low pH and when oxygen is scarce, the T form is favored and Hb O_2 release is increased. Binding of O_2 by a first subunit leads to an increase in affinity for the following ones. The subunits of Hb therefore practice cooperative interactions when it comes to oxygen binding. The switch from one form to another depending on the binding or the release of oxygen causes a change in the quaternary conformation of the protein (28) (Figure 6).

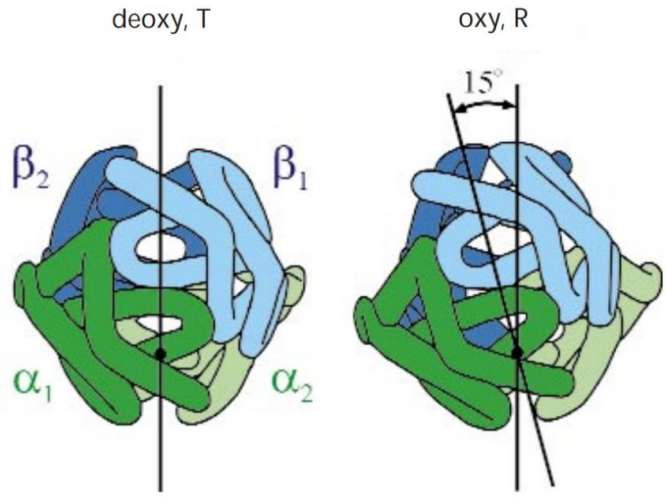

Figure 6 | Structural schematic representations showing difference in quaternary structure between the T and R forms of hemoglobin with a noticeable relative 15° rotation angle of two $\alpha\beta$ dimers. Figure adapted from Eaton, *et al*. (28).

While adapted to molecules at the equilibrium, kinetics studies revealed that MWC model does not consider intermediates that are present at much higher concentrations than at equilibrium. A tertiary two-state allosteric model has then been added to the MWC model

to solve this issue (29). It consists in assuming that tertiary conformations of individual subunits play the primary role instead of the quaternary conformations of the tetramer. This modified model thus gives better quantitative descriptions of Hb oxygen binding kinetics, especially for mutant Hb like HbS (30,31).

The sensitivity of Hb to pH comes from the fact that cells containing high amounts of carbon dioxide (CO_2) have a more acidic pH because of the following reaction:

$$CO_2 + H_2O \leftrightarrow H_2CO_3 \leftrightarrow HCO_3^- + H^+$$

Once the Hb has discharged its load of O_2 it can then help to evacuate the excess CO_2 and H^+ ions from the tissues. CO_2 binds to the N-terminus of each of the four globin chains to form carbaminohemoglobin. 2,3-Diphosphoglycerate (2,3-DPG), a glycolytic intermediate, is present at high concentration in RBCs. It binds to the central cavity of deoxyhemoglobin (the T-form) by interacting with positively charged side chains in the β-globin subunits. The 2,3-DPG reduces the affinity of Hb for oxygen by stabilizing the T-form. The transition from T- to R-form expels it from the cavity. 2,3DPG has been shown to increase in case of anemia or under high altitude condition. Moreover, it also increases during RBCs aging.

The curve of O_2 saturation as a function of the pO_2 is sigmoid, reflecting the cooperation (Figure 7). The affinity of Hb for O_2 can be assessed by measuring the p50 (the pO_2 value for which 50% of Hb is saturated by O_2), which is influenced by environmental conditions such as pH, or concentrations in 2,3-DPG or in CO_2.

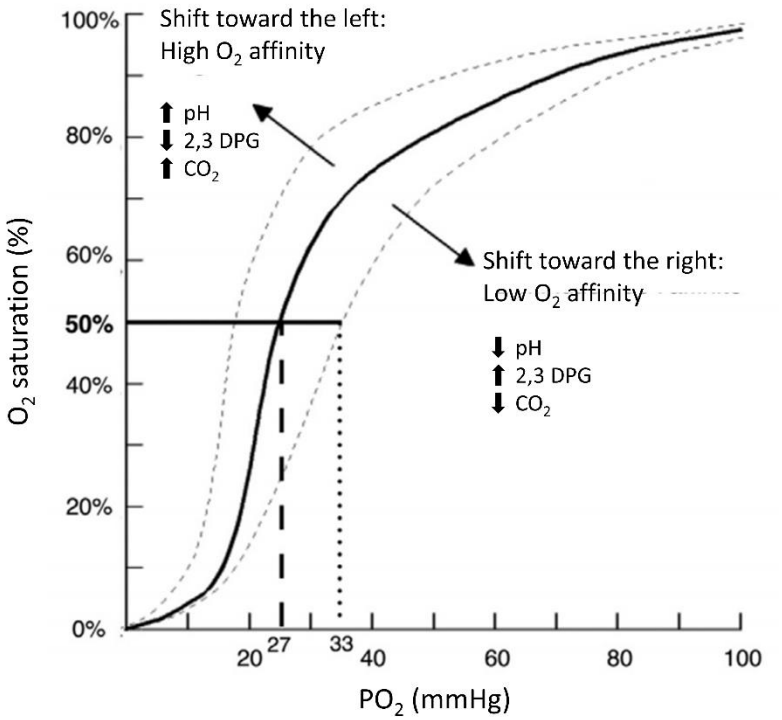

Figure 7 | Relationship between hemoglobin dioxygen saturation and PO_2. A decrease in p50 ("left shift") corresponds to an increase in the affinity of Hb for O_2. An increase in p50 ("right shift") corresponds to a decrease in the affinity of Hb for O_2. pO_2 (x-axis) indicates partial pressure of O_2; O_2 saturation (y-axis) indicates the percentage of Hb sites occupied by O_2. Figure adapted from Pincez, *et al*. (32).

3.2.3. Genetic of the Human hemoglobins

Widely studied, the genes encoding globin chains were, in 1976, among the first to be cloned (33). The different globin chains have the particularity of being encoded by genes grouped in a cluster, which means that they are located next to each other in the same region of the genome. The genes encoding the alpha-type chains are located on the short arm of the chromosome 16 (16p13.3) and form the alpha cluster (α-cluster). The beta-type chains form the beta cluster (β-cluster), which is located on the short arm of the chromosome 11 (11p15.5) (Figure 8).

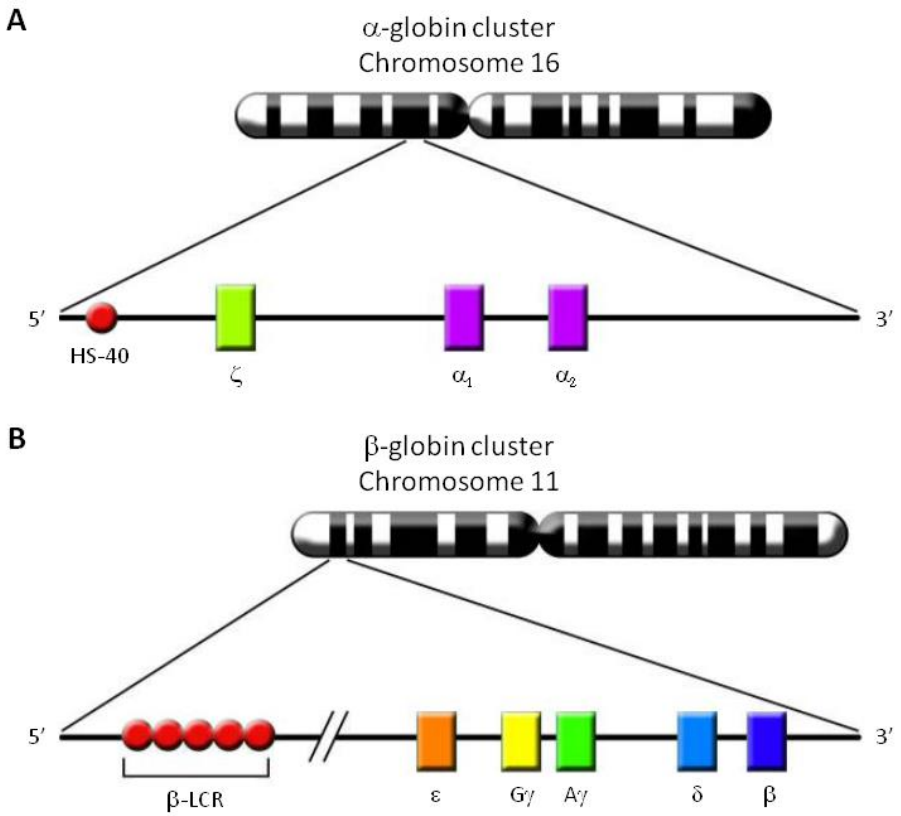

Figure 8 | Chromosomal organization of the gene clusters of the α- and β-globin chains. (**A**) The *HBZ* (ζ), *HBA1* (α1) and *HBA2* (α2) genes preceded by their major positive regulation element HS-40. (**B**) The *HBE1* (ε), *HBG2* (Gγ), *HBG1* (Aγ) *HBD* (δ) and *HBB* (β) genes preceded by the β-locus control region (β-LCR). Figure adapted from Frenette and Atweh (34).

The α-cluster consists of 3 genes: *HBZ* and the two duplicated genes *HBA1* and *HBA2,* encoding for the zeta- (ζ), alpha 1- (α1) and alpha 2-globin chains (α2), respectively. These 3 genes are preceded by the HS-40 region, the main positive regulator of their expression (35). Within the cluster, the genes are in the same order in which they are expressed during development.

The β-cluster consists of 5 genes: *HBE1*, *HBG2*, *HBG1*, *HBD* and *HBB,* encoding for the epsilon- (ε), G gamma- (Gγ), A gamma- (Aγ), delta- (δ) and beta-globin chains (β), respectively. Their expression is finely regulated by the beta-locus control region (β-LCR), a sequence composed of 5 regulatory hypersensitive sites (HS) regions (HS-1 to HS-5) located far upstream (between 6 and 20 kb 5' of *HBE1* gene) (36). similarly, the genes in this cluster are in the same order in which they are expressed during development.

The Hb molecule is always composed of 2 α-type chains and 2 β-type chains. Depending on the developmental stage, globin genes are sequentially expressed, and

different assemblies can be observed, each giving a different type of Hb (Figure 9). RBCs are produced from a physiological process named erythropoiesis. During the development, primitive erythropoiesis is followed by definitive erythropoiesis. The first takes place in the yolk sac during the first 6 to 8 weeks post-conception and gives rise to nucleated erythroblasts containing the embryonic hemoglobins Gover 1 ($\zeta_2\varepsilon_2$), Portland ($\zeta_2\gamma_2$) and Gover 2 ($\alpha_2\varepsilon_2$). Definitive erythropoiesis, producing enucleated RBCs, decomposes into two phases: fetal and then adult. After the embryonic period, a first Hb switch occurs with the cessation of the synthesis of the ζ- and ε-globin chains, which are replaced by the α- and γ-globin chains, respectively. RBCs, then produced in the fetal liver and, in a lesser level, in the spleen, contain mainly fetal hemoglobin, HbF ($\alpha_2\gamma_2$). Finally, shortly after birth, a second Hb switch occurs at the same time as erythropoiesis migrates to the bone marrow. HbF is gradually replaced by adult hemoglobin, HbA ($\alpha_2\beta_2$), which becomes predominant after 6 months of age (37,38). The δ-globin chain is expressed in the same time as β-globin, but the resulting HbA2 ($\alpha_2\delta_2$) is found in very low quantity (less than 2% of total Hb).

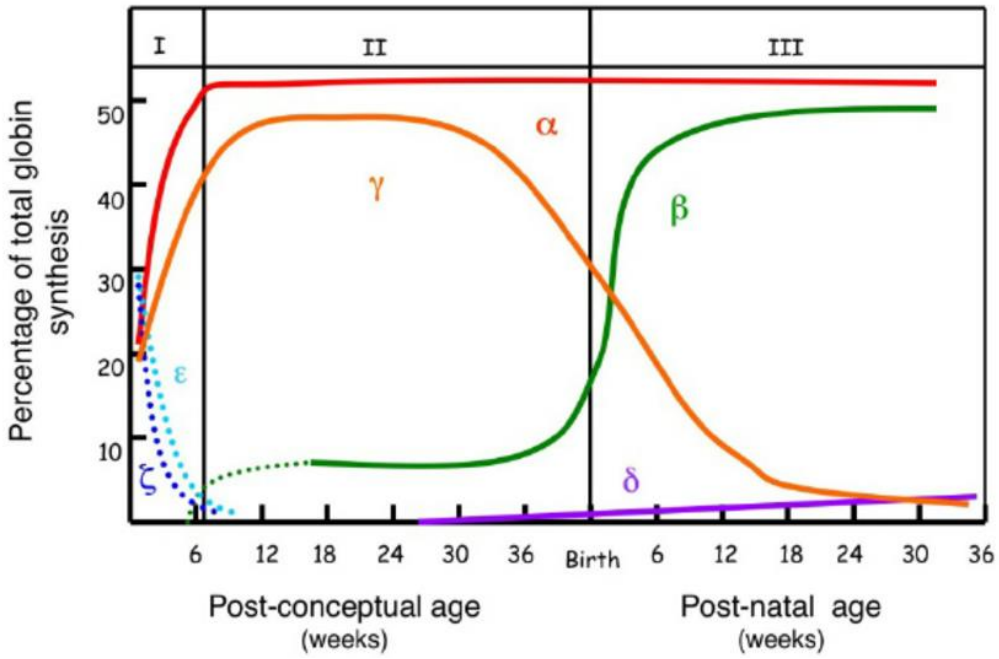

Figure 9 | Changes in globin genes expression profile during development. The first embryonic-to-fetal switch (from ζ- to α-globin and from ε- to γ-globin) occurs within 6 weeks after conception, and the second fetal-to-adult switch (from γ- to β-globin) occurs shortly after birth. The x-axis represents the age in weeks. The y-axis corresponds to the expression of each globin gene as a percentage of total globin gene expression. Time of birth is denoted with a vertical line. The embryonic genes are expressed during the first six weeks of gestation. (I: embryonic; II: fetal; III: adult). Figure from Grosso, *et al.* (39).

This fetal-to-adult Hb switch is finely regulated by several erythroid-specific and ubiquitous transcription factors leading to the repression of the expression of γ-globin genes (*HBG1* and *HBG2*) (40) (Figure 10). Expression of the individual globin genes relies on direct physical interactions between the globin promoters and the β-LCR, and transcriptional suppression of the preceding gene. The first four HS sites of the β-LCR (HS1 to HS4) act as erythroid cell-specific enhancers that are required for proper order of activation of the globin genes during ontogeny. The last hypersensitive site (HS5) acts as a structural and insulator element (41). The zinc-finger transcription factor B-cell lymphoma/leukemia 11A (BCL11A), is a major element of this switch (42). It cooperates with SOX6, GATA1 and FOG1 in a protein complex to repress the expression of γ-globin genes in adult erythroblasts. In addition, this complex drives the recruitment of epigenetic factors such as the nucleosome remodeling and deacetylase (NuRD) repressor complex, histone deacetylase (HDAC1 and HDAC2), lysine-specific demethylase (LSD1), and DNA methyltransferase (DNMT1) (43). The expression of BCL11A is regulated by the transcription factor Krüppel-like factor 1 (KLF1). It contributes to directly activate the *HBB* gene in adult life by inducing the formation of chromatin loops favoring interactions of the HS2 and HS3 sites in the β-LCR with the *HBB* promoter (44). In addition, KLF1 also drives expression of the transcription factor LRF/ZBTB7A in erythroid cells and is associated with γ-globin synthesis repression through interaction with NuRD repressor complex (45,46).

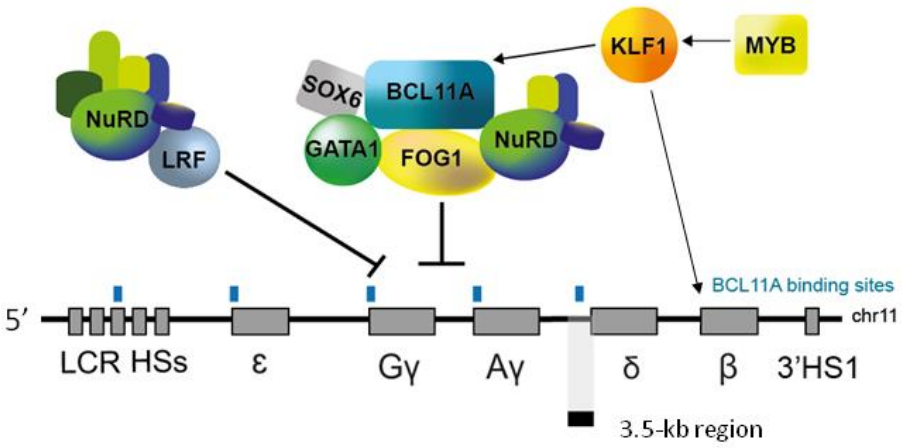

Figure 10 | Major elements involved in the fetal-to-adult hemoglobin switching. MYB upregulates the expression of KLF1, which in turn positively regulates the expression of BCL11A. The latter interacts with SOX6, GATA1, FOG-1, and the NuRD repressor complex to inhibit the expression of γ-globin genes in adult erythroblasts. Additionally, KLF1 directly activates β-globin gene expression. Independently, the transcription factor LRF silences γ-globin expression through the NuRD complex. Blue squares indicate BCL11A binding sites. Figure adapted from Cavazzana M. et al. (47).

3.2.4. The hemoglobinopathies

Hemoglobinopathies is a term which includes all the hereditary blood diseases that affect the Hb. There are two main types. Quantitative defect in the synthesis of one of the globin chains is termed thalassemia. Alpha thalassemia (α-thal) or beta thalassemia (β-thal) are used to discriminate whether the abnormality affects the *HBA1* and/or *HBA2* genes or the *HBB* gene, respectively. The other hemoglobinopathies result from the production of a Hb variant with impaired solubility, stability or affinity for oxygen. The phenotypic and clinical consequences are very variable, ranging from mild to very serious.

The HbVar database, which is accessible online and references the Hb genetic variants, contained in April 2020, 1818 different entries of which 505 were associated with thalassemia (*http://globin.cse.psu.edu/hbvar/menu.html*) (48,49). According to a study conducted by the World Health Organization (WHO), an average of 24% of people around the world are carriers of at least one Hb variant and more than 5% carries a variant of clinical significance which can leads to hemoglobinopathy (50). The most common variant is the β^S-globin, which in the homozygous state (β^S/β^S) or in the form of various composite heterozygosity (i.e. β^S/β^C, β^S/β-thal and others) is responsible for SCD.

Hemoglobin SC (β^S/β^C genotype) is the second most common type of SCD. β^C-globin results from the substitution of the glutamic acid amino acid with a lysine at the 6th position of the β-globin chain (E6K substitution). HbC molecules tend to crystalize within RBCs (51). SC patients, who suffer the same complications as SS patients, typically have less severe disease and longer lifespans than homozygous SCD patients (52).

3.3. The “S” mutation of the hemoglobin and its deleterious gain of function

The substitution on the β-globin of a glutamic acid in the sixth position by a valine is responsible for the production of the abnormal HbS ($\alpha_2\beta^S_2$) present in RBCs of individuals with SCD. It is a "gain of function" mutation because it gives to the HbS a new property: the capability to polymerize under low oxygen conditions (when the Hb is not bound to oxygen). Hb hybrid tetramers, with a single β^S-globin subunit ($\alpha_2\beta^S\beta$), can also polymerize, however less efficiently than HbS.

In addition, while glutamic acid is negatively charged, valine is neutral. The resulting HbS molecule is more positively charged than HbA.

3.3.1. Molecular mechanisms of HbS polymerization

The observation by Stetson *et al*. in 1966 of sickle-shaped RBCs by electron microscopy showed the presence of long, thin intracellular crystals of reduced Hb (53). These intracellular fibers follow the same organization as *in vitro* purified and crystallized HbS. The comparison of the crystalline forms shows that the intracellular fibers are not the result of a crystallization process but of an intracellular polymerization (54). Other analyzes by electron microscopy and X-ray diffraction have shown that one single HbS fiber consists in 7 double-stranded filaments twisted around a single axis (Figure 11). It contains only deoxygenated HbS molecules (meaning no oxygenated HbS molecules) and its diameter is approximately 20 nm (55,56).

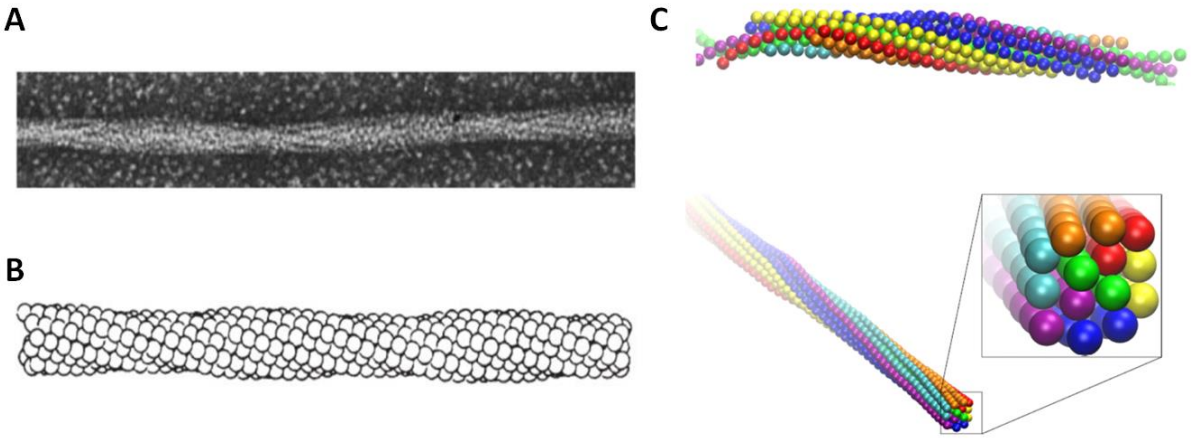

Figure 11 | Structure of the HbS fiber. (**A**) Photograph of an HbS fiber by electron microscopy. (**B**) Reconstruction of the HbS fiber with a sphere model in which only deoxy-HbS can enter. (**C**) Organization of the HbS fiber into a 7 double-stranded filaments with a cross section in a hexagon shape. Figure adapted from Li, *et al*. (57).

The study of molecule-molecule interactions at the amino acid level allowed to identify the residues directly and indirectly involved in polymerization (58). Obviously the first is the valine at the sixth position, which initiates the polymerization process. Valine is a non-polar aliphatic amino acid and it replaces the glutamic acid, a negatively charged polar amino acid, in the β^S-globin. This residue is located at the molecular surface of the protein and is therefore prone to interact with other molecules. Into HbS fibers, the side chain of the valine of the first Hb molecule interacts with a hydrophobic pocket on the surface of a β subunit of the adjacent molecule. This interaction only occurs in T state, because of the conformational modification. This pocket is naturally present on the HbA and is formed between the phenylalanine and leucine residues at positions 85 and 88 (F85 and L88) on the one hand, and alanine at position 70 (A70) on the other hand. This interaction is further stabilized by the presence of an energetic hydrogen bond between the threonine at positions 4 (T4) on the first Hb molecule and asparagine at position 73 (D73) on the adjacent molecule (59) (Figure 12). Several other contacts, intra-strand (called axial contacts) and inter-strand (called lateral contacts) participate in stabilizing the fibers, also including residues of the α-globin chains (60) (Figure 13).

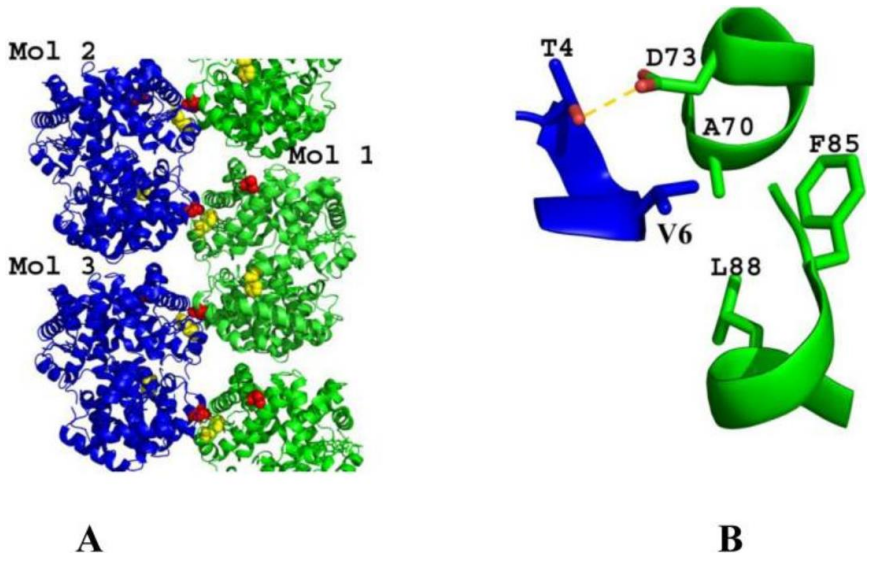

Figure 12 | Initiation of the lateral contact between HbS molecules. Lateral contact is initiated between the valine β-6 of a first HbS molecule (blue) and the hydrophobic pocket of an adjacent molecule (green). (**A**) Representation of the HBS fiber. (**B**) Magnification of the interaction induced by the valine β-6 residue (blue) and the hydrophobic pocket (green). The hydrogen bond is represented in yellow. Figure from Ghatge, *et al*. (59).

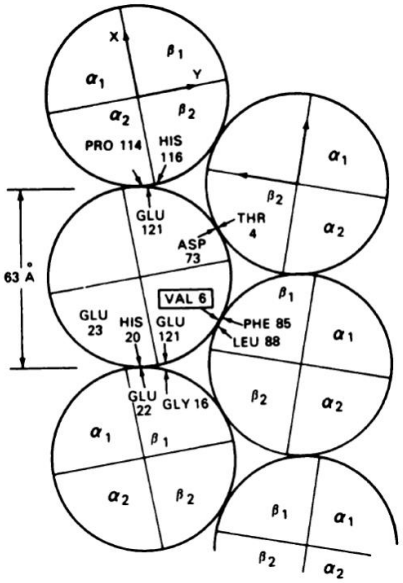

Figure 13 | Lateral and axial interactions between HbS molecules. The first lateral contact is initiated by β-VAL 6 amino acid with β-PHE 85 and β-LEU 88 and is then stabilized by lateral contact involving β-ASP 73 and β-THR 4 and by axial contacts between β-GLU 121 and α-PRO 114, β-HIS 116; β-GLU 22 and α-HIS 20; β-GLU 121 and β-GLY 16. Figure from Noguchi and Schechter (60).

In 1917, Victor Emmel, through *in vitro* blood cells cultures, showed that the RBCs of individuals with SCD can adopt sickle shape. In 1966, Chandler Stetson *et al*., following the observation of the long intracellular filaments by electron microscopy concluded that "the rapid growth of these crystals causing tenting of the cell membrane is responsible for the bizarre distortion of the erythrocytes and presumably of the disease itself" (53). The sickle-shaped erythrocytes are thus called sickle cells.

In vivo observation of these orthogonal to the axis of elongation fibers of sickle cells taken from a vein, therefore in hypoxic condition, confirms this phenomenon as well as their role in the disease (Figure 14). It is however important to note here that sickle cells without any noticeable intracellular HbS filaments can be observed as well as fibers organizations following more anarchic patterns (61). These observations suggest that there are different types of polymerization.

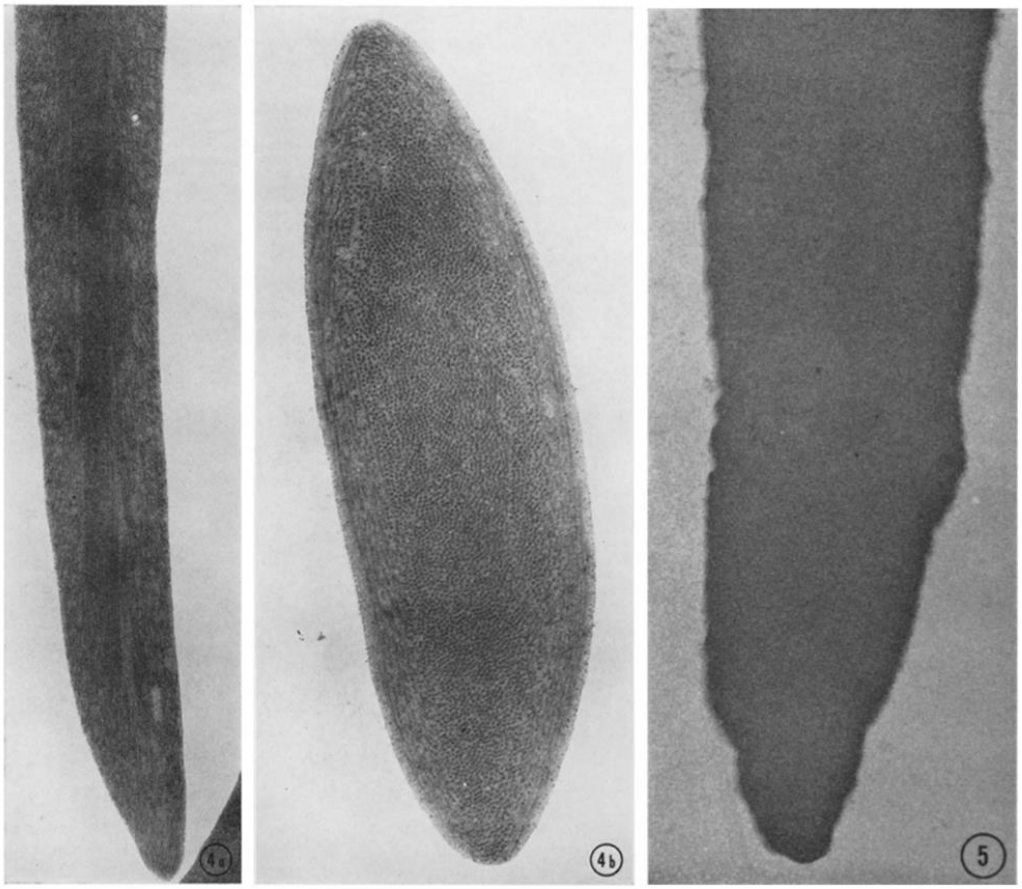

Figure 14 | Electron microscopy photographs of sections of sickle cells fixed with glutaraldehyde. Left: longitudinal section of sickle cell showing parallel HbS fibers (x 26800). Middle: cross section of a sickle cell (x 57600). Right: longitudinal section of a sickle cell with no noticeable intracellular structures (x36000). Figure from Döbler and Bertles (61).

3.3.2. Kinetics and properties of HbS polymerization

HbS polymerization, whether in solution or within RBCs, follows a specific kinetic. Polymerization can be achieved *in vitro* by lowering the pO_2, by increasing HbS concentration and/or by increasing the temperature. The polymerized fraction in solution takes the appearance of a hyper viscous gel. The curve for fiber formation as a function of time shows a characteristic "delay time" (also called lag phase), fibers appearing only after this time (Figure 15) (62–64). Delay time can be long or short depending on the experimental conditions but also on the sensitivity of method used to detect fiber formation (65,66).

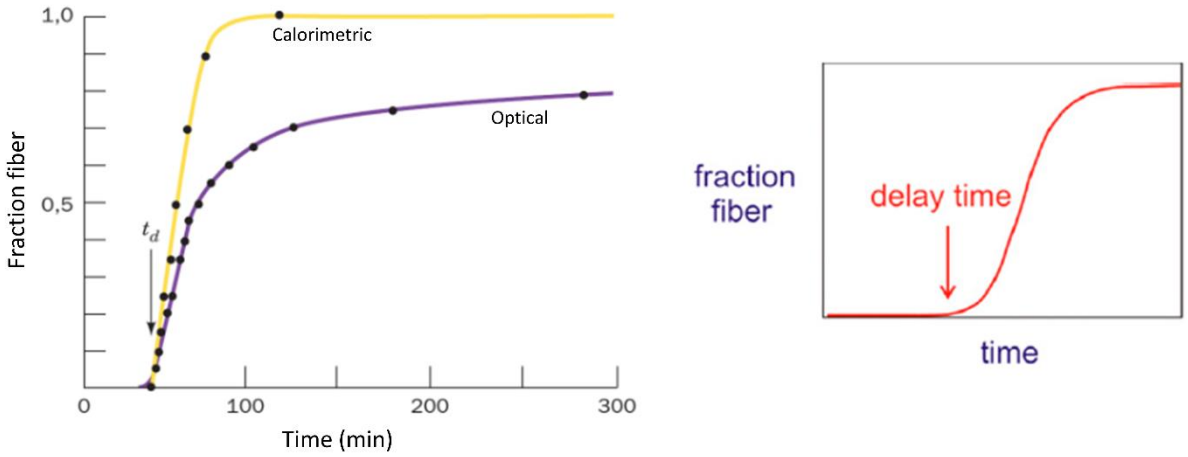

Figure 15 | Kinetic of HbS fiber formation. Gelation of a 0.233 g/mL deoxyHbS solution by rapid increase in temperature and measured by calorimetry (yellow) and optic method (purple). t_d corresponds to the delay time. Figures from Voet, and from Henry, et al. (66,67).

The appearance of HbS fibers is a two-step process (Figure 16). First, the HbS molecules aggregate sequentially to form a nucleus made up of *n* HbS molecules. Before its formation, aggregates are unstable and break down easily, but once the nucleus is formed, it assumes a stable structure that quickly elongates to form the HbS fiber. The initial process is called homogeneous nucleation because it occurs without any interaction with other fibers. Second, when one fiber is formed, it can initiate the formation of other fibers of which nucleations initiate from the surface of existing fibers. This heterogeneous nucleation is responsible for the rapid and exponential growth of polymerized HbS. New fibers will in turn initiate the formation of other fibers in an autocatalytic process. This exponential growth results in the observed delay time (62,66,68–70). Studies of the two-step nucleation of HbS polymerization

has become the basis for other peptide aggregation mechanisms as observed in Alzheimer's disease (71).

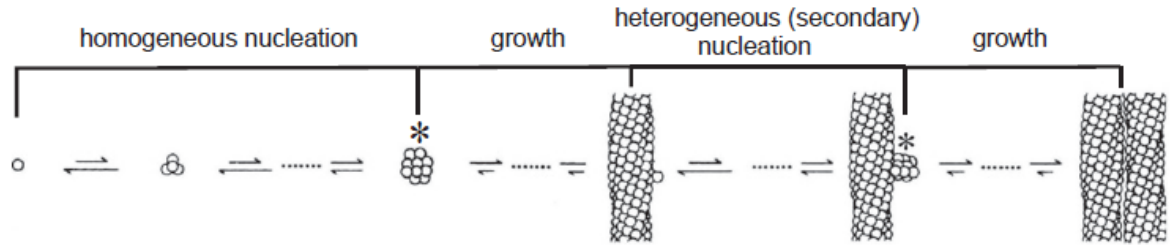

Figure 16 | The double nucleation mechanism for HbS polymerization. First step consists in homogeneous nucleation. The secondary heterogeneous nucleation quickly follows the nucleus formation. Fibers are nucleated on the surface of previous ones in an autocatalytic mechanism as more fibers form, increasing surface area for nucleation. Asterisks (*) denote initial instable aggregation until a critical nucleus is formed; the relative length of the arrows shows the more thermodynamically favorable process. Figure from Henry, *et al.* (66).

The kinetics of polymerization influences the shape of the RBCs. In case of a slow process, long fibers will line up parallel with a homogeneous orientation giving the cell its characteristic "sickle" shape. If the polymerization is faster, many short fibers will be formed, and the cell will be shaped as a "holly leaf". Finally, when the polymerization is very fast, the short fibers will not have time to pair up and the orientation will be random. The red blood cell is then said to be "granular" (65).

HbS polymerization is not a fully reversible process. Once RBC is re-oxygenated in the pulmonary circulation, part of aggregates can remain in the cell. During its next deoxygenation, these remaining aggregates will facilitate the nucleation, reducing the delay time and increasing the polymerization kinetic (72). Repeated oxygenation and deoxygenation cycles lead to the formation of irreversible sickle cells, which can be noticed even at atmospheric pO_2.

3.3.3. Factors influencing HbS polymerization

a. Hemoglobin affinity for oxygen

The higher p50 value measured for HbS is due to the polymerized fraction, which only contains deoxygenated Hb. Polymerization blocks the T state, which has a reduced affinity for O2. The p50 can reach 33 mm Hg for HbS by comparison with 27 mm Hg for HbA. This reduced affinity of the polymer induces a lower oxygen association rate which therefore decreases the transition speed from T- to R-form. Consequently, it induces more HbS polymerization, which in turn further reduces the affinity of HbS for O_2. In addition, the affinity of HbS for oxygen is further reduced by 2,3-DPG, through its interaction with β-globin subunits in the T-state. This effect is exacerbated in SCD patients because in hypoxic conditions, anaerobic glycolysis within RBC is promoted, leading to an increase in its intracellular concentration (73,74).

Recent studies have shown an indirect role of sphingosine-1-phosphate (S1P) in lowering the affinity of HbS for O_2. This molecule, increased in the RBCs of individuals with SCD, can bind to the central cavity of deoxyHb and stabilize the T form. In addition, it induces its translocation to the plasma membrane causing an increase in glycolysis activity and the production of even more 2,3-DPG (75). Inflammation is believed to be responsible for S1P increase in RBCs (76).

b. Partial pressure in O_2 (pO_2)

Oxygen availability plays a crucial role in both kinetics and level of HbS polymerization. Indeed, interactions between two HbS molecules can only occur under hypoxic conditions. The measurement of Hb solubility as a function of O_2 saturation has shown that solubility slowly increases at low saturation levels and then increases rapidly at high saturation levels (60,65).

The Monod, Wyman, and Changeux (MWC) quaternary two-state allosteric model gives a good description of fiber formation according to O_2 saturation (27,77). In this model, HbS polymer binds oxygen non-co-operatively and with a more reduced affinity for oxygen than T-state molecules in solution. A recent study has showed that applying the tertiary two-state allosteric model in addition to the MWC model allows to demonstrate that *in vivo* fiber formation is very far from equilibrium and follows a particular kinetics according to the oxygen explaining the long delay time observed in SCD (66).

c. Intracellular HbS concentration

James Hofrichter and William Eaton discovered that the delay time is greatly dependent on the HbS concentration (62). It is inversely proportional (to a power of about 30) to its concentration (60). Therefore, an even small decrease in the intracellular HbS concentration, whether caused by an increase in cellular volume or by the parallel presence of other types of Hb, has the effect, even at low pO_2, of reducing polymerization. In α-thal, the reduced synthesis of α-globin subunits promotes the formation of unstable β^S tetramers (formed of four β^S-globin subunits), which are proteolyzed. Iron deficiency also results in a decrease in Hb synthesis. These two conditions result in a lower HbS concentration and slowing down its polymerization.

d. Fetal hemoglobin and HbA2

Fetal hemoglobin (HbF) ($\alpha_2\gamma_2$) has a vital role in oxygen transport from maternal to fetal circulation. The structure of HbF is very similar to that of HbA. The α-chains are identical in the two hemoglobins but β- and γ-chains differ in 39 of their 146 amino acid (though not in number). These substitutions account for the different properties of HbF as compared to HbA, namely: a higher affinity for O_2, because of less positive charge and the capability to inhibit HbS polymerization. The HbF oxygen dissociation curve is left-shifted in comparison to HbA. The pO_2 at which HbF is half saturated with oxygen (p50) is 19 mm Hg, compared to 27 mm Hg for HbA. This value indicates that HbF has a high affinity for oxygen, giving HbF the ability to bind oxygen more readily from the maternal circulation (78).

HbF is a major modulator of sickle cell disease severity. Its synthesis in RBCs lowers HbS intracellular concentration and it presents a natural capability to directly interfere with the HbS polymer elongation. Following the first publications describing the disease in the 1910s and the demonstration of its hereditary nature, a surprising observation was quickly made: newborns show few symptoms of the disease, even several months after birth according to individuals. In 1948, it was proposed that the presence of HbF, which represents 60 to 80% of total Hb at birth and which can persist for several months depending on the individual, has a protective effect in SCD (79). This protective effect has been demonstrated in 1974 (80).

Wild-type human β-globin is a relatively poor inhibitor of HbS polymerization since it is incorporated into HbS aggregates and only acts by mere dilution (81). On the other hand, the addition of HbF to dilute deoxy-HbS solutions results in an increased delay-time with a much stronger effect than that of HbA. Moreover, HbF strongly inhibits the aggregation of deoxy-HbS and increases the solubility of HbS by inhibiting the formation of nuclei composed of deoxy-HbS, as well as the growth of the nuclei (82).

The protective effect of HbF results primarily from a decrease in the intracellular concentration of HbS homotetramer ($\alpha_2\beta^S_2$) because of polymerization kinetics being highly sensitive to HbS concentration (83). Dissociation of Hb tetramers into $\alpha\beta$ dimers and their random re-association result in mixtures of 3 tetramers containing mostly $\alpha_2\beta^S_2$ and $\alpha_2\gamma\beta^S$ and fewer $\alpha_2\gamma_2$ (84). This dimer re-association thereby further lowers the fraction of the HbS homotetramer (Figure 17A).

By comparison with the β-globin, the threonine at position 87 (T87) is replaced by a glutamine (Q87) in the γ subunit, which results in a much less favorable intermolecular lateral contact with β6 valine. Therefore, while the $\alpha_2\gamma_2$ homotetramer does not enter the polymer, the $\alpha_2\gamma\beta^S$ hybrid tetramer can enter the fiber but to a very few extent, much lower than the $\alpha_2\beta^S_2$ homotetramer or the $\alpha_2\beta^S\beta^A$ hybrid tetramer, resulting in the inhibition of HbS polymerization (Figure 17B) (85,86).

Kinetic studies have proved that conversion from T87 to Q87 is the main parameter responsible for most of the sickling inhibiting activity among other amino acid differences between β and γ-globin sequences (87).

Because the amino acids differences at positions 22 and 87 between δ- and β-globin sequences are the same as between γ- and β-globin, HbA2 ($\alpha_2\delta_2$), also strongly inhibits HbS polymerization to an extent similar to HbF (88). Re-expressing its synthesis is however a bad therapeutic target because of its very weak promoter.

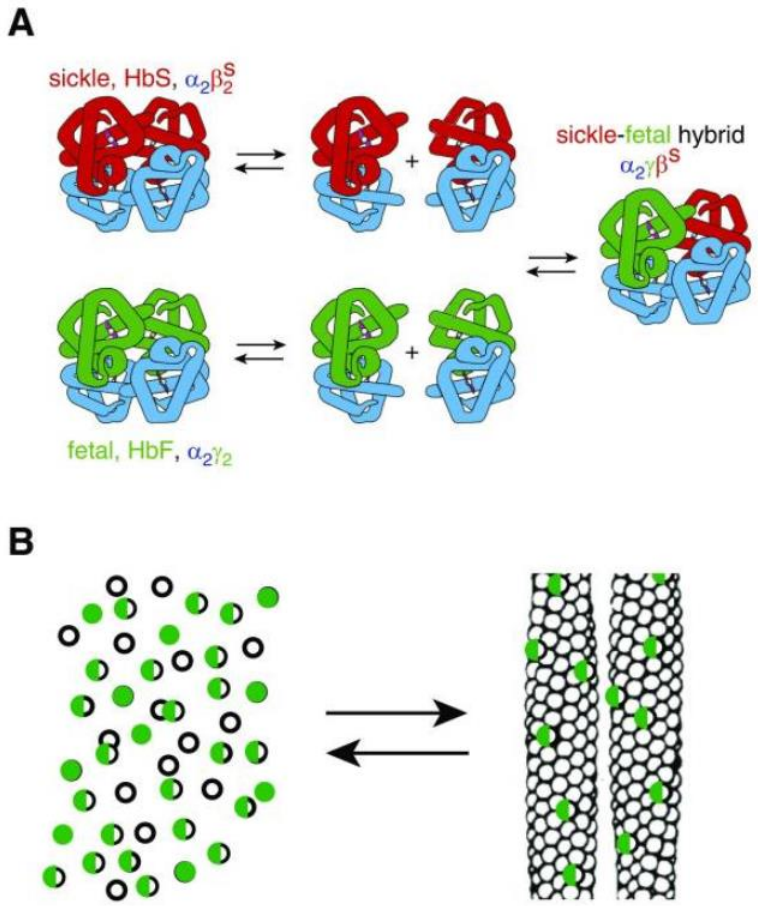

Figure 17 | Inhibition of HbS polymerization by HbF. (**A**) Dissociation of Hb tetramers into dimers and reassociation in mixtures of HbS and HbF resulting in the formation of sickle-fetal hybrid, lowering the fraction of the HbS homotetramer ($\alpha_2\beta^S_2$). (**B**) Cartoon of polymerization equilibrium in HbS-HbF mixture. Hb tetramers are present in 2 phases: the solution phase (left) or the fiber phase (right). Fibers are mostly composed of HbS homotetramers (empty circles), but there is also some copolymerization of hybrid tetramers ($\alpha_2\beta^S\gamma$) (half-green, half-empty circles). HbF homotetramers ($\alpha_2\gamma_2$) (full-green circles) cannot enter the fiber. Figure adapted from Eaton and Bunn (89).

3.4. Consequences of HbS polymerization on red blood cells

The consequences of HbS polymerization on RBC biology are numerous. As described above, HbS polymerization triggers the formation of long intracellular fibers, which align into parallel rod, distorting the shape and changing physical and biological properties of RBCs. These impairments directly or indirectly induce ischemia, a decreased arterial blood supply to an organ, anemia, a decrease in the hemoglobin level below its normal value, vaso-occlusion, or blood vessel occlusion, and eventually, multiple organ damage. These alterations and their involvement in SCD pathophysiology will be described in chapter 3, after a review of the physiological RBC biology in the next chapter.

Chapter 2 – Physiological red blood cell biology

1. The erythropoiesis

Because of its relative access facility, the RBC is probably chronologically and quantitatively the first, most studied cell in the organism. German documents from the 17th century (shortly after the invention of the microscope) describe its morphology but also some of its fundamental properties with exceptional precisions (90). Since then, many studies have described the process allowing its generation, its different physical and biological properties and its behavior throughout its life in the body. Erythroid homeostasis is highly regulated to maintain a sufficient number of RBC for efficient oxygen delivery to the tissues, while avoiding viscosity problems associated with overproduction.

1.1. The erythroid differentiation

Erythropoiesis is the set of physiological mechanisms ensuring the production of RBCs at a sufficient level and in line with their role as oxygen carrier to the various tissues of the body. Also named erythrocytes, RBCs represent the most common cell type in the blood of an adult, which in humans contains approximately $5x10^6$ cells per microliter (91). In mammals these cells are characterized by the absence of nucleus and of the major cell organelles: endoplasmic reticulum, Golgi apparatus and mitochondria, a lack which consequently leads to the fact that they are no longer able to proliferate. With an average lifespan of 120 days, maintaining the necessary number of RBCs for oxygenation requires the generation of approximately $2x10^6$ cells every second, i.e. the renewal of 1/20th of the total erythrocyte mass every day. From birth, new erythrocytes are produced in the bone marrow which provides a favorable cellular microenvironment composed of endothelial cells, osteoblasts, stromal cells, hematopoietic cells and extracellular matrix (91).

Erythroid differentiation is characterized by the commitment of a multipotent hematopoietic stem cell (HSC) that gives rise to all the blood cells, into a myeloid differentiation pathway and then into early erythroid progenitors called BFU-E (Burst Forming Units Erythroid). The latter differentiates into CFU-E (Colony Forming Units Erythroid), which are the later progenitors. They will undergo several successive stages of maturation until their terminal differentiation into enucleated RBC (92). As these different progenitors differentiate, their number increases while their proliferative capacity decreases. The different cellular stages of erythroid differentiation can easily be visualized by simple staining. This is due to the progressive hemoglobinization of the cytoplasm from the proerythroblast to the orthochromatic erythroblast, (Hb being acidophilic) gradually masking the cytoplasmic basophilia which is linked to ribonucleic acids (RNA). The different cells leading to RBCs make up the erythrocyte lineage (Figure 18). At the end of the process, reticulocytes are characterized by the expulsion of the nucleus and the persistence of cytoplasmic organelles. They enter the bloodstream where they differentiate into mature RBCs, corresponding to the ultimate stage of maturation of the erythroid lineage, having lost its cytoplasmic organelles and assumed its characteristic biconcave form. A morphological study of these cells under a microscope shows that erythroid differentiation is accompanied by a reduction in cell and nuclear volumes as well as a strong condensation of the chromatin. *In vivo*, 4 to 5 mitoses make it possible to go from one proerythroblast to 32 or 64 RBCs in 5 to 6 days.

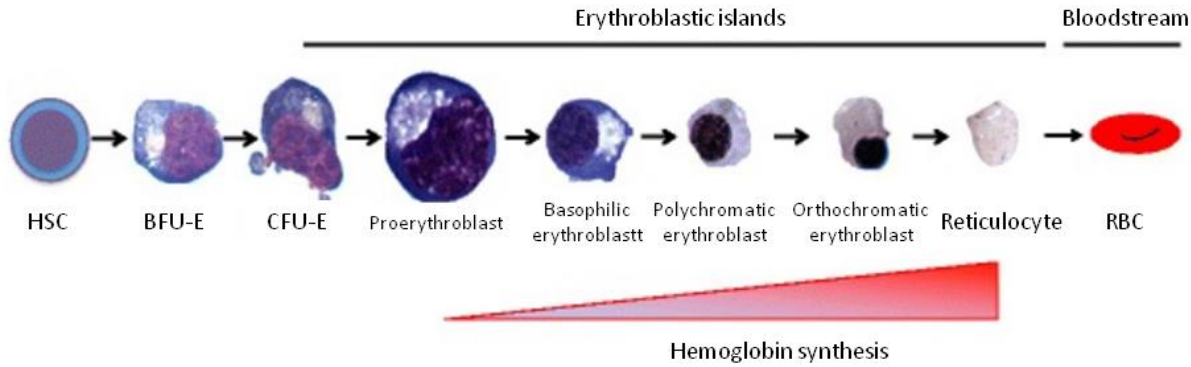

Figure 18 | Overview of the erythropoiesis from the hematopoietic stem cell (HSC) to the red blood cell (RBC). Figure from Zivot, *et al.* (93).
BFU-E: Burst forming unit-erythroid. CFU-E: Colony forming unit-erythroid.

1.2. The erythroblastic island

First described in 1958, the erythroblastic island, which is a structure within in the bone marrow, is composed of a central macrophage with long cytoplasmic extensions around which the maturing erythroblasts organize themselves in crowns (Figure 19) (94).

The central macrophage plays several roles: supporting the proliferation of erythroblasts, providing necessary iron for the synthesis of Hb, promoting enucleation and degrading the expelled nuclei by phagocytosis (95). In addition it is involved in the clearance of abnormal maturating erythroblasts, as observed in β-thalassemia, thanks to its phagocytic capabilities (96–98). The formation and integrity of erythroblast islands involve numerous adhesion molecules, present on both the surface of the macrophage and erythroblasts or only on one of them. These proteins include erythroblast macrophage protein (EMP), α4β1 integrin, which is present on erythroblasts and its receptor, vascular adhesion molecule 1 (VCAM-1), which is present on the macrophage, as well as intercellular adhesion molecule-4 (ICAM-4), which interacts with αV integrins of the macrophage (98,99).

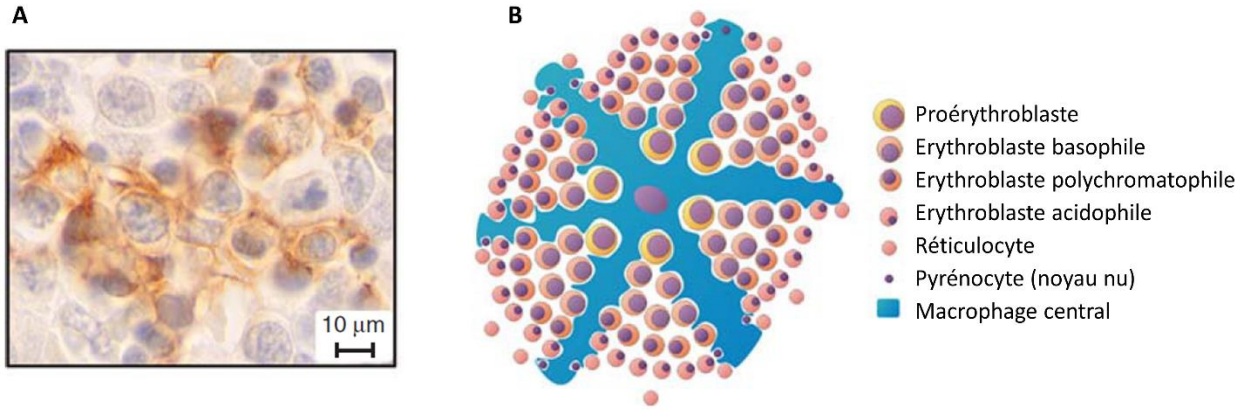

Figure 19 | The erythroblastic island. (**A**) Erythroblastic island in E13.5 fetal liver. The cytoplasmic extensions of the central macrophage (brown) are surrounding erythroid cells at various stages of differentiation. (**B**) Schematic drawing of an erythroblastic island. Figure from Dzierzak and Philipsen (91).

1.3. Erythropoiesis regulation

Physiologically, erythropoiesis is finely regulated at different stages of differentiation by a balance between Fas-Ligand-induced apoptosis and protection against cell death. This regulation notably involves growth and transcription factors. The key factor is the erythropoietin hormone (Epo), a glycoprotein produced by kidney cells that protects erythroblasts against apoptosis while inducing erythroid differentiation (100). In hypoxia, induction of Epo synthesis via the transcription factor hypoxia induced factor-alpha (HIF-α) adapts the number of circulating RBCs to maintain optimal oxygenation of all body tissues. Its receptor, Epo-R, from the family of receptors with tyrosine kinase activity, induces an activation of the Janus kinase 2 / signal transducer and activator of transcription 5 (JAK2/STAT5) signaling pathway, which activates genes fundamental for erythroid progenitor survival, proliferation and differentiation (101). The main erythroid transcription factors involved are GATA-1, GATA-2 and the Krueppel-like factor 1 (KLF1). The first two have a reciprocal expression pattern during erythropoiesis. GATA-1 promotes differentiation while GATA-2 regulates the proliferation and maintenance of hematopoietic progenitors (102).

Iron is critical for hemoglobin synthesis and plays a key role in the regulation of erythropoiesis. The liver peptide hepcidin is the master regulator of systemic iron homeostasis. It facilitates surface expression of ferroportin, an iron export protein that is largely expressed in enterocytes, hepatocytes and macrophages, and facilitates iron absorption (103). Within bloodstream, iron is transported by the glycoprotein transferrin with two ferric iron molecules (Fe^{3+}) per transferrin protein.

1.4. Stress erythropoiesis

Under steady state conditions, HSCs are mainly localized within the bone marrow in specialized microenvironments termed niches, maintaining their survival and functions. Under emergency conditions, such as inflammation, anemia, myelofibrosis and bone marrow failure, extramedullary hematopoiesis occurs outside the bone marrow, including the spleen and liver (104). In part of those contexts, the constant production of erythrocytes might be inhibited or unable to maintain RBC numbers and new erythrocytes must be rapidly made to increase

hemoglobin levels. To maintain homeostasis an alternative stress erythropoiesis pathway is activated.

Stress erythropoiesis is defined as an increase in erythroid output in response to anemic stress and is better characterized in mice. Characteristics of stress erythropoiesis include the use of specific signals and distinct progenitor cells that migrate from bone marrow (105). Among these signals are bone morphogenetic protein 4 (BMP4) and growth differentiation factor 15 (GDF15) which drive the expansion of a population of specialized stress erythroid progenitors into BFU-E (106). BMP4 functions in concert with stem cell factor (SCF) and Epo under hypoxia condition to induce stress erythropoiesis (107).

In humans, stress erythropoiesis often exhibits properties of fetal erythropoiesis with increased synthesis of HbF, associated with a reduced expression of *BCL11A* (106,108). Analysis of bone marrow progenitors from SCD patients identified a population of progenitor cells that express CD34 and glycophorin A (GPA) on their surface. These cells also express CD71 and SCF receptor (KIT) and can be differentiated into erythroid cells with higher proportion of HbF containing cells than normal bone marrow progenitors (109). Such a phenomenon has also been described in patients receiving bone marrow transplantation (108,110). While stress erythropoiesis is not well characterized and documented, its properties represent a potent therapeutic target in SCD and β-thalassemia.

2. Physical and biological properties of red blood cells

2.1. Erythrocyte membrane properties

Development from the pro-erythroblast to the reticulocyte results in a progressive reduction in cell size. Mature RBCs have a diameter of only 6–8 µm. Their small size and biconcave shape create an excess of surface as compared to their volume. It results in a large surface area optimized for rapid gas exchange.

Erythrocyte membrane deformability allows the cells to enter the micro-capillaries in the tissues, the smallest diameter of which being about a third of their own, with a minimum direct contact with endothelial cells. This flexibility is due to the structural organization of their plasma membrane. This consists of a phospholipidic bilayer in which are embedded many cholesterol molecules as well as proteins allowing it to be anchored to a very elastic and

dynamic cytoskeleton. Erythrocyte transmembrane proteins are very often exclusive to the erythroid lineage and participate in various biological properties.

2.1.1. Composition of the phospholipidic bilayer

The lipid composition of the RBC membrane participates in its physical properties of fluidity and deformability. Cholesterol and phospholipids are in equal proportions in terms of weight. Enclosed between the phospholipids, cholesterol molecules participate in the fluidity of the plasma membrane and are evenly distributed within the two layers. The five major phospholipids are asymmetrically distributed between the inner and the outer layer. Phosphatidylcholines and sphingomyelins are found in the outer surface while phosphatidylethanolamines, phosphatidylserines, and phosphoinositols are confined to the inner layer (111). This asymmetry is maintained by proteins of the translocase family, whose function is to displace phospholipids. The energy-dependent flippases move the phospholipids from the outer layer to the inner one and the energy-independent floppases do the opposite. These migratory activities are active transport, moving against a concentration gradient (112). On the opposite, scramblases move the phospholipids toward both directions in a passive way, following the concentration gradient (113).

The maintenance of lipid asymmetric distribution, and primarily maintenance of phosphatidylserines (PS) in the inner layer, plays a crucial role in the survival of RBCs. Indeed, its externalization, which acts as an apoptosis signal and is recognized by macrophages, induces the engulfment of the cell by phagocytosis (114,115). In addition, PS interacts with the internal spectrin network, participating in the regulation of the mechanical properties of the membrane. Another important aspect of the lipid asymmetry in the plasma membrane is the enrichment of negatively charged phospholipids in the inner leaflet. Indeed, mainly PS and phosphoinositols, both being negatively charged, contribute to the generation of a static negative surface potential of −25 mV (116,117).

2.1.2. Transmembrane structuring proteins

In RBC, the plasma membrane and cytoskeleton are closely connected and form a complex structure called the membrane skeleton (111). This connection is ensured by protein-protein interactions including both transmembrane proteins, cytoskeletal proteins as well as

binding intermediate proteins. Lipid-protein interactions participate in the cohesion of the membrane. The transmembrane proteins serve as anchors allowing the cytoskeleton to be attached to it. This influences the topology of the transmembrane proteins by restricting their lateral and rotational mobility. The phospholipid bilayer is linked to the cytoskeleton by two major protein complexes: the ankyrin complex and the junctional complex (also known as the 4.1R complex) (Figure 20). In the first one, ankyrin is the binding intermediary between cytoskeletal spectrins and band 3 transmembrane proteins and RhAG. The 4.1R protein allows the binding between actin and spectrin filaments of the cytoskeleton with the C (GPC), D (GPD), XK, Rh Kell and Duffy glycophorins (118,119). These protein-protein interactions play a key role in the stabilization of the lipid bilayer and also participate in the prevention of microvesicles formation. These interactions are regulated by numerous post-translational modifications.

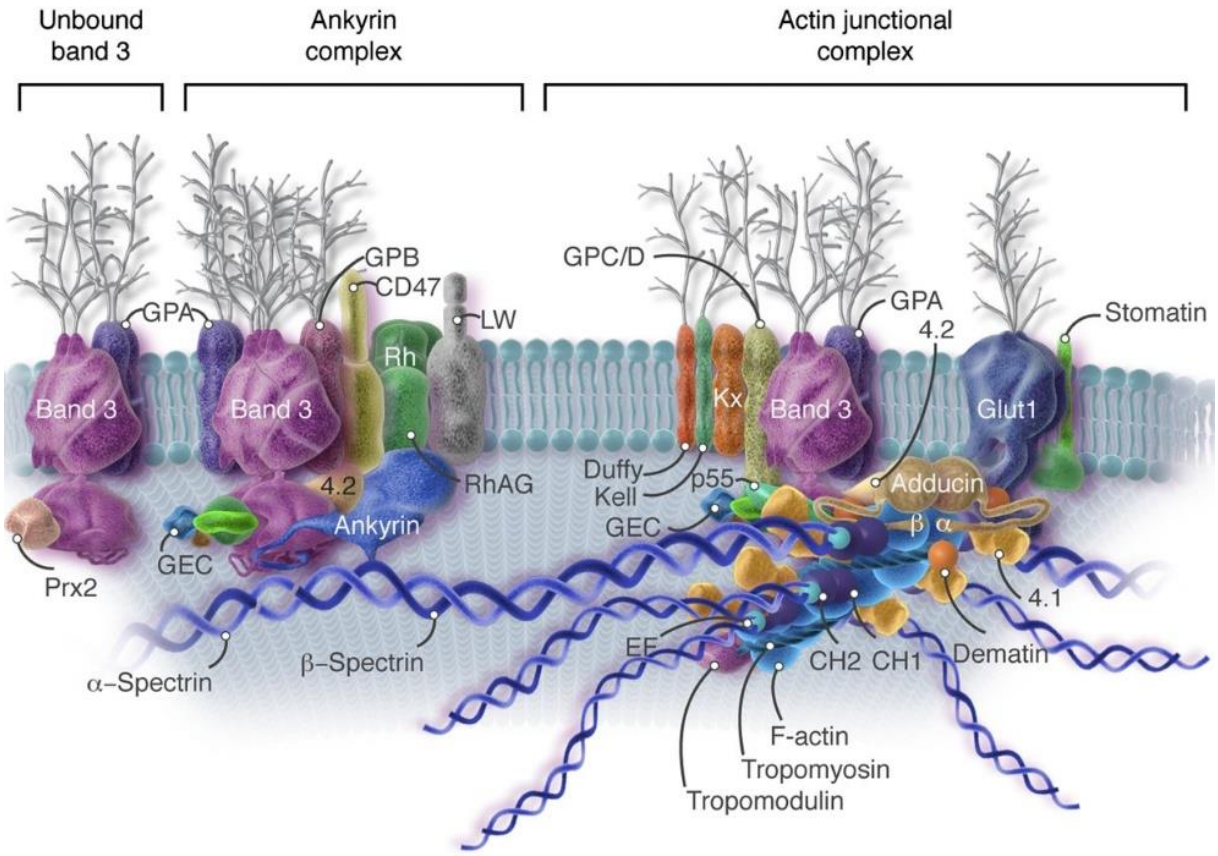

Figure 20 | Schematic representation of the protein complex interactions constituting the erythrocyte membrane skeleton. The transmembrane protein band 3 is associated with several other proteins in the two major complexes of cohesion and binding of the phospholipid bilayer to the cytoskeleton. Although in minority, unbound forms of band 3 protein are also observable. Figure from Lux (119).

2.1.3. Cell deformability and aggregation

Throughout its life, RBC will undergo a huge number of extensive deformations and distortions as it passes through the blood microcapillaries and the inter-endothelial slits in the spleen. The structure of its plasma membrane gives it properties of great fluidity and deformability while maintaining extremely high resistance.

Studies have identified three RBC characteristics regulating its deformability potential: its biconcave shape, the physical and elastic properties of its membrane and the internal (cytosolic) viscosity (120).

The RBC unique biconcave disc shape offers a very high surface-to-volume ratio, which corresponds to an excess of membrane as compared to its volume. This extra-membrane is crucial for its survival. It allows the cell to elongate and deform while protecting it from mechanical destruction. To both maintain this shape and prevent loss of material by vesiculation, the phospholipid bilayer and the cytoskeleton must be in close contact. The integrity of the plasma membrane is ensured by the interactions of the distal junction complex.

The membrane viscoelasticity properties are ensured by the intrinsic characteristics of the cytoskeleton proteins and the lipid bilayer properties. The dynamic dissociation of spectrin tetramers into dimers during the distortion of RBCs is followed by their very rapid reassociation in order to restore the characteristic shape of the cell.

The intracellular viscosity is essentially determined by intracellular Hb concentration. A slight increase in Hb concentration induces a simultaneous and exponential increase in viscosity, which can thus compromise the deformability. This intracellular Hb concentration is tightly regulated (121).

Membrane deformability can be assessed by ektacytometry using the laser optical rotational red cell analyzer (LORRCA) and is carried out at +37°C. The blood sample is mixed with a viscous iso-osmolar solution of polyvinylpyrrolidone (PVP, viscosity ≈ 30 cP) at 2% hematocrit in order to be able to apply physiological and supra-physiological shear stresses. It makes it possible to study erythrocyte deformability at different increasing shear stresses (from 0.3 Pa to 30 Pa). The viscosity of PVP is greater than that of the cytoplasm of GR. The latter therefore deforms into an ellipse when forces are applied. A laser passes through the

sheared RBC solution and the image of the deformed RBCs is captured by a camera. An elongation index (EI) is then calculated (120).

In addition, the osmoscan is a measure of deformability at constant shear stress but under an osmotic gradient. The obtained curve represents the EI as a function of osmolality and is the reference technique for the diagnosis of red cell membrane diseases. The osmoscan provides information on both cell deformability and membrane stiffness. In healthy individuals, the maximum deformability (EI max) corresponds to physiological osmolality. When osmolality is reduced, water enters the RBC until it reaches a maximum swelling for O min. Conversely, when osmolality is increased water leaves the cell, the RBC dehydrates, and its deformability decreases. Three parameters can thus be extracted from this curve: O min, EI max (and O EI max), and O hyper (Figure 21).

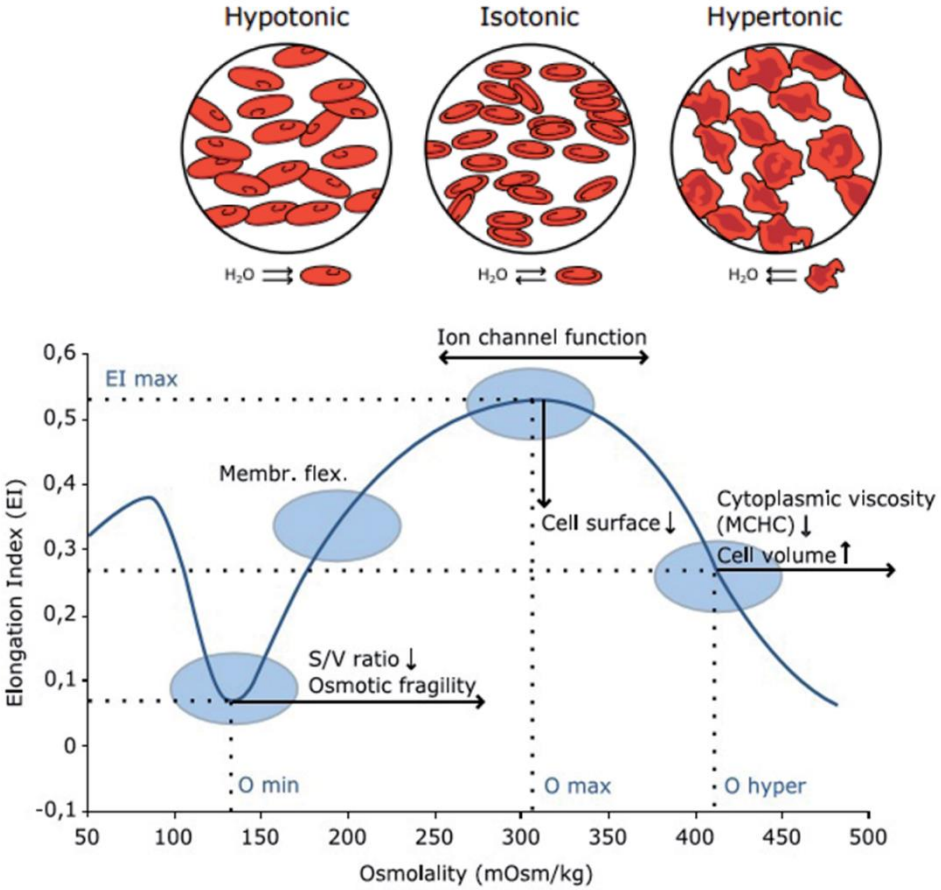

Figure 21 | Measurement of RBCs deformability under osmolality gradient using the LORRCA system. For normal RBCs, the EI max is measured at physiologic osmolality (isotonic condition). Under hypotonic condition (i.e. when osmolality is decreased), water enters the RBC until it reaches a maximum swelling for O min. Conversely, under hypertonic condition (i.e. when osmolality is increased), water leaves the cell and the RBC dehydrates. O hyper, which corresponds to the osmolality for which 50% of the maximum deformability is obtained, reflects Hb concentration (MCHC) and cell volume. Figure from the LORRCA user manual www.rrmechatronics.com.

The O min point reflects the osmotic fragility and the surface to volume (S/V) ratio. EI max depends on membrane deformability. O hyper, which corresponds to the osmolality for which 50% of the maximum deformability is obtained, reflects Hb concentration and cell volume, thus cytoplasmic viscosity. A global shift toward the left of this curve as compared to control (i.e. both reduced O min and O max), as observed in individuals with SCD or hereditary spherocytosis, indicates the presence of dehydrated red cells and is associated with reduced cell deformability whatever the shear stress applied (120,122,123).

Erythrocyte membrane deformability is essentially dependent on the volume of the cell, which itself is mainly determined by the intracellular cation content. For that, many membrane channels regulate the flow of sodium and potassium ions.

Aggregation is another rheological feature of RBCs. It consists in the reversible formation of “rouleaux” where RBCs stack on top of each other because of their discoid shape and occurs at low shear rate. It is the main determinant of blood viscosity at low shear rate. Increased RBC aggregation has been shown to increase axial migration through vessels thereby facilitating blood flow (124). This phenomenon leads to an apparent decreased in hematocrit and in blood viscosity (Fharaeus effect), and in endothelium wall shear stress (125,126).

2.1.4. Ionic transport

RBCs plasma membrane is selectively permeable to cations and anions allowing the maintenance of a high intracellular content in potassium (K), low content in sodium (Na) and even lower content in calcium (Ca). Several transport mechanisms exist depending on the type of ion to be transported and whether it is a passive or active transport (Figure 22).

Disruption of any of these flows, whether innate or acquired, usually leads to changes in the hydration of RBC. This causes an increase or a decrease in MCHC and leads to an associated pathology, which severity is often correlated with the degree of the disturbance (127).

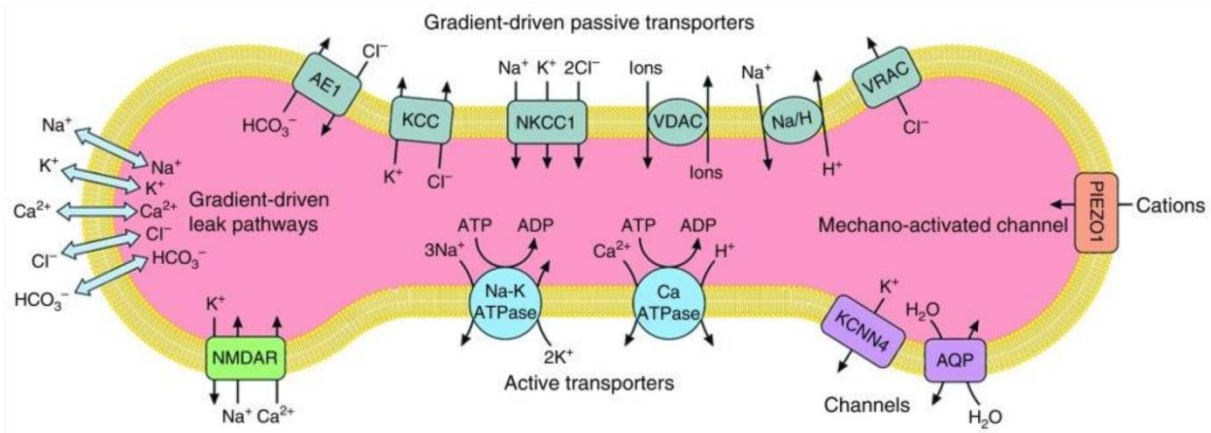

Figure 22 | Schematic representation of the protein complexes participating in the erythrocyte ionic homeostasis. Gradient-driven transport pathways include AE1: anion exchange protein 1 (AE1) or band 3, K-Cl cotransporters of the family of chloride-cation cotransporters (KCC), Na-K-Cl cotransporter 1 (NKCC1), voltage-dependent anion channels (VDAC), sodium/hydrogen exchanger 1 (Na/H) and voltage-regulated anion channels (VRAC). PIEZO1 is a mechano-activated channel. Other erythrocyte membrane channels are the aquaporins, water channels (AQP1 and AQP3), and the Gardos channel (KCNN4), a calcium-activated potassium channel. Active transporters are the calcium (Ca) and the sodium-potassium (Na-K) ATPase. The multicomponent N-methyl d-aspartate receptor (NMDAR) participates in calcium regulation. Gradient-driven leak pathways, not otherwise identified and indicated by the arrows, also exist in some pathology. Other transport pathways (e.g., CO_2, amino acids, glucose, urea, etc) are not shown. Figure from Gallagher (127).

2.2. Energetic metabolism

The primary functions of the erythrocyte, gas transport and exchange, are maintained through several metabolic process. They aim at maintaining membrane integrity and the sodium/potassium osmotic gradient, keeping heme iron in its reduced ferrous form, and protecting hemoglobin (Hb) from oxidative denaturation (128). Because RBCs lack mitochondria, they do not undergo oxidative phosphorylation and do not store glycogen; thus, they must constantly catabolize glucose from the blood stream. Fructose and mannose are also metabolized almost readily. Erythrocytes incorporate glucose from the plasma through the membrane glucose transporter 1 (GLUT1).

More than 90% of the glucose is processed through the Embden-Meyerhof pathway, which consists in anaerobic glycolysis with the catabolism of 1 mole of glucose yielding 2 moles of adenosine triphosphate (ATP) and 2 moles of lactate (Figure 23). It is the primary source of

ATP, 2,3-DPG and nicotinamide adenine dinucleotide reduced form (NADH) in RBCs. The methemoglobin reductase is the specific enzyme which reduces ferric (Fe^{3+}) metHb to the ferrous (Fe^{2+}) form. To ensure its proper function, this enzyme activity needs reduced NADH.

Between 5 and 10% of the glucose enters the Hexose Monophosphate Shunt (pentose phosphate pathway) leading to fructose-6-phosphate and glyceraldehyde-3-phosphate, intermediates in the glycolytic pathway (Figure 23). This pathway is the primary source of reduced nicotinamide adenine dinucleotide phosphate (NADPH), with 2 moles of NADPH produced for each mole of glucose metabolized. NADPH is required for the reduction of oxidized glutathione (GSSG). Reduced glutathione (GSH) is restored by glutathione reductase and protects erythrocytes from oxidants, which are produced as byproducts of the oxidation of heme by oxygen.

Lastly, a small fraction of glucose (less than 1%) is converted to glucose-1-phosphate and then to glycogen. (129–131).

There is a competition between the two main pathways to maintain the energy-dependent volume and ionic homeostasis and the generation of antioxidant molecules. A dysregulation of the balance might reduce the Embden-Meyerhof pathway activity and thus a decrease in ATP levels which are required for the activity of ionic transports, then triggering changes in RBC hydration. In addition, a reduced in the pentose phosphate pathway activity could result in less effective antioxidant capability (132).

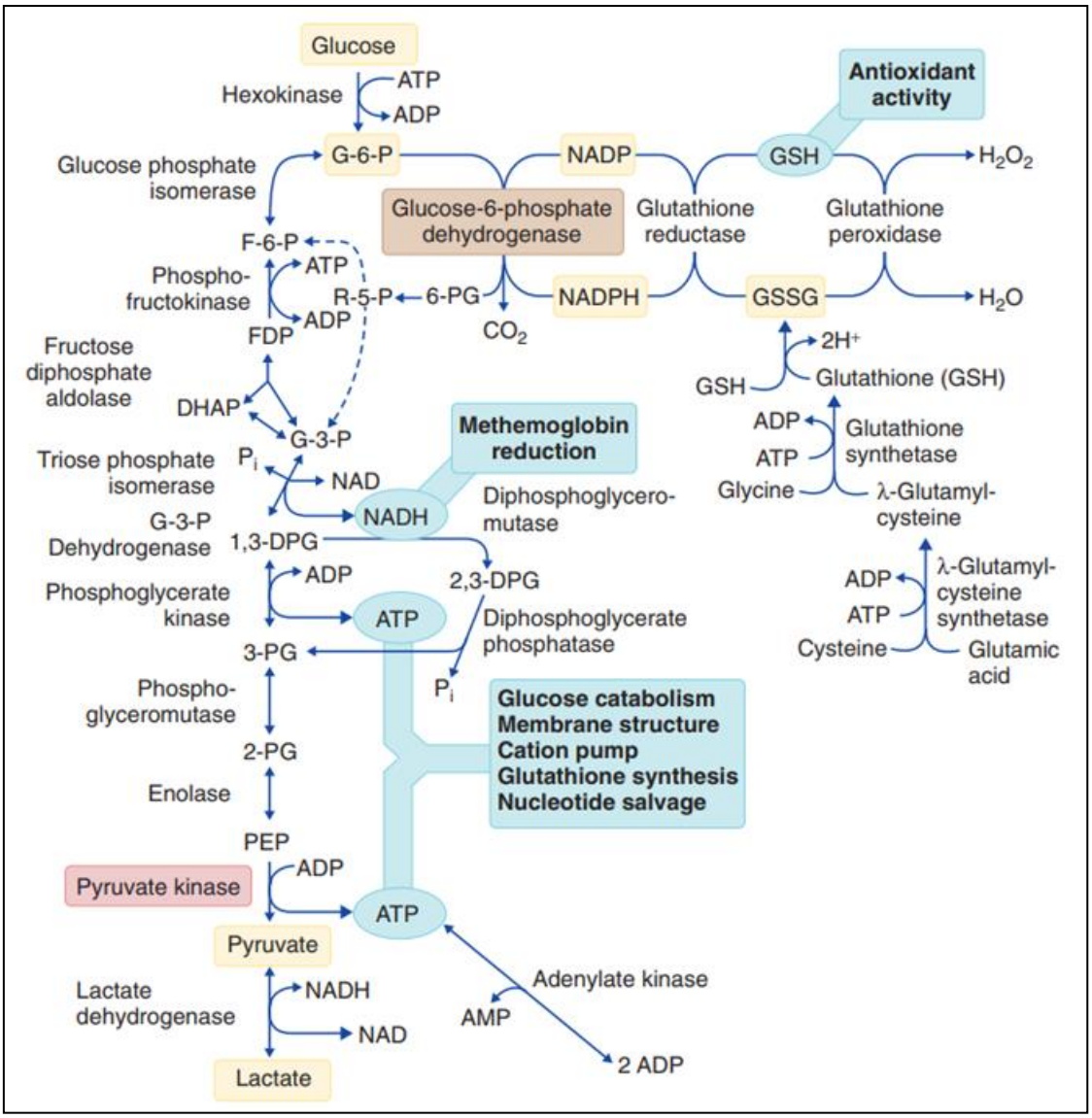

Figure 23 | Pathways of energy metabolism in erythrocytes. Glucose-6-phosphate may be degraded anaerobically to lactate through the Embden-Meyerhof pathway or oxidatively through the hexose monophosphate shunt. 2,3-Diphosphoglycerate (2,3-DPG) may be generated instead of adenosine triphosphate (ATP) through diversion of triose through the Rapoport-Luebering shunt. Glutathione may be synthesized directly from constituent amino acids; its cycling from oxidized (GSSG) to reduced forms (GSH) depends on reduced NADPH generation. Figure from Gallagher (133).

ADP = adenosine diphosphate; DHAP = dihydroxyacetone phosphate; FDP = fructose-1,6-diphosphate; NAD = nicotinamide adenine dinucleotide; NADP = nicotinamide adenine dinucleotide phosphate; NADPH = nicotinamide adenine dinucleotide phosphate, reduced form; PEP = polyestradiol phosphate.

2.3. Intrinsic antioxidant activity

2.3.1. Main sources of oxidation

Hb auto-oxidation is one of the main sources of oxidation within RBCs. In functional Hb, the iron atom is in the ferrous form (Fe^{2+}). Oxidation of this atom to ferric iron (Fe^{3+}) generates methemoglobin (metHb), which cannot bind O_2 molecules. Hb auto-oxidation is favored under low oxygen conditions, such as when RBCs pass through the blood capillaries (134). This reaction produces superoxide ions that are quickly converted into highly oxidizing hydrogen peroxide (H_2O_2), which in turn can react with Hb and generate other superoxide ions, amplifying the phenomenon (135). Hb oxidation is prevented thanks to catalase and peroxidases, which neutralize hydrogen peroxide (H_2O_2) from oxidative reactions.

The affinity of heme for metHb is much lower than for unoxidized Hb (136). The degradation of heme by superoxide ions induces the release of iron which, whatever its form, induces via the Fenton reaction the generation of hydroxyl radicals (HO·) responsible for numerous oxidative damage. Heme is a hydrophobic molecule that can interact with membrane lipids and proteins promoting oxidation reactions (137).

Partially oxygenated Hb, especially if Hb is unstable, is responsible for the majority of ROS generated at the RBC membrane (138). ROS located at the plasma membrane are not readily accessible to the cytoplasmic antioxidant system and can easily oxidize membrane lipids and proteins, causing oxidative damage. Lipid peroxidation and protein oxidation result in a loss of membrane lipid organization and a reduced cellular deformability. Additionally, the resulting disruption of the physiological asymmetry of phospholipids causes PS exposure to the outer membrane (139).

Oxidized hemoglobins also tend to denature and precipitate as hemichromes, which consist in all the intermediate products of Hb oxidative denaturation starting from metHb until complete dissociation and release of heme and iron. Hemichromes have a high affinity for the cytoplasmic domain of band 3 and mediate the oxidative crosslinking through disulphide bonds (140). This results in band 3 clusterization and dissociation from cytoskeletal proteins through disruption of ankyrin binding, leading to membrane blebbing and microparticle generation. As band 3 binds glycolytic enzymes, the resulting dislodgement of these enzymes from oxidized band 3 leads to the activation of glycolysis and reduced NADPH production.

Reduction in the levels of NADPH decreases the antioxidant capacity of RBCs and further exacerbates oxidative stress.

Oxidative stress has also an effect on cytoskeletal proteins. ROS activate the KCC channel leading to an exit of K^+ and water from the cell. They also trigger an increase of intracellular Ca^{2+} which in turn can activate the Gardos channel which in turn promote loss of K^+. In addition, both ROS and Ca^{2+} activate caspase-3, which partially degrades band 3, affecting its interaction with the cytoskeleton. ROS can also promote oxidation of protein 4.1, actin and spectrin resulting in impaired interaction (141). The different RBC intracellular oxidative events are summarized in Figure 24.

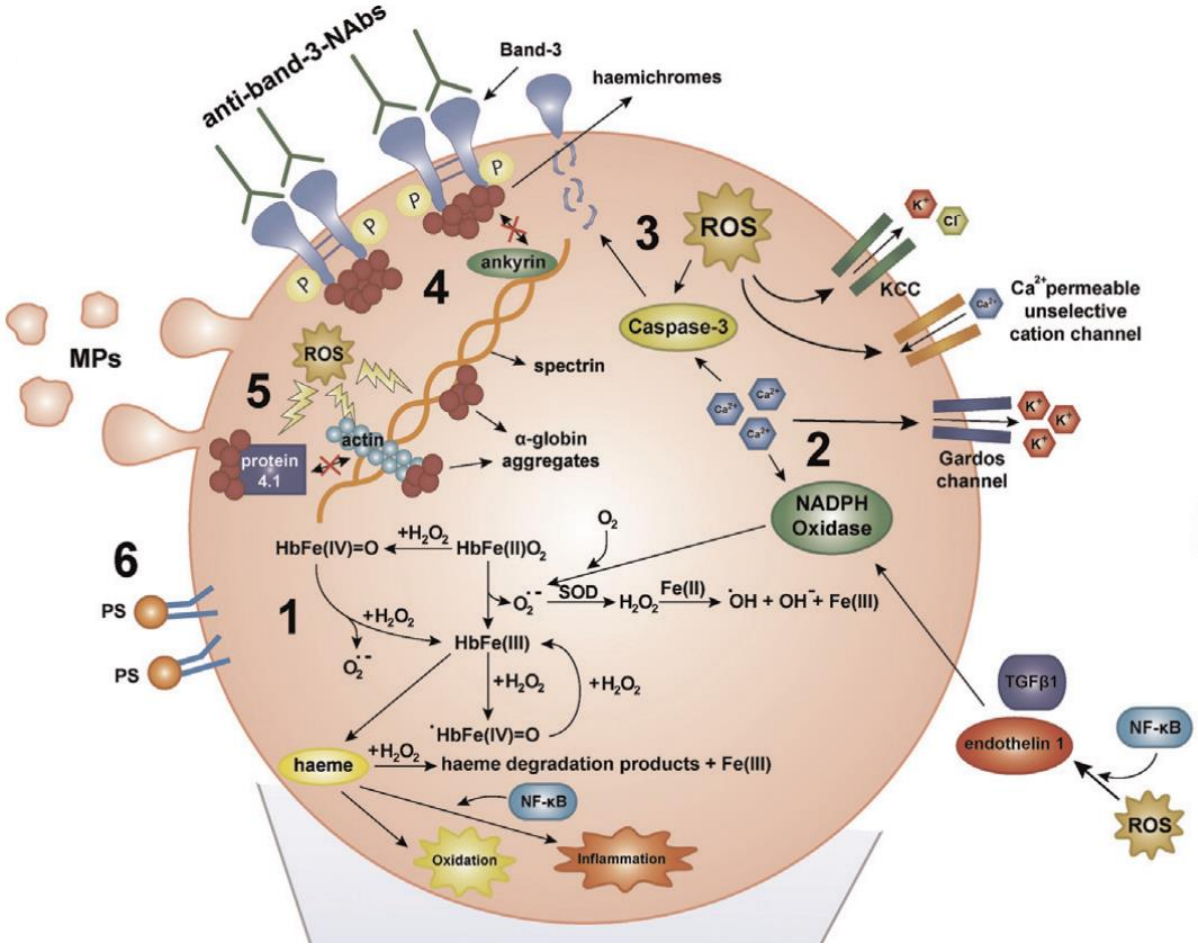

Figure 24 | RBC intracellular oxidative events. **1**: Oxidative denaturation of Hb resulting in the production of ROS, free heme and iron. **2**: Enzymatic generation of superoxide by NADPH oxidase. **3**: ROS activating caspase-3, which partially degrades band-3, affecting its interaction with the cytoskeleton. **4**: Hemichromes mediate the oxidative crosslinking and phosphorylation of band-3 leading to band 3 clusterization and dissociation from cytoskeletal proteins. **5:** ROS promote oxidation of protein 4.1, actin and spectrin resulting in impaired interaction. **6:** PS exposure results from ROS-induced disruption of normal membrane organization. Figure adapted from Voskou, *et al.* (135).
Nab: natural antibodies; MPs: microparticules.

2.3.2. RBC enzymes and antioxidant molecules

Erythrocytes have many enzymatic or chemical reducing systems, allowing the level of metHb to be physiologically maintained at around 1%. NADH produced by glycolysis is the main reducing agent of metHb. The reaction is catalyzed by the NADH-dependent cytochrome b5 reductase enzyme (142). On the other hand, NADPH is the cofactor of the metHb reductase enzyme.

Chemical reduction occurs through reduced glutathione or ascorbic acid. Glucose-6-phosphate is used for the reduction of $NADP^+$ to NADPH. NADPH is the reducing agent used by glutathione reductase for the reduction of oxidized glutathione (GSSG) to two molecules of glutathione (GSH). GSH is an important antioxidant molecule reducing some of the metHb. Finally, ascorbic acid, which enters the cell through GLUT1, has a very effective reducing action of metHb by direct transfer of an electron. The dehydroascorbic acid obtained is then reduced by the GSH present in the cell (143).

Thioredoxin and superoxide dismutase are other antioxidant enzymes in RBCs. They reduce oxidized proteins and neutralize H_2O_2 to water and oxygen, respectively (144).

2.4. Dynamic aspects: physiological lifespan and senescence

2.4.1. Erythrocyte lifespan

Physiologically, RBC population is constant. In humans, 2 million erythrocytes enter the bloodstream every second, implying that roughly the same number is removed by a finely regulated clearance mechanism (121).

The elimination of so-called "aged" RBCs takes place approximately 120 days after they entered the bloodstream from the bone marrow. This phenomenon thus participates in their renewal in the blood. This consensus time comes from experimental experiments consisting in *ex vivo* labeling of RBCs followed by their autologous reinjection in humans. It is thus possible to study the behavior of either a representative sample of the entire RBC population of an individual, or a fraction of interest after purification. Then, a longitudinal follow-up allows the measurement of the decrease in the population of labeled RBCs, allowing determination of the half-life (time after which 50% of the labeled re-injected RBCs have

disappeared). The calculation must obviously consider the natural elution factor of the product used for the label (145).

Several methods have been used for the measurement of RBCs half-life after autologous re-injection, using different molecules for the labeling: rapidly decaying radioisotopes, non-radioactive isotopes and biomolecules, all giving substantially the same results. The most frequently used radioactive element is the chromium 51 isotope (^{51}Cr), in a method which was developed in the early 1950s (146), and which is still the reference in the United States. It has been used for transfusion studies or for evaluation of *ex vivo* generated RBCs (147,148). Less frequently used radioactive elements include ^{59}Fe (iron), ^{14}C-glycine (carbon) or ^{99}Tc (technetium). The use of non-radioactive chromium isotopes or ^{15}N-glycine, apart from the lack of radioactive exposure to the subject, has the disadvantage of being poorly available and less specific (145). The most used biomolecule is biotin, which gives half-life results comparable to those obtained with ^{51}Cr (Figure 25) and can be easily detected by analyzing RBCs thanks to flow cytometry (149). This latter method is still also in use, including in studies conducted on newborns (150,151).

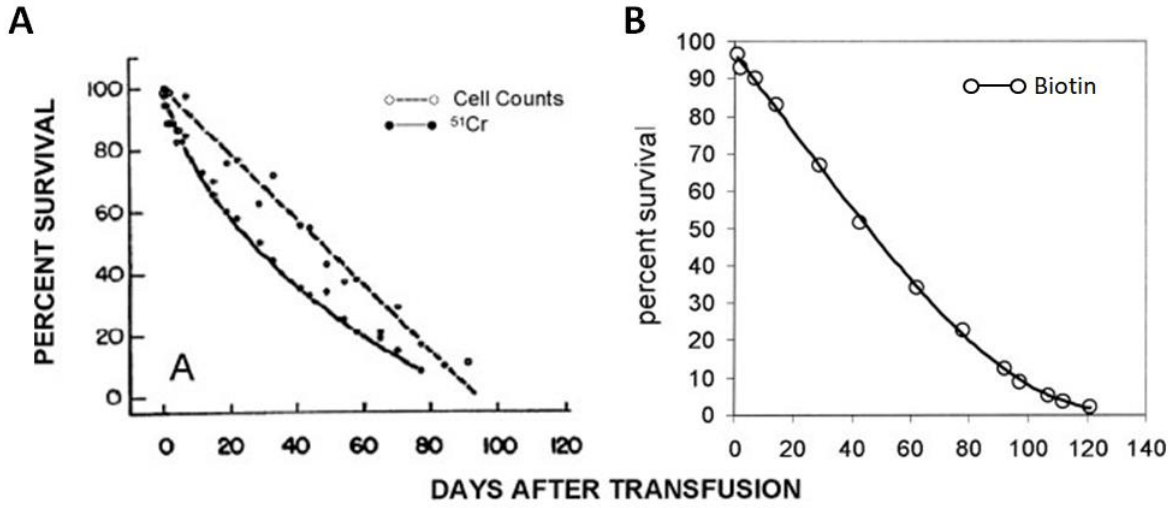

Figure 25 | Red blood cell lifespan measurements. (**A**) Percent of survival according to days after transfusion of RBCs labeled with ^{51}Cr and (**B**) RBCs labeled with biotin. Figure adapted from Franco (145).

Another non-invasive method for determining RBC lifespan consists in measuring exhaled carbon monoxide (CO). Indeed, metabolically the physiological endogenous production of CO is only due to the catabolism of heme with a stoichiometric ratio of 1 molecule of CO for 1 molecule of heme (152). Exhaled CO (eCO), which corresponds to the

alveolar (endogenous) plus the atmospheric CO, can easily be assessed. Endogenous CO is produced by the degradation of heme by heme oxygenase and is eliminated following the pulmonary route. By subtracting the atmospheric CO from the eCO (alveolar), and considering the rate of degraded heme which comes from hemoglobin (the other part originating from myoglobin) it is possible to deduce the production of CO. Studies have evaluated RBC lifespan by measuring endogenous CO and Hb concentration, with an excellent correlation compared to the reference methods (153,154).

2.4.2. Physiological changes associated with red blood cell aging

The physiological aging of RBCs, named senescence, is accompanied by numerous changes in their properties, both located on the membrane and in the cytoplasm. Multiple studies have shown a decrease in MCV associated with an increase in MCHC (155–157). This phenomenon was also observed during the conservation of RBCs in a suitable solution for transfusion purposes (158). This dehydration, leading to an increase in Hb concentration, induces an increase in intracellular viscosity which correlates with a decrease in the cell deformability. A physiological increase in the density of erythrocytes is therefore observed during aging, allowing their separation and analysis in laboratory by using density gradients.

Rheoscope measurements of RBCs separated according to their age by density gradient demonstrated that the decrease in deformability is a result of the increase in their MCHC (156). This loss of elasticity is also accompanied by an accumulation of intracellular calcium, responsible for the dehydration, thus contributing to the increased Hb concentration (159). Externalization of PS is also observed in RBCs stored in appropriate solution because of the reduced flippase activity also induced by an increase in intracellular calcium (160).

An increase in the glycation of hemoglobin, the covalent addition of a sugar molecule resulting in glycated hemoglobin, has also been correlated with RBCs aging (155). Glycated Hb includes several forms of glycation: HbA1a corresponds to the link of a fructose 1,6 diphosphate (HbA1a1) or a glucose 6 phosphate (HbA1a2); HbA1b corresponds to the link of a pyruvate and HbA1c, the most abundant glycated Hb found in RBCs, corresponds to the link of a glucose. Glycated Hb levels can be measured through high pressure liquid chromatography (HPLC). HbA1c value is greatly influenced by plasmatic sugar levels and represents the glycemic status of an individual over the last two to three months. Obviously, it is commonly measured in diabetics, as well as in those with impaired glucose tolerance, to

assess their glycemic status during this period (161). However, HbA1c is not only affected by blood sugar levels, and there are various factors influencing the quantity of HbA1c (162). HbA1c was shown to be identical to HbA, except that a glucose molecule reacts with the N-terminal valine of both β-globin chains to form an aldimine linkage which then undergoes an Amadori rearrangement to form a more stable product (163–165). HbA1c can be formed *in vitro* by incubating either whole blood or purified Hb in the presence of glucose at 37°C and *in vivo* studies of the slow kinetics of conversion of HbA to HbA1c further showed that the process is not mediated by a red cell enzyme (166,167). Thus, HbA1c is formed throughout the life span of the red cell as a post-traductional modification of HbA and can thus be used as a relative marker of RBC senescence. Of note, HbS can also be glycated in the same way.

As erythrocytes age, glucose utilization and ATP levels fall, leading to decreased membrane deformability. Lower potassium levels, higher sodium levels, and decreased membrane lipids are also seen in ATP-deficient, aging erythrocytes (133).

Finally, RBCs endure a huge number of cycles passing from oxygenated to deoxygenated states and are exposed to constant oxidative stress during their life. These elements contribute to an overall increase in oxidative stress which, associated with the decrease in the membrane flexibility, lead to the appearance of senescence signals (in particular PS exposure, band 3 protein clusterization and membrane vesiculation) which ultimately trigger the clearance of aged RBCs.

2.5. Physiological clearance of red blood cells

The physiological destruction of RBCs is dictated by numerous senescence signals, mainly deleterious changes in their plasma membrane. On the one hand, the loss of deformability induces a difficulty for the senescent RBCs to slip through the inter-endothelial slits located at the level of the red pulp of the spleen. It results in an increased time in which senescent PS-exposing RBCs can interact with resident macrophages and trigger phagocytosis (168–170). By itself, this stiffening alone would seem to be sufficient to induce a phagocytosis signal through activation of myosin II and local reorganization of the macrophage cytoskeleton (171).

On the other hand, other membrane signals, mainly induced by the oxidative stress, are elements triggering senescent RBCs recognition by phagocytes. For example, oxidation

and then clusterization of the band 3 protein induces its recognition by natural antibodies promoting complement activation via recognition by the C3 fragment (172,173). Exposure of PS to the outer membrane of a cell is a well-studied signal of phagocytosis, involved in apoptosis (115). All these membrane changes are recognizable signals by macrophages, not only within the spleen, that allow them to clear these senescent RBCs from circulation. This physiological process is called erythrophagocytosis.

The liver is also an organ involved in the clearance of senescent RBCs through Kupffer cells, as well as in iron recycling (174). It has been demonstrated in mice that monocytes having ingested stressed or senescent RBCs are recruited to the liver where they differentiate into iron-recycling macrophages (175).

2.6. Protective mechanisms against cell-free hemoglobin and heme

A damaged or aged RBC is recognized and phagocytosed by macrophages. In the absence of enough erythrophagocytosis capacity or after physical damage, lysis of RBCs can occur in the circulation, releasing cell-free Hb. Hb-toxicity is mostly determined by heme-iron oxidation because superoxide and peroxide are formed. Haptoglobin is the natural scavenger of cell-free Hb. The high affinity irreversible binding between the haptoglobin and the Hb αβ dimer occurs at a 1:1 stoichiometry ratio. By sequestering Hb, it prevents its oxidation and stabilize the globin-heme interaction (176,177).

In case of oxidation, Hb releases cell-free heme, which is lipophilic and can transfer to cell membrane components disturbing cell surface receptors and lipids (178). Hemopexin is the natural scavenger of cell-free heme. Like Hb-haptoglobin, heme-hemopexin binding is irreversible, blocking its oxidative reactivity. Several proteins with lower affinity for heme exist, such as albumin and alpha-1-microglobulin.

Hb-haptoglobin and heme-hemopexin complexes are recognized and phagocytosed by macrophages through interaction with the specific membrane receptors CD163 and CD91, respectively (179,180). These macrophages can then eliminate degrade heme into CO and biliverdin through heme oxygenase 1 (HO-1). HO-1 is expressed in many cell types and is highly inducible. Biliverdin can then be converted in bilirubin by the biliverdin reductase. Heme degradation releases iron, which can be stored within cells with ferritin or exported through the ferroportin in order to be taken by transferrin and recycled (Figure 26) (181).

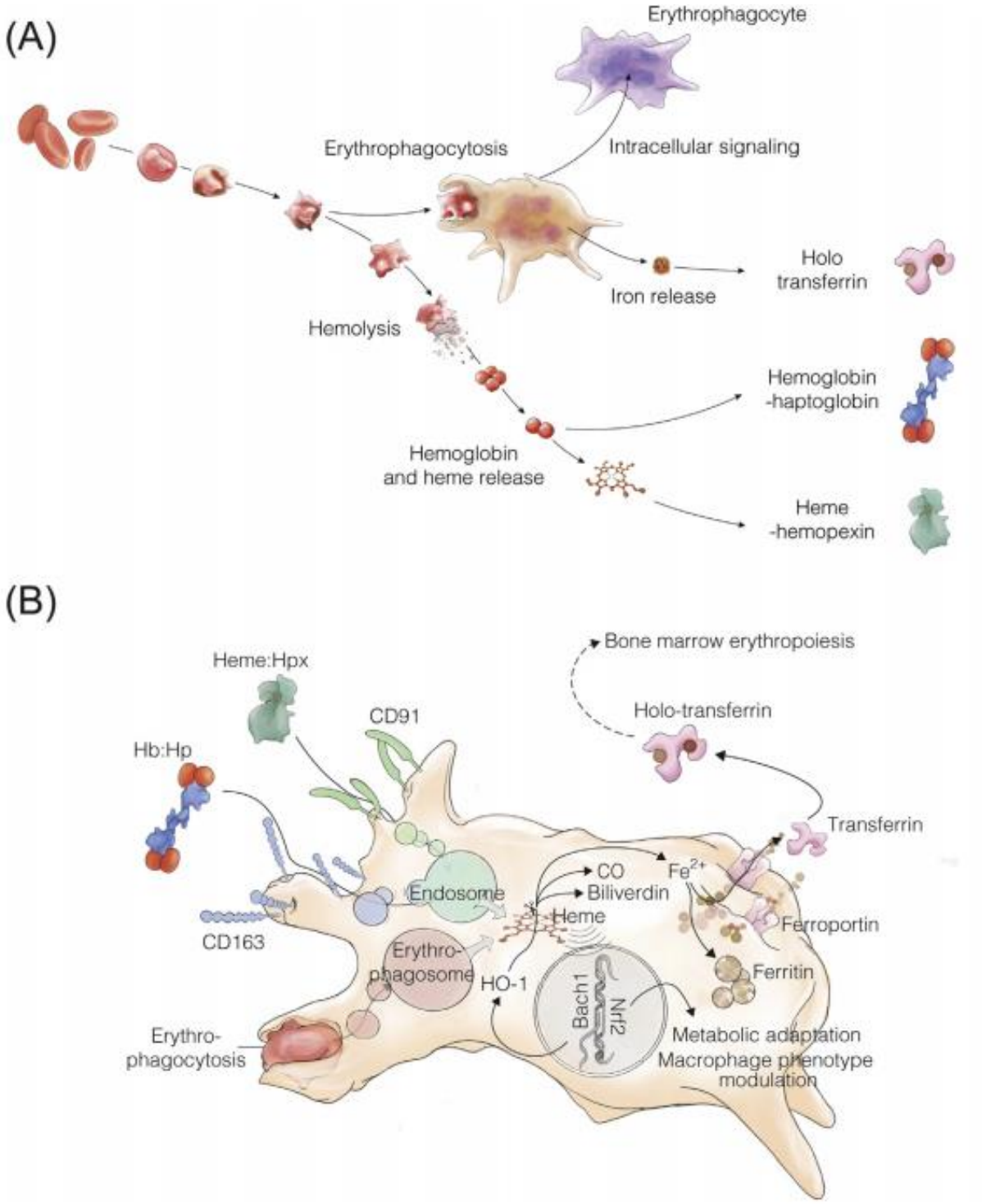

Figure 26 | Red blood cell damage and protective pathways. (**A**) Hb and heme can be bound and detoxified by the plasma scavenger proteins haptoglobin (Hp) and hemopexin (Hpx), while iron released by the macrophage is bound to transferrin. (**B**) Specific scavenger receptors CD163 and CD91 mediate endocytosis of Hb–Hp and heme–Hpx complexes, respectively. Phagocytosed RBCs are degraded by the macrophage. Finally, heme is metabolized to biliverdin, carbon monoxide, and iron through heme-oxygenase 1 (HO-1). Iron can be stored in a complex with ferritin or exported from macrophages by the iron-transporter ferroportin. In the extracellular space, iron is bound by transferrin and transported to hematopoietic tissues to support erythropoiesis. Nerf2 and Bach1 are inducers of HO-1 synthesis. Figure from Buehler, *et al.* (181).

2.7. Classical red blood cell laboratory evaluation parameters

From a blood sample, the total Hb mass is evaluated by measuring the hematocrit (Ht - expressed as a percentage), the ratio of the volume occupied by RBCs to the total volume of blood, and by the blood hemoglobin concentration (Hb - expressed in g/dL). Ht and Hb are both dictated by the absolute number of cells (RBC - expressed in millions/µL) and by their volume. The latter, called mean corpuscular volume (MCV - expressed in fL), also allows calculating the mean corpuscular hemoglobin concentration (MCHC - expressed in g/100mL). Finally, the ratio of total hemoglobin to the number of red blood cells gives the mean corpuscular hemoglobin content (MCH - expressed in pg/cell). As each cell taken individually does not have the exact same volume, red cell distribution width (RDW - expressed as a percentage) represents this variability. Finally, the reticulocyte count (retic) - expressed either as a percentage of RBCs or as a number per µL) gives information about the stimulation level of the erythropoiesis. Routinely, these data are measured and calculated by automatic devices during the complete blood count (CBC) (121).

While informative on the general state of RBC population, these results represent an average observation. They neither consider the qualitative aspects, nor the state of each individual cell. A method providing information about the distribution would be of interest for a complete and reliable analysis of cell dynamics, particularly in the context of a clinical monitoring.

Chapter 3 – Pathophysiology of sickle cell disease

1. Alterations of erythrocyte properties and involvement in sickle cell disease pathophysiology

HbS polymerization is the main first event in the disease. It alters the physical and biological properties of RBCs, triggering phenomenon inducing a large variety of symptoms, syndromes and clinical manifestations. The hallmarks of SCD are chronic hemolytic anemia and painful vaso-occlusive crises (VOC). HbS polymerization under hypoxic condition induces a variety of impairments, including RBC sickling, reduced hydration, decreased deformability, hemolysis and abnormal interactions with other blood cells. On the one hand, sickling results in impaired blood rheology. On the other hand, hemolysis, through the release of toxic intracellular contents, induces endothelial dysfunction. These pathobiological processes contribute to inflammation in patients, exacerbating VOC frequency or severity (Figure 27). Ultimately, the overall decrease in oxygen transport, the resulting relative hypoxia, and the vascular impairments induce extensive organ damage.

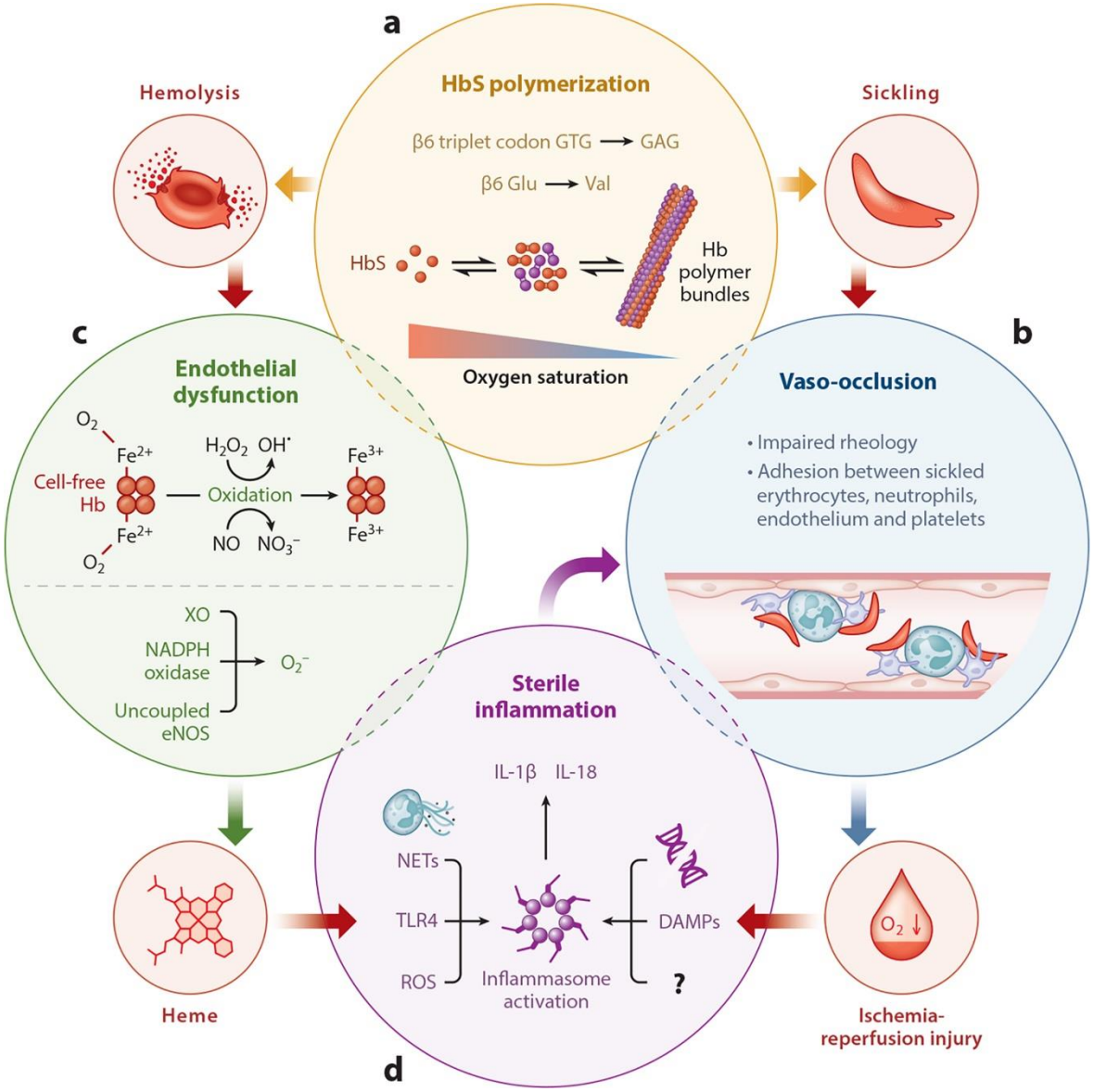

Figure 27 | Molecular pathophysiology of sickle cell disease. (**a**) Following deoxygenation, HbS molecules polymerize resulting in erythrocyte sickling. (**b**) Sickling leads to impaired rheology of the blood and aggregation of sickle erythrocytes with neutrophils, platelets, and endothelial cells to promote vaso-occlusion. HbS polymerization also promotes lysis of erythrocytes, which releases cell-free Hb into the blood circulation. (**c**) Oxygenated Hb (Fe^{2+}) promotes endothelial dysfunction by depleting endothelial nitric oxide (NO) and by forming reactive oxygen species (ROS) and metHb (Fe^{3+}). (**d**) ischemia-reperfusion injury, ROS generation, Toll-like receptor 4 (TLR4) activation by cell-free heme and neutrophil extracellular trap (NET) can contribute to sterile inflammation by the release of interleukins IL-1β and IL-18, further promoting adhesion and vaso-occlusion. Figure from Sundd, *et al*. (182).
DAMP: damage-associated molecular pattern.

1.1. Altered erythrocyte membrane biology

1.1.1. Increased dehydration and reduced deformability

A characteristic of SCD is the cellular heterogeneity in term of volume and Hb concentration, with the presence of cells with increased MCHC because of dehydration (183,184). It is a multimodal process, which takes place throughout the life span of sickle cells. The reduced cell hydration is involved in SCD pathophysiology. It induces an increased intracellular HbS concentration, promoting its polymerization. The opening of the K-Cl co-transporters leads to a loss of K^+ and Cl^- ions as well as water, accentuating the dehydration even more. Third, reduced hydration also leads to a lowered deformability, thus promoting vaso-occlusion.

A biomarker of the cellular dehydration is the percentage of dense RBCs (DRBCs), which are cells characterized by a high MCHC. They are defined as red cells having a density >1.11 mg/mL (185,186). The density curve, measured with the phthalate density method, accesses the pathological dehydration process (due to channel activation) and provides the percentage of the subpopulation of DRBC which is associated with organ damages (187).

DRBCs are highly rigid and comprise a lot of irreversible sickle cells. Both mature RBCs and reticulocytes can be found in the high-density fraction of SCD patients' blood. They play an important role in SCD pathophysiology because of their hemorheological properties, including a low deformability level, and their hemolytic propensity (188). They can also form stickier aggregates able to further impair microvascular blood flow (189). PS exposure related to an increased intracellular Ca^{2+} can be observed in DRBCs. The percentage of DRBCs is strongly associated with hemolytic markers, such as reticulocyte count, bilirubin or lactate dehydrogenase (LDH) and with chronic vasculopathy manifestations including renal dysfunction, skin ulcer or priapism (190). DRBCs do not exist in normal RBC populations.

The biological process leading to the formation of DRBCs is still unclear. Deoxygenation induces membrane permeability, and, mainly because of oxidation, several ion channels become dysfunctional. The loss of K^+ and dehydration of sickle cells are mediated by three ion transport pathways: the K-Cl cotransports (KCC), the Ca-activated K channel (Gardos/KCNN4) and P_{sickle}. The latter, only present in sickle erythrocytes, is activated by deoxygenation and is defined as a non-selective cation conductance, most likely mediated by PIEZO1 (191,192).

PIEZO1, a mechanosensitive channel, opens upon direct physical deformations of the lipid bilayer, such as increased membrane tension (193). The K-Cl co-transport activity is increased by oxidation and is favored by acidification of plasma (194). Erythrocyte membrane permeability leads to a loss of K^+ and an increase in Na^+ ions. This increased permeability also results in an important increase in Ca^{2+} which will activate the Gardos channel, also promoting loss of K^+ and water (195).

The pathophysiology of SC disease has been attributed to erythrocyte dehydration, associated with an increase in intracellular HbS concentration to critical levels. The leak of cations and water in SC erythrocytes is due to an overactivity of KCC channels (196). This activity has been shown to correlate with disease severity in those individuals (197). HbC is known to interact with KCC molecules present in the red cell membrane and with the cytoplasmic region of band 3 (51,198). These interactions probably result from both protein conformation and electrostatic charge, because HbC is positively charged. While the inner plasma membrane is negatively charged. A similar process might be involved in sickle erythrocyte dehydration as HbS is also positively charged (less than HbC but more than HbA), and has been shown to interact with the membrane (199,200).

Sickle red cells are less deformable as compared to RBCs from normal individuals, even when fully oxygenated (201,202). Sickle RBC deformability declines hastily with deoxygenation and polymerization (203). The presence of dehydrated irreversible sickle cells impacts directly on the mean deformability of the whole RBC suspension (204). Therefore, they do not easily flow through the microcirculation, promoting vaso-occlusive episodes in affected patients. Newborns usually have almost normal RBC deformability because of the protective effect of HbF while deformability decreases in older patients (205). Their RBCs also usually present a decreased surface to volume ratio, and an increased cytosolic viscosity, mainly because of HbS polymerization which triggers cell dehydration and auto-oxidation, the latter leading to the membrane cytoskeleton disorganization.

Blood rheology is influenced by hematocrit, plasma viscosity, and erythrocyte deformability. The increased plasma viscosity contributes to impaired flow of blood through microcirculation in tissues, where the oxygen is released from RBCs (206). Because of low hematocrit and the inability of sickle shaped RBCs to aggregate, aggregability is usually found lower in SCD patients (207). However, once formed, sickle RBC aggregates are 2- to 3-fold

more robust than healthy RBC aggregates, a phenomenon that might be due to the enhanced oxidative stress (208).

In addition, when RBCs lose their deformability, they become more fragile and prone to hemolysis, which is the root cause of chronic hemolytic anemia in SCD (189).

1.1.2. Phosphatidylserine exposure

In SCD, the lipid bilayer and erythrocyte membrane proteins have been shown to be abnormal as compared to normal RBCs from healthy volunteers. PS is exposed on the surface of subpopulations of sickle cell erythrocytes and was found predominantly among the densest and the very light sickle cells. PS exposure can occur at different stages in the life of the sickle RBC and it correlates with the loss of flippase activity. The additional requirement of scramblase activation may occur during transient increases in cytosolic Ca^{2+} (209). Erythrocytes circulating and exhibiting PS has a role in many pathophysiological events, including increased hemolysis, endothelial activation and interaction between erythrocytes, white blood cells and platelets (210–212).

1.1.3. Microparticles release

HbS have a high auto-oxidation potential. It triggers the generation of hemichromes, which in turn affect membrane proteins with structural functions, especially the band 3 protein. The displacement of ankyrin from band 3 leads to release of the spectrin/actin cytoskeleton from the membrane, which can promote unwanted membrane vesiculation (213). This alteration leads to the release of erythrocyte microparticles (MPs). They are submicron membrane vesicles that possess cell surface markers, cytoplasmic proteins and microRNAs derived from their cell of origin (214).

The increased level of MPs in SCD is linked to intravascular hemolysis and PS exposure of RBCs (215). The high amount of externalized PS at the surface of most of the MPs is responsible for their pro-coagulant property. It has also been demonstrated that *ex-vivo* generated sickle RBC-MPs, when infused in sickle cell mice, promoted kidney vaso-occlusions. RBCs derived MPs might also deliver toxic heme to endothelial cells, increasing the production of ROS, the expression of endothelial cell adhesion molecules, and promoting their apoptosis, participating in the endothelial dysfunction (216,217).

1.2. Hemolysis

Hemolysis is a key feature in SCD. It is defined as abnormal shortening of RBC survival, leading to the anemia. There are two types of hemolysis. Intravascular hemolysis is the destruction of RBCs in the circulation with the release of cell contents into the plasma, while extravascular hemolysis corresponds to the removal and destruction of RBCs with membrane alterations by the macrophages of the spleen and the liver and by circulating monocytes (218). The consequences of hemolysis include the immediate effect of RBC loss, such as anemia and expansion of erythropoiesis with increased reticulocytosis. Hemolysis intensity is usually evaluated via the increase in serum lactate dehydrogenase (LDH), bilirubin and aspartate aminotransferase (ASAT) levels. LDH, abundant in RBCs is released during hemolysis, while bilirubin is a product of Hb breakdown.

Extravascular hemolysis is exacerbated in SCD. Sickle red cells, with PS externalization and band 3 clustering associated with natural antibodies at their membrane, are easily recognized as abnormal, thus promoting RBC phagocytosis in the spleen, the liver and the circulation (219,220). Abnormal RBCs can then be trapped in the hepatic and splenic sinuses, contributing to vaso-occlusion. In addition, the reduced RBC deformability and the increased adherence properties result in sickle RBCs being prone to be trapped within the spleen. Splenic resident macrophages express high level of CD163, the receptor of hemoglobin-haptoglobin complexes and the HO-1 enzyme, which degrades heme into CO and biliverdin. The high number of macrophages in the spleen is responsible for the enhanced RBC clearance in SCD (206), leading to frequent functional hyposplenism and splenic sequestration (221). The presence of stressed or damaged RBCs has been shown to induce a rapid recruitment of monocytes in the liver, giving rise to transient macrophages equipped to RBC clearance (175). Then it has been shown that a subset of patrolling monocytes with high phagocytic activity, expressing high level of HO-1 and present exclusively in SCD patients, can clear hemolysis-damaged endothelial cells (222). Moreover, the same team recently showed that these patrolling monocytes engulf sickle RBCs and not normal RBCs adhered to the vascular endothelium leading to inhibition of vaso-occlusion in SCD (223). The CD47 interacts with the macrophage self-recognition receptor signal regulatory protein alpha (SIRPα), which protects from phagocytosis. Thrombospondin (TSP) is a ligand of CD47 which is highly expressed on

RBC (224,225). Oxidative stress can induce CD47 conformational change switch from a protective signal to a pro-phagocytosis signal (226).

Free hemoglobin and heme, released in the plasma in high amount, cannot be fully neutralized by their natural scavengers, haptoglobin and hemopexin, respectively, causing their depletion and leading to several damages (227,228). Hemolysis products are considered erythrocyte DAMPs that promote and propagate sterile inflammation and oxidative stress, further impairing the redox balance (229).

The accumulation of Hb in the plasma affects the bioavailability of nitric oxide (NO), resulting in its consumption (230). NO plays a major role in vascular homeostasis by triggering vasodilatation (231). Moreover, hemolysis leads to the release of the arginase contained in erythrocytes into the plasma. Free arginase hydrolyzes arginine, which is the precursor to NO, thereby exacerbating the decrease in its bioavailability (232). The decrease in NO bioavailability could also be responsible for the enhanced platelet activation observed in SCD patients (233). Heme, hemoglobin, and red cell ADP and ATP also activate platelets resulting in thrombospondin-1 (TSP) and platelet derived growth factor (PDGF) release, leading to promotion of inflammation and vasculopathy (234). Furthermore, plasma heme can activate neutrophils and promote the release of neutrophil extracellular trap (NET) in SCD (235).

Hb and heme are also major sources of oxidative stress. The resulting excessive production of ROS leads to endothelial damage, through peroxidation of the lipid membrane, potentially leading to cellular apoptosis (236). Heme is released following Hb oxidation, and is an agonist of TLR4, a membrane receptor expressed on endothelial cells and macrophages. Heme-induced TLR4 activation contributes to endothelial recruitment of leukocytes by increasing the expression of P-selectin (237). Its activation also leads to the production of inflammatory cytokines such as IL-1β, IL-6 or tumor necrosis factor (TNF) via NF-κB signaling pathway, increasing cellular adhesion (227). Heme has also been shown to activate the complement alternative pathway triggering deposition of C3 on the surface of RBCs (238). In line with this, endothelial cells exposure with heme also results in deposition of C3 on the surface of the cells contributing to endothelial damage (239,240).

The process of intravascular hemolysis directly damages blood vessels, and the resulting anemia exerts additional stress on the cardiovascular system. Hemolysis contributes to a pro-inflammatory and pro-coagulant state in SCD, characterized by activated leukocytes, platelets, endothelial cells, NO depletion, and generation of ROS, all contributing to an

increased red cells adhesiveness leading to vaso-occlusion (Figure 28). Hemolysis is also strongly associated with various organ damage (232,241–243).

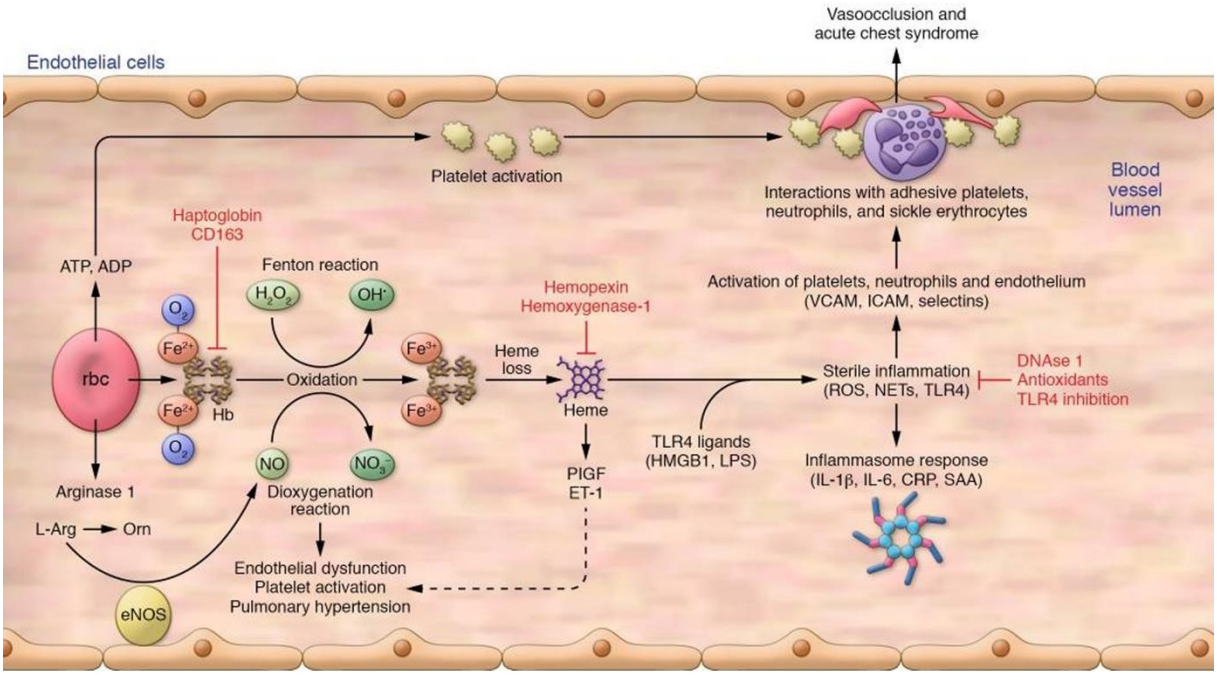

Figure 28 | Summary of intravascular hemolysis process in sickle cell disease. Hemolysis results in RBC content release in the plasma. Free Hb drives Fenton reactions to produce oxidants and scavenges NO while arginase 1 can deplete plasma L-arginine (L-Arg), the required substrate for NO production by eNOS. Oxidized Hb releases free heme, which activates TLR4, leading to sterile inflammation with production of ROS, neutrophil extracellular traps (NETs), and downstream activation of the inflammasome. Intravascular hemolysis also releases adenine nucleotides, including ATP and ADP, which further contribute to platelet activation. Proteins on the surface of the activated endothelium (P-selectin, E-selectin, VCAM1, ICAM1) interact with adhesive platelets, neutrophils, and sickle erythrocytes, promoting vaso-occlusion. Figure from Kato, *et al.* (227).

1.3. Vasculopathy in sickle cell disease

Amalgams are often made, and it is important to point out that HbS polymerization does not necessarily mean sickling. RBC sickling does not necessarily mean vaso-occlusion. Vascular damage does not necessarily mean vaso-occlusion.

Vaso-occlusion, or blood vessel occlusion, is the predominant pathophysiology responsible for acute painful VOC in SCD patients and the requirement for emergency medical care (244). Hoover, in 1979, was the first to demonstrate the increased adhesiveness of sickle RBCs to the vascular endothelium in SCD (245), a phenomenon confirmed a few years later by other studies (242,246,247). While not completely understood, it is now clear that VOC in SCD

is a multi-parameter phenomenon. It is the result of interplay among impaired blood rheology, increased adhesiveness of erythrocytes with inflammatory cells and vascular endothelium, and hemostatic activation (248). At similar hematocrit, blood viscosity of SCD patients is above blood viscosity of healthy individuals. Poorly deformable sickle erythrocytes combined with increased plasma viscosity, contribute to impaired blood flow through capillaries and postcapillary venules of tissues with high oxygen demand. Reduced bloodstream eventually leads to RBCs becoming mechanically sequestered in the microcirculation, which promotes vaso-occlusion. Indeed, HbS polymerization is not instantaneous, allowing most of the RBCs to escape the microvasculature into the larger venules before sickling occurs (249). If the regional blood flow decreases, the transit time of the RBCs through the microvasculature is prolonged, and sickling occurs while the RBCs are still in the capillaries. Thus, vaso-occlusion will depend on the delay time between deoxygenation and polymerization of HbS and the blood flow rate in the microvasculature. The latter is influenced by the increased RBCs adhesiveness observed in SCD.

Sickling-dependent damage of erythrocyte membranes promotes exposure of adhesion molecules and binding motifs not normally expressed on erythrocytes, including PS, Lutheran/basal cell adhesion molecule-1/ (Lu/BCAM), α4β1 integrin, integrin-associated protein (IAP also known as CD47), and intercellular-adhesion-molecule-4 (ICAM-4) (250). These adhesion molecules interact with exposed sub-endothelial laminin and fibronectin on the surface of endothelial cells lining the vasculature (251,252). Thus, sickle red cells not only adhere to the endothelium but also interact with circulating leukocytes and platelets. Moreover, because of chronic anemia, high amounts of reticulocytes, expressing adhesion molecules such as α4β1 integrin (VLA-4) and CD36, are released.

Activated platelets release TSP that mediates adhesion of sickle red cells to endothelial cells via both CD47 and CD36 cell surface molecule present on both erythroid and endothelial cells (253,254).

Endothelial dysfunction and inflammation may also contribute to upregulation of P-selectin, E-selectin, VCAM-1 and ICAM-1 on endothelial cells (248). The inflammatory state observed in SCD may also promote activation of neutrophils, monocytes, and platelets, leading to their elevated levels. They contribute to adhesion and endothelium activation and correlate with disease severity (255–257).

2. Sickle cell disease pathophysiology

2.1. Severity of the disease

There are very wide variations in clinical severity in individuals with SCD. This is partly explained by genetic factors, starting with the genotype of the *HBB* gene itself. HbAS heterozygous individuals (β/β^S), are said to be "healthy" carriers or “sickle cell trait” and are exceptionally symptomatic. The following genotypes are responsible for SCD: homozygous HbS (β^S/β^S) or composite heterozygous, i.e. the association of a β^S allele with a β^0-thalassemia (β^S/β^0), or a β^+-thalassemia allele (β^S/β^+), consisting in β-globin deletion or synthesis defect, respectively, or with a β^C allele (β^S/β^C), corresponding to the substitution of glutamic acid in position 6 by a lysine (Figure 29).

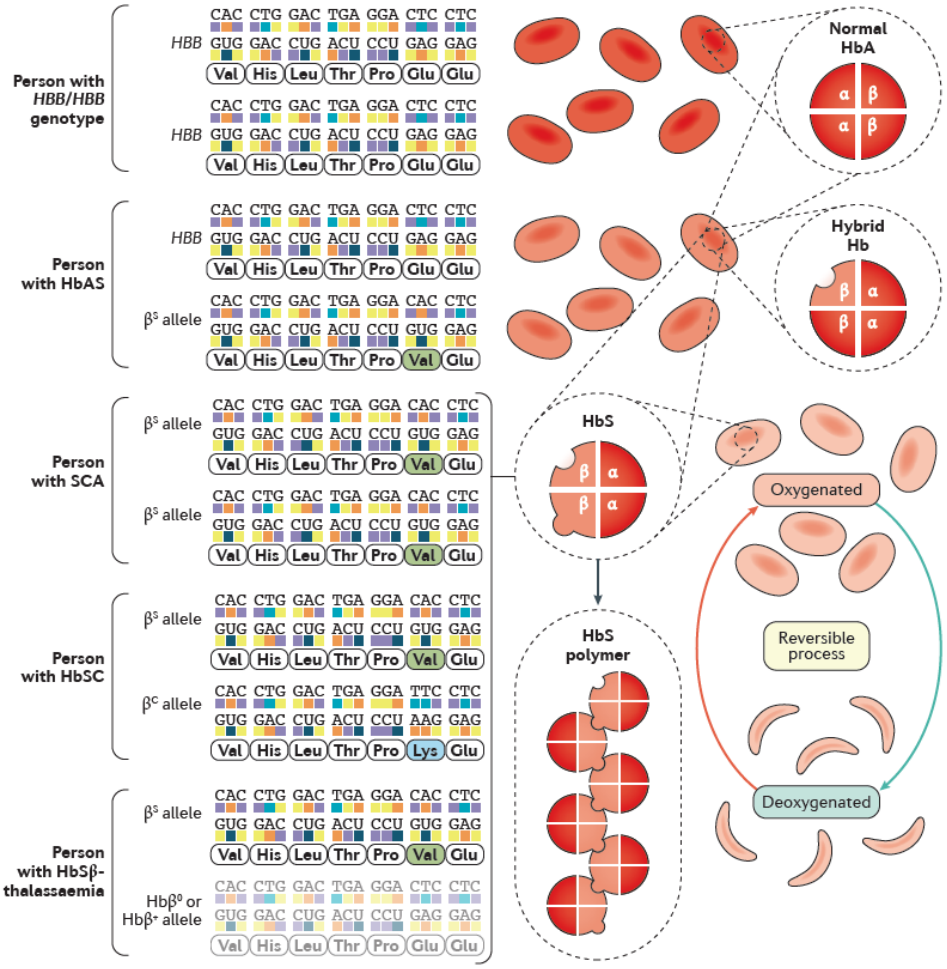

Figure 29 | Genetic alterations in the *HBB* gene resulting in the polymerization of abnormal hemoglobin S and sickle cell disease. Figure from Kato, *et al.* (20).

Much more uncommon, composite heterozygosity associating the β^S allele with β^D, β^E, HbOArab and Hb Lepore alleles, also results in a severe form of SCD (20).

Other genetic factors have also been proposed as modulator of SCD clinical severity, mainly those affecting HbF synthesis, but also transmission of α-thal. Hereditary persistence of fetal hemoglobin (HPFH) with an HbF percentage corresponding to at least 20% of the total Hb is associated with a relatively mild form of the disease despite SCD genotype (258). An associated α-thal can reduce HbS intracellular concentration and therefore its polymerization. In some studies, it has been shown that haplotypes, the simultaneous transmission of a set of genetic polymorphisms, are associated with attenuated severities of the disease (i.e. Senegal). Although often geographically restricted, these haplotypes are mostly related to different levels of HbF expression, including the following, named according to their region of location: Bantu, Cameroon, Benin, Arab Indian and Senegal. (20,79,259).

Environmental factors have also been studied as modulator of the clinical severity of the disease, including the living environment (altitude, climate, air quality), socio-economic status, nutrition or access to healthcare (260). For example, in the United Kingdom, a climate with both high wind and low relative humidity was associated with an increase in the frequency of hospital admissions. These two factors can cause rapid changes in skin temperature associated with more frequent manifestations of the disease (261). A large study conducted in France, including all public hospitals of Paris conurbation for 8 years (approximately 4500 patients) showed an influence of temperature drop, higher wind speed and low CO air concentrations where associated with an increased risk of SCD-related hospitalizations (262). Despite their probable implication in the disease, such studies remain infrequent.

2.2. Clinical manifestations

2.2.1 Chronic hemolytic anemia

Anemia consists in the decrease in Hb level in the blood. Individuals suffer from excessive tiredness and a feeling of weakness. In SCD, anemia is hemolytic, meaning it is caused by a pathological and exacerbated destruction of RBCs. In patients, it is most often associated with a reticulocytosis, an increased production of reticulocytes, which can represent up to 20% of RBCs in the most severe patients. Besides the less efficient transport of oxygen in the body, the effects of hemolysis are numerous, as shown previously.

2.2.2 Vaso-occlusive crises and acute pain episodes

VOCs are caused by the obstruction of the blood capillaries and are manifested by sharp and brutal pain, which can occur in all parts of the body, most affected being the back, abdomen, extremities and thorax. These painful episodes, which usually last three to ten days, are difficult to predict. Individuals with a high VOC frequency are characterized by a higher hematocrit, and therefore an increased blood viscosity, than others. They are also at greater risk of developing osteonecrosis. Moreover, the associated transmission of α-thal promotes a higher hematocrit in these individuals (263).

Among these crises, acute chest syndrome (ACS) (a VOC taking place in the pulmonary vascularization) is manifested by fever, discomfort or difficulty in breathing (dyspnea), cough, and chest pain. Lungs radiograph shows pulmonary infiltrates. ACS is a serious complication that must be treated urgently. In children it is often secondary to or associated with pulmonary infection. ACS is the second most common reason for hospitalization and a cause of death in individuals with SCD. It is often related and precedes an acute pain event (264). The severity increases with age. In adults, over 10% of cases are fatal or complicated by following neurological events or total organ failure (265,266).

The complex mechanisms and causes of VOC in SCD have been and are still widely studied.

2.2.3. Organ damage

As individuals with SCD age, acute and chronic complications promote organ dysfunction, contributing to mortality (Figure 30). Improvements in general medical care, early diagnosis and comprehensive treatments led to better management of chronic complications in high-income country (267). However, life expectancy is still reduced by around 30 years and most of these advances have not reached low-income countries (268).

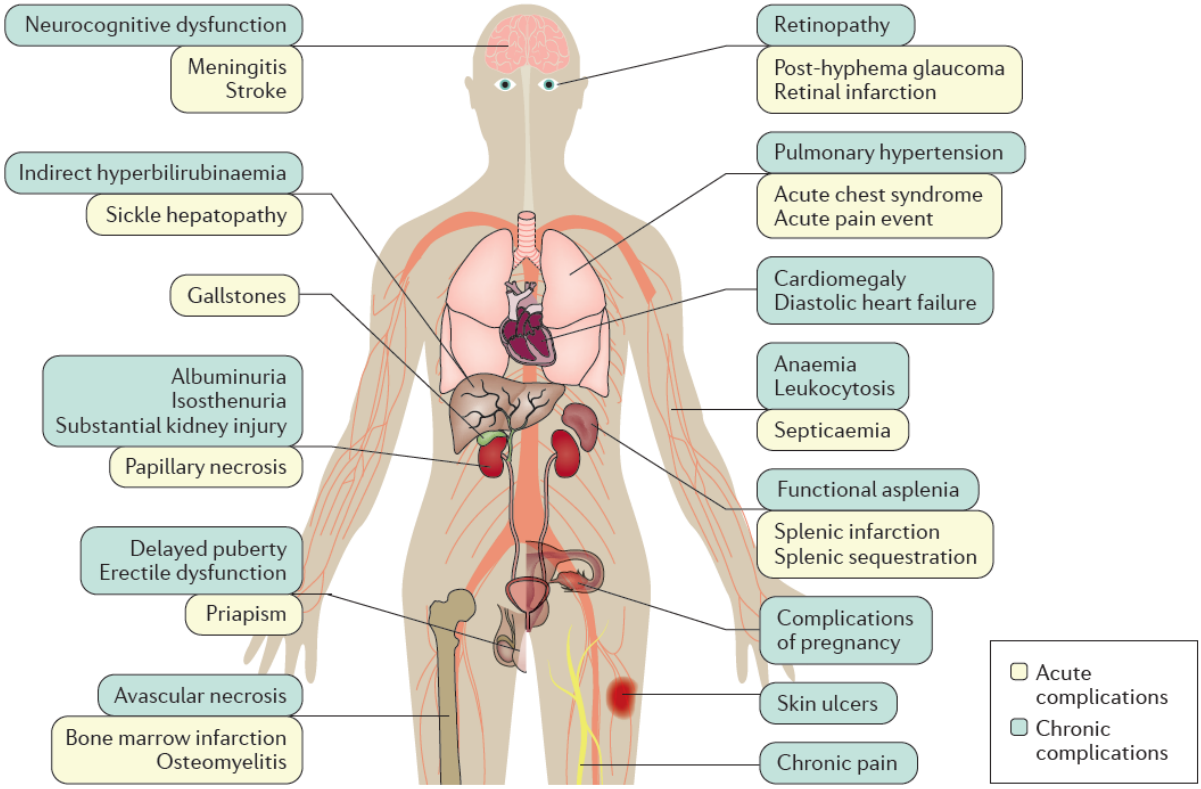

Figure 30 | Sickle cell disease clinical complications can affect a wide range of organs through the body. Chronic complications require long term management while acute complications need rapid medical care. Figure from Kato, *et al*. (20).

The most common complications of SCD are the acute clinical events that punctuate periods of reasonable health. However, increased life expectancy, brought to light many complications that result from damage to a wide range of organs (15). Some SCD complications are associated with clinical sub-phenotypes, which are not mutually exclusive and contribute to the high variability among individuals with SCD (20). The vaso-occlusive sub-phenotype presents a higher risk of frequent VOC, ACS, osteonecrosis or retinopathy. Patients have a higher hematocrit, responsible for a higher blood viscosity (263). The hemolysis and vasculopathy sub-phenotype is characterized by a lower hematocrit and a higher hemolysis

level. Patients are more at risk of ischemic stroke, pulmonary hypertension, leg ulcer, priapism and nephropathy (232). Strokes are severe acute complications in individuals with SCD, mainly in children. Symptoms often appear and disappear suddenly, and risk of recurrence is high. Children may be unharmed, but in many cases the stroke causes brain damage, leaving motor and/or intellectual sequelae. Hemolysis has been proposed as a cause of or contributing to several complications in SCD, including pulmonary hypertension, priapism, leg ulcers and stroke (241).

Chapter 4 – Treating sickle cell disease: from drugs to gene therapy

1. Pharmacological treatments for sickle cell disease

1.1. Approved drugs

Since Hydroxyurea (HU), the first drug approved for the treatment of SCD in 1998, three additional compounds have now been licensed by the US Food and Drug Administration (FDA) (Table 1).

1.1.1. Hydroxyurea

Some chemotherapeutic or cytotoxic agents that impose regenerative hematopoietic stress increase HbF production in erythrocytes. One of the first of these chemical agents used to reactivate HbF was 5-azacytidine, a DNA methyl transferase (DNMT) inhibitor (269,270). However, its toxicity and carcinogenicity quickly led to its abandonment as a potent treatment for SCD.

Hydroxyurea, or hydroxycarbamide, a ribonucleotide reductase inhibitor, was then used. HU acts mainly by increasing HbF synthesis (271), an increase associated with extended RBC survival (272,273). A decrease in the pathological percentage of DRBCs under HU has also been shown, associated with a reduced complement activation (186,190,240).

HU has been shown to prevent VOC and ACS (274,275), to improve splenic function regeneration (276), cerebrovascular involvement in children (277,278), or to treat early adult glomerular disease (279), reflecting its broad clinical effects. Importantly HU decreases the rate of mortality, mainly, but not exclusively, in an HbF dependent way (275,280).

Several mechanisms of action of HU have been described: a decrease in Lu/BCAM phosphorylation (281), inhibition of α4β1–Lu/BCAM interaction via phosphodiesterase 4A (282), inhibition of leukocyte recruitment via phosphodiesterase E9 (283), or inhibition of ion

Table 1 | Approved drugs for pharmacological treatment of SCD. Modified from Ballas (284).

Compound	Company	Structure	Mechanism of Action	Indication
Hydroxyurea	Numerous	Hydroxycarbamide $CH_4N_2O_2$ 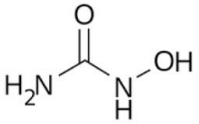	An antineoplastic agent that inhibits DNA synthesis through the inhibition of ribonucleotide diphosphate reductase. HbF Induction, reduces inflammation and hemolysis	Sickle cell anemia; Myeloproliferative disorders, certain cancers
L-glutamine (Endari)	Emmaus Medical Inc.	2-Amino-4-carbamoylbutanoic acid 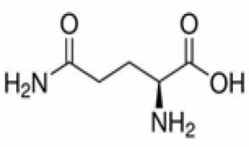	Not well known. It may improve the NAD redox potential in sickle RBCs through increasing the availability of reduced glutathione.	Reduction of the acute complications of sickle cell disease in adult and pediatric patients 5 years of age and older
Crizanlizumab-tmca	Novartis	Monoclonal antibody	Anti-P-selectin	Reduces the frequency of VOCs in adults and pediatric patients aged 16 years and older
Voxelotor (Oxbryta, GBT440)	Global Blood Therapeutics Inc.	Benzaldehyde, 2-hydroxy-6-((2-(1-(1-methylethyl)-1H-pyrazol-5-yl)-3-pyridinyl)methoxy) 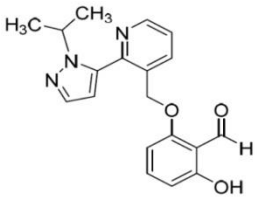	HbS Polymerization inhibitor	Treatment of sickle cell disease in adults and pediatric patients 12 years of age and older

leakage preventing cell dehydration (186,285). Clinical effects of HU indicate a complex mechanism of action involving different pathways. The main biological response parameter is the increase in HbF which, through its anti-polymerizing action, constitutes a major therapeutic target. In addition, because of its cytotoxicity, HU induces a reduced number of

total leukocytes. Then HU has a protective effect on endothelial cells (286). These two mechanisms of action contribute in the reduced incidence of VOC observed in patients under HU. While it increases hemoglobin, it has been demonstrated that the improvement in RBC deformability and the decrease of RBC aggregates induced by HU limit the consequences on blood viscosity (26137960).

Dosing strategies and pharmacokinetic profiles of HU are highly variable among individuals. Recently, it has been proposed to use a personalized dose of HU for children with SCD, with better improvements (287,288).

However, HU does not improve HbF synthesis in all patients and its expression is generally heterocellular when increased (289).

1.1.2. L-glutamine

L-glutamine is the most abundant amino acid in human blood (290). It is converted to L-glutamate, the glutathione precursor, by the glutaminase enzyme. Glutamate is a precursor used for the synthesis of the antioxidant GSH.

L-glutamine was the second FDA approved drug for treatment of SCD in 2017. *In vitro* studies have shown that depletion of glutamine contributed to RBC membrane damages and adhesion in SCD (291). L-glutamine appears to increase NADH and NAD redox potential. A phase 3 clinical trial showed that it decreases VOC frequency by around 25% while also reducing the frequency of ACS and hospitalization (292). However, this study did not show any changes in biologic parameters such as anemia and the mechanism whereby L-glutamine exerts its effects remains uncharacterized. Of note, this drug is still not approved by the European Medicines Agency.

1.1.3. Voxelotor

Voxelotor (GBT440) was licensed in 2019 by the FDA. It targets HbS polymerization. The molecule binds specifically to the N-terminus of the alpha subunit of HbS and inhibits sickling *in vivo* by preferential binding to the high-oxygen affinity R quaternary conformation, thereby shifting the T-R quaternary conformational equilibrium toward R state, which cannot enter the sickle fiber (293). Preclinical studies have shown that voxelotor increases the affinity between Hb and oxygen, decreases sickling of HbS, improves sickled RBCs deformability and

decreases blood viscosity (294). It also reduces hemolysis and improves anemia in most patients with SCD (295).

1.1.4. Crizanlizumab

Crizanlizumab, also licensed in 2019 by the FDA, targets vaso-occlusion. It is a humanized monoclonal antibody directed against P-selectin, a mediator of leukocyte, platelets and endothelial cells adhesion. Effective in reducing VOC frequency, it did not affect biologic parameters (296,297).

1.2. Other molecules currently studied

Several candidates are being explored either to inhibit HbS polymerization or to prevent symptoms or organ damages in SCD.

Small molecules have been proposed to re-activate γ-globin expression. They include epigenetic drugs such as histone deacetylase (HDAC), DNMT or lysine-specific histone demethylase 1 inhibitors, with clinical trials ongoing. Other HbF inducers are also under study, including pomalidomide, initially used to treat multiple myeloma, and metformin, the most widely used medication for diabetes orally taken. These two drugs have been shown to reactivate HbF synthesis up to 30% in primary HSCs *ex vivo* culture (298).

Targeting vaso-occlusion is also a therapeutic option explored to treat SCD. In addition to Crizanlizumab, Rivipansel, another pan-selectin inhibitor is tested in a clinical trial. Heparinoids, which also exhibit P-selectin inhibition properties, could also be used to prevent VOC in SCD patients.

Lastly, reducing the chronic inflammatory state in SCD patients could prevent organ damage. To this purpose, several therapeutics have been proposed including intravenous immunoglobulins, inhibitors of the coagulation activation cascade or Canakinumab, a humanized monoclonal antibody targeting the inflammatory IL-1β cytokine (289,299).

2. Blood transfusion

Parallel to the medications, blood transfusions, either simple RBC transfusion or exchange transfusion (used to rapidly exchange the patient erythrocytes with donor RBCs) remain an effective therapeutic option for preventing SCD complications. Bloodletting is also used to reduce blood viscosity in case of elevated Hb concentration. Blood transfusion improves oxygen delivery and microvascular perfusion by decreasing the number of circulating sickle erythrocytes. However, transfusions can induce potential adverse effects such as, iron overload, alloimmunization or delayed hemolytic reactions. Iron overload can be managed by using iron-chelating drugs. To reduce the other associated risks, many blood centers have adopted systematic extended red cell phenotyping as well as molecular genotyping in some centers. Blood transfusion has been demonstrated to be one of the best strategies to prevent primary and secondary strokes and can prevent VOC in SCD patients (300,301).

3. Bone marrow transplantation

Bone marrow transplantation, which consists in hematopoietic stem cell transplant (HSCT), is the only available curative and definitive treatment for SCD. HSCT can establish donor-derived erythropoiesis and can stabilize or restore function in damaged organs of SCD patients (302). Worldwide, it has been estimated that about 2,000 SCD patients have received HLA-identical (human leukocyte antigens) match sibling donor HSCT with an overall survival superior to 90% (303). More recent data reported at least 95% cure rate in 234 children and young adults (<30 years) with SCD, showing that myeloablative HSCT can be a safe option for patients <15 years old (304). Donor can either be HbAA or HbAS.

Most of these patients received myeloablative conditioning, using chemotherapy, in order to remove receiver's HSCs and fully replace them by HSCs from a normal donor. However, this procedure is highly toxic and some adult patients with pre-existing organ dysfunction cannot endure such treatment. The need to reverse sickle hematopoiesis without complete replacement of the patient's bone marrow led to the development of reduced intensity conditioning (305,306). Studies showed that a myeloid donor chimerism of more than 20% was sufficient to reverse sickle hematological genotype (more than 20% HSCs are from the donor), resulting in RBC donor chimerism close to 100% (307). Indeed, a minority of

donor myeloid cells is adequate because of the vast differences in RBC survival between donor and recipient.

While now limited by the huge improvements of HSCT, severe adverse effects include acute and chronic graft versus host disease (GVHD) or graft rejection. Although HSCT from the bone marrow of a healthy sibling donor can cure SCD, this therapy is limited by the lack of suitable donors and is available only in high-income countries (308). For example, in the US, it has been estimated than less than 15% of SCD patients have a sibling donor. Alternative donor sources have thus been proposed such as haplo-identical family members and matched unrelated donors. Both options recently showed promising results for the treatment of β-hemoglobinopathies (299). However, associated risks and donor availability still remain a huge limitation of this approach.

4. Gene therapy

Gene therapy using autologous, genetically modified HSCs is thus an alternative to allogenic HSCT for treating β-hemoglobinopathies. It circumvents the need for a matched unrelated donor and thus avoids the risk of GVHD and graft rejection after HSCT. Furthermore, the conditioning regimen required to allow the engraftment of genetic modified cells does not include immunosuppressive drugs because it uses the patient's own stem cells.

The genetic defect in the sickle HSCs can be corrected via several approaches. However, they are all based on the same principle: modifying HSCs so that HbS polymerization will be inhibited in arising RBCs, in order to cure SCD patients. This inhibition can be achieved using erythroid-specific expression of transgenic anti-sickling hemoglobin so that only RBCs will produce this Hb. A similar result can be reached by reversing the fetal-to-adult HbF expression synthesis, either using gene addition or genome editing strategies. Lastly, genome editing could also be considered in the future to directly correct the point mutation in the *HBB* gene.

4.1. Basic principles of gene therapy

Gene therapy consists in treating genetic diseases by achieving durable expression of a therapeutic gene, or transgene. The goal is to achieve its expression at a level sufficient to ameliorate or cure disease symptoms with minimal adverse event. Two basic strategies exist:

the use of an integrating vector, which is introduced into progenitor or stem cells, or the use of a nonintegrating vector, which is introduced into long-lived postmitotic or slowly dividing cells (309). In the first case, the vector is designed to integrate in the patient's chromosomes and transduction is generally an *ex vivo* process. In the second case, the transgene is stabilized extra-chromosomally and delivery is generally an *in vivo* process.

Non integrating strategies mainly use recombinant adeno-associated viral (AAV) vectors, engineered from parvovirus. The majority of these vectors are maintained in targeted cells as stable episomes expressing the therapeutic transgene. Because recombinant episomal DNA does not integrate into host genomes, it will eventually be diluted over time as the cell undergoes replication. AAV vectors also present size limitation on the length of complementary DNA that can be incorporated (309). Obviously, such strategy is not suitable for β-hemoglobinopathies because of the high rate of RBC production, which require the genetic modification of HSCs. In addition, the size limitation cannot afford both β-globin gene and regulatory expression elements.

Gamma-retroviral (RV) vectors were the first type of integrative vectors proposed and used for gene therapy. After entering the host cell, a single-stranded retroviral RNA genome is released into the cytoplasm and converted into a double-stranded DNA by virus-encoded reverse transcriptase. The viral DNA then forms a large nucleoprotein structure, termed pre-integration complex, containing proteins necessary for nuclear localization and insertion of viral DNA into the host genome by integrase. To be successful, transgene must be integrated into the genome so that any daughter cells are genetically corrected, must be stably and sufficiently expressed, and must not interfere with the functional integrity of the target cells. The latter is the major risk of integrating vectors, which comes from the RV vector potential for insertional mutagenesis as it inserts and disrupts a functional element of the genome (310,311). Indeed, it has been observed that treatments of various disorders with HSCs transduced with RV vector could led to leukemia or myelodysplasia. This was attributed to vector insertion near protooncogenes, which were activated by enhancer sequences present in the retroviral long terminal repeats (LTRs). Safer vectors were thus investigated and lentiviral (LV) vectors were developed to improve gene therapy safety and efficiency requiring genome integration (312). Lentiviruses are members of the viral family *Retroviridae* (retroviruses) that are characterized by their use of viral reverse transcriptase and integrase for stable insertion of viral genomic information into the host genome. The majority of LV

vectors are based on the human immunodeficiency virus type 1 (HIV-1) (313). As compared to RV vectors, they offer several attractive properties: the capability of infecting both dividing and non-dividing cells (312) and a safer integration pattern in the genome because they mainly integrate in transcribed regions (314). Like AAV, LV vectors lack the capacity for ongoing replication and are said to be self-inactivated. In case of a cell co-infected by both the vector and a wild-type virus could result in theory in replication-competent virus. Therefore, numerous assays are mandatory before any infusion to a patient.

Genome engineering has expanded the possible genetic therapy options for many hematopoietic diseases. Targeted nucleases, such as zinc-finger nucleases (ZFNs), transcription-activator like effector nucleases (TALENs), and the clustered regularly interspaced palindromic repeats (CRISPR)-associated nuclease Cas9, have each programmable DNA-binding modules that allow introduction of site-specific double-strand breaks into the human genome. In the cell, double-strand breaks can be repaired through homology-directed repair (HDR), non-homologous end-joining (NHEJ), or microhomology-mediated end joining (MMEJ) (315,316). Unlike gene addition strategies, genome engineering approaches rely on an *ex vivo* intervention and do not result in permanent insertion of foreign DNA into the genome. Because of its high-fidelity properties, HDR is a preferred mechanism allowing the site-specific integration of a homologous DNA donor template. NHEJ and MMEJ are preferred to obtain permanent gene inactivation or disruption of regulating elements mainly through insertion or deletions (317).

4.2. Development of gene therapy for β-hemoglobinopathies

Gene therapy for genetic blood diseases is currently based on transplantation of autologous hematopoietic stem cells (HSCs) genetically modified with integrating viral vectors expressing the transgene of interest. *Ex vivo* transduction is achieved by extracting progenitor and stem cells from the patient. Once HSCs ($CD34^+$ enriched) are isolated, they are transduced with the gene of interest, and are then returned to the patient in a procedure similar to hematopoietic stem cell transplantation (Figure 31). The transplantation of these genetically corrected autologous HSCs avoids the immunological risks associated with allogeneic HSCT (318). In addition, it does not require the use of immune suppressive associated treatments.

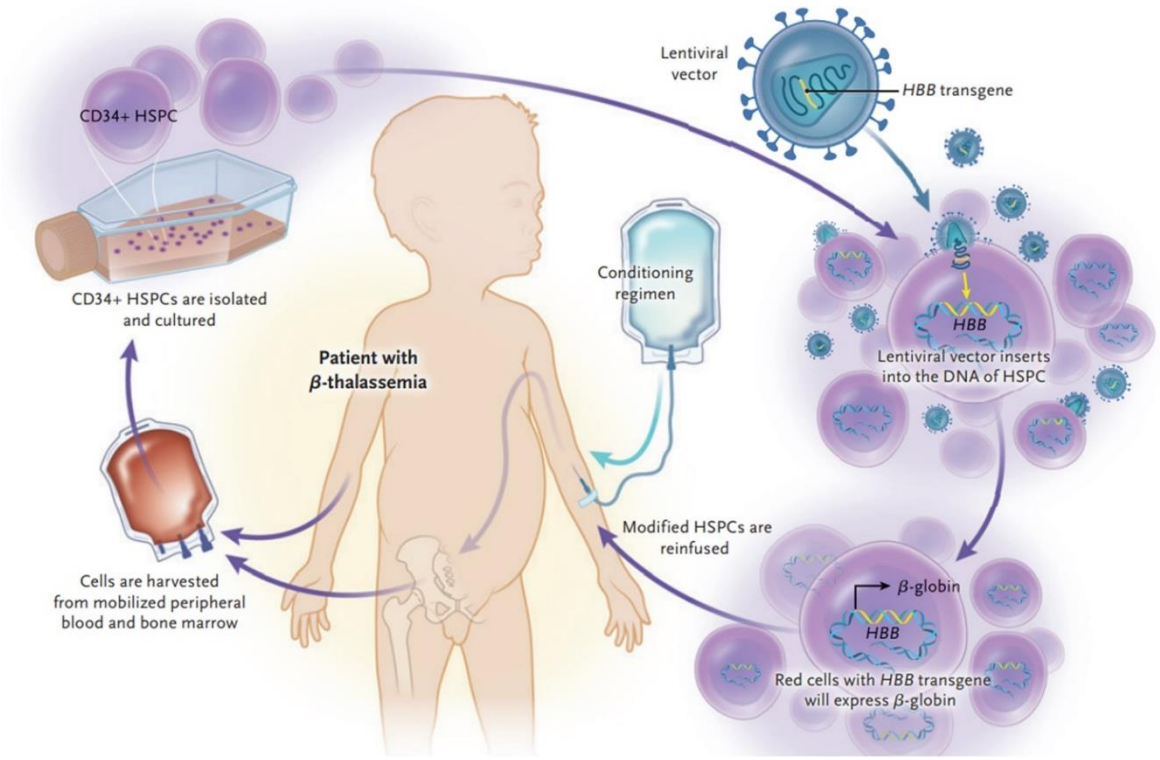

Figure 31 | *Ex vivo* delivery of gene therapy for the treatment of β-thalassemia. HSCs (CD34+) are harvested from the bone marrow or from the mobilized peripheral blood of the patient and isolated. After a brief *ex vivo* culture period, they are subjected to gene transfer with an integrating lentiviral vector encoding the β-globin complementary DNA under the control of an erythroid-specific promoter. The patient receives a conditioning regimen that depletes the endogenous HSCs from the bone marrow. The gene corrected HSCs are then reinfused intravenously and engraft in the bone marrow, where they self-renew and differentiate into all hematopoietic lineages, including erythroid lineage expressing the transgene. Figure from High and Roncarolo (309).

The correction of β-hemoglobinopathies by gene addition has required years of research. Earlier gene therapy studies were conducted using recombinant RV, derived from the Moloney leukemia virus, as vector to deliver a copy of the β-globin gene into murine repopulating HSCs (319,320). While successful, the level of expression of the transgene was variable and low. A higher level of expression was reached using a modified RV including a single hypersensitive site of the locus activation region of the human β-globin-like gene cluster but resulted in an increased risk of activating the expression of non-globin genes (321).

The discovery of the β-globin LCR in 1989 (322,323), associated with the development of HIV-1-derived LV vectors in 1996 (312), opened up new perspectives in gene therapy for β-hemoglobinopathies. Following these breakthroughs, two first LV vectors containing fragments of the β-globin gene, including the promoter, and critical β-LCR HS enhancers were designed. The additional optimization of the vector titer (by deleting a portion of the second

β-globin intron and removing multiple cryptic polyadenylation and splicing signals) (324,325) led to proof of concept studies complementing murine models of β-thalassemia (326,327) and SCD (328). Following, other laboratories demonstrated that LV vectors expressing the human β- or γ-globin (also under the control of β-globin promoter) and including β-LCR elements improved β-thal phenotypes in murine models (329,330).

The first phase 1/2 clinical trial (LG001) started in France in 2006, for gene therapy of transfusion-dependent β-thalassemia. It used the LV vector HPV569, expressing the modified β-globin transgene $\beta^{A\text{-}T87Q}$. This vector carries two copies of the core of the chicken β-globin HS4 (cHS4) chromatin insulator, displaying enhancer-blocking activity, to prevent activation of adjacent genes (331). This trial resulted in one patient becoming transfusion-independent (332).

Following these results, the use of the BB305 LV vector, which is an improved version of the HPV569 used in the LG001 study, has been shown to efficiently reduce or eliminate transfusion-dependency in 22 patients with severe β-thal (333). Recently, Zynteglo, a gene therapy using this LV vector to modify HSCs for autologous transplantation has been approved by the European Medicines Agency for the treatment of adolescents and young adults suffering from non β^0/β^0 transfusion-dependent β-thal.

4.3. Gene addition strategies to treat sickle cell disease

4.3.1. Hemoglobin variants with anti-sickling properties

Engineering recombinant HbF and HbA by adding additional substitutions can enhance the capacity of the molecule to inhibit HbS polymerization. The design of anti-sickling globins is based on genetic considerations, HbF being the major modulator of the disease clinical severity. Modified β-globin chains based on HbF native properties and amino acid sequences have been proposed as transgenes with the aim to be used for gene therapy purposes. Mutations that disrupt the ability of HbS to form polymers by interfering with axial and lateral contacts in the polymer were introduced into the normal human β-globin gene *HBB* by site-specific mutagenesis (334). Substitutions such as glutamic acid at position 22 replaced by an alanine (E22A) and threonine at position 87 replaced by a glutamine (T87Q) confer potent anti-sickling activity.

An advantage of these modified hemoglobins is the ease with which the contribution of various globin chains can be assessed. Because the erythropoietic stress associated with HSCT may lead to elevated endogenous γ-globin expression, the capacity to distinguish exogenous from endogenous globin chains facilitates evaluation of gene addition efficacy (335).

Based on these studies, a modified β-globin chain harboring the point mutation T87Q alone ($\beta^{A\text{-}T87Q}$) has been tested under erythroid-specific expression to efficiently correct a murine model of SCD for gene therapy purposes (328). Present in the γ-globin chain, this substitution prevents HbS polymerization by interfering with the formation of lateral contacts between the Hb tetramers (Figure 32).

Other investigators developed a triple-mutant β-globin chain that disrupts both axial and lateral contact in the HbS polymer, with potent anti-sickling properties (336). This mutant carries the T87Q substitution and two additional ones. First, the E22A substitution contributes to the anti-sickling activity by disrupting axial contacts between Hb tetramers. Second, the substitution of the glycine at position 16 by an aspartic acid (G16D) increases its affinity for the α-chain (Figure 32). This latter substitution confers to this triple-mutant β-globin a competitive advantage toward endogenous β^S to interact with α-globin. The formation of Hb tetramer including this mutant is supposed to be greater than Hb tetramer including β^S-globin similarly to what is observed in sickle cell trait patient but in a more important way. The expression of the so-called β^{AS3}-globin also corrects a murine model of SCD.

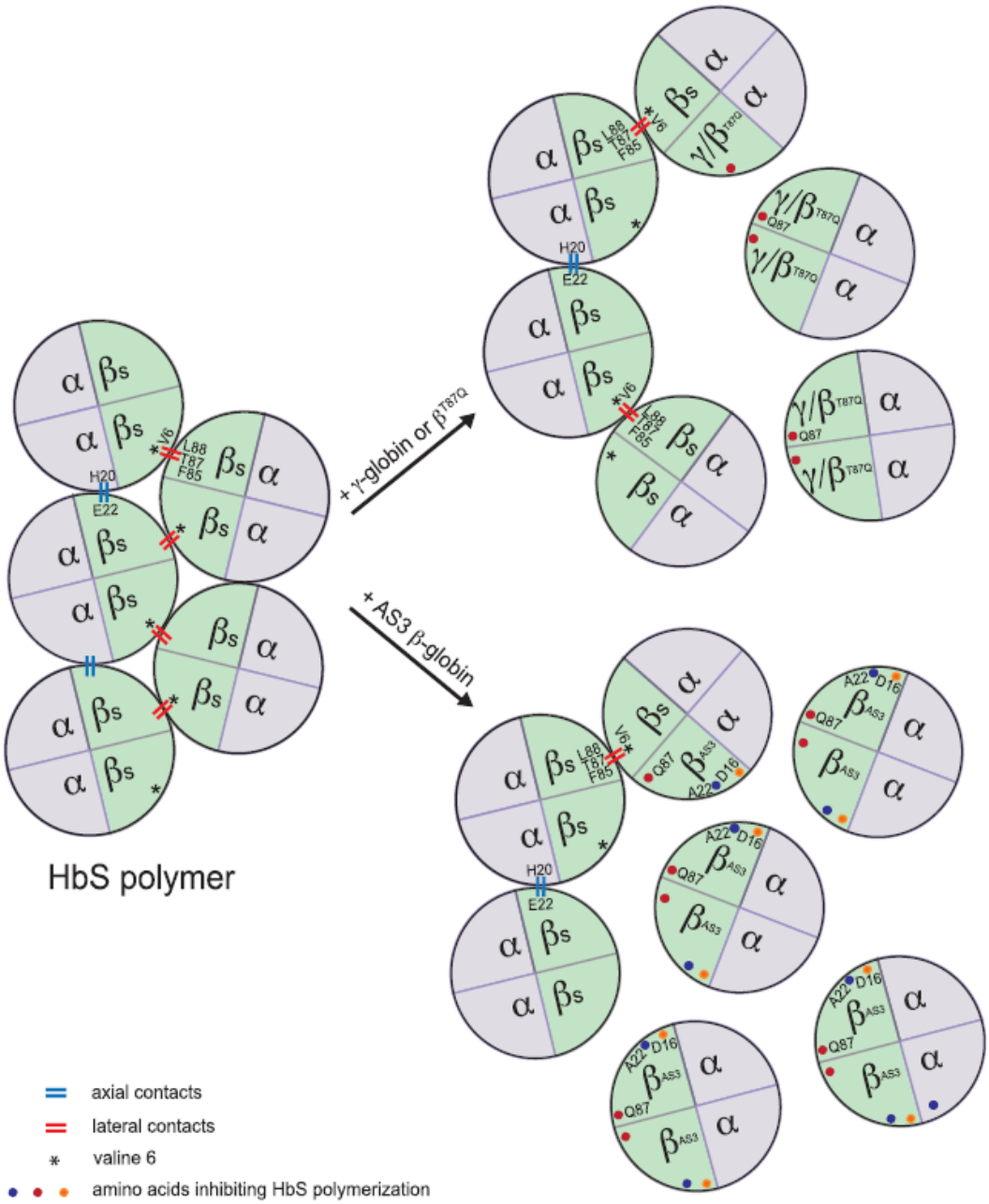

Figure 32 | Inhibition of HbS polymerization by anti-sickling β-like globins. In HbS polymers, the valine at position 6 (V6) of the β^S-chain forms a lateral contact with the phenylalanine and leucine residues at positions 85 and 88 (F85 and L88) of the β^S-chain of the adjacent tetramer. Additionally, a glutamic acid (at position 22) of the β-chain interacts with a histidine residue (at position 20) of the α-globin of a neighboring tetramer (axial contact). Like γ-globin, the β^{T87Q}-globin, in which the threonine at position 87 is replaced by a glutamine (T87Q), prevents HbS polymerization by interfering with the formation of lateral contacts between the Hb tetramers. The β^{AS3}-globin, in which the glutamic acid at position 22 is replaced by an alanine (A22) in addition to the T87Q amino acid substitution, prevents HbS polymerization by disrupting both lateral and axial contacts between Hb tetramers. Moreover, in β^{AS3}, the glycine at position 16 is replaced by an aspartic acid (D16), thus increasing its affinity for the α-globin polypeptide. Figure from Cavazzana, *et al*. (47).

4.3.2. Anti-sickling hemoglobin as transgene to treat sickle cell disease

The results obtained in patients with severe β-thal encouraged attempts to extend gene therapy clinical trials for the treatment of SCD patients. The vectors used in these studies harbor expression cassettes based on the same β-globin promoter and LCR elements that are used for treating β-thal. They however express modified β-globin transgenes with the potential to interfere with HbS polymerization.

The first patient treated with success in France, in the HGB-205 study (NCT02151526), was reported in 2017 (337). He received autologous HSCs genetically modified with the BB305 LV vector, expressing the $\beta^{A\text{-}T87Q}$-globin. The patient achieved a level of therapeutic Hb around 50% and transfusion independence, with a clinical status comparable to that of a sickle cell trait individual. Two other SCD patients were recruited in this study. The results obtained in the first patient encouraged the treatment of additional severe SCD patients in the context of another clinical trial ongoing in the United States (HGB-206 study - NCT02140554).

As modification at β-16 (glycine to aspartic acid), which confers a competitive advantage over β^S-globin for binding to α-globin, and modification at β-22 (glutamic acid to alanine), which disturbs axial contact with α-20 histidine, the triple-mutant β^{AS3}-globin is expected to exhibit greater anti-sickling properties compared to the T87Q alone modified variant (338). This triple-mutant is currently being tested in a clinical trial (NCT02247843) using the LV vector βAS3-FB to modify autologous HSCs. Another clinical trial which aims at evaluating the safety and efficacy of the GLOBE1 LV vector to treat SCD has started recently in France (NCT 03964792). It also consists in re-injection of autologous genetically modified HSCs with the aim to express the anti-sickling β^{AS3}-globin in RBCs.

Lastly, expression of unmodified γ-globin under the control of β-globin promoter through a LV vector has also been proposed as a gene therapy strategy to treat SCD (339,340). The comparison of two vectors in a mouse model demonstrated improvements in anemia and in secondary organ pathology (341). These results lead to an ongoing clinical trial aiming at the expression of a modified γ-globin transgene using LV vector in the United States (NCT02186418). This vector expresses a γ-globin with the point mutation (G16D), increasing its affinity for the α-globin chain.

4.3.3. Reactivation of endogenous fetal hemoglobin expression

Another option to inhibit HbS polymerization using gene therapy consists in the reactivation of endogenous HbF levels. It can be achieved through the downregulation of nuclear factors involved in the repression of γ-globin expression. To this purpose, reversing the fetal-to-adult Hb switch has been proposed (342). It requires the comprehensive knowledge of the transcription factors involved in this inhibition, the prominent among these regulators being BCL11A, a transcriptional repressor that inhibits adult-stage HbF expression (40,42,343). The inactivation of *BCL11A* in the erythroid lineage of genetically engineered mice prevents RBCs from sickling and other sickle cell disease–associated phenotypes, such as hemolysis and organ damage (344). By using RNA interference, a short-hairpin RNA (shRNA) expressed in the erythroid lineage, it has been demonstrated that an increase in γ-globin can be achieved with a concomitant decrease in β-globin synthesis (345). However, ubiquitous down-regulation of *BLC11A* in HSCs impairs their engraftment in recipients showing that a fine modulation of *BCL11A* expression levels is necessary (346,347). Thus, β-LCR-driven expression of shRNA for *BCL11A* has been tested and has been shown to overcome the *BCL11A* knock-down associated toxicity in HSCs. This approach allowed *BCL11A* reduction in RBCs derived from normal and SCD HSCs, with HbF representing up to 70% of the total Hb content. Moreover, the transplantation of HSCs expressing the *BCL11A* shRNA improved clinical manifestation of SCD in a mouse model (348). In this context, preclinical studies of the BCH-BB694 LV vector showed that down-regulation of *BCL11A* using an erythroid-specific expression and an adapted short-hairpin, effectively bypasses the engrafting inability of HSCs with ubiquitous *BCL11A* inhibition (349). These results led to the beginning a phase 1 clinical trial for SCD using this approach (NCT03282656).

Another alternative way to increase the level of endogenous HbF is to directly control the genomic interactions at the β-LCR locus (44). To this purpose a LV vector encoding a fusion protein between a zinc-finger domain (which binds to the γ-globin promoters) and LIM domain-binding protein 1 (LDB1) (a factor involved in the LCR/β-like promoters interaction) has been generated. The resulting forced chromatin looping led to γ-globin synthesis in primary erythroblasts from SCD patients (350,351).

4.4. Genome-editing strategies to treat sickle cell disease

Genome-editing has been investigated to achieve *ex-vivo* reversion of the point mutation in the *HBB* gene (e.g. A>T) by using ZFN (352) or CRISPR/Cas9 systems (353–355). While promising, this approach needs high accuracy in order not to generate a deletion in the *HBB* gene instead of the correction of the sickle mutation, which could lead to a β-thalassemia.

An alternative approach consists in increasing HbF level in RBCs by re-creating naturally occurring mutations in HSCs. Indeed, the co-inheritance of mutations responsible for γ-globin synthesis in adult life, as observed in HPFH, reduces the clinical severity of SCD. HPFH is caused by either large genomic deletions encompassing *HBB* and *HBD* genes, or mutations in *HBG1* and *HBG2* gene promoters. The first requires the generation of two double-strain breaks and such deletions mediated by CRISPR/Cas9 and using NHEJ repair system in the β-globin locus have been showed to induce HbF synthesis (356–358). The disruption of the BCL11A repressor binding site in the promoters of *HBG1* and *HBG2* genes also leads to HbF reactivation, using either CRISPR/Cas9 or TALEN systems (359–361). Lastly, the downregulation of *BCL11A* can also be obtained by deleting enhancer elements controlling its expression in the erythroid lineage by CRISPR/Cas9-mediated genome editing (347,362).

A clinical trial based on genome-editing strategy using CRISPR/Cas9 mechanism has been approved to treat SCD (NCT03745287). It consists in autologous $CD34^+$ HSCs modified with CRISPR/Cas9 at the enhancer of the *BCL11A* gene with the aim to induce HbF synthesis.

Part 2: Results

Chapter 5 – Assessment of fetal hemoglobin distribution among red blood cell populations

1. Development of an individual red blood cell fetal hemoglobin quantification assay for clinical purposes

1.1. Developing a new tool for the quantification of fetal hemoglobin

Because of its biochemical properties, HbF is a major modulator of SCD severity by inhibiting the HbS polymer elongation, decreasing clinical manifestation and mortality (280,363). Studies have shown that individuals with 20% or more HbF are mostly few symptomatic (364–366). Such high levels of HbF are mostly associated with genetic factors including HPFH, beta-thalassemia or other polymorphisms. In most of these individuals HbF is homogeneously distributed among the RBC population. Therefore, all the RBCs are protected from HbS polymerization in the same way. However, the vast majority of SCD patients does not present those genetic factors. They express low levels of HbF, and its distribution is mostly heterogeneous (367). Moreover, it has been described in patients that an increase in HbF expression is not associated with a clinical improvement and inversely, some patients with low HbF levels can have few symptoms (368–370). These observations support the hypothesis done by Steinberg *et al.* in 2014 that rather than the percentage of HbF, there is a threshold of HbF content in each RBC allowing the inhibition of HbS polymerization (371).

In the last decades, several techniques have been developed to detect HbF in RBCs. The routinely used high pressure liquid chromatography (HPLC) provides a global percentage of HbF in a hemolysate and therefore does not consider the distribution (372). A variety of immunological methods have been proposed to estimate RBCs containing HbF (373–381). Based on a variable positivity threshold, these methods are limited to a qualitative measurement of HbF, providing a percentage of HbF positive RBCs named F cells.

Therefore, HbF distribution is probably one of the most critical point to explain the clinical discrepancies observed between patients having identical %HbF. As exemplified in

Figure 33, patients A and B have the same % HbF as assessed by routinely used HPLC. Assuming 30% of HbF, as observed in SCD patient with HPFH, these two patients should be "protected" and less symptomatic. However, VOC frequency for patient B is significantly higher than for patient A. The HbF content in individual RBCs of these two patients shows that HbF is homogeneously distributed among the RBC population for patient A, while the distribution is heterogeneous for patient B. Assessment of HbF distribution can easily be performed by using a method allowing single cell analysis, such as flow cytometry. HbF distribution in patient A reveals that almost all RBCs from patient A contain enough HbF to inhibit HbS polymerization. In contrast, for patient B, a sub-population of RBC contain high level of HbF while it is not the case for the other RBC sub-population. Inside these latter RBCs, HbS polymerization still occurs, probably explaining the clinical manifestation differences observed between these two individuals. Obviously, the same reasoning could be applied to any anti-sickling hemoglobin such as the genetically modified β-globins used in gene therapy, namely $\beta^{A\text{-}T87Q}$ and βAS3.

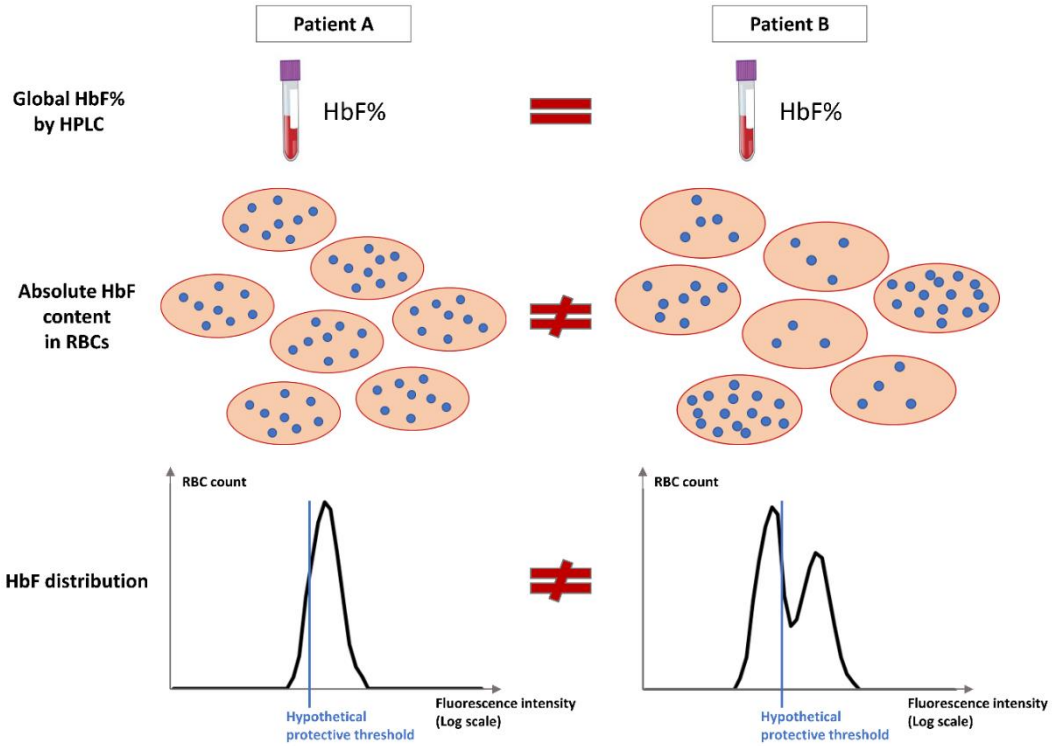

Figure 33 | Relevance of the HbF quantification in individual red blood cells. Example of two patients (A and B) presenting the same HbF%. Percentages of HbF, measured by routinely used HPLC on a hemolysate from a blood sample, give the same value between the two patients. When looking at the single cell level, HbF is homogeneously distributed among the RBC population for Patient A, while distribution is heterogeneous for Patient B, as measured by a method allowing single cell analysis such as flow cytometry. The blue vertical barre represents the hypothetical protective threshold to reach.

Our team has previously developed a new tool to quantify HbF in individual RBCs, providing a quantitative HbF distribution. This new method is based on the use of a Mouse anti-Human-HbF monoclonal antibody coupled to phycoerythrin (PE) fluorochrome and flow cytometry to allow the quantification of HbF per RBC (HbF/RBC). This method has been patented in 2016 (Patent n° FR3058525A1). As a proof of concept, and to validate the method, a study has been performed on 14 SCD patients treated by the well-known HbF inducer HU. This previous work showed first, the feasibility of HbF quantification in individualized RBCs by flow cytometry, second, the changes in HbF distribution induced by HU treatment, and third, the association of HU effectiveness with exceeding HbF content thresholds that accompanies the increase in %HbF (382). In a clinical context, a standardized, reliable and reproducible assay is mandatory.

The aims of my work were:

- to assess the reliability of the HbF quantification per RBC method for clinical purpose, by performing analysis of reproducibility and repeatability,
- to determine biological and clinical protective thresholds of HbF/RBC in SCD,
- to demonstrate the utility of the assay in patients' clinical follow-up or to evaluate new therapeutics aiming to induce HbF synthesis such as gene therapy.

1.2. Methods

a. Patients

Eligible patients (all ≥ 18 years) were selected from the Erythropedie collection monitored in our referral center (Henri Mondor Hospital, Creteil, France). This protocol was approved by the local ethics committee (CPP–Île-de-France IV Saint-Louis Hospital, IRB 00003835). In accordance with the Declaration of Helsinki, all patients gave their signed informed consent. All data were rendered anonymous to protect patients' privacy and confidentiality.

A first group of patients (group A) was recruited for method development. Inclusion criteria in group A were: patients carrying HPFH, $\beta-$ or $\delta\beta-$Thalassemia genotype, or genetic hemochromatosis (as controls with very low HbF). Exclusion criteria were SCD (S-S, S/β-Thalassemia or S/C) or sickle cell trait (A/S), blood transfusion within 3 months preceding the enrolment and pregnancy.

A second group of patients (group B) was recruited to assess changes produced by HU treatment. Inclusion criteria in group B were: S/S or S/β^0-thalassemia genotype at steady state (>1 month from a VOC and >3 months from a transfusion) and undergoing a treatment with hydroxyurea (HU). Exclusion criteria were S/C or S/β^+-thalassemia genotype, chronic transfusion program, erythropoietin treatment and pregnancy. We collected samples and biologic parameter values before treatment (D0), between 15 days and 1 month (D15-M1), 3 and 4 months (M3-4) and ≥6 months (≥M6) on HU.

All other patients were S/S or S/β^0-thalassemia genotype at steady state (>1 month from a VOC and >3 months from a transfusion).

b. Sample pretreatment

20 mL of blood were drawn and collected in EDTA tubes. Samples were processed within 24 hours. RBCs were separated from whole blood by centrifugation at 1200 g for 10 minutes at room temperature. The RBC fraction was washed with phosphate buffered solution (DPBS - Thermo Fischer Scientific) and centrifuged at 1200 g for 5 minutes at room temperature. Supernatant was removed and the washing procedure was repeated at least 3 times. About 1 mL of packed RBC was collected for experiments on fresh RBCs while 7 mL were frozen at –80°C in multiple aliquots of 200 µL in cryotubes using 57.7% (v/v) glycerol (B. Braun) as cryoprotective agent. To prevent precipitation, one-third of the glycerol volume was added to packed RBCs prior to incubation for 10 minutes at room temperature and thereafter the remaining volume was added. Thawing RBCs consisted in placing cryotubes containing frozen RBCs in a pre-warmed water bath at 37 °C followed by washing cells with decreased concentration of 0.9% NaCl solutions (B. Braun) in order to completely remove the cryoprotective agent.

c. %HbF determination on HPLC

HbF dosage was performed through ion exclusion HPLC using a Variant II Hemoglobin Testing System (Bio-Rad). The different Hb were eluted from column based on ionic interaction with carboxyl group and then introduced in a photometer detector using 2 different wavelengths of 690 nm and 415 nm for baseline and sample detection, respectively.

The chromatography system run time was 6 minutes and HbF was eluted up to 0.5 minute. Results were acquired with CDM 5.2 software.

d. Complete blood count

RBC count, total Hb and mean corpuscular hemoglobin (MCH) were determined using a Horiba ABX Micros ES 60 counter (HORIBA Medical). Mean Corpuscular HbF (MCHbF in pg) was calculated using the following equation (383):

$$\text{MCHbF}=\frac{(\%HbF \times MCH)}{100}$$

e. HbF detection by flow cytometry

Prior to intracellular staining, RBC membrane was fixed and permeabilized using Fetal Cell Count™ kit reagents (Cat IQP-363, IQ Products) according to the manufacturer's instructions using 5 µL of packed RBC.

Mouse monoclonal anti-human HbF antibody conjugated with R-phycoerythrin (R-PE) (reagent F, Fetal Cell Count™ kit, IQ Products) was used for immunologically based HbF detection. 20 µL of a R-PE mouse IgG1 Kappa (BD Pharmingen) were used as a negative isotypic control. RBCs were incubated for 15 minutes shielded from light at room temperature. Thereafter, RBCs were washed with PBS and centrifuged at 300 g for 3 minutes. Stained RBCs were immediately analyzed on flow cytometer.

HbF fluorescence in RBCs was acquired using a BD FACSCanto II system including an 8-color flow cytometer (BD Biosciences). Data were analyzed using FlowJo v10 software (Miltenyi Biotec). Light scatter thresholds were used to select RBC population and exclude cellular debris. Every PE fluorescence intensity (FL-2) was monitored with a photomultiplier tube (PMT) voltage set at 400V. 1 x 10^5 cells were gated on forward scatter area (FSC-A) versus side scatter area (SSC-A) plot and recorded. Doublet were excluded by selecting single cells on FSC-H (FSC-Height) plotted against FSC-W (FSC-Width) and then on SSC-H versus SSC-W. The anti-carbonic anhydrase (CA) contained in the Fetal Cell Count™ kit was never used, first, to avoid fluorescence interference on the measured signal from the anti-HbF because of spectral overlap of fluorescein isothiocyanate (FITC) and R-PE emission spectra and second, because all the quantifications were performed on adult RBCs (not from a fetus). In parallel, quantitation beads (BD Quantibrite™ Beads PE, BD Biosciences) were analyzed on flow

cytometer using the same settings as used for RBCs (384). A minimum of 1 x 10^4 beads was recorded allowing 4 fluorescence levels corresponding to a number of PE molecules by bead which is batch specific. A linear regression involving bead fluorescence intensity and number of PE molecules per bead was then obtained (Figure 34).

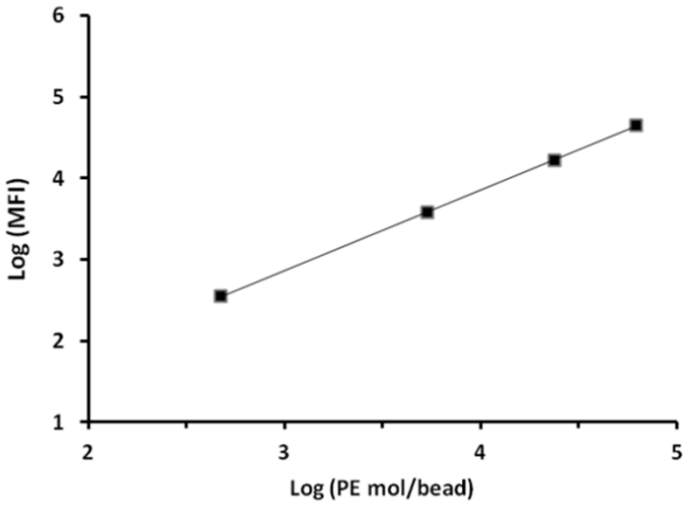

Figure 34 | Example of linear regression obtained with the BD Quantibrite Beads (R^2 = 0.999). Each point represents one of the 4 fluorescence levels measured (beads being conjugated with 4 different levels of PE), which corresponds to 4 known numbers of PE molecules per beads.

f. HbF determination method in individual RBCs

A method for HbF quantification in single RBC was developed from samples collected from patients assigned in group A. Mathematically, we applied a correction factor to the measured PE fluorescence intensities to consider the variability of the degree of coupling of the antibody which can differ from one batch to another. Using the linear regression curve obtained with the quantitation beads, the PE fluorescence value of each RBC was converted into a corresponding PE molecules per RBC, giving a normalized HbF fluorescence. Because MCHbF corresponds to an average HbF content per RBC when homogeneous HbF distribution is observed, a linear regression associating the normalized HbF fluorescence and MCHbF was obtained. This linear regression can then be used to measure HbF/RBC in any sample.

g. Assessment of the variability, repeatability and reproducibility of the HbF assay.

To consider the variability of the degree of coupling of the antibody which can differ from one batch to another, 3 different batches were tested. Fluorescence:protein ratios were 1.2, 1.04 and 0.66 for batch 1, batch 2 and batch 3, respectively.

To assess the effect of freezing on the quantification, samples from 3 SCD patients (SS) and 1 healthy donor (HD) were collected and split in 2 parts. One was used freshly to perform the HbF/RBC assay (in triplicate) and the other was frozen as described to allow later quantification (in triplicate).

Repeatability and reproducibility of the method were assessed using RBCs from 3 different samples: 1 adult HD; 1 cord blood (CB) and 1 homozygous SCD patient (SS). RBCs from unique samples were washed and frozen into aliquots as described above and then thawed for each experiment. Repeatability was assessed by performing 5 independent replicates the same day for each sample and reproducibility was assessed by performing 5 independent replicates at 5 different days. The same antibody batch (n°3) was used for all these experiments. HD and CB samples were obtained from the Etablissement Français du Sang after signed informed consent. Results were expressed as mean ± standard deviation and coefficient of variation was calculated in percentage.

h. F cell detection methods

F cell percentages were assessed by using two different methods as previously described (380,381). Briefly, cells were analyzed by flow cytometry as above. The F cell percentage was calculated as the fraction of positive cells when incubated with the anti-HbF antibody compared to a threshold set up according to the fluorescence intensity of unstained cells (method 1) or cells incubated with the isotypic control (method 2) (Figure 35).

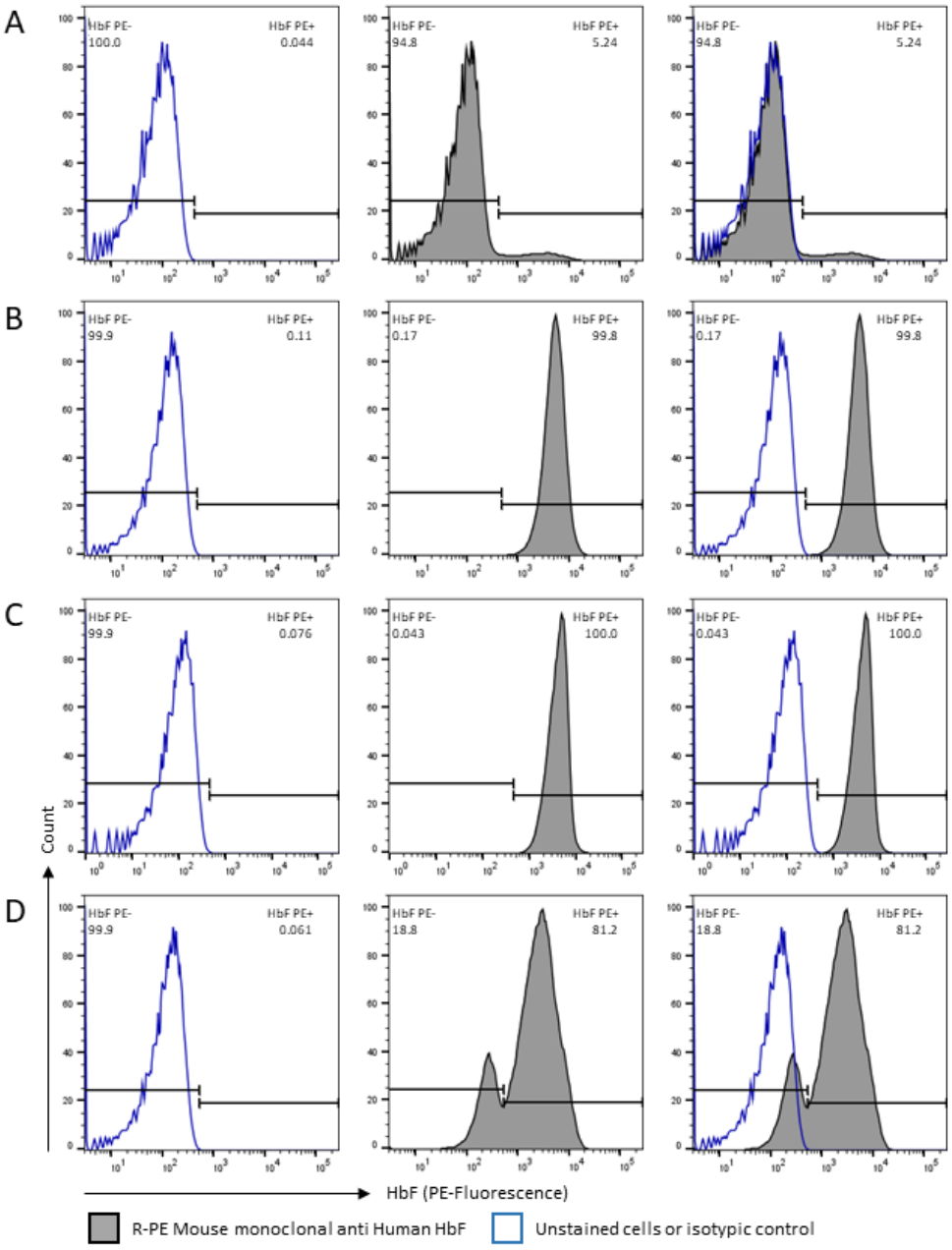

Figure 35 | Representative histograms of F cells detection strategy. 5 µl of packed RBCs were fixed then permeabilized prior to incubation with R-PE-coupled anti Human-HbF monoclonal antibody and were analyzed by flow cytometry. The threshold of positivity was set up according to the fluorescence intensity measured on corresponding unstained RBCs or incubated with the isotypic control (blue). The same threshold was applied on RBCs incubated with the R-PE-coupled anti Human-HbF monoclonal antibody to determine F cell frequency (middle). Overlays (right). (**A**): Healthy donor. (**B**): Cord blood. (**C**): Patient A-2. (**D**): SCD patient. One representative experiment (n = 5). Gray histograms represent the HbF and blue lines represent the unstained cells or the isotypic control. Horizontal axis shows the R-PE fluorescence (log scale); vertical axis shows the RBC count.

i. Association between HbF/RBC and vaso-occlusive crisis incidence

Numbers of VOC were collected from computerized patient's file from Henri Mondor Hospital for each group B patient. The VOC incidence during the 3 years period before the beginning of HU treatment was compared to HbF/RBC measured at D0, and the VOC incidence during the 3 years period after 6 months of HU treatment at stable dose was compared to HbF/RBC measured at ≥M6 (Figure 36). VOC was defined as pain or tenderness, affecting at least one part of the body, including limbs, ribs, sternum, head (skull), spine, and/or pelvis, that required opioids, was associated with a hospitalization and was not attributable to other causes.

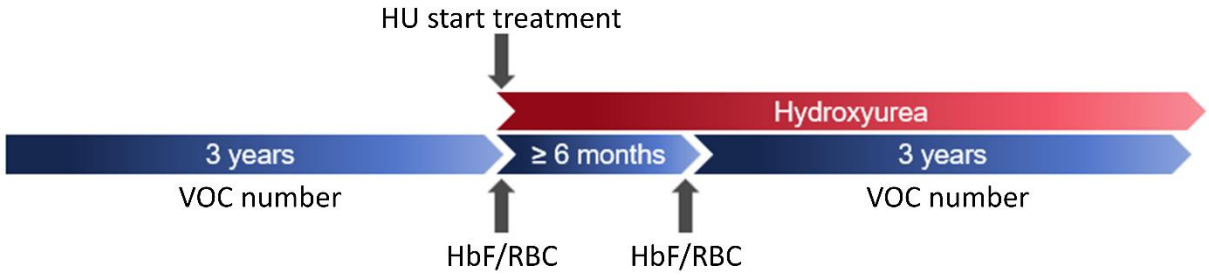

Figure 36 | Study design of hospitalized VOC incidence during HU treatment.

j. In vitro sickling assay

Blood samples were collected from 46 SCD patients from the Erythropedie collection and not included in group B. Total blood was washed as described and RBCs were diluted 400-fold in PBS pH = 7.4 containing 5 mM glucose (Sigma-Aldrich). The oxygen was enzymatically depleted by adding glucose oxidase and catalase (Sigma-Aldrich) to diluted blood to final concentrations of 12.5 IU/mL and 100 IU/mL with the following reaction:

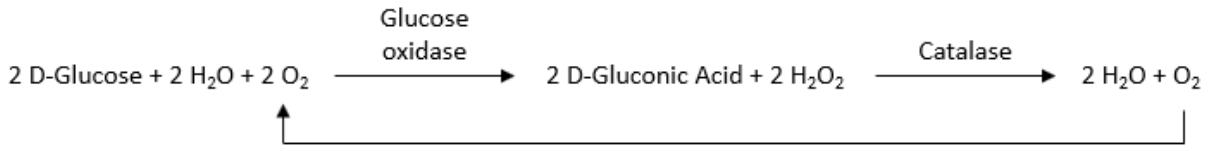

This method presents the advantage of a rapid consumption of all available O_2, deoxygenating RBCs within approximatively 30 seconds, which is more physiologic than long incubation time of RBCs under hypoxic conditions. Samples were rested for at least 2 minutes at room temperature and then observed under an inverted microscope (Zeiss AxioObserver) (385). Pictures were analyzed using ImageJ 1.52a software (NIH). Results were expressed as the ratio of sickle RBCs on total RBCs.

k. CD71 and HbF detection by flow cytometry

Prior to intracellular staining, RBC membrane was fixed and permeabilized as described above. 2 µL of a mouse monoclonal anti-human CD71 antibody conjugated with allophycocyanine-Hilite 7 (APC-H7) (BD Pharmingen) were added in the same time as 50 µL of the mouse monoclonal anti-human HbF antibody conjugated with R-phycoerythrin (R-PE) (reagent F, Fetal Cell CountTM kit, IQ Products) for immunologically based CD71 and HbF detection, respectively. 2 µL of an APC-H7 mouse IgG1 Kappa (BD Pharmingen) were used as a negative isotypic control. RBCs were incubated for 15 minutes shielded from light at room temperature. Thereafter, RBCs were washed with PBS and centrifuged at 300 g for 3 minutes. Stained RBCs were immediately analyzed on flow cytometer as described above.

l. HbF/RBC quantification in patients with severe SCD treated with sh-BCL11A gene therapy

Patients were enrolled in the clinical trial (NCT 03282656). Blood samples were collected, RBCs were isolated and then frozen in Boston Children's Hospital and sent on dry ice to Henri Mondor Hospital. After thawing, RBCs were fixed, permeabilized and incubated with the mouse anti-Human HbF monoclonal antibody and HbF/RBC quantification was performed as described above. Results for one patient (BCL-006) are shown.

m. Statistical analysis

Association between MCHbF and normalized HbF fluorescence was assessed by a Pearson correlation. The log-normal distribution of HbF was assessed by D'Agostino & Pearson normality test. The normalized HbF fluorescence of each RBC was calculated and 500 events were randomly selected to test the normality. A homogeneous HbF distribution was considered when P value was >0.05.

Comparisons of biologic parameters between D0 and ≥M6 were performed using Wilcoxon matched pairs signed rank tests. Comparisons of HbF/RBC at D0, D15-M1, M3-M4 and ≥M6 were performed using Friedman tests. Correlations between %RBC above HbF thresholds and biologic parameters or number of VOC before and after HU treatment were performed using Spearman correlation tests. ROC (receiver operating characteristics) analysis were performed by applying a cut-off for VOC incidence of ≤1 over 3 years.

Comparisons of %CD71-positive and %CD71-negative cells classified according to their HbF content were performed using Wilcoxon matched-pairs signed rank tests.

Statistical analyzes were performed using Prism 8 software (GraphPad) or STATA 15.1 software (Statacorp). All tests were 2-tailed using a significance level set at 0.05.

1.3. Determination of HbF in individualized RBCs: the HbF/RBC assay

The quantification of HbF/RBC is based on the correlation between MCHbF and the fluorescence intensity measured by flow cytometry (382). HbF distribution was assessed by flow cytometry (Figure 37) for the 18 group A non SCD individuals (Table 2). A log-normal distribution, as verified by D'Agostino & Pearson normality tests, indicates a homogeneous HbF content among the RBC population (Table 3). Patients A-1 to A-6 and A-8 to A-12 were selected for further study while A-7 and A-13 to A-18 were excluded because of a non-log-normal distribution.

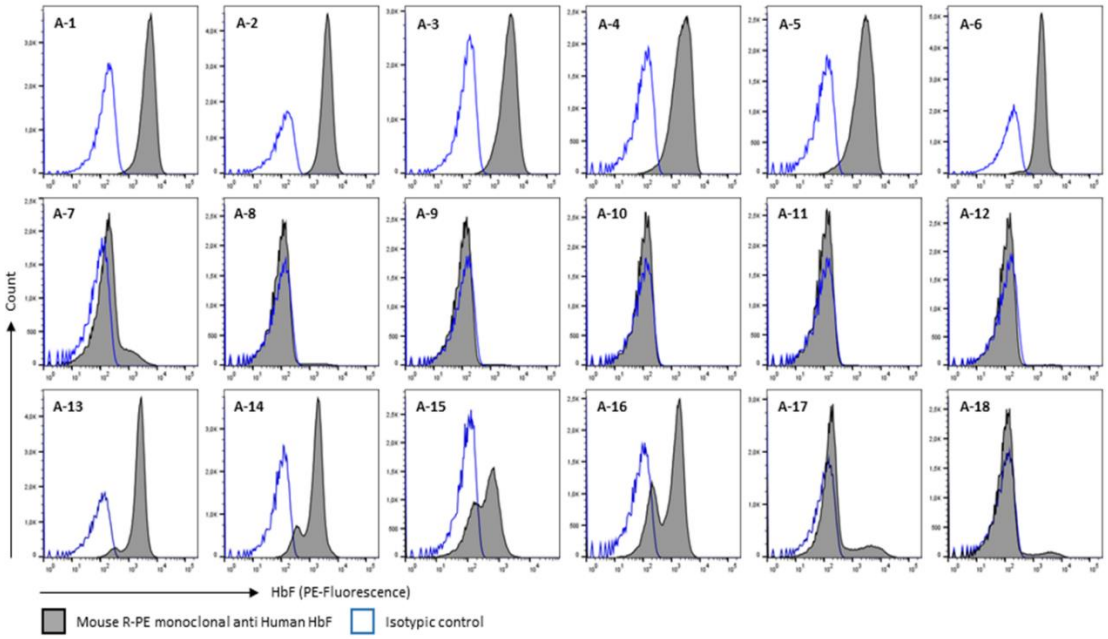

Figure 37 | Individual histograms of the 18 non-SCD individuals analyzed. A log-normal distribution of fluorescence (gray histograms) indicates a homogeneous distribution of HbF (patients A-1 to A-6 and A-8 to A-12) (one representative experiment). Blue lines represent the isotypic control. The horizontal axis shows the R-PE fluorescence (log scale); the vertical axis shows the RBC count.

The linear regression obtained between MCHbF and mean normalized HbF fluorescence for each non SCD individual functions as a standard curve, allowing the determination of HbF/RBC according to the measured fluorescence intensity (Figure 38).

Therefore, determining HbF/RBC in any sample consists in (1) assessing HbF fluorescence distribution by flow cytometry, (2) converting the fluorescence of each individual RBC in pg of HbF using the linear regression, (3) expressing results as a quantitative distribution in %RBC according to their HbF content, and (4) calculating HbF/RBC thresholds, which correspond to percentages of RBC containing at least arbitrary chosen HbF quantities (in picograms of HbF) (Figure 39).

Table 2 | Demographical, genetic and HbF characteristics of the 18 non SCD individuals.

Patient	Age at inclusion (years)	Gender	Genotype	%HbF	MCHbF (pg)
A-1	49	F	β-Thal / Secondary hemochromatosis	97.4	31.01
A-2	18	M	δβ-Thal	100.0	24.86
A-3	60	M	β-Thal	73.5	21.68
A-4	48	M	Eβ-Thal	63.1	13.31
A-5	45	M	β-Thal	62.1	12.66
A-6	49	F	HPFH	35.9	8.51
A-7	48	F	Genetic hemochromatosis	1.9	0.76
A-8	54	M	Genetic hemochromatosis	0.6	0.22
A-9	57	M	β-Thal	0.9	0.18
A-10	71	M	Genetic hemochromatosis C282Y homozygous	0.5	0.17
A-11	75	F	Genetic hemochromatosis	0.6	0.17
A-12	73	M	genetic hemochromatosis C282Y and H63D heterozygous	0.4	0.16
A-13	38	F	β-Thal	27.9	7.76
A-14	37	M	β-Thal	21.0	5.00
A-15	36	M	β-Thal	14.9	2.76
A-16	42	F	β-Thal	16.4	3.87
A-17	48	F	Genetic hemochromatosis	2.0	0.76
A-18	35	M	Genetic hemochromatosis	0.9	0.33

Table 3 | D'Agostino normality test results for HbF distribution in RBCs form patients enrolled in group A.

Patient	K^2	*p*	Log-normal distribution?
A-1	2.45	0.294	Yes
A-2	3.353	0.187	Yes
A-3	2.394	0.302	Yes
A-4	5.130	0.077	Yes
A-5	3.186	0.203	Yes
A-6	5.945	0.051	Yes
A-7	12.310	0.002	No
A-8	3.203	0.202	Yes
A-9	3.517	0.172	Yes
A-10	3.511	0.173	Yes
A-11	3.587	0.166	Yes
A-12	4.048	0.132	Yes
A-13	11.97	0.002	No
A-14	9.671	0.008	No
A-15	6.252	0.044	No
A-16	8.895	0.012	No
A-17	33.21	< 0.001	No
A-18	18.58	< 0.001	No

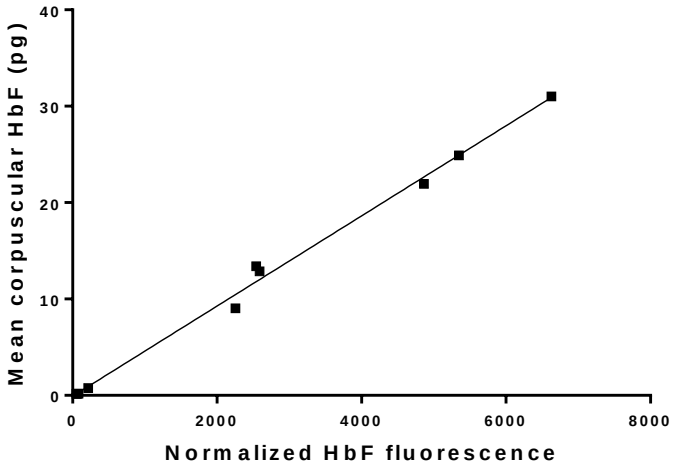

Figure 38 | Linear regression between the mean corpuscular HbF (assessed by HPLC) and the mean normalized HbF fluorescence. (Pearson correlations)

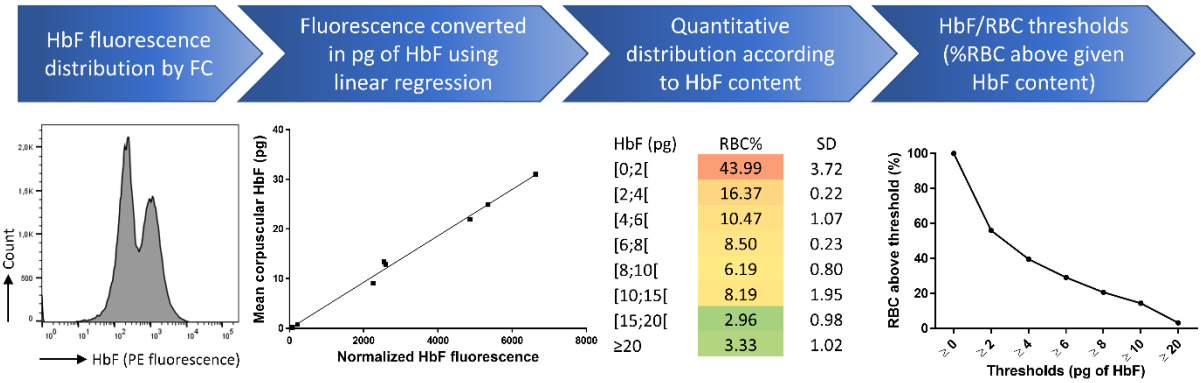

Figure 39 | HbF/RBC assay overview. Example of HbF/RBC quantification for one SCD patient. Once fluorescence is converted in pg of HbF, results can be expressed as %RBC classified according to their HbF content. Subsequently, HbF/RBC thresholds, which correspond to %RBC containing at least a given HbF quantity (in pg), can be calculated. (FC: flow cytometry; SD: standard deviation).

1.4. Assessment of the reliability of the assay

1.4.1. Variability

To consider a variability introduced by the use of different HbF monoclonal antibody batches, linear regressions were independently determined as the relationship between MCHbF and mean normalized HbF fluorescence for each group A individual using 3 different

batches (n°1; 2 and 3) (Figure 40). The linear regressions obtained were similar for the 3 batches (r = 0.9911 and P = 0.0010; r = 0.9930 and P <0.0001; r = 0.9978 and P <0.0001 for batches n°1, 2 and 3 respectively). We thus calculated a mean linear regression including all the data measured with the 3 batches (r = 0.9984; P <0.0001). This mean linear regression was used for the HbF quantifications.

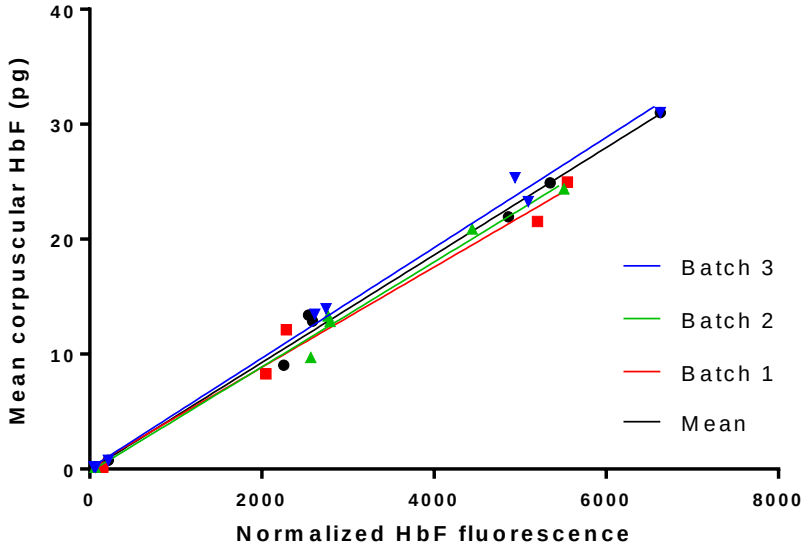

Figure 40 | Linear regressions between the mean corpuscular HbF (assessed by HPLC) and the mean normalized HbF fluorescence using different antibody batches. 3 batches (batch n°1, 5 patients, n = 3; batch n°2, 6 patients, n = 4; and batch n°3, 11 patients, n = 4) were independently used (Pearson correlations).

To allow the analysis of several samples from patients' follow-up in the same time, RBCs can easily be frozen in glycerol. We compared results of HbF/RBC quantification obtained from fresh and frozen RBCs. Freezing of the RBCs does not alter the quantification as we observed similar distributions (Figure 41).

1.4.2. Repeatability and reproducibility of the method

Repeatability (Figure 42) and reproducibility (Figure 43) experiments gave good precision results with highest coefficients of variation (CV) (> 20%) only observed for ranges containing less than 1% of total RBC what is expected due to the low mean %RBC in the corresponding ranges (as CV is a ratio of the SD to the mean).

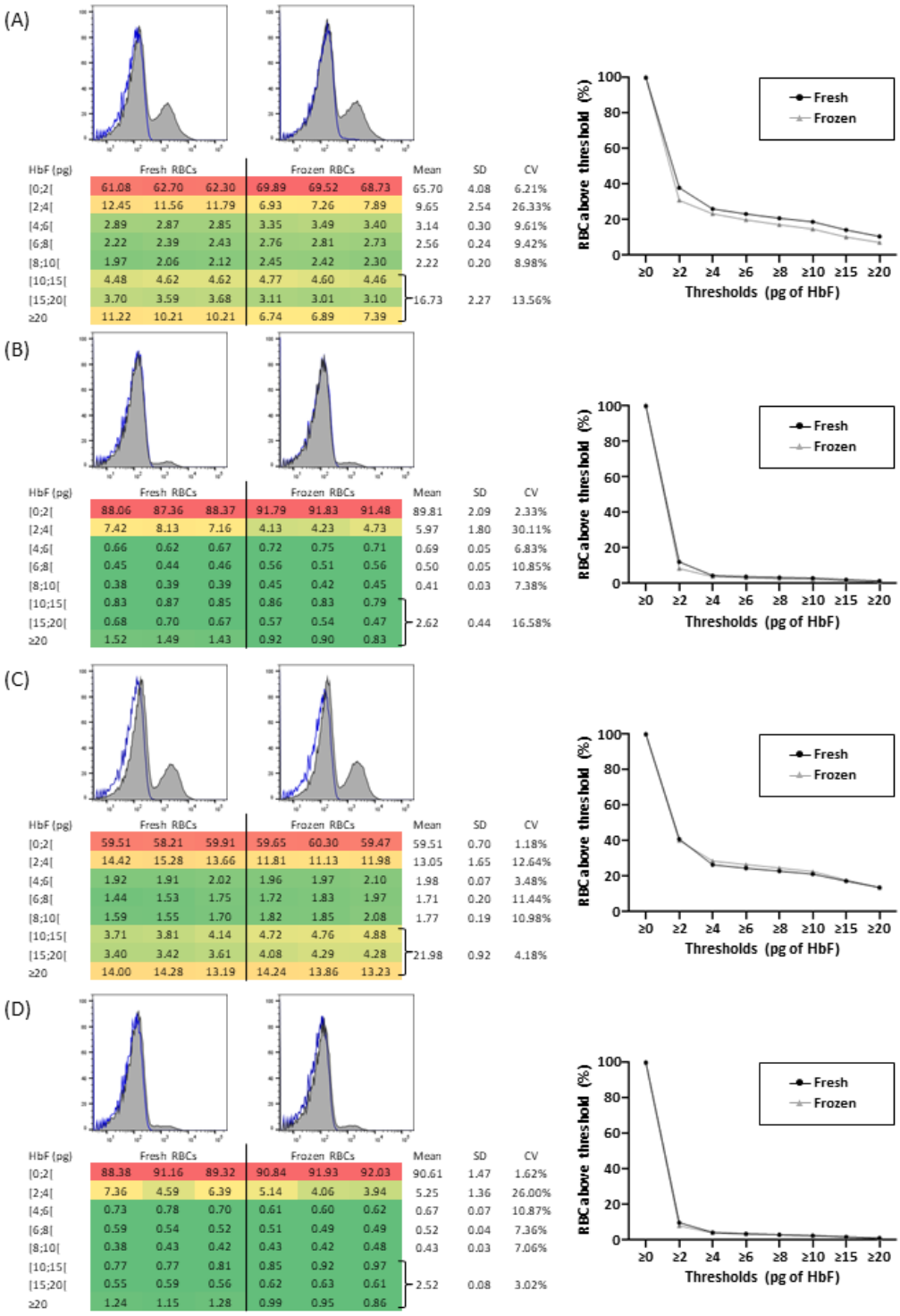

Figure 41 | Comparison of HbF/RBC measurement between fresh and frozen samples. HbF fluorescence distribution in RBCs and quantification of HbF/RBC assessed by flow cytometry after intracellular staining of HbF. 5µl of packed RBCs from 3 SS patients (**A**, **B** and **C**) and 1 HD (**D**) were fixed then permeabilized prior to incubation with R-PE-coupled anti Human-HbF monoclonal antibody and were analyzed by flow cytometry (n = 3 independent replicates performed the same day). Representative histograms obtained from fresh (left) and frozen (right) samples (upper panels). Gray histograms represent the HbF and blue lines represent unstained cells or isotypic control. Horizontal axis shows the R-PE fluorescence (log scale); Percentage of RBC classified by HbF/RBC (lower panel) (SD: Standard deviation; CV: coefficient of variation). Percentages of RBCs containing at least the indicated quantity of HbF (thresholds) (right curves).

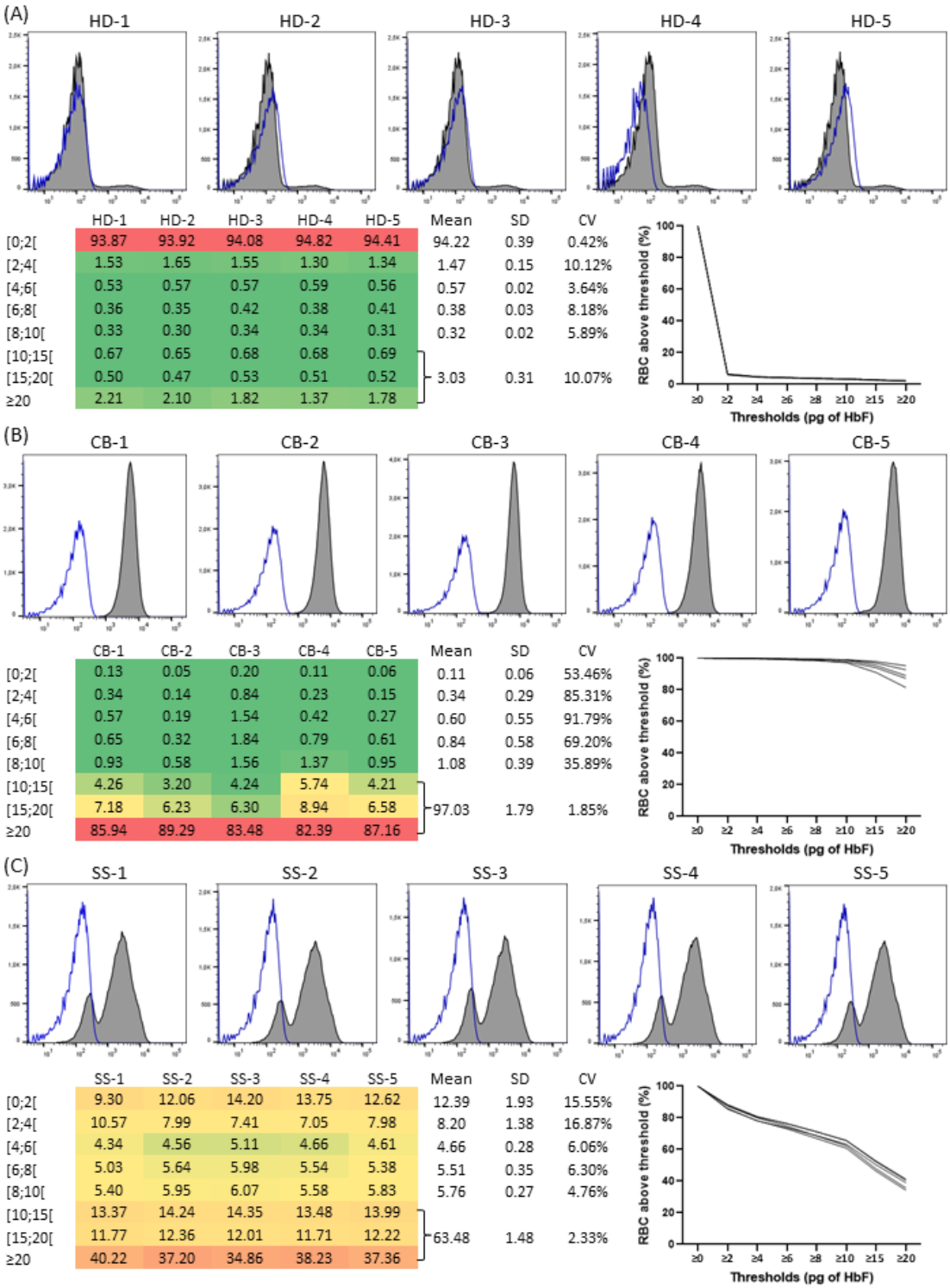

Figure 42 | Repeatability of the method. HbF fluorescence distribution in RBCs and quantification of HbF/RBC assessed by flow cytometry after intracellular staining of HbF. 5µl of packed RBCs from 1 HD (**A**), 1 CB (**B**) and 1 SS (**C**) patient were fixed then permeabilized prior to incubation with R-PE-coupled anti Human-HbF monoclonal antibody and were analyzed by flow cytometry (n = 5 independent experiments performed the same day). Histograms of the 5 replicates of each sample (upper panel). Gray histograms represent the HbF and blue lines represent unstained cells or isotypic control. Horizontal axis shows the R-PE fluorescence (log scale), vertical axis shows the RBC count. Percentage of RBC classified by HbF/RBC (lower panel) (SD: Standard deviation; CV: coefficient of variation) and percentages of RBCs containing at least the indicated quantity of HbF (thresholds).

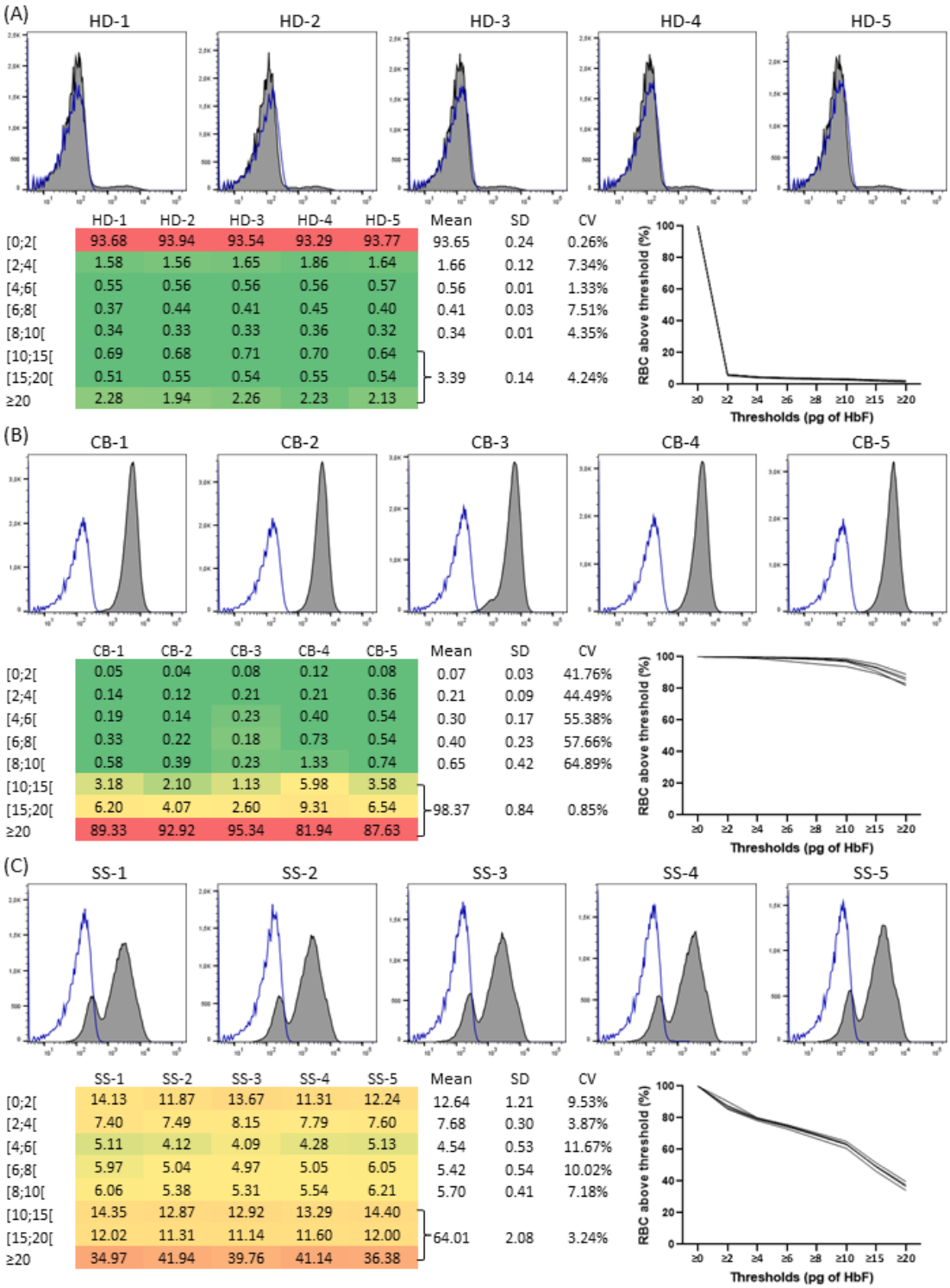

Figure 43 | Reproducibility of the method. HbF fluorescence distribution in RBCs and quantification of HbF/RBC assessed by flow cytometry after intracellular staining of HbF. 5µl of packed RBCs from 1 HD (**A**), 1 CB (**B**) and 1 SS (**C**) patient were fixed then permeabilized prior to incubation with R-PE-coupled anti Human-HbF monoclonal antibody and were analyzed by flow cytometry (n = 5 independent experiments performed on 5 different days). Histograms of the 5 replicates of each sample (upper panel). Gray histograms represent the HbF and blue lines represent unstained cells or isotypic control. Horizontal axis shows the R-PE fluorescence (log scale); vertical axis shows the RBC count. Percentage of RBC classified by HbF/RBC (lower panel) (SD: Standard deviation; CV: coefficient of variation) and percentages of RBCs containing at least the indicated quantity of HbF (thresholds).

2. Assessment of HbF biological and clinical protective thresholds in sickle cell disease

2.1. Quantitative measurements of HbF/RBC upon HU treatment

In the hypothesis of an « HbF per red blood cell threshold » in SCD, we used the above validated method to analyze HbF quantitative distribution in SCD patients before, during and after treatment by HU. 14 adult SCD patients (11 women and 3 men; mean age (± SD) = 34.9 ± 8 years) were included in the study. Table 4 provides the biologic parameters assessed before and after ≥6 months of HU.

HbF distributions were assessed by flow cytometry before and during HU treatment showing different types of response (Figure 44). R-PE fluorescence intensity was collected for each RBC, normalized and referred to the mean linear regression to calculate the corresponding amount of HbF/RBC in picograms. Percentages of RBC were classified according different ranges of HbF/RBC which were compared during HU treatment for the 14 group B patients (Figure 45).

Statistically significant variations were only found in low ranges of HbF/RBC (HbF <2 pg, P = 0.001 and 2≤ HbF <4 pg, P <0.001; Friedman test) with a 16,6 % decrease between D0 and ≥M6 in RBCs containing less than 2 pg and a 1.7-fold increase in RBCs containing between 2 and 4 pg. Interestingly, the increase in cells containing 2-4 pg HbF (+7.36%) accounted for almost 40% of the sum of the increase of cells containing more than 2 pg HbF (+15.69%). Concomitantly, RBC population with HbF/RBC >20 pg increased up to 3.5-fold but this change was not statistically significant (P = 0.135; Friedman test).

To analyze these results, thresholds of HbF/RBC, which correspond to the percentage of RBC containing at least a given HbF quantity in pg were calculated for each patient for thresholds of 2, 4, 6, 8 and 10 pg of HbF (Figure 46). Upon HU treatment, an increase in mean %RBC for every threshold was observed, statistically significant for the number of RBCs containing at least 2 pg of HbF (P = 0.0015; Friedman test).

Table 4 | Changes in biological parameters during hydroxyurea treatment for group B patients (Median [first quartile - third quartile]) (Wilcoxon matched-pairs signed rank test).

	D0	≥M6	*p*	mv
%HbF	6.2 [2.8-8.4]	14.2 [7.7-21.1]	**0.001**	2
Total hemoglobin (g/dL)	8.4 [7.3-9.4]	9.5 [8.3-10.5]	**0.006**	3
Red blood cells (10^{12}/L)	2.6 [2.2-3.4]	2.8 [2.4-3.4]	0.865	3
Reticulocytes (10^9/L)	245.5 [190.5-260.0]	120 [78.5-211.0]	**0.008**	4
MCV (fL)	89.5 [83.0-94.5]	100.5 [91.2-115.2]	**0.002**	2
MCHC (g/dl)	34 [33-35]	33 [32-34]	**0.016**	3
MCH (pg)	30 [28.0-32.9]	34.5 [32-40.7]	**0.001**	2
Leucocytes (10^9/L)	10.3 [9.7-12.1]	6.5 [5.4-8.5]	**0.002**	3
Platelets (10^9/L)	432.5 [329.0-529.2]	354.5 [269.0-468.5]	**0.005**	2
LDH (U/L)	360 [223-511]	327 [213-383]	0.067	3
Total bilirubin (µmol/L)	42 [34.2-53.7]	33.5 [24.2-46.2]	**0.005**	2
ASAT (U/L)	36 [26.0-54.7]	29 [26.2-46.5]	0.060	2
F cells (%) method 1	40.3 [20.6-48.2]	54.6 [41.1-73.3]	**0.001**	0
F cells (%) method 2	35.6 [18.3-42.7]	52.8 [31.8-70.2]	**0.001**	0

mv (missing value); MCV (Mean Corpuscular Volume); MCHC (Mean Corpuscular Hemoglobin Concentration); MCH (Mean corpuscular Hemoglobin); LDH (Lactate Dehydrogenase); ASAT (aspartate aminotransferase).

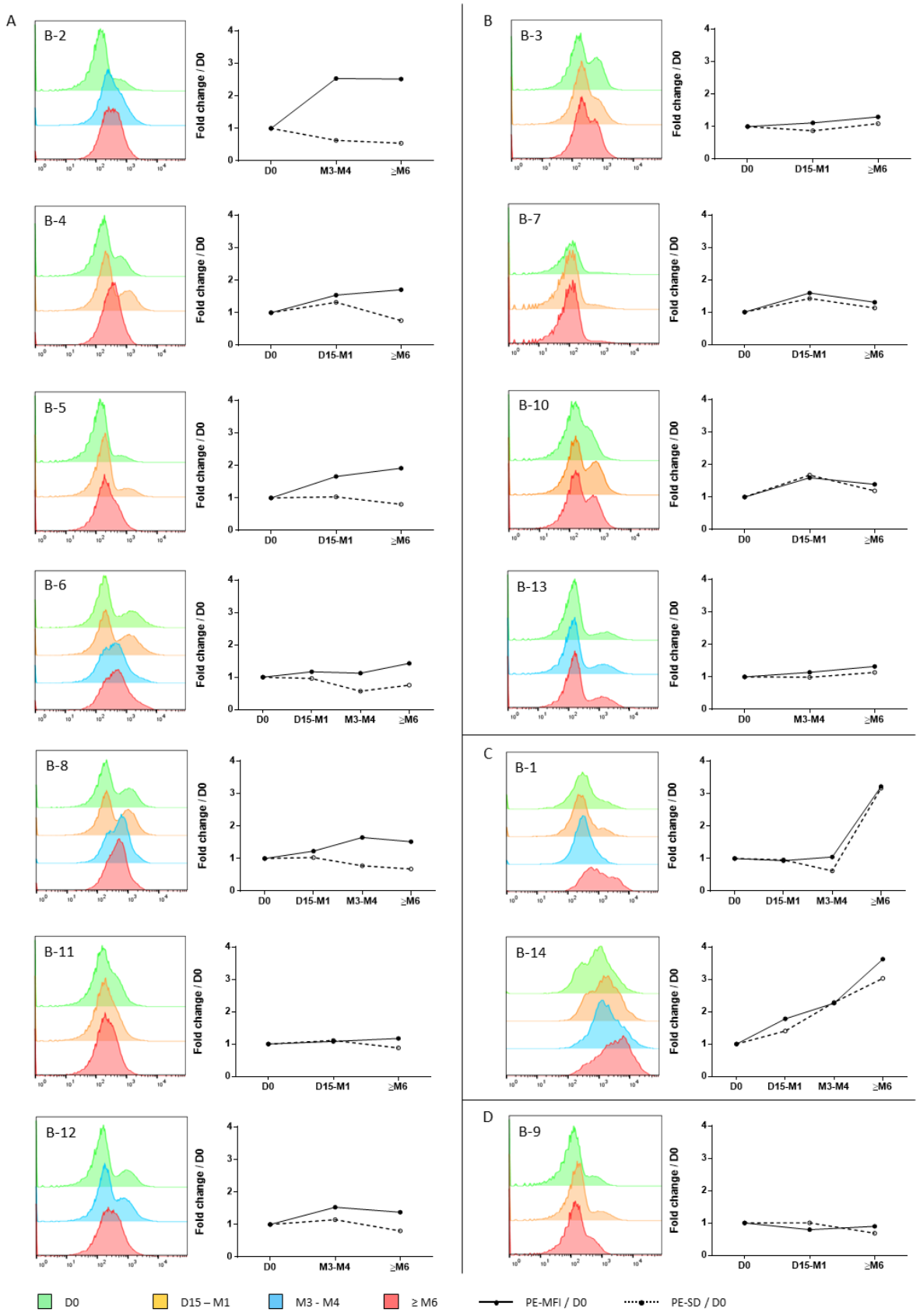

Figure 44 | Evolution of HbF distribution during HU treatment. For the follow-up, 5 µl of packed RBCs from group B patients were fixed then permeabilized prior to incubation with R-PE-coupled anti Human-HbF monoclonal antibody and were analyzed by flow cytometry. HbF fluorescence intensity (PE-MFI) and fluorescence standard deviation (PE-SD) values were extracted after analysis with FlowJo

v10 software and were expressed as the fold-change from D0. (**A**) 7 patients presenting an increase in HbF and a homogenization of the HbF distribution. (**B**) 4 patients presenting an increase in HbF but little change in the distribution. (**C**) 2 patients presenting an increase in both HbF and heterogeneity of distribution. (**D**) 1 patient for whom HbF level did not change but the distribution became more homogeneous. Histograms (left): the horizontal axis shows the R-PE fluorescence (log scale), the vertical axis shows the RBC count. Curves (right): the vertical axis shows the PE-MFI or PE-SD fold-change from D0.

	HU follow up				
HbF/RBC (pg)	D0	D15-M4	≥M6	*P*	n
[0;2[	75.21	65.10	62.69	**0.001**	14
[2;4[	10.36	14.88	17.72	**<0.001**	14
[4;6[	5.46	7.37	6.52	0.223	14
[6;8[	2.97	4.06	3.01	0.223	14
[8;10[	1.77	2.38	1.79	0.145	14
[10;15[	0.88	1.23	1.42	0.257	14
[15;20[	2.11	2.88	2.52	0.135	14
≥20	1.24	2.11	4.34	0.135	14
Mean HbF	6.2%	7.9%	15.2%		

Colorimetric scale (% of RBC):

1	5	10	15	20	30	40	50	60	70	80	90	100

Figure 45 | Percentages of RBC classified by HbF/RBC ranges before and under HU. Data represents mean % of RBCs in each range of HbF/RBC for the 14 group B patients at D0, between D15 and M4, and at ≥M6 of HU (Friedman test). Mean %HbF was assessed by HPLC. The color scale shows the %RBC by range.

(A)

	HU follow-up				
HbF/RBC (pg)	D0	D15-M4	≥M6	*p*	*n*
≥0	100	100	100		
≥2	24.79	34.90	37.31	**0.001**	14
≥4	14.43	20.02	19.59	0.395	14
≥6	8.97	12.65	13.07	0.135	14
≥8	6.00	8.60	10.06	0.223	14
≥10	4.23	6.22	8.27	0.257	14
≥20	1.24	2.11	4.34	0.135	14

Colorimetric scale (% of RBC):

1	5	10	15	20	30	40	50	60	70	80	90	100

(B)

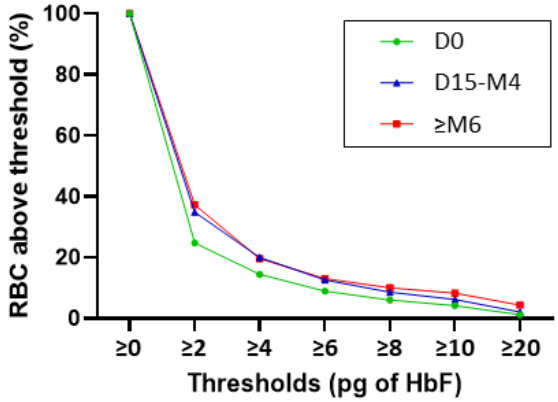

Figure 46 | Evolution of %RBC above HbF thresholds upon HU treatment. (**A**) Mean percentage of RBC according to HbF/RBC thresholds before and during HU for the 14 group B patients. (Friedman test). The color scale shows the %RBC by range. (**B**) Mean percentages of RBC containing at least the indicated quantity of HbF (thresholds) at D0 (green), between D15 and M4 (mean value – blue) and ≥M6 (red) for the 14 group B patients.

2.2. Protective effects according to HbF/RBC content

2.2.1. Correlations between biologic parameters and HbF/RBC thresholds

Correlations were evaluated between percentages of RBC by each HbF/RBC threshold and biologic parameters, independently of the duration of HU treatment (Figure 47). Increase in mean %HbF, MCV and MCH and decrease in RBC count were significantly associated with the number of RBC containing at least 2 pg of HbF ($P < 0.0001$; < 0.0001; < 0.001; and < 0.001, respectively). Interestingly, LDH, total bilirubin and ASAT were statistically not correlated with a HbF/RBC threshold.

Moreover, when looking at the evolution between day 0 and ≥6 months, the median increase in %RBC with more than 2 pg of HbF/RBC (+12.06% [4.09 - 22.0]; median [interquartile range]) was correlated with the median increase in %HbF (+7.8% [2.2 – 14.1]) ($r = 0.7426$; $P = 0.0074$), and correlated with the median decrease in total bilirubin (-8.0 µmol/L [13.5 – 0.7]) ($r = -0.5860$; $P = 0.0371$) and in reticulocytes (-78.0 109/L [159.5 – 3.5]) ($r = -0.7133$; $P = 0.0118$) (Spearman correlations).

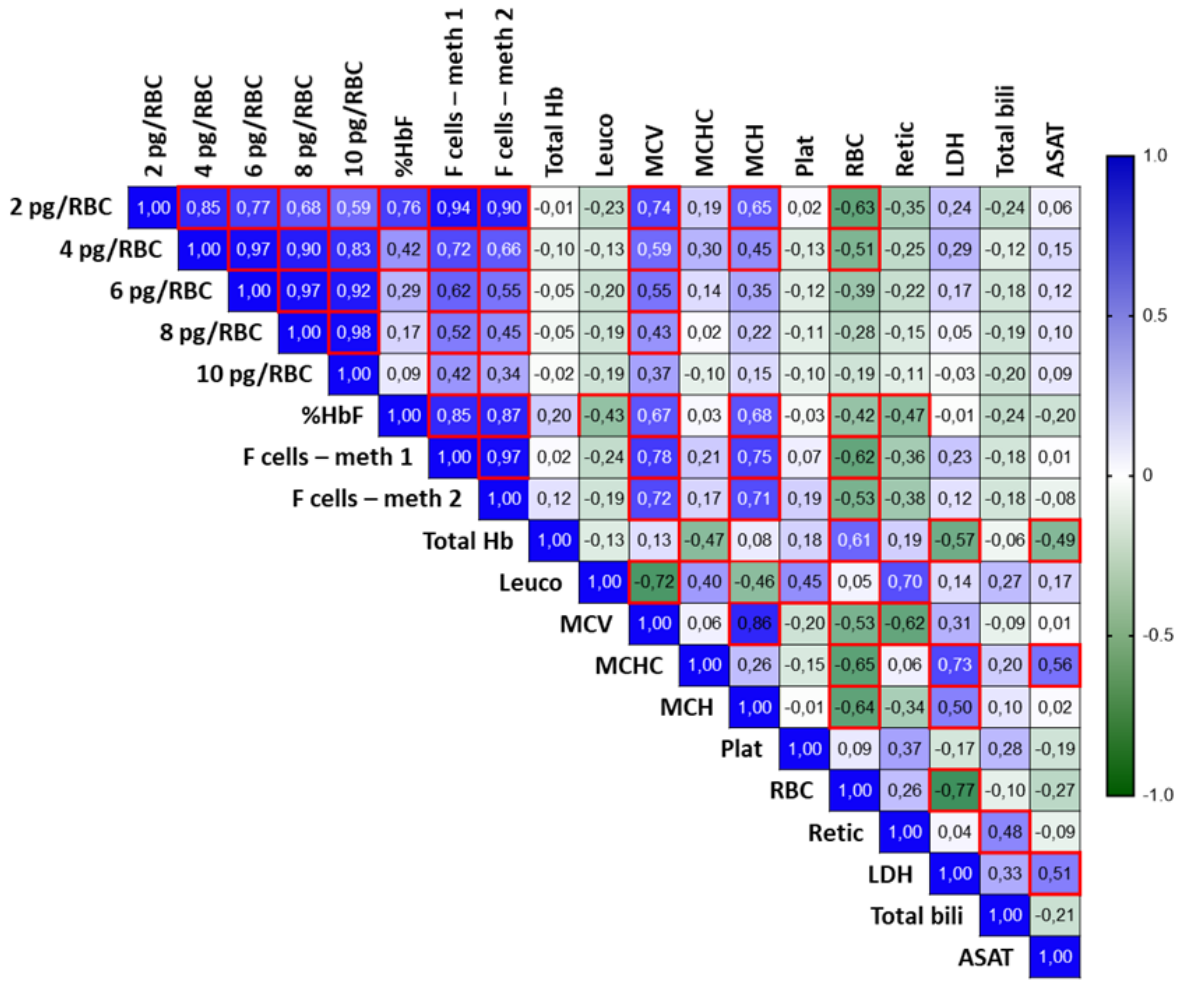

Figure 47 | Triangular heat map representing the pairwise correlation coefficients between biologic parameters and %RBC containing at least the indicated quantity of HbF (2, 4, 6, 8 and 10 pg). The color scale shows the value of the Spearman correlation coefficient (r). Blue values represent positive correlations and green values represent negative correlations. Values in red frame correspond to statistically significant correlations (P <0.05).

Total Hb: total hemoglobin; Leuko: leukocytes; MCV: mean corpuscular volume; MCHC: mean corpuscular hemoglobin concentration; MCH: mean corpuscular hemoglobin; Plat: platelets; RBC: red blood cells; Retic: reticulocytes; Total bili: total bilirubin; LDH: lactate dehydrogenase; ASAT: aspartate aminotransferase.

2.2.2. Associations between HbF/RBC thresholds and VOC incidence

VOC incidence for the 14 group B patients was collected for the 3 years preceding D0 and the 3 following years after 6 months of HU at stable dose. The VOC number/3 years before and after HU was not statistically different (P = 0.4414; Wilcoxon test). Among the 14 patients, 6 decreased their VOC incidence after HU treatment (B-2; -6; -10; -11; -12 and -14), 4 did not change (B-1; -4; -8 and –13) and 4 increased (B-3; -5; -7 and –9). When looking at the HbF distribution, 66.6% of patients with decreased VOC incidence (4/6) had pancellular distribution while 75% of patients with increased VOC (3/4) had heterocellular distribution after HU (Figure 44).

Percentage of HbF determined by HPLC, and F cell frequency assessed by the two methods, were not significantly related to VOC incidence (r = -0.036; P = 0.856, r = -0.203; P = 0.299, r = -0.287; P = 0.139, respectively – Spearman correlation). Hypothesizing that a threshold of HbF/RBC could impact the VOC incidence, we analyzed hospitalizations for VOC for the two 3-year periods (before and after HU treatment) with corresponding HbF/RBC thresholds. The association of VOC incidence over 3 years was statistically significant with the percentage of RBC above HbF/RBC thresholds of 4, 6, 8 and 10 pg, with a trend toward association with threshold of 2 pg.

ROC analyzes were performed to compare %HbF, F cell frequency and HbF/RBC thresholds as a predictive value of the VOC incidence with a threshold of ≤1 VOC over a period of 3 years (Figure 48). For each threshold, area under curve (AUC) was higher than %HbF (AUC = 0.549; P = 0.659) or F cells frequency (AUC = 0.734; P = 0.139 and AUC = 0.693; P = 0.086, for methods 1 and 2, respectively). Moreover, only ROC curves performed with %RBC above the different thresholds of HbF/RBC were statistically significant as compared to global %HbF and F cell frequency.

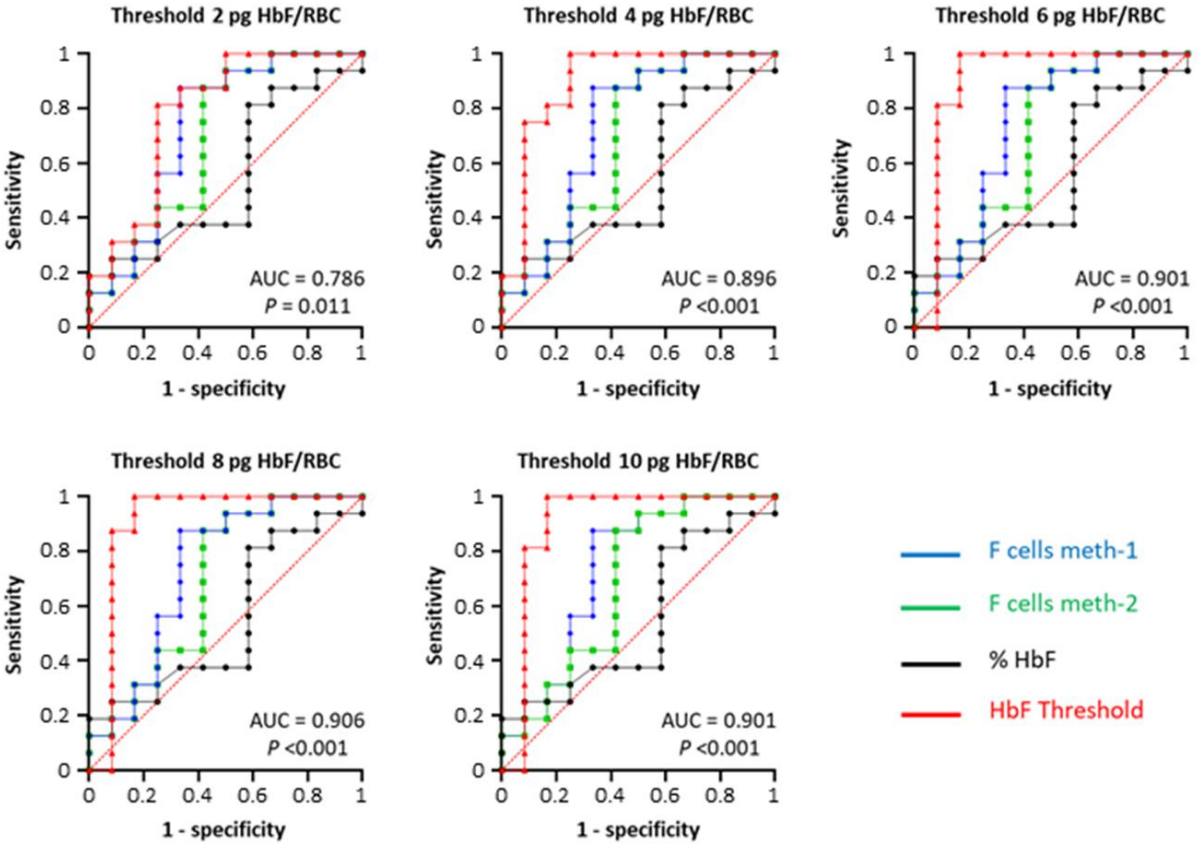

Figure 48 | ROC curves of %HbF, F cell frequency (by method 1 and 2) and %RBC containing at least the indicated threshold of HbF for a VOC incidence cut-off of ≤1 over 3 years. Indicated AUC corresponds to HbF threshold.

To assess the minimal quantity of HbF/RBC corresponding to the level of detection of F cells by flow cytometry, we performed HbF/RBC quantification on SCD patients and applied the two described methods (Figure 35). The lowest value of fluorescence intensity was extracted and then converted into pg of HbF. We measured a variable HbF positivity threshold of 1.86 pg ± 0.47 (ranging from 0.91 to 2.80 pg) and 3.21 pg ± 1.26 (mean ± SD) (ranging from 0.87 to 6.04 pg) for methods 1 and 2, respectively (n = 71) (Figure 49), inducing higher values of F cell frequencies measured by method 1 for group B patients (Table 4).

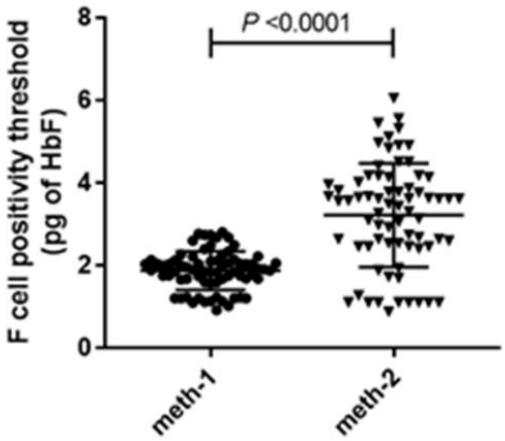

Figure 49 | Variability of F cell detection threshold measured by flow cytometry with method 1 (meth 1) and method 2 (meth 2) (n = 71) showing discrepancy according to the method used (Wilcoxon test).

2.2.3. Associations between HbF/RBC thresholds and *in vitro* RBC sickling

To confirm the results obtained on VOC*, in vitro* sickling assays by enzymatic deoxygenation were performed on RBCs from 56 SCD patients treated by HU or not (n = 13 and n = 43, respectively) and healthy donors as control (n = 4) (Figure 50). Mean %HbF and mean percentage of sickle cells were 15.3% ± 10.2 and 36.5% ± 18.0 for treated patients and 8.9% ± 6.8 and 57.2% ± 11.6 for untreated patients. Percentage of sickle cells was inversely correlated with global %HbF and HbF/RBC thresholds of 2, 4, 6, 8 and 10 pg (Spearman correlations) (Figure 51).

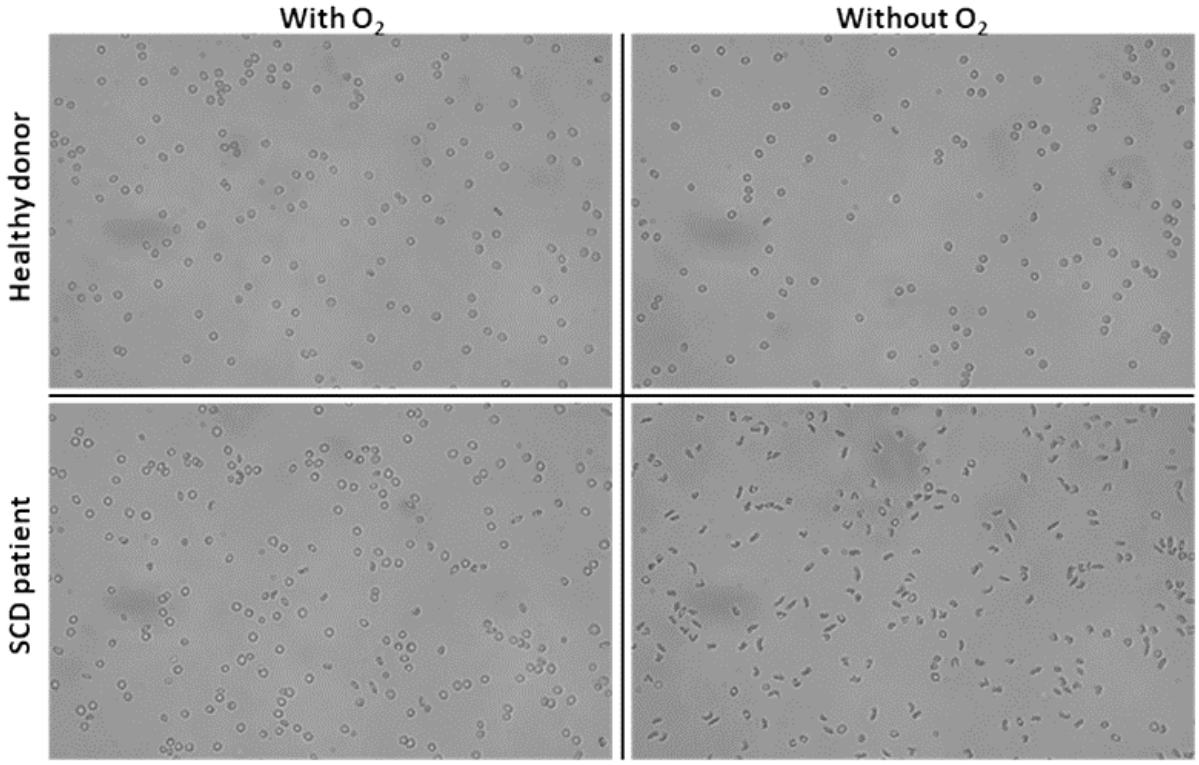

Figure 50 | Representative pictures of in vitro sickling assay before (left panel) and after (right panel) enzymatic deoxygenation for one healthy donor (n = 4) and one SCD patient (n = 56) (magnification = 200).

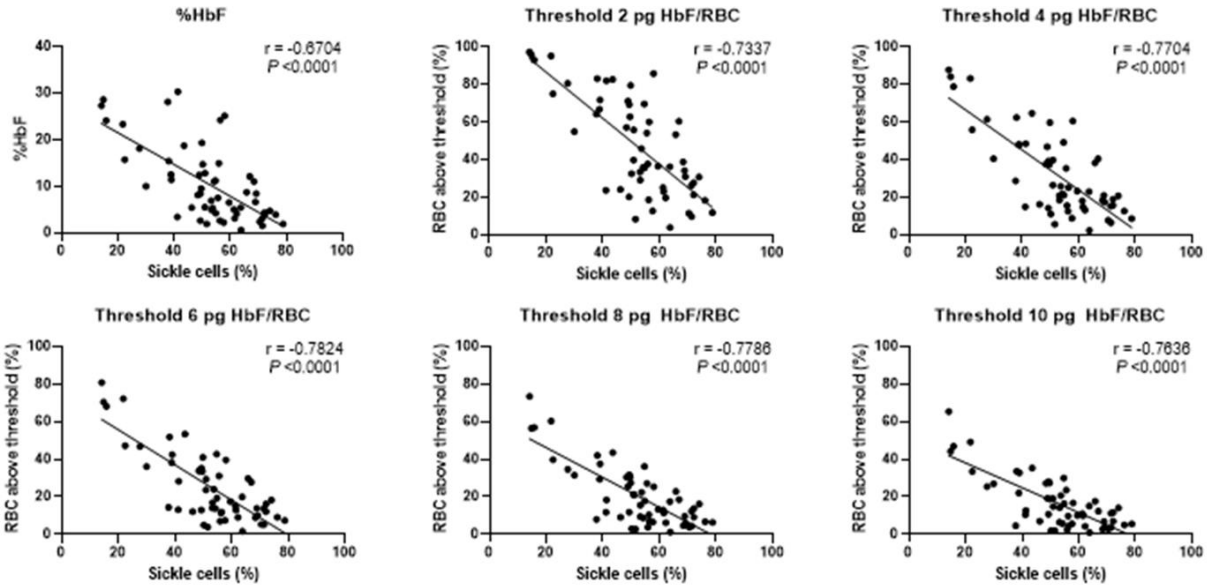

Figure 51| Association between global %HbF of %RBC containing at least the indicated threshold of HbF/RBC and percentage of sickle cells counted after enzymatic deoxygenation (n = 46) (Spearman correlations).

3. Comparison of HbF content in reticulocytes and mature erythrocytes in sickle cell disease patients

3.1. Analysis of HbF content in reticulocytes

Among several specific markers, reticulocytes still express transmembrane proteins such as the transferrin receptor CD71, allowing their discrimination from mature erythrocytes. The addition of an anti-human CD71 monoclonal antibody couple to APC-H7 fluorochrome during the incubation with the anti-human HbF antibody allows the measurement of HbF content in reticulocytes in a blood sample (Figure 52). HbF histogram overlays showed the same distribution in mature erythrocytes (CD71-negative cells) and in reticulocytes (CD71-positive cells in samples from cord blood or healthy donors.

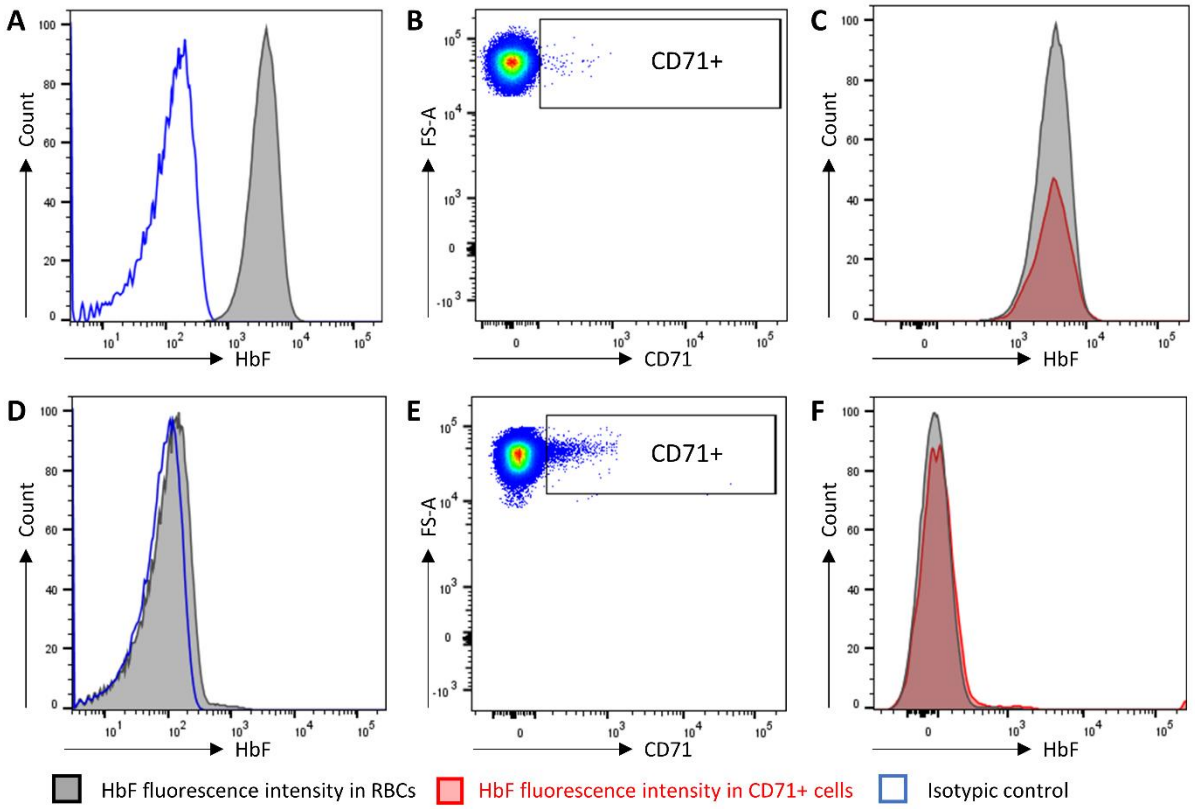

Figure 52 | Assessment of HbF in mature RBCs and reticulocytes. Representative FACS analysis of RBCs isolated from cord blood (A-C; *n* = 3) and from healthy donors (D-F; *n* = 5). (**A and D**) HbF fluorescence distribution in total RBCs, including CD71 positive cells. (**B and E**) Discrimination of CD71 positive cells from negative cells. (**C and F**) Histogram overlays of HbF fluorescence distribution in CD71 negative cells (gray histograms) and CD71 positive cells (red histograms) showing identical distribution between the two populations. Blue lines represent isotypic control. Horizontal axis shows the R-PE (HbF) or APC-H7 (CD71) fluorescence (log scale), vertical axis shows the RBC count or forward scatter (FSC-A).

3.2. Accumulation of high HbF containing RBCs in circulating blood of SCD patients by comparison with their reticulocytes

3.2.1. Comparison of quantitative distribution between reticulocytes and mature erythrocytes

Using this discrimination, we assessed HbF quantitative distributions in reticulocytes (Retic; CD71-positive cells) and in mature erythrocytes (RBCs; CD71-negative cells) from 12 SCD selected patients presenting a heterogeneous distribution of HbF. We observed for all patients, at varying degrees, an increase in the RBC populations containing high HbF level by comparison with reticulocytes (Figure 53). Statistically significant lower percentages of Retic containing between 6-8 pg, 8-10 pg and ≥10 pg of HbF (P <0.001; P <0.001 and P <0.001, respectively) by comparison with percentages of RBCs were observed (Figure 54A). This difference was associated with a statistically significant higher percentage of Retic containing less than 4 pg of HbF (P < 0.001) by comparison with percentage of RBC. In contrast, quantifications done on cells from HD showed no statistically significant differences between %RBC and %Retic (Figure 54B).

We then calculated mean fold-increase values (enrichment), from Retic to RBCs, which correspond to the ratio of %RBC/%Retic for each range of HbF/cell, for the 12 selected SCD patients (Figure 54C). Enrichments were not calculated for HD because no differences between Retic and RBCs were observed. For SCD patients, mean enrichments were 0.86, 1.48, 2.51, 3.35 and 2.92 for cells containing between 0-4 pg, 4-6 pg, 6-8 pg, 8-10 pg and ≥10 pg of HbF, respectively.

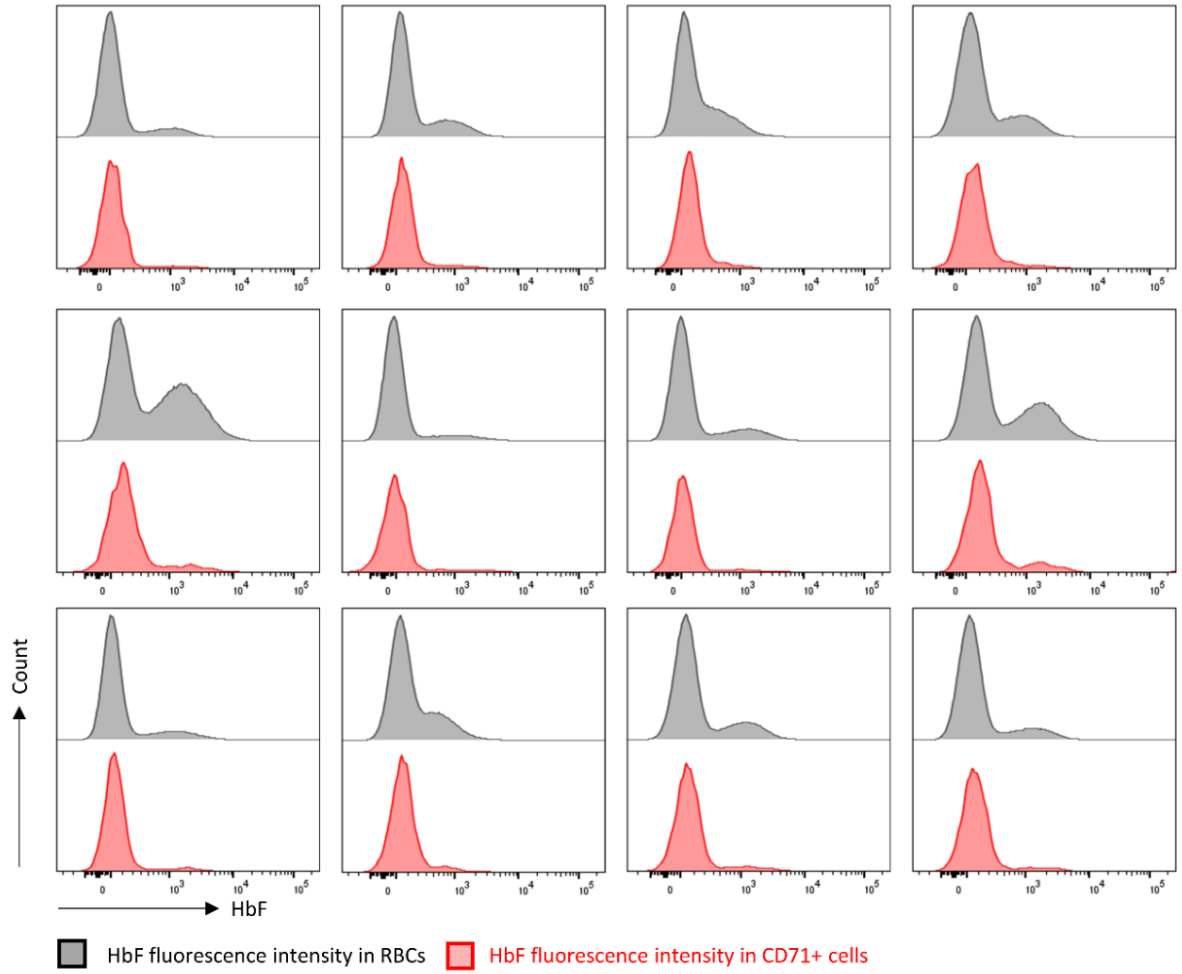

Figure 53 | Assessment of HbF distribution in mature RBCs and reticulocytes from SCD patients presenting a heterogeneous distribution. Representative histograms showing an increase in the RBC populations containing high HbF level by comparison with corresponding reticulocytes (12 patients, *n* = 2). Horizontal axis shows the R-PE (HbF) fluorescence (log scale), vertical axis shows the RBC count.

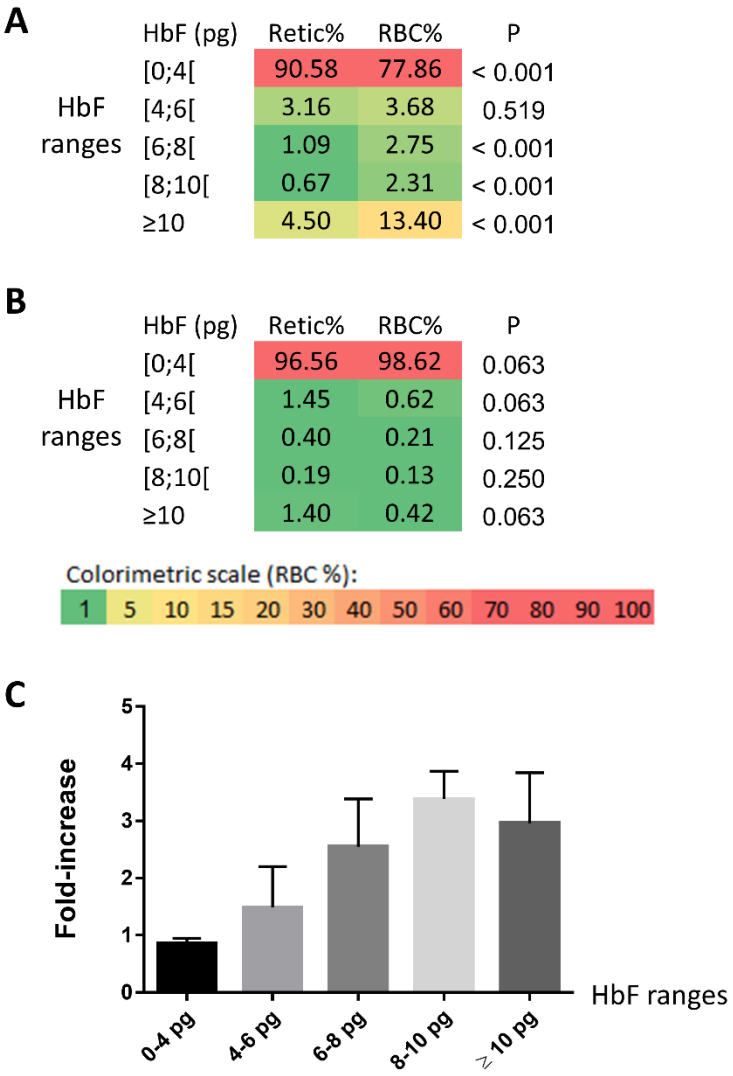

Figure 54 | Quantitative HbF distribution in reticulocytes and in mature RBCs. (**A**) (left) Mean reticulocyte (Retic) and RBC percentages classified by HbF content for the 12 SCD patients presenting a heterogeneous HbF distribution (Wilcoxon test). (**B**) Mean Retic and RBC percentages classified by HbF content for HD (*n* = 5) (Wilcoxon test). (**C**) Mean fold-increase (enrichment) calculated as the ratio of mean %RBC to mean %Retic according to HbF content for the 12 SCD patients. (Wilcoxon test).

3.2.2. Comparison of reticulocyte and mature erythrocyte percentages above HbF thresholds

To determine if a threshold of HbF/cell could be associated with the differences we observed between Retic and RBCs, the percentages of Retic and RBCs above different HbF thresholds were compared. As observed in the quantitative distribution of cells from HD, no differences were observed between mean Retic and RBC percentages above the different HbF

thresholds (Figure 55A). In contrast, mean percentages of Retic from the 12 SCD patients above the different thresholds of HbF were lower than mean percentages of RBC (Figure 55B). These differences between mean percentages of Retic and RBC were statistically significant for all the thresholds ($P = 0.022$, $P < 0.001$, $P < 0.001$, $P < 0.001$ and $P < 0.001$, for HbF thresholds of ≥ 2 pg, ≥ 4 pg, ≥ 6 pg, ≥ 8 pg and ≥ 10 pg, respectively) with %Retic lower than %RBC for each thresholds (Figure 55C). We thus calculated mean fold-increase values (enrichment), from Retic to RBCs, which correspond to the ratio of %RBC/%Retic above each HbF thresholds, for the 12 selected SCD patients (Figure 55D). A slight mean enrichment (1.09) was observed for the threshold of 2 pg of HbF. Mean enrichment was 2.38 ± 0.55 (mean ± SD) for cells with ≥ 4 pg. Mean enrichments raised to 2.88 ± 0.74 for cells with ≥ 6 pg of HbF and were 2.95 ± 0.80 and 2.92 ± 0.86, for cells with ≥ 8 pg and with ≥ 10 pg of HbF, respectively.

These results suggest an accumulation in circulating RBCs containing ≥ 4 pg of HbF and is more pronounced for RBCs containing ≥ 6 pg of HbF.

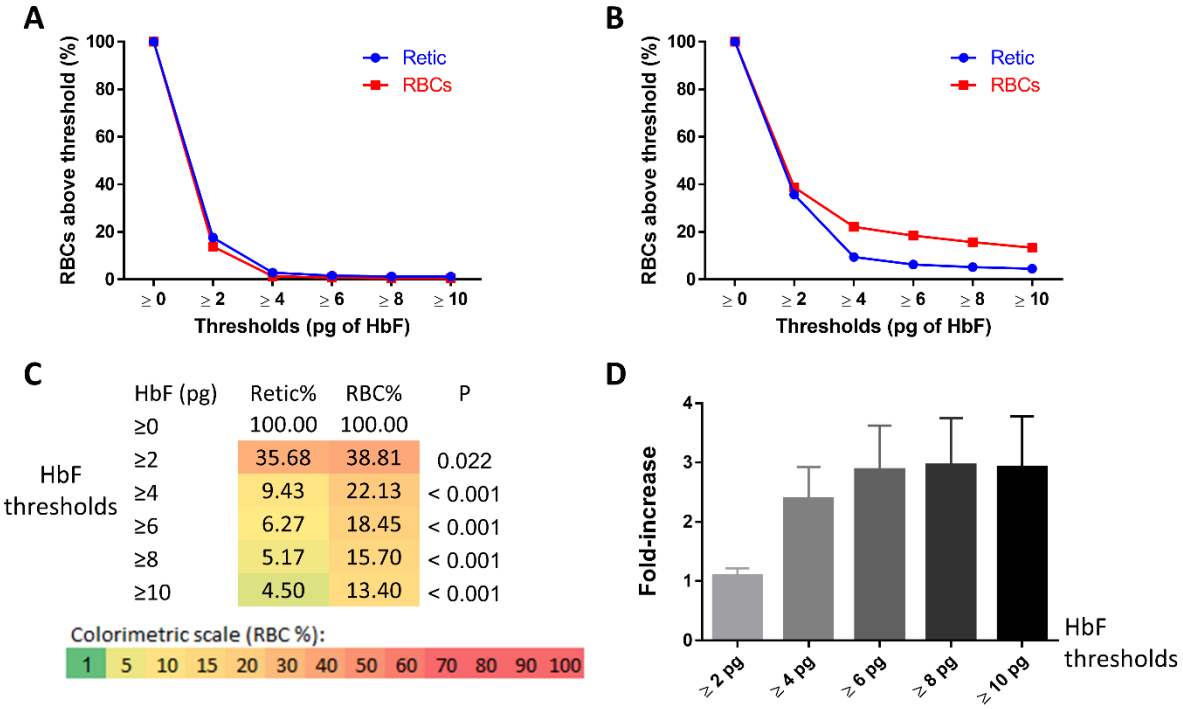

Figure 55 | Enrichments in %RBC as compared to %Retic according to HbF thresholds. (**A**) Mean percentages of cells containing at least the indicated quantity of HbF (thresholds) for Retic (blue) and RBCs (red) from HD (*n* = 5). (**B**) Mean percentages of cells containing at least the indicated quantity of HbF (thresholds) for Retic (blue) and RBCs (red) from the 12 SCD patients. (**C**) Mean percentages of Retic and RBC according to HbF/cell thresholds for the 12 SCD patients (Wilcoxon test). (**D**) Mean fold-increase (enrichment) calculated as the ratio of mean %RBC to mean %Retic containing at least the indicated HbF content for the 12 SCD patients.

4. HbF/RBC quantification in patients with severe SCD treated with sh-BCL11A gene therapy

4.1. HbF/RBC quantification as a measure of endogenous HbF expression induced by gene therapy

The results presented here represent a perfect example of the vast possible use of this new method in the field of gene therapy for SCD. They are part of a collaborative work with the Boston Children's Hospital in the pilot and feasibility gene therapy study (NCT03282656), which evaluates the safety of infusion of LV vector BCH-BB694 transduced autologous CD34+ cells in patients with severe SCD. First data from the full adult cohort which has completed enrollment with > 6 months of follow up in all patients was reported in 2019 at the annual meeting of the American Society of Hematology (386).

4.2. Quantitative single cell HbF determination

Quantitative HbF/RBC quantification showed a 75.9% decrease in RBC containing less than 2 pg of HbF associated with a >5-fold increase in RBC% containing at least 4, 6, 8 and 10 pg of HbF (5.35-, 5.24-, 5.40- and 5.50-fold increase, respectively) only 4 months after drug product infusion by comparison with before (Figure 56). Of note, the patient was transfused before gene therapy, so the quantification includes RBCs from healthy donors (HbA was 33.4% of total Hb). RBCs from HD mainly contain HbA with very few amount of HbF. Thus, the fold increase calculated here might be slightly different if the quantification was only performed on patients' own RBCs. 4 months post gene therapy HbA was 4.6% of total Hb.

A

	pre-GT*			4 months post-GT	
HbF (pg)	RBC%	SD	HbF (pg)	RBC%	SD
[0;2[	78.86	1.01	[0;2[	18.97	1.51
[2;4[	11.06	0.49	[2;4[	19.69	0.95
[4;6[	1.94	0.77	[4;6[	12.71	0.13
[6;8[	1.48	0.43	[6;8[	8.52	0.26
[8;10[	1.23	0.09	[8;10[	6.58	0.23
≥10	5.43	2.78	≥10	33.53	2.41

Colorimetric scale (RBC %):

1 5 10 15 20 30 40 50 60 70 80 90 100

B

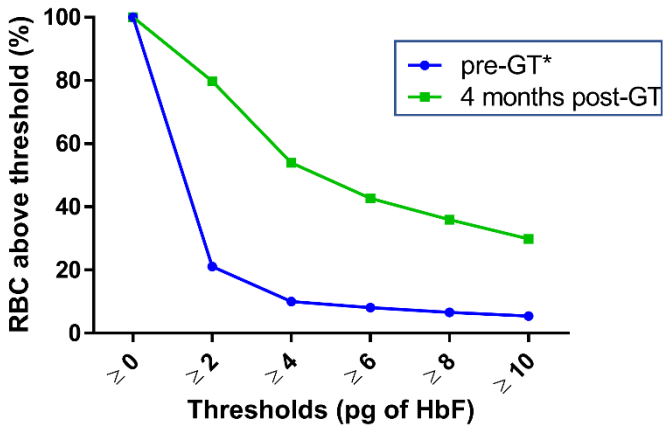

Figure 56 | HbF/RBC quantification in a patient with SCD before and after sh-BCL11A gene therapy. (**A**) Percentages of RBC classified by HbF/RBC ranges before (pre-GT) and 4 months after gene therapy drug product infusion (4 months post-GT). Data represents mean % of RBCs in each range of HbF/RBC (*n* = 3). (**B**) Mean percentages of RBC containing at least the indicated quantity of HbF (thresholds) before (blue) and after (green) gene therapy. (GT: Gene therapy).

*patient was under chronic RBC transfusions before gene therapy (HbA = 33.4%).

Chapter 6 – Analysis of red blood cell properties in patients with severe sickle cell disease treated with LentiGlobin gene therapy in the HGB-205 study

1. Assessing RBC properties in SCD patients treated with gene therapy

RBCs of SCD patients are known to present physical, biochemical and functional abnormalities. They are more rigid, due to the increased density related to dehydration which promotes the HbS polymerization. They have increased adhesion properties and they present an impaired oxygen transport. Moreover, a high intra vascular hemolysis level and percentage DRBCs have been shown to be strongly correlated with chronic complications (190,241).

The results presented in this chapter are from a clinical trial coordinated by Pr. Marina Cavazzana at Necker hospital, with a collaborative work between our team and Dr. Annarita Miccio at the Imagine institute, in Paris. Part of this project focuses on analyzing the effects of HbA^{T87Q} production on RBC properties in SCD patients treated with LentiGlobin gene therapy during the Phase 1/2 HGB-205 clinical trial (NCT02151526). Presently, three patients have been treated in this study in France (387).

To this purpose, we have analyzed RBC hemoglobin content, extent of HbS polymerization, membrane properties and hemolysis markers.

2. Methods

a. Patients

Three patients (P1, P2 and P3) with severe SCD (≥2 ACS or ≥2 VOC in the preceding year or the year before regular transfusions) were recruited in the HGB-205 study (NCT02151526). $CD34^+$ HSCs were obtained by bone marrow harvest. Following collection, cells were transduced with the LV vector BB305. Patients underwent myeloablative busulfan conditioning and were infused with transduced cells. After 2 years in HGB-205, patients transitioned into the long-term follow-up study LTF-303 (NCT02633943). Whole blood samples were obtained from the 3 patients during their clinical follow-up and were processed within 36 hours after blood draw. Results obtained from patients were compared to β^S/β^S patients (SS) non treated with HU, selected from the Erythropedie collection monitored in our referral center (Henri Mondor Hospital, Creteil, France), and to healthy donors (HD) (collected from the Etablissement Français du Sang).

b. Hemoglobin content

Hemoglobin content in RBCs was assessed by HPLC using a Bio-Rad Variant II Hb analyzer (Biorad). β-like globin chains proportions were assessed in total RBCs and in reticulocytes (CD71-positive cells sorted – anti-CD71 Microbeads; Miltenyi Biotec) by reverse-phase HPLC (RP-HPLC). RP-HPLC analysis was performed using a NexeraX2 SIL-30AC chromatograph and the LC Solution software (Shimadzu). Globin chains were separated by HPLC using a 250x4.6 mm, 3.6 µm Aeris Widepore column (Phenomenex). Samples were eluted with a gradient mixture of solution A (water/acetonitrile/trifluoroacetic acid, 95:5:0.1) and solution B (water/acetonitrile/trifluoroacetic acid, 5:95:0.1). The absorbance was measured at 220 nm.

c. HbS level of polymerization

HbS polymerization extent was assessed by *In vitro* $Hb–O_2$ dissociation and association curves on a Hemox analyzer (TCS scientific) to evaluate the O_2 saturation at various PO_2 pressures at pH = 7.4 and 37°C (performed at month 36 (M36) and M8 for P1 and P3, respectively) and by measuring the level of sickling by microscopic observation (performed at

M12, M25 and M36 for P1 and at M8, M15 and M18 for P3) after RBCs were incubated 20 minutes under 10% O_2 at 37°C.

d. Membrane property analyzes

RBC deformability was determined by laser diffraction analysis (ecktacytometry), using the Lorrca (Laser Optical Rotational Cell Analyzer – RR Mechatronics) in polyvinylpyrrolidone (PVP) as measurement of elongation index (EI) under increasing shear force (from 0.3 to 30 Pa) at physiological osmolality and at 37°C. Osmotic gradient ektacytometry (EI under increasing osmotic gradient) was performed in PVP at stable shear stress (30 Pa) and at 37°C. Measurements were performed at M31, M36, M42 and M43 for P1 and at M6, M8, M12 and M15 for P3. EI is calculated as the ratio of the length (A) and width (B) of cells pattern of diffraction with the following formula: (A−B)/(A+B). O min (i.e., the osmolality at which RBC deformability reaches a minimum in the hypotonic region) reflects osmotic fragility and surface to volume ratio. O hyper (i.e., the osmolality at half of the EImax) reflects internal viscosity, mainly influenced by the MCHC.

In vitro RBCs adherence to surfaces coated with thrombospondin (TSP) or fibronectin (FIB) was performed under physiological flow conditions using a capillary flow chamber VENA 8 ENDO+ (Cellix) in DPBS with Ca and Mg (Gibco) with 0.4% BSA (Sigma Aldrich) at a hematocrit of 0.25%, under 0.5dyne/cm² for 5 min and counted in 6 representative areas along the centerline of the microslides using an AxioObserver Z1 microscope (Carl Zeiss) under 3 shear stress (at 0.5, 2 and 5 dynes/cm² for 5, 2.5 and 2.5 min, respectively).

e. Hemolysis markers

Monitoring of hemolysis, and biologic markers were performed according to the local laboratory tests by collecting reticulocyte count, serum haptoglobin, LDH and bilirubin. In addition, using two spectral methods patented by our team, we measured levels of cell-free Hb, cell-free heme and hemopexin.

3. Clinical status post drug product infusion

SCD patients and treatment characteristics are given in Table 5. The 3 patients had a reported follow-up of 54, 24 and 24 months for P1, P2 and P3, respectively. The first patient (P1) treated with LentiGlobin for SCD experienced only one vaso-occlusive pain episode or ACS post-treatment: vaso-occlusive pain episode, which developed at 30 months after LentiGlobin gene therapy following a case of acute gastroenteritis with fever, dehydration and an increase in blood viscosity. SCD P2 had 2 serious adverse event (SAEs) of ACS approximately 6 and 8 months after LentiGlobin gene therapy. The patient resumed chronic transfusions and HU treatment and subsequently experienced 2 SAEs of vaso-occlusive pain; no additional SAEs of vaso-occlusive pain or ACS were reported during the follow-up of HGB-205. SCD P3 had no episode of vaso-occlusive pain or ACS post-LentiGlobin gene therapy (clinical data are from M. Cavazzana laboratory – Necker Hospital (387)).

Table 5: SCD patient and treatment characteristics

Patient characteristics	**P1**	**P2**	**P3**
Age at enrollment (years)	13	16	21
Genotype	β^S/β^S with a single 3.7-kb α-globin gene deletion	β^S/β^S	β^S/β^0
Treatment characteristics			
Busulfan AUC† daily average, µM*min	4.841	5.022	5.447
Drug product VCN vector copies/diploid genome	1.0/1.2‡	0.7/1.0‡	0.8/0.5‡
Drug product cell dose x10^6 CD34+ cells/kg	5.6	4.7	3.0
Follow-up (months)	52.5	28.5	25.5

AUC, area under the curve; VCN, vector copy number (number of vector copies per diploid genome)

†Busulfan plasma levels were monitored daily and busulfan dose was adjusted to meet the daily target average AUC of 4000 – 5200 µM*min

‡Corresponds to 2 drug products from 2 separate bone marrow harvests per patient

4. Analysis of red blood cell properties

4.1. RBC hemoglobin content

Total Hb levels were 13.0 g/dL (P1, M54), 9.4 g/dL (P2, M24), and 9.8 g/dL (P3, M24), with corresponding HbA^{T87Q} contributions of 47.9%, 7.9%, and 25.8%, respectively (Figure 57A). After drug product infusion, we observed a robust expression of HbA^{T87Q} and HbS ≤ 60% with ≥ 6 months of follow-up post-LentiGlobin treatment in the 2 patients without transfusion. All treated patients show a rising trajectory of HbA^{T87Q} expression through 6 months (Figure 57B). In P1 and P3, who were no longer on transfusions since M3 and M1, respectively, HbA^{T87Q} expression remained stable for up to 4.5 years following LentiGlobin treatment. In P2, the decrease in HbA^{T87Q} level followed exchange transfusions. (Results are from M. Cavazzana laboratory – Necker Hospital – (387)).

We also compared Hb content in whole RBCs to Hb content in reticulocytes by RP-HPLC in the two patients without transfusion (P1 and P2). We observed a stable over time accumulation in $\beta^{A\text{-}T87Q}$-globin and γ-globin in whole circulating RBCs (48.43% at M36; 49.10% at M42 and 24.58% at M8; 27.00% at M12, for P1 and P2, respectively) as compared to respective Hb levels in their CD71-positive reticulocytes (37.65% at M36; 32.55% at M42 and 6.82% at M8; 7.85% at M12, for P1 and P2, respectively) (Figure 57C). The subsequent enrichment was calculated as the ratio of %Hb in RBCs to %Hb in reticulocytes (fold-increase) (Figure 57D). Enrichments in HbA^{T87Q} were 1.5 and 3.5 for P1 at M42 and P3 at M12, respectively. No enrichment in HbF was observed for P1 (1.0) while for P3, enrichment in HbF was 2.0 at M12.

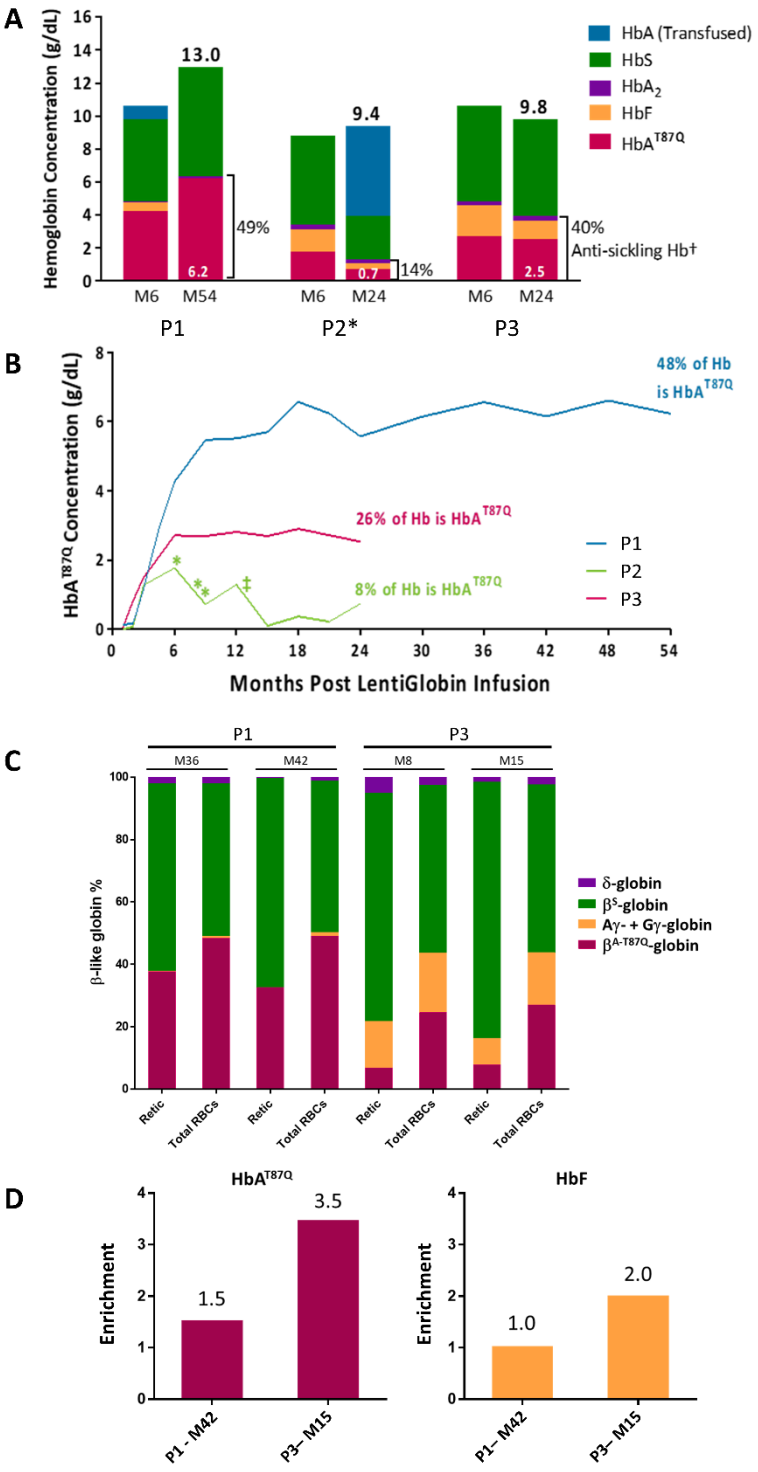

Figure 57 | Anti-sickling Hb expression post LentiGlobin gene therapy. (**A**) Hb levels in P1, P2 and P3 at M6 and M54 or M24 assessed by HPLC showing HbS ≤ 60% in the 2 patients off-transfusion. (**B**) %HbA^{T87Q} over time following gene therapy remaining stable from M6 for the 2 patients off-transfusion. (**C**) β-like globin chains content assessed by RP-HPLC in reticulocytes (CD71+ cells sorted; Retic) and total circulating RBCs from P1 and P3 showing a stable over time increase in $\beta^{A\text{-}T87Q}$-globin and γ-globin in total RBCs by comparison with Retic. (**D**) Enrichment in %HbA^{T87Q} and %HbF in total circulating RBCs relative to their percentages in reticulocytes. Figures A and B and corresponding results are from M. Cavazzana laboratory – Necker Hospital – (387).
*: P2 received exchanged transfusion at M6 and 8 due to ACS and at M9 for ACS prophylaxis. ‡: Starting M13, P2 received chronic infusions ~ every 30 days.

4.2. Extent of HbS polymerization

In vitro Hb–O_2 dissociation and association curves were plotted to evaluate the O_2 saturation at various pO_2 pressures at pH = 7.4 and 37°C. p50 were higher for SS (31.6 [29.4–34.5] Torr; n = 12) than AA (26.2 [25.3–27.2] Torr; n = 12) (medians [IQR]). A hysteresis, which characterizes the property of a system whose evolution (O_2 binding to Hb) does not follow the same path depending on whether an external cause (pO_2) increases or decreases, was observed, initiated by the formation and dissociation of HbS polymers (388,389) (Figure 58A). Measurements were performed at M36 and at M8 for P1 and P3, respectively (Figures 58B and 58C). In accordance with the anti-sickling capability of HbA^{T87Q}, we observed an improvement in the hysteresis in RBCs from the two patients no longer transfused, with p50 lower for P1 (27.3 Torr) and P3 (29 Torr) than untreated SS, approaching values for HD.

These results were strengthened by *in vitro* sickling assays after oxygen deprivation showing a statistically significant better anti-sickling phenotype for RBCs from P1 and P3 during their follow-up than for RBCs from SS patients (Figure 58D). With both methods, we observed that RBCs from P1 had better anti-sickling performance than those of P3, which is in accordance with more anti-sickling Hb (Figure 57A and 57B).

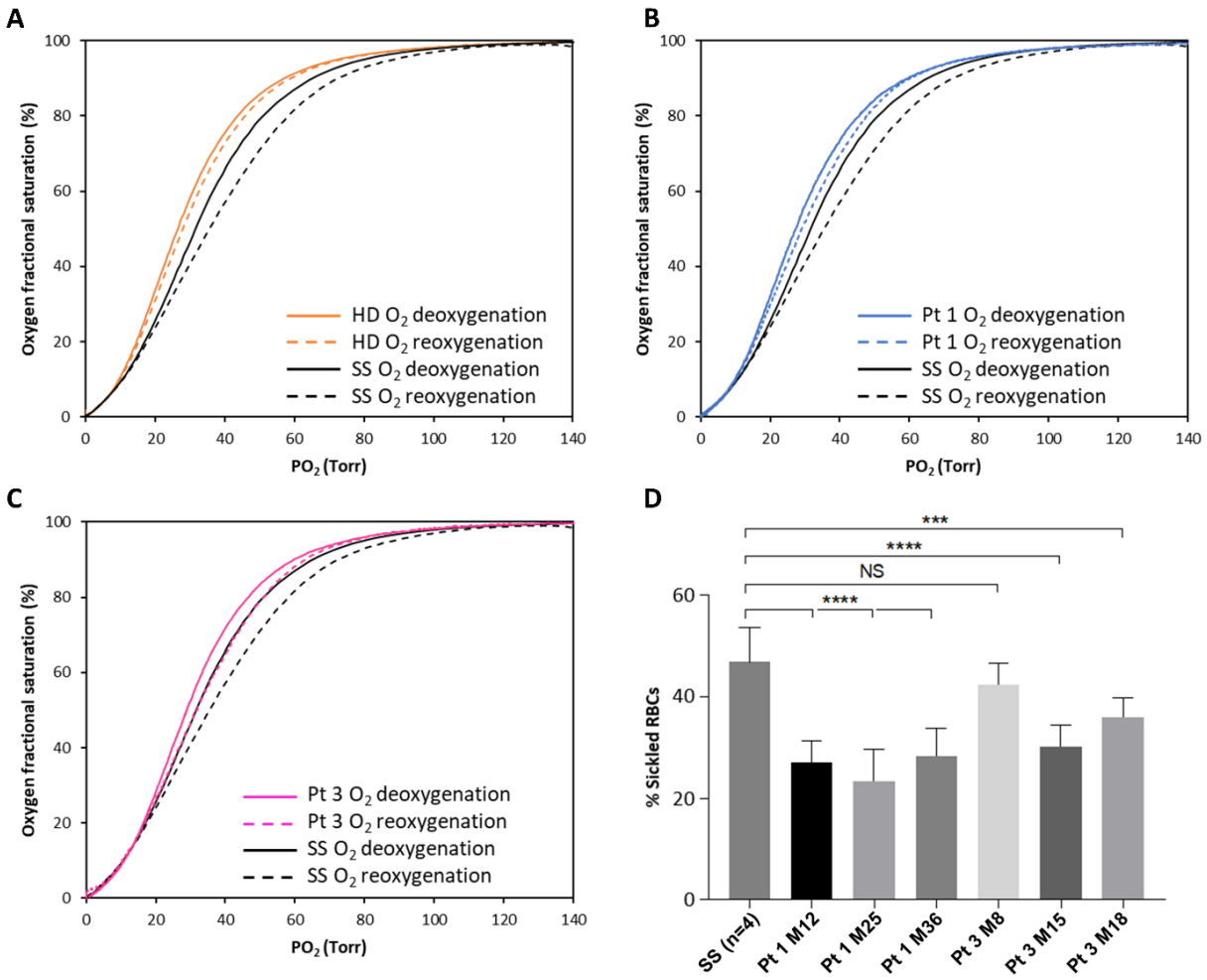

Figure 58 | Extent of HbS polymerization post LentiGlobin gene therapy. (**A**) Dissociation and association of O_2 curves for RBCs isolated from healthy donors (HD) (orange lines; n=12), compared to untreated SCD patients (SS) (black lines; n=12) showing reduced p50 in RBCs from SS and hysteresis initiated by HbS polymers. (**B**) Dissociation and association of O_2 curves for RBCs isolated from patient 1 at M36 (blue lines) and compared to untreated SS curves. (**C**) Dissociation and association of O_2 curves for RBCs isolated from patient 3 at M8 (purple lines) and compared to untreated SS curves. Full lines represent O2 dissociation and dotted lines represent subsequent O2 reassociation. (**D**) *in vitro* sickling assay of isolated RBCs from patients 1 and 3 at M12, 25, 36, and M8, 15 and 18, respectively, compared to RBCs from untreated SS (n=4). Mann-Whitney test (****: P<0.0001 - ***: P<0.0002 – ns: not statistically significant). Figure D and corresponding results are from Wassim El Nemer – INTS, Paris.

4.3. Hemolysis level

Measurement of hemolysis markers showed a global normalization for the two patients off transfusion by comparison with SS, AS and HD individuals (Figure 59). Reticulocyte counts remain elevated but normalized shortly after LentiGlobin infusion. LDH levels were in ≤ 300 U/L for P1, P2 and P3 by comparison with SS patients (417 ± 118 U/L, n = 16, mean ± SD) and total bilirubin was below normal upper value for P1 and P3, by comparison with SS patients (41.5 ± 19 µM, n = 16). Plasmatic free Hb level was elevated for P1 (21.3 ± 18.9 mg/dL) and very low for P3 (≤ 5.5 mg/dL) by comparison with SS patients (22.4 ± 23 mg/dL), which correlate with its natural scavenger haptoglobin level, mainly undetectable for P1, as for SS, and measured in almost normal levels for P3 (0.42 and 0.52 g/L). Low levels of plasmatic free heme were detectable for P1 (≤0.58 µM) and for P3 (≤ 0.38 µM), which correlates with normal values of its natural scavenger, hemopexin (≥0.55 and ≥0.38 g/L for P1 and P3, respectively). By comparison, free heme and hemopexin levels for SS patients were 2.82 ± 3.15 µM and 0.19 ± 0.13 g/L, respectively. In addition, plasma Hb, heme and hemopexin values for P1 and P3 were more similar to values measured for sickle cell trait individuals than for values measured for SS patients.

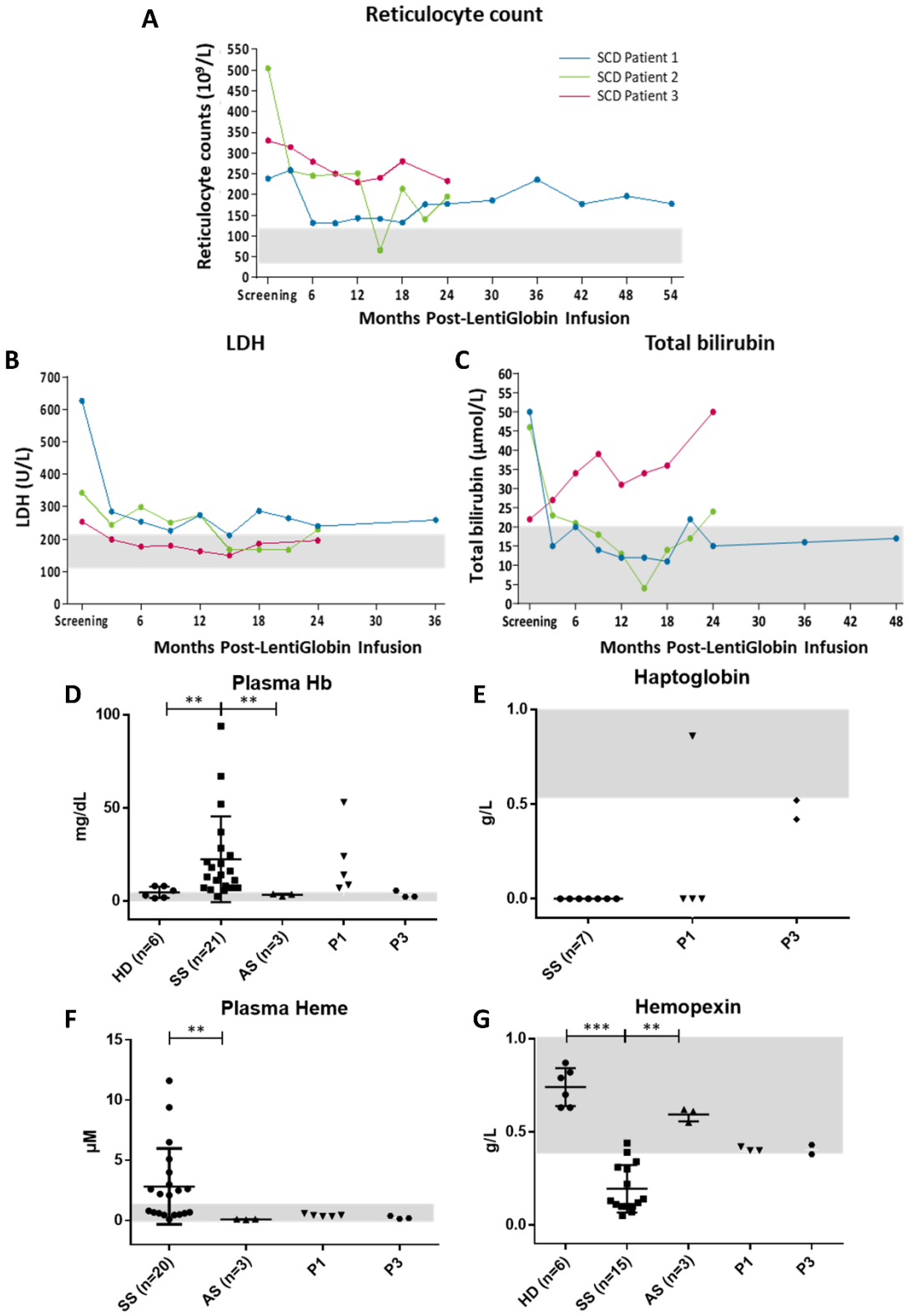

Figure 59 | Hemolysis profile post LentiGlobin gene therapy. (**A**) Reticulocyte counts, (**B**) LDU and (**C**) Total bilirubin assessed for P1, P2 and P3 during the follow-up. (**D**) Plasma Hb, (**E**) Haptoglobin, (**F**) plasma heme and (**G**) hemopexin levels assessed after gene therapy for P1 and P3 and compared to values measured for SS, AS and HD. (**D-G**) Different time points during follow-up are shown for P1 and P3. Gray areas correspond to normal values. Mann-Whitney test (***: P<0.001 - **: P<0.01 - *: P<0.05). Figures A, B and C and corresponding results are from M. Cavazzana laboratory – Necker Hospital – (387).

4.4. Membrane properties

4.4.1. RBC deformability

RBC deformability was assessed in isotonic solution, under increasing shear stress and at 37°C. An intermediate state of deformability for P1 and P3, assessed at M15 and at M42, respectively, was observed as compared to median values measured for RBCs from HD, AS and SS individuals (Figure 60A).

According to osmolality, assessed at 37°C and at constant shear stress (30 Pa), the overall curve of RBCs from SS patients is shifted toward the left by comparison with the curve of RBCs from HD (Figure 60B). This shift corresponds to the presence of dehydrated RBCs as stated by the lower O min median values (97 and 140 mOsm/kg for SS and HD, respectively) lower O EI max median values (221 and 312 mOsm/kg for SS and HD, respectively) and lower median O hyper values (382 and 464 mOsm/kg for SS and HD, respectively). In addition, RBCs deformability from SS patients is also lower than RBCs from HD, as stated by the EI max (0.563 and 0.617 for SS and HD, respectively). A similar but less important effect was also observed for AS individual with O min, O EI max and O hyper values of 133, 293 and 446 mOsm/kg, respectively.

As compared to RBCs from HD, a shift toward the left was also observed for RBCs from P1 and P3 at M42 and M15, respectively. O min, O EI max and O hyper values were 95, 235 and 404 mOsm/kg, for P1 and 97, 236 and 372 mOsm/kg for P3, respectively. RBCs maximum deformability (EI max) was improved for P1 and P3 by comparison with SS patients. EI max values for P1 at M42 and P3 at M15 were 0.586 and 0.593, respectively. These values were closer to those measured for HD individuals (median value of 0.617) than median value for SS patients (0.541).

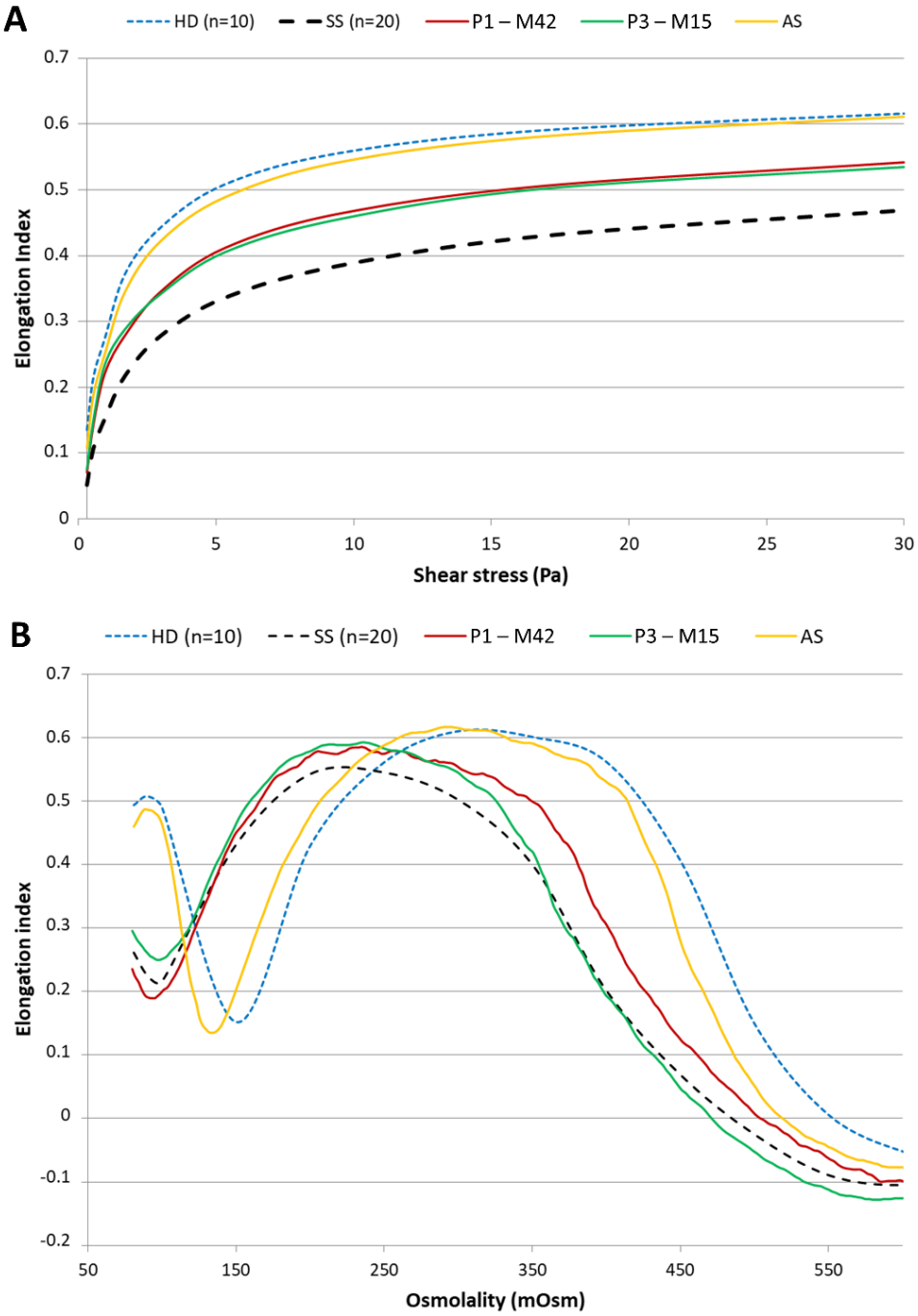

Figure 60 | Membrane deformability post LentiGlobin gene therapy. (**A**) Deformability measured in isotonic solution, under increasing shear stress (from 0.3 to 30 Pa) and at 37°C, for RBCs from P1 and P3 and compared to median data from HD (*n* = 10), SS (*n* = 20) and AS individuals. Results show an intermediate state of deformability for P1 and P3 as compared to SS and HD, with a profile for AS RBCs lower than HD RBCs. (**B**) Deformability according to osmolality at constant shear stress (30 Pa) and at 37°C, for RBCs from P1 and P3 and compared to median data from HD (*n* = 10), SS (*n* = 20) and AS individual. Maximum deformability for P1 and P3 was similar to HD and AS and higher than SS patients. The shift toward the left observed under osmotic gradient is due to the presence of dehydrated RBCs as compared to HD.

4.4.2. RBC adherence profile

Under controlled increasing shear stress (0.5, 2 and 5 dynes/cm²), adherence on surface coated with TSP of RBCs isolated from P1 and P3 was consistently lower by comparison with adherence measured with RBCs from untreated SS, whatever the applied shear stress (Figure 61). Adherence level of each patient was more similar to levels obtained with RBCs from HD. Similar results were obtained with adherence on FIB (data not shown).

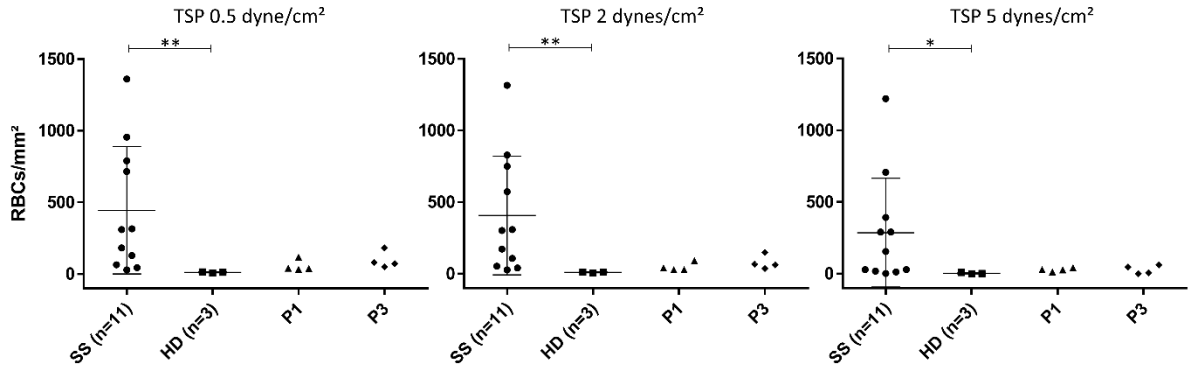

Figure 61 | RBCs adherence on TSP post LentiGlobin gene therapy. Results are expressed as mean RBCs/mm² for untreated SS (n=11) and HD (n=3) and different time points are shown for P1 (M31, M36, M42 and M43) and P3 (M6, M8, M12 and M15). Mann-Whitney (**: P<0.01 - *: P<0.05).

Chapter 7 – Improving the HbF/RBC assay to assess erythrocyte chimerism

1. Objective

The HbF/RBC assay allows to quantify HbF content in individual RBCs. By using monoclonal antibodies against other type of Hb, such as HbS, could be of interest to precisely determine the erythrocyte chimerism after gene therapy or HSCT. In addition, the possibility to discriminate SCD patients' own RBCs in case of blood transfusion would allow to perform the HbF/RBC in those cells, excluding the transfused RBCs.

To this purpose, the selection of a monoclonal antibody with good specificity is mandatory. Moreover, most monoclonal antibodies are mouse antibodies. Therefore, since we aim to combine the different quantifications within the same sample, it prevents the use of a secondary fluorescent antibody. In addition, the latter are mainly polyclonal, which might interfere with results.

The data presented in this chapter consist in preliminary results of the improvement we are willing to develop in order to assess both HbF and HbS content in RBCs.

2. Methods

a. Patients

Eligible patients (all ≥ 18 years, either S/S, A/S or S/C genotype) were selected from the Erythropedie collection monitored in our referral center (Henri Mondor Hospital, Creteil, France). In accordance with the Declaration of Helsinki, all patients gave their signed informed consent. All data were rendered anonymous to protect patients' privacy and confidentiality. Cord blood (CB) and healthy donors (HD) samples were obtained from the Etablissement Français du Sang.

b. HbS detection by flow cytometry

Prior to intracellular staining, RBC membrane was fixed and permeabilized using Fetal Cell Count™ kit reagents (Cat IQP-363, IQ Products) according to the manufacturer's instructions using 5 µL of packed RBC.

Indirect HbS detection: Unconjugated mouse monoclonal anti-human HbS antibody was used for immunologically based HbS detection. RBCs were incubated for 15 minutes shielded from light at room temperature. Thereafter, RBCs were washed with PBS and centrifuged at 300 g for 3 minutes. 2 µL of a secondary Rat anti mouse IgG1 conjugated with Alexa Fluor 405 (AF405) (BD Pharmingen) were added and incubated for 30 minutes shielded from light at room temperature. Negative controls were performed using the secondary antibody alone, without incubation with the anti-HbS. Thereafter, RBCs were washed with PBS and centrifuged at 300 g for 3 minutes. Stained RBCs were immediately analyzed on flow cytometer.

Direct HbS detection: RBCs were incubated for 15 minutes shielded from light at room temperature with a mouse monoclonal anti-human antibody. Thereafter, RBCs were washed with PBS and centrifuged at 300 g for 3 minutes. Stained RBCs were immediately analyzed on flow cytometer.

HbS fluorescence in RBCs was acquired using a BD FACSCanto II system including an 8-color flow cytometer (BD Biosciences). Data were analyzed using FlowJo v10 software (Miltenyi Biotec). Light scatter thresholds were used to select RBC population and exclude cellular debris. 1 x 10^5 cells were gated on forward scatter area (FSC-A) versus side scatter area (SSC-A) plot and recorded. Doublet were excluded by selecting single cells on FSC-H (FSC-Height) plotted against FSC-W (FSC-Width) and then on SSC-H versus SSC-W.

c. Simultaneous HbF and HbS detection by flow cytometry

Prior to intracellular staining, RBC membrane was fixed and permeabilized using Fetal Cell Count™ kit reagents (Cat IQP-363, IQ Products) according to the manufacturer's instructions using 5 µL of packed RBC.

Both 50 µl of mouse anti-human HbF (IQ products) and 5 µL of mouse anti-human HbS were incubated with RBCs for 15 minutes shielded from light at room temperature. Thereafter, RBCs were washed with PBS and centrifuged at 300 g for 3 minutes. Stained RBCs were immediately analyzed on flow cytometer.

d. HbF quantification in individual RBCs

Every HbF/RBC quantification were performed as described above.

3. Validation of the specificity of an anti-human HbS monoclonal antibody

To assess the specificity of the monoclonal anti-HbS antibody, RBCs samples from HD, CB, heterozygous (AS and SC) and homozygous (SS) individuals were fixed and permeabilized prior to incubation with the anti-HbS. A secondary anti-mouse-IgG-AF405 was then used for measurement by flow cytometry. The quantity of HbS in each samples (assessed by HPLC) was compared to the AF405 mean fluorescence intensity (MFI) measured (Figure 62). For HD and CB, MFI were similar to those measured when using only secondary antibody in the absence of the anti-HbS. MFI values measured for AS and SC patients were lower than those measured for SS. These results indicate that the anti-HbS is specific for HbS and does not cross react with HbA, HbF nor HbC.

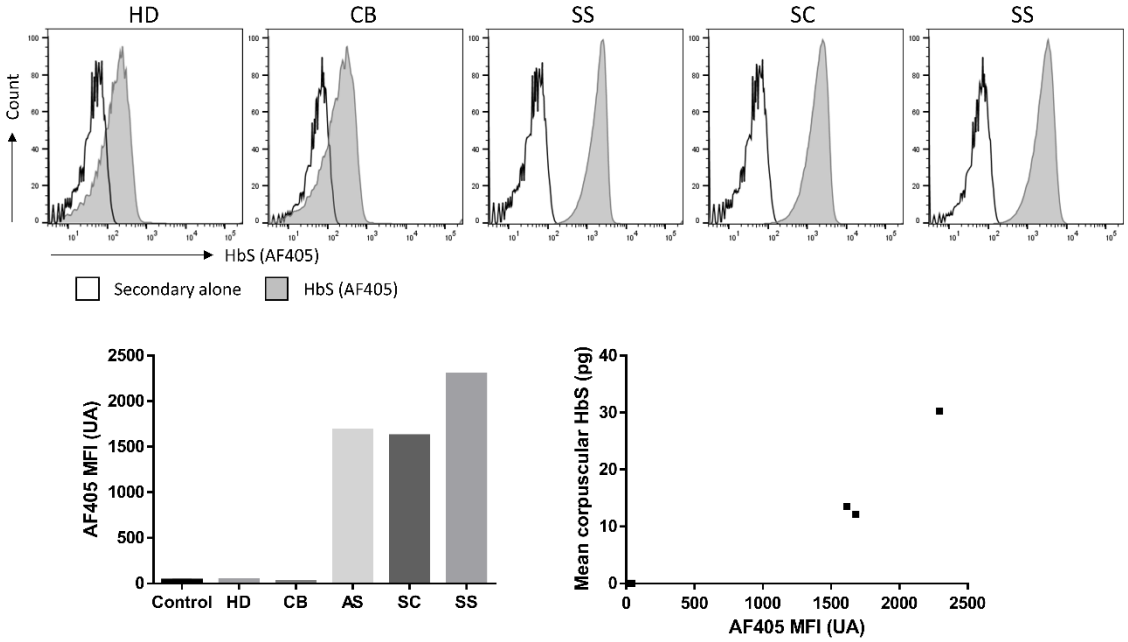

Figure 62 | Specificity of the mouse anti-HbS monoclonal antibody. Representative histograms of HbS measured for HD, CB, AS SC and SS RBCs. MFI was collected for each sample and compared to the mean corpuscular HbS content in pg.

4. HbF/RBC quantification in transfused SCD patients

To evaluate the possibility to discriminate HbS positive RBCs from HbS negative RBCs, we mixed RBCs form HD (AA-RBCS) with RBCs from non-transfused SCD patients (SS-RBCs) in known proportions (0%, 20%, 40%, 60%, 80% and 100%). Mixed RBCs were then fixed and permeabilized prior to be incubated with the anti-HbS. Percentages of HbS-positive RBCs were evaluated by flow cytometry. The correspondence between expected %SS-RBCs and measured %SS-RBCs was satisfactory (R^2 = 0.991) (Figure 63).

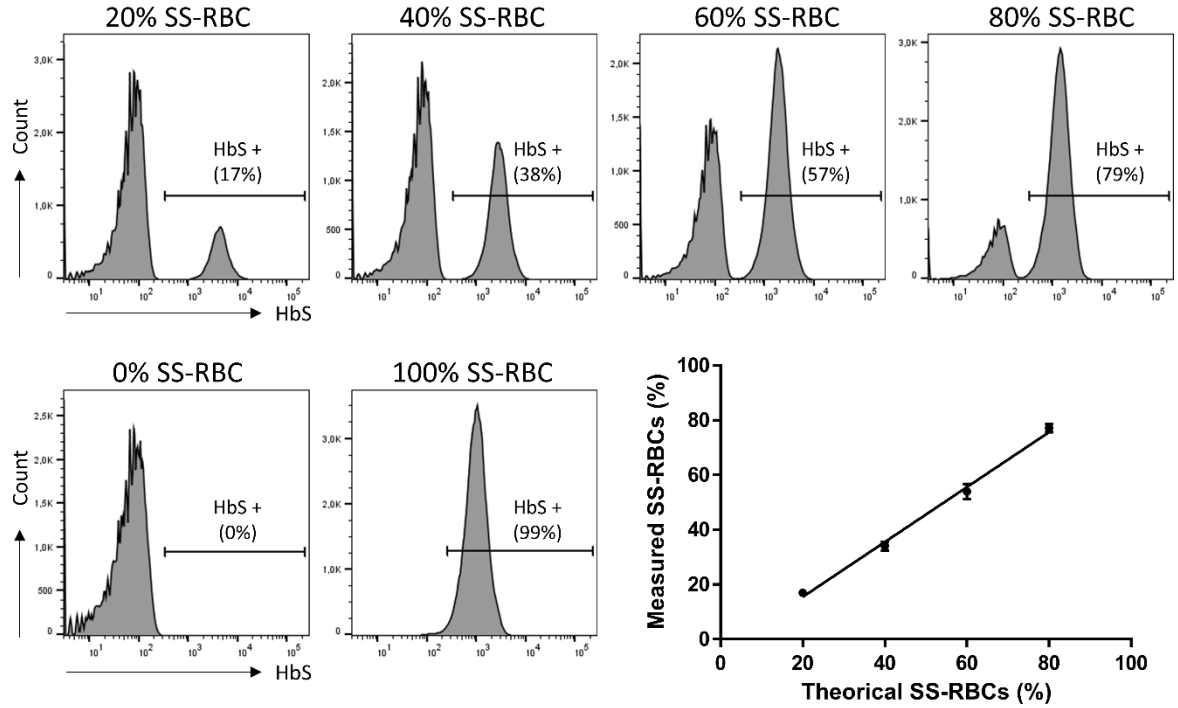

Figure 63 | Discrimination between HbS-positive and HbS-negative RBCs. Representative histograms obtained with known SS-RBCs percentages (0; 20; 40; 60; 80 and 100%) mixed with AA-RBCs (*n* = 3). Indicated percentages correspond to either theorical (above histograms) or measured (inside histograms) %SS-RBCs as compared to total RBCs. Vertical axes represent count and horizontal axes represent HbS.

Therefore, we performed co-staining of HbF and HbS within the same samples to assess the possibility to measure HbF/RBCs in transfused patients. As a proof of concept, HbF/RBC quantification was performed in a patient under blood exchange procedure because of allogenic HSCT with a stimulation of HbF synthesis probably due to conditioning. Whole blood analysis revealed that >85% of RBCs contained less than 4 pg of HbF (Figure 64A). Own patient's HbS-positive and transfused HbS-negative RBCs were discriminated using the anti-HbS (Figure 64B). We then performed HbF/RBC quantification in both population (i.e. donors'

RBCs and patient's RBCs). While most HbS-negative RBC contained less than 4 pg of HbF (>95%) (Figure 64C), 41% of HbS-positive RBCs contained less than 4 pg of HbF and 49% of it contained more than 10 pg of HbF (Figure 64D). These results indicate the possibility to discriminate patients' own RBCs in case of blood transfusion and to perform HbF/RBC quantification in those selected erythrocytes. Similar results were obtained for other transfused SCD patients with lower levels of HbF (data not shown).

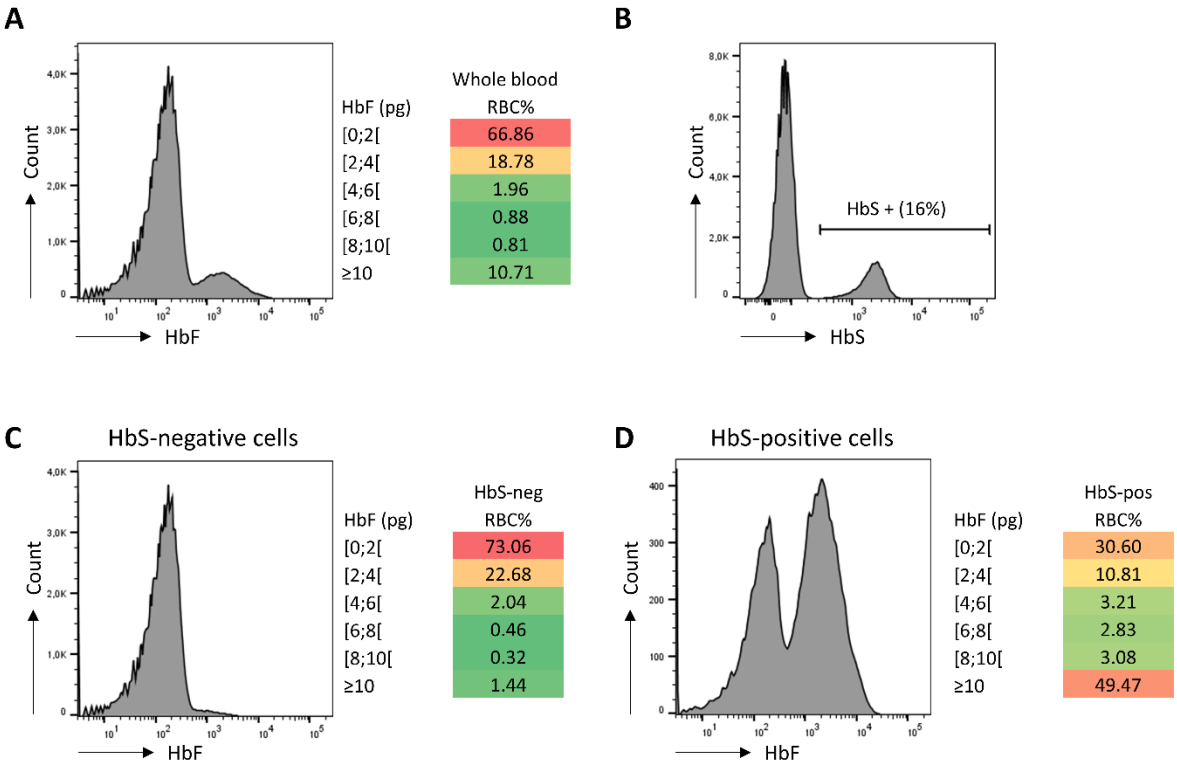

Figure 64 | HbF/RBC quantification in only HbS-positive RBCs in case of blood transfusion. (**A**) HbF/RBC quantification performed on whole blood. (**B**) Discrimination of HbS-negative and HbS-positive RBCs. (**C**) HbF/RBC quantification in HbS-negative RBC population. (**D**) HbF/RBC quantification in HbS-positive RBC population. Vertical axes represent count and horizontal axes represent HbF or HbS. RBC were classified according to their HbF content.

Discussion

1. Gene therapy for the treatment of sickle cell disease

1.1. Developing new strategies to cure SCD

Numerous studies to better understand SCD molecular basis have contributed to a better characterization of its pathophysiology. In the last decades, a vast scientific investment leads to the approval of three new medications in addition to the historical treatment, hydroxyurea. Moreover, massive improvements in allogeneic bone marrow transplantation have been done. Finally, the development of several gene therapy strategies represents a promising alternative to cure SCD (299). However, one of the biggest challenges remains the clinical complexity and wide variability that cannot be only explained by the disease genotype itself. Lives of patients with SCD are characterized by frequent painful vaso-occlusive events, acute organ dysfunction and progressive multi-organ damage. While it is estimated that mortality under the age of 5 years is between 50% to 90% in low-income countries (390), median life-expectancy is only about 45-58 years in high-income countries, compared to the overall life expectancy of 78.2 years. Therefore, the lifetime health care cost has been estimated to be over $8 million for a patient with a 50-year life expectancy in the United States (391). This cost is significantly increased for patients with end-organ damage, such as stroke, chronic kidney or renal disease, and pulmonary hypertension (392). With around 20 million people affected worldwide, SCD is a health and socio-economic burden.

The principal element that determines SCD severity is the time it takes for RBCs to transit through the microcirculation relative to the delay time for HbS polymerization (89). Thus, targeting HbS polymerization is probably one of the best strategies to cure SCD. To this purpose, modifying patient's genome through expressing anti-sickling Hb in RBCs, including HbF and genetically engineered recombinant β-globin such as $\beta^{A\text{-}T87Q}$- or β^{AS3}-globin,

represents potent promising strategies to improve SCD clinical manifestations and cure individuals thanks to gene therapy.

1.2. Chimerism induced by gene therapy

Gene therapy strategies for β-hemoglobinopathies are procedures similar to HSCT, except that donor HSCs are those of the patient himself after being *ex vivo* genetically modified. Following HSCT, patients may develop mixed chimerism.

To avoid any confusion, it is important to point out that mixed chimerism induced by HSCT corresponds to a cellular chimerism. Cellular chimerism is the proportion of donor-derived circulating cells. After gene therapy, two kinds of chimerism can be observed. The first one is the cellular chimerism, similar to the one obtained after HSCT. The second one is an intra-cellular chimerism, which corresponds to the ratio of therapeutic Hb to total Hb, per RBC.

Cellular chimerism is typically quantified in total circulating white blood cells, especially in the absence of a standard widely accepted test for erythrocyte-specific engraftment (393). It reflects the level of bone marrow engraftment. This common phenomenon can result in clinical control of the disease with, in some cases, fully peripheral blood RBCs replaced by donor-derived erythrocytes (394–396). Only 20% of cellular chimerism in HSCs is sufficient to replace most sickle RBCs in circulating blood after HSCT (307). This observation is based on the selective advantage within the bone marrow and peripheral blood of normal erythroid cells (397). Thus, in β-hemoglobinopathies, assessing RBC cellular chimerism is of interest.

In gene therapy, cellular chimerism corresponds to the proportion of cells that have been transduced. The intra-cellular chimerism results from the level of transduction, and the level of synthesis of the therapeutic Hb at the single cell level. This intra-cellular chimerism must be considered because it also conditions the efficacy of the treatment. Therefore, because of the transduction, the level of bone marrow cellular chimerism to reach after gene therapy may be higher than 20% to obtain a complete control of the disease.

Pre-clinical mouse studies using LV vectors to express a therapeutic anti-sickling Hb showed that its level in blood correlates with vector copy number (VCN) values measured in peripheral blood mononuclear cells (PBMCs) after the gene therapy procedure. VCN in PBMCs

is related to the level of HSCs correctly engrafted and transduced and is influenced by both transduction efficiency and cellular chimerism. The latter also depends on the degree of myeloablation obtained after conditioning. An average VCN of 1 has been shown to result in the production of therapeutic Hb corresponding to around 20% of the total Hb level (398,399). This observation is coherent with the results of the first SCD patient treated with gene therapy for whom therapeutic Hb level was about 50% of total Hb with a VCN value of around 2 in whole blood (337).

Assuming that the same level of transduction (i.e. VCN = 2 and therapeutic Hb in every single RBC = 50% of total Hb) is obtained in all transduced HSCs, cellular chimerism after transplantation corresponds to what is observed in case of allograft with an A/S donor. A recent study conducted in SCD patients receiving HSCT, showed that a myeloid donor cellular chimerism level ≤30% was not always enough to prevent VOC in patients with A/S donors (400). In this study, the authors also showed that a myeloid donor cellular chimerism level above 30% was sufficient to no longer display clinical manifestations of SCD, whatever donors being A/A or A/S, but suggest that this threshold should reach more than 50% to normalize hemolysis markers.

Therefore, in addition to the cellular chimerism, the intra-cellular chimerism is an important aspect to consider in particular for the comparison of HSCT and gene therapy

1.3. Developing new assays to evaluate sickle cell disease treatments efficacy

Currently, the level of both chimerisms needed to control SCD after gene therapy procedure are not known. By comparison, reaching a condition similar to sickle cell trait individuals or SCD patients with HPFH and homogeneous distribution of ≥30% HbF will obviously result in complete remission. Therefore, developing new tools, based on single cell analysis, to assess gene therapy induced chimerism are of interest. They represent potent indicators of treatment efficacy at the biological and functional level. In addition, such assays could also be used as predictive markers in the future.

2. Assessment of hemoglobin content in individual red blood cells

2.1. HbF content measurement in individual RBCs for clinical purpose

To date, chromatography (i.e. HPLC or reverse-phase [RP] HPLC) is the gold standard assay for Hb detection in a blood sample (372). It provides a measure of each Hb as a percent of total hemoglobin. The same method is used in case of gene therapy to determine therapeutic Hb levels (337). However, these methods do not consider the cellular distribution. In this context, a precise tool allowing the assessment of individual RBC HbF content is required.

The new method presented in this study allows the precise and direct measurement of HbF content distribution in RBCs at the single cell level. The development of this technique has been possible by using samples from non-SCD subjects presenting a homogeneous distribution of HbF, for whom the mean HbF fluorescence can be directly related to the MCHbF. Interestingly, when we integrate individuals with heterogeneous HbF distribution, the standard curve we obtained was modified, with some of these values far away from the linear regression, resulting in a decrease in the R^2 coefficient. Therefore, we have chosen to use only individuals with homogenous HbF distribution as a prerequisite to perform the linear regression that allows HbF/RBC quantification.

Despite the choice of an accurate monoclonal antibody from a commercial kit used to diagnose fetomaternal hemorrhage, the slight variability we observed came from the batch. Indeed, conjugation of fluorochromes to antibodies, which makes the molecule of interest detectable, may be variable from one reaction to another (401). The degree of coupling corresponds to the ratio of optical densities between the fluorochrome and the antibody, measured by spectrophotometry. Thus, integrating the variability of the degree of coupling of PE molecule per antibody, by applying a correction factor to the measured fluorescence intensities, allows greater accuracy of the assay. In addition, in a clinical context, it would be necessary to reperform the linear regression obtained from patients with homogeneous HbF distribution for every new batch. Moreover, focusing on the use of a monoclonal antibody with a fluorochrome/protein ratio close to 1:1 might attenuate the variations we observed between the different batches.

The present method displays excellent results in term of precision, which is of interest in a clinical context. Moreover, when we compared quantifications performed on the same sample but using different batches, we obtained similar HbF/RBC quantitative distribution, attesting of the accuracy of this assay (data not shown). In addition, the capability to perform HbF quantification on frozen samples presents several advantages. It allows distant analysis when the sampling site is far away from the facility performing the assay. Then, in case of a clinical follow-up to demonstrate efficacy of a given treatment, collecting and analyzing all the samples from a same patient on the same day may be of interest to avoid batch-to-batch variations.

To our knowledge, only one attempt to precisely quantify HbF/RBC has been done using a fluorescent antibody (367). The method developed by Horiuchi *et al*., consisted of HbF content measurement in F cells assessed by fluorescence microscopy. While this method showed a good correlation between total fluorescence intensity and %HbF, it is time consuming and requires technical expertise for reproducible smear preparation. Contrary to flow cytometry assay, RBCs size, in terms of MCV, could also affect the fluorescence density quantification because of the variation of the inner hemoglobin concentration, making correlation with standards unreliable.

2.2. Changes in HbF/RBC distributions upon HU treatment

As a proof of concept, we applied this method to measure HbF content in SCD patients during HU treatment, a well-known inducer of HbF synthesis (271). After at least 6 months of treatment, median %HbF for the 14 included patients increased from 6.2% to 14.2%, as expected. During the longitudinal follow-up we observed a statistically significant decrease in %RBC containing a very low HbF level (<2 pg) as well as a statistically significant increase in %RBC containing between 2 and 4 pg of HbF. These results are consistent with published data showing that HU treatment leads to an increase in both %HbF and F cell frequency (186,402,403).

HbF distribution, assessed by flow cytometry, showed different types of response. On the one hand, half of the included patients presented an increase in global HbF, associated with a distribution becoming homogenous. On the other hand, while global HbF increased, the distribution did not change for 4 patients. We also observed an increase in global HbF

associated with a more heterogeneous distribution than basal state for 2 patients, as well as no changes in global HbF associated with a homogenization of the distribution for 1 patient. These different response-profiles reflect the known variability in SCD patients' response to HU (404). Indeed, mechanisms of action by which HU induces γ-globin synthesis, which involve several transcriptional events and signaling pathways, are still not well understood. HU administration is followed by increased intra-erythrocyte levels of NO, activation of guanylyl cyclase and synthesis of guanosine cyclic monophosphate (cGMP), which in turn activates downstream signaling pathway responsible for γ-globin mRNA synthesis. The activation of mitogen-activated protein kinases (MAPK) signaling pathway leading to HbF synthesis by HU has also been demonstrated (405). Genetic factors, including polymorphisms, have been hypothesized as an explanation of a differential response to HU (406,407).

2.3. The HbF/RBC assay as a tool to determine protective thresholds in sickle cell disease

In compound heterozygotes for HbS and HPFH, total HbF level is around 30%. HbF is commonly homogeneously distributed in RBCs of those individuals. Each erythrocyte contains about 30 pg of hemoglobin, endowing each cell with approximatively 10 pg of HbF. This level represents a sufficient concentration to confer protection from sickle cell complications despite their high HbS fraction. In solubility experiments, a combined HbF and HbA2 concentration of 30% in the presence of HbS (70%) had an equivalent solubility to hemolysate from patients with sickle cell trait containing 60% HbA and 40% HbS (408).

The protective HbF/RBC threshold initially calculated and believed to be around 10 pg per cell by Steinberg *et al*. (371), might be lower according to our results. In the present study, we show that assessing the distribution of HbF/RBC allows analyzing any possible protective threshold against SCD phenotypes. The number of RBC containing at least 2 pg of HbF was significantly associated with an increase in mean %HbF, MCV and MCH and a decrease in RBC count. Hemolytic markers such as LDH, bilirubin and ASAT were not correlated with a HbF threshold, whereas we observed a decrease in bilirubin and reticulocytes count between D0 and ≥M6, which were correlated with an increase in the %RBC with HbF/RBC higher than 2 pg. These results are consistent with published data showing that hemolytic markers did not correlate with RBC survival improved by HbF level (409). It has indeed been demonstrated that

HU treatment decreases DRBCs percentage (186,279), the latter being related to increased hemolysis. These observations suggest that HU treatment also improves RBCs hydration, in addition to HbF synthesis. Therefore, the effect of HU treatment on hemolysis is probably more complex, in part because method to assess hemolysis markers are not enough precise.

The present study also shows that %RBC above thresholds of HbF/RBC even from 2 pg of HbF could have a clinical significance according to VOC incidence. We indeed calculated statistically significant correlations between VOC incidence and HbF/RBC from the threshold of 4 pg per cell in our study. As expected, the effect on VOC is more pronounced in case of %RBC reaching higher levels of HbF/RBC. ROC analyzes showed that the highest AUC was observed for threshold of 8pg, with the threshold of 6 pg giving an AUC very similar.

These results were strengthened by performing *in vitro* sickling assays using samples from another cohort of SCD patients treated or not with HU. The method we used consisted in a rapid enzymatical deoxygenation (in a few seconds), which is closer to physiologic processes than incubating red cells under hypoxic condition for several minutes (385). Percentages of sickle RBCs were correlated with the thresholds of 4, 6, 8 and 10 pg of HbF/RBC in a stronger way than %HbF and F cell.

Interestingly, the HbF threshold could explain the discrepancy between some studies showing a positive effect of the %HbF on survival (267,275,280,410), and those without a close relationship (411,412). While studied on a small cohort, the distribution of HbF (i.e., pancellular or heterocellular), which is of interest from a biological point of view, seems to be associated with the VOC incidence, heterocellular distribution having a negative effect, as reported (413).

Currently, several immunological methods, using fluorescence microscopy or flow cytometry, have been proposed to assess the frequency of F cells. In the present study, we compared the two most used methods to determine F cell frequency. We showed that using a positivity threshold corresponding to the fluorescence intensity of unstained cells gave fewer variable but higher results than using an isotypic control. In our cohort, improvements in biological parameters were also associated with F cell frequency, whatever the method used. Indeed, like for HbF/RBC threshold of 2 pg, statistically significant correlations with MCV, MCH and RBC count were observed. However, this was not the case when we performed ROC analyzes to determine if F cell frequency could impact the VOC incidence over 3 years in this

study. This result might be explained by the fact that F cells corresponds to only one threshold of HbF content and methods used can induce, as we showed, the setting of either a too variable or a too low positivity threshold, resulting in no clinical significance.

A study in larger cohorts of patients including their clinical manifestations, treatments and genetic analysis should be considered to evaluate the best threshold of HbF/RBC and the proportion of cells above it. In addition, these studies could also focus on genetic factors associated with HbF synthesis. Pharmacogenomics aims at understanding the influence of individuals' acquired or inherited genetic variations on pharmacokinetics and drug response. Indeed, multiple genetic factors have been hypothesized as an explanation of a differential response to HU (406,407,414,415). A better understanding of these genetic factors might be helpful in developing new therapeutics, such as the epigenetic drugs currently tested, as potential HbF inducers. These genetic differences also strongly suggest that a personalized HU dose according to drug bioavailability determination, coupled with the study of the thresholds, might attenuate these differences (287,288).

The determination of the best threshold is of major interest in gene therapy since these procedures focus on expressing anti-sickling Hb. Different thresholds probably exist, corresponding to different desired effects. For example, thresholds and %RBC above it to reach inhibition of VOC, inhibition of a given associated organ damage or inhibition of hemolysis are probably not the same. Therefore, they would represent therapeutic targets to reach to better evaluate new therapies or prognostic biomarkers for each patient.

2.4. Utility of the HbF/RBC assay to characterize response to gene therapy aiming to repress *BCL11A* expression

The effect of HU on HbF distribution was undertaken as a proof of concept of a new method for HbF measurement in each RBC. This method opens up interesting prospects for analysis of new therapeutic approaches, including epigenetic and gene therapy HbF inducers. The best example of its application to gene therapy purpose was the quantification we performed in patients included in the study aiming to reverse the fetal-to-adult Hb switch by expressing a shRNA targeting *BCL11A* expression (NCT03282656). While in our cohort of

patient on HU, HbF level reached up to 29.4% after six months of treatment, some patients included in this gene therapy clinical trial exhibit up to 40% of HbF (expressed as HbF / [HbF+HbS]) (386). Higher HbF synthesis leads to subsequent higher %RBC reaching the protective thresholds we estimated in the present study. Not surprisingly, we measured >50%, >40% and >35% RBCs above 4 pg, 6 pg and 8 pg of HbF/RBC, respectively, only 4 months after gene therapy procedure. These results suggest that the re-expression of endogenous HbF resulting from *BCL11A* repression might occur shortly after gene therapy procedure. Moreover, they are in accordance with the correlation established between the different thresholds of HbF/RBC and VOC incidence over 3 years in our cohort of SCD patients on HU treatment. They highlight the clinical interest in assessing HbF content distribution in SCD in case of any treatment aiming to induce HbF synthesis.

While the response is presented for only one patient, the other individuals included in this clinical trial display similar responses.

3. Improving the HbF/RBC assay

Using flow cytometry not only allows analysis of thousands of RBCs but also subpopulations of interest such as reticulocytes or patients' RBCs in the case of a chronic transfusion program. This method could also be applied to other hemoglobins with appropriate antibodies such as HbAS3 or HbA^{T87Q}. Moreover, combining quantitative measurements of different Hb and the total amount of Hb per RBC, would inform about their relative concentration, which is of interest for an anti-polymerization effect, using the corpuscular Hb concentration (MCHC) per RBC (371). However, the latter requires an individual volume measurement which is difficult to obtain when cell shape is not regular as in SCD. To this purpose, imaging flow cytometry, which has already been used to analyze SCD erythrocytes morphology, could be coupled to the quantitative Hb measurement (416).

Moreover, Improving the HbF quantification assay we developed by adding the concomitant determination of HbS content per RBC would be of major interest in SCD. Such an improvement presents three advantages.

First, because of chronic blood transfusion, SCD patients' RBCs are diluted with normal RBCs. This is the case before any HSCT or gene therapy procedure. The resulting HbF

quantification in individual RBCs is then currently determined in both S/S and A/A RBCs, with no possibility to discriminate between those two population. It thus results in an overestimated percentage of RBCs with low HbF content. The addition of an anti-HbS monoclonal antibody would allow to do this discrimination and to analyze only SS patients' own RBC population. This is of particular interest in strategies aiming at re-activating the endogenous HbF expression since transgene addition might be effective in a few days (the time for erythropoiesis to produce new RBCs), while it will be only measured several weeks after the procedure (as transfused RBCs are eliminated) without such a discrimination.

Second, in any gene addition procedure, the expression of anti-sickling Hb transgene, or re-expression of endogenous HbF is expected to be accompanied with a subsequent decrease in HbS content in RBCs. In theory, this HbS decrease would be more important in RBC expressing high levels of anti-sickling Hb. Therefore, a method allowing the assessment of HbS content in individual cells would give significant information on the degree of gene therapy procedure efficacy and the relative decrease in HbS, leading to the inhibition of polymerization.

Third, as HSCT induces a mixed cellular chimerism in receivers, it can be difficult to assess the efficacy of this procedure in case of a donor with A/S genotype. Indeed, evaluation is currently performed by measuring the global %HbS by HPLC, expecting it to reach level similar to what is observed in sickle cell trait individuals. However, the use of attenuated conditioning combined with A/S donors, might generates RBC chimerism which could only be assessed at the single-cell level. Thus, having a method able to discriminate RBC populations between those originating from A/S donors and those originating from the remaining S/S receiver's HSCs would have a major interest in transplantation follow-up.

Moreover, the possibility to assess both HbF and HbS content in reticulocytes would inform about the relative survival advantage of any red cell population. To this purpose, we have already begun to work on the improvement of the HbF assay to allow both determination of HbF and HbS content in individual RBCs, coupled to reticulocytes discrimination. Our preliminary results showed that it is easily possible to discriminate and analyze RBC sub-populations including A/A RBC in case of blood transfusion, A/S RBC and S/S RBCs, the two later presenting significant differences in fluorescence intensities according to their relative HbS content.

4. Selective survival advantage of RBCs containing anti-sickling hemoglobin

4.1. Fetal hemoglobin extends sickle RBCs lifespan

Thanks to its natural anti-polymerizing capability, HbF is a major modulator of the clinical severity of sickle cell disease. As a result, RBCs that contain more HbF survive longer than those with small amounts or no HbF. This has been demonstrated by RBC lifespan measurements carried out in SCD patients. The reinjection of biotin-labeled RBCs showed an extension of F cells lifespan, estimated to six weeks, by comparison with cells which do not contain HbF, for which survival was estimated to be around two weeks (383). Therefore, these results suggest that F cells might have a 3-fold improved survival advantage by comparison with non-F cells. As HbF is mostly heterogeneously distributed among RBCs from SCD patients, survival of F cells may be dependent on the concentration of HbF at the individual cell level. The demonstration of this survival advantage of cells with high levels of HbF is strengthened when HbF content is compared between reticulocytes and mature erythrocytes. Several studies have indeed reported that mature erythrocytes contain more HbF than reticulocytes in SCD patients (417–421).

The analysis of any subpopulation of interest, such as reticulocytes, simultaneously with HbF quantification is possible by flow cytometry. To this purpose, the addition of an anti-human-CD71 monoclonal antibody to the anti-HbF allows discriminating between reticulocytes (CD71-positive cells) and matures erythrocytes (CD71-negative cells) within the same sample. Here we found that while most reticulocytes contain less than 4 pg of HbF (90.6 ± 5.0 % of total retic [mean ± SD] for 12 SCD patients), the mature erythrocyte population containing more than 4 pg is 2.38-fold increased by comparison with reticulocytes. This enrichment is further increased for cells containing at least 6 pg of HbF and reaches a plateau for upper thresholds of HbF content. Statistically significant enrichments in mature erythrocytes by comparison with reticulocytes of 2.88-fold, 2.95-fold and 2.92-fold, for cells containing at least 6 pg, 8 pg and 10 pg of HbF, respectively, were calculated. These results are consistent with a previous study in which the authors showed, using flow cytometry, that F-reticulocyte percentages were always lower than those of F-erythrocyte percentages and that most reticulocytes contain a small amount of HbF in SCD patients (420). As already

reported, no statistically significant changes in HbF content between reticulocytes and erythrocytes from healthy donors were observed, in which no selective advantage of any RBC sub-populations is expected (421).

The survival advantage of sickle red cells may rely on the amount of HbF they contain, as already hypothesized (422). Our results indicate that the survival advantage of sickle red cells may be mainly dependent on the HbF level in individual cells from the threshold of 4 pg. Furthermore, they also suggest that there is a potential survival selection among RBCs containing more than 4 pg of HbF. However, in the present study, this selective advantage seems to reach a plateau from 6 pg of HbF, suggesting that an increase in HbF content over this threshold has limited effect, if no effect at all, on corresponding RBCs lifespan improvement in SCD patients. These thresholds of 4 pg and 6 pg of HbF/RBC are in accordance with the correlations we observed with VOC incidence over 3 years in our cohort of patients on HU treatment.

Interestingly, this enrichment was only observed in patients presenting a heterogenous distribution of HbF in RBC population and does not seem to be related to HU treatment. Indeed, we found out no changes in HbF quantification between reticulocytes and mature erythrocytes in patients presenting a homogeneous HbF distribution (data not shown). This observation confirms the results obtained in a previous study conducted on SCD patients, in which the authors did not observe any enrichment in percentages of F-erythrocytes by comparison with percentages of F-reticulocytes in two HPFH-sickle patients presenting a homogeneous HbF distribution (417). They however calculated a 2-fold increase in another HPFH-sickle patient for whom HbF was found heterogeneously distributed among RBCs. Despite a small cohort, we observed that at least 6 months of HU treatment induced a homogenization of HbF distribution in 50% of our patients. However, we did not assess HbF content in reticulocytes of those patients. The results presented here strongly suggest that, to be as much effective as possible, induction of anti-sickling Hb might need to be achieved in most HSCs, resulting in a pan-cellular distribution in reticulocytes.

4.2. Anti-sickling HbA^{T87Q} accumulation in RBCs as compared to reticulocytes following gene therapy

A similar accumulation was observed in erythrocytes from the two patients with no transfusion treated with LentiGlobin gene therapy in the HGB-205 study. Comparison of HbA^{T87Q} and HbF levels between reticulocytes and total circulating red cells reveals a 1.5-fold and a 3.5-fold enrichment in HbA^{T87Q} for P1 (at M42) and P3 (at M15), respectively, as well as a 2.0-fold enrichment in HbF for P3 (at M15). This accumulation in circulating RBCs by comparison with reticulocytes indicate an improved survival of RBCs exhibiting a higher expression of anti-sickling hemoglobin with a better enrichment in HbA^{T87Q} than in HbF in those two patients. To our knowledge, this is the first report of an improved selective advantage of RBCs resulting from the expression of an anti-sickling Hb following gene therapy procedure. No HbF accumulation in total circulating RBCs by comparison with reticulocytes for P1 was observed, which is consistent with the low HbF amount measured for this patient (<1.5%). Interestingly, HbA^{T87Q} enrichment was found more pronounced than HbF enrichment. These results suggest that the anti-sickling HbA^{T87Q} exhibits potent protective effect, at least similar to HbF, in improving survival of RBCs containing high levels of anti-sickling Hb.

4.3. Reticulocytes are involved in sickle cell disease pathophysiology

Taken together, these data suggest that the content of anti-sickling Hb in reticulocytes conditions their protection and durability in the blood. While the benefit of reticulocytosis under hemolytic anemia is to increase oxygen transport, it has been linked to increased mortality in children with SCD (423). Previous studies showed that sickle reticulocytes are more susceptible to cell dehydration and are less likely to resume discoidal shape on reoxygenation at the arterial oxygen tension than erythrocytes (420,424). The presence of reticulocytes among the DRBCs indicates that a portion of young red cells became dehydrated very quickly (425). This phenomenon is exacerbated in red cells with very low HbF content (419). In addition, sickle reticulocytes have reduced membrane deformability, suggesting an increased vaso-occlusive potential, in particular with the high numbers observed in patients (426). They also present phagocytosis signals, including inside-out PS-exposed autophagic vesicles, on their surface (427). In addition to transferrin receptor (CD71), they express

enhanced levels of the adhesive molecules glycoprotein IV (CD36) and α4β1 integrins, probably because of their premature release from the bone marrow. The CD36 is implicated in RBC binding endothelial lining of blood vessels through its interaction with TSP (250,428). The binding of integrin α4β1 to VCAM-1 and fibronectin occurs on the endothelial lining of blood vessels (429). Interestingly, an inverse relationship between percent of CD36 positive red cells and percent of F cells in sickle patients has been reported (430). However, hereditary nonexistence of CD36 receptor has not been shown to change the manifestation of SCD suggesting that CD36 might not be implicated in sickle reticulocytes adherence (431).

All these properties participate in making reticulocytes being believed to contribute to vaso-occlusion risk, with a higher risk in patients with splenic dysfunction. Indeed, hyposplenism, is frequently observed in SCD individuals and may results in failure to remove the inside-out PS-exposed red cells, exacerbating vaso-occlusion and clinical severity (432). Of note, long term engraftment of donor HSC occurs after transplantation and results in normalizing reticulocyte count as anemia improves (305,433). Furthermore, in the first published report of gene therapy in patient with SCD, reticulocyte counts decreased substantially after the transduction of the anti-sickling gene therapy vector (337).

Considering their reduced lifespan by comparison with reticulocytes containing more than 6 pg of HbF, these observations strongly suggest that reticulocytes and erythrocytes with low amounts of anti-sickling Hb (less than 4 pg of HbF) might represent an important biomarker of severity. Moreover, any treatment which reduces reticulocytosis is of particular interest in SCD.

4.4. Ineffective erythropoiesis in sickle cell disease

In addition to the increased survival of mature erythrocytes containing high level of anti-sickling Hb by comparison with reticulocytes, a similar selection has already been reported at the level of the early erythroid precursors (395,400). This selective advantage of donor erythroid precursors could be attributed to the existence of a dyserythropoiesis in SCD. In β-thalassemia, dyserythropoiesis is the major cause of anemia in affected patients. It is characterized by high levels of apoptotic erythroblasts during the last stages of terminal differentiation because of the aggregation of free α-globin chains (434,435).

A growing number of evidence strengthens the hypothesis of an ineffective erythropoiesis in SCD. Indeed, it has been shown that after HSCT, S/S erythroblasts presented a competitive disadvantage compared to donor's A/S erythroblasts, resulting in a predominance of donor's maturing erythroblasts, even with low levels of donor engraftment. (436). Erythroblasts differentiated *in vitro* or isolated from bone marrow of SCD patients were shown to sickle under hypoxic conditions (437). In line with this, structural abnormalities in S/S erythroid precursor cells, including sickle-shaped cells, and a depletion in BFU-E and CFU-E precursors, while compensated by an increase in their proliferation, have been described in a SCD mouse model (438). In addition to HbS polymerization, these alterations could be favored by the bone marrow vasculature defects observed in a SCD mouse model with sinusoids obstructed by both mature erythrocytes and nucleated erythroid precursors by comparison with non SCD mice (439). More recently, a study highlighted the existence of ineffective erythropoiesis in SCD patients using bone marrow aspirates. They showed high cell death rates at late stages of terminal erythroid differentiation (440). In addition, the authors also showed that HbF levels play a role in the preferential survival of erythroblasts.

All these data strongly suggest that the selective survival advantage induced by the anti-sickling Hb is not simply the consequence of the increased lifespan of F cells vs. non-F cells. It results from a complex balance between erythropoiesis, erythroblast maturation and reticulocytes production. The link between all these cells is their anti-sickling Hb level, which will protect them from HbS polymerization and confer them improved selective survival.

4.5. Increased removal of red cells with low amount of anti-sickling hemoglobin

The observation of the selective survival advantage during erythropoiesis on the one hand, and at the reticulocyte and erythrocyte levels on the other hand, strongly suggests that cells with low amounts of, or no, anti-sickling Hb are quickly eliminated. During erythropoiesis, the central macrophage at the erythroblastic island is involved in the clearance of abnormally maturated erythroblasts.

Several processes have been hypothesized to play a role in the clearance of the abnormal sickle RBCs such as phagocytosis within spleen and liver or by circulating patrolling monocytes.

These observations suggest that these monocytes/macrophages are able to discriminate signals on RBCs that promote their removal and that these signals are reduced according to anti-sickling Hb content. Oxidative stress induced by HbS polymerization induces band 3 clustering, opsonization by natural antibodies or complement C3b fragments and finally, recognition by Fc-receptors (173). PS exposure can be induced by cytosolic Ca^{2+} increased concentration as a result of oxidative stress (98). Least, RBC rigidity has been demonstrated has a signal of phagocytosis, activating macrophages myosin-II (171). This physical-based recognition is strong enough to pass by the CD47 interaction with the macrophage SIRPα, which protects from phagocytosis.

Furthermore, in patients with SCD, TSP plasma levels are elevated at baseline and further elevated in vaso-occlusive crisis, and high plasma TSP levels correlate with an increased risk of vaso-occlusive complications (441,442). In addition, it has recently been shown in a mouse model of SCD that both TSP and CD47 are upregulated in the lungs and also in SCD patients with pulmonary hypertension (254). TSP stimulates increased superoxide anion production in vascular endothelial cells, through CD47, contributing to vasculopathy (443).

We believe that this quick removal of unprotected red cells (with low amount of anti-sickling Hb) contributes to the difficulty to control hemolysis after HSCT or gene therapy. Therefore, it is probable that patients with a total reticulocyte count becoming normal after such a procedure might present improved hemolysis profile (400).

Red cell rigidity, oxidative stress (which leads to membrane impairments) and RBC adherence represent interesting signals to investigate in order to determine the functional protective effects of the expression of anti-sickling Hb in SCD. To this purpose, the use of an *in vitro* model of erythrophagocytosis might be of interest. The development of an assay using either autologous or non-autologous monocytes and/or macrophages or human cell lines such as THP-1 could answer these questions. Comparing SCD patients presenting different anti-sickling Hb levels and different patterns of distribution with normal RBCs could help to better understand their involvement in SCD pathophysiology.

To this purpose, a model like those already developed (444,445) but allowing in the same time the HbF and/or HbS content quantification using immunofluorescence, would be of interest to assess a more precisely a protective threshold of anti-sickling Hb content per cell.

5. Protective effect of anti-sickling hemoglobin synthesis in patients treated with LentiGlobin gene therapy in the HGB-205 study

While informative, Hb content quantification in individual RBCs is not the only way to evaluate protective effects of anti-sickling Hb expression. Sickle RBCs are known to present several alterations in their biological and physical properties because of HbS polymerization. As compared to normal RBCs, these alterations include a more rigid, less deformable profile, a global dehydration, an increased adhesion profile and an exacerbated trend toward hemolysis. Thus, assessing these properties represents another way to evaluate the functional protective effects induced by the expression of anti-sickling Hb, in particular in gene therapy trials.

To this purpose, RBC properties were analyzed in SCD patients treated with LentiGlobin gene therapy in the HGB-205 study during their clinical follow-up. Because of blood transfusion, results from patient 2 could not be exploited, however, our results show global improvement in RBC properties for the two patients with no transfusion (P1 and P3).

The extent of HbS polymerization, assessed by O_2 dissociation and re-association curves and by *in vitro* sickling assay, was clearly lower for P1 and P3 than for untreated SCD patients. Interestingly, results were better for P1 than P3, which is correlated with their respective total amount of anti-sickling Hb (HbA2 + HbF + HbA^{T87Q}). These results attest of the *in vivo* anti-sickling capability of HbA^{T87Q} in patients treated with LentiGlobin gene therapy.

Adherence profile under increasing shear stress on surface coated with TSP was also consistently lower for RBCs from P1 and P3 than mean value of RBCs from untreated SCD patients. Similar results were obtained on surface coated with fibronectin. Not surprisingly, RBCs adherence level for untreated SCD patients was very variable as already stated using laminin or endothelial cells under perfusion (281,286). Adherence profile of RBCs from P1 and P3 was relatively stable over the time and was more similar to the profile measured with RBCs from healthy donors.

Ektacytometry uses laser diffraction to provide a convenient measure of red cell deformability. Previous studies showed that rigid red cells do not align or deform properly in response to increasing shear stress (446). Here we show that the deformability level of RBCs from P1 and P3, assessed under physiological osmolality, was intermediate between levels measured for HD or AS individuals and untreated SCD patients. Osmotic gradient ektacytometry (osmoscan) measures erythrocyte deformability as a continuous function of changes in the osmolality of the suspending medium. In addition to deformability, the osmotic gradient curve provides additional information regarding surface to volume ratio, cellular hydration, and cytoplasmic viscosity. A study showed moderate correlation between deformability index and %HbF in SCD patients not treated with HU, indicating that HbF level is not the only determinant of RBC deformability (447). α-thalassemia plays also a role on RBC deformability, resulting in better cell deformability, less cellular dehydration and less dense cells than in patients with SCD and four α-globin genes (448). This is consistent with the improved osmoscan profile obtained for P1, who expresses more anti-sickling Hb and presents a heterozygous α-thal (−α/αα), as compared to P3. In addition, Parrow *et al*. reported osmoscan profiles shifted toward the left for RBCs from non-transfused SCD patients with %HbF ranging from 3.4% to 27.6% (447). However, it is unknown if HbF is homogeneously or heterogeneously distributed in those patients. Interestingly, whatever the %HbF, the osmoscan curve was shifted toward the left in those patients, which indicates the presence of dehydrated cells. These results are in accordance with our obtained for P1 and P3 in the present study. They indicate an improved deformability in P1 and P3 as compared to SS patients even in the presence of dehydrated cells. They also suggest that correcting dehydration might necessitate either higher levels of anti-sickling Hb or a more homogeneous distribution of it, as deformability is influenced by cell heterogeneity.

Least, we measured plasmatic hemolysis markers in those patients. We observed a trend toward normalization of the hemolysis in P1 and P3 as compared to SCD patients and HD. In particular, we measured very low level of cell-free plasma heme, similar to levels measured in A/S individuals. These levels were associated with the presence of normal value of its scavenger hemopexin, which is known to be depleted in SCD patients, as we measured.

It is important to note that these results of RBC properties must account for the fact that all these assays are performed using the red cell population. As such, it is difficult to

account for the contributions of pancellular or heterocellular distribution of HbA2, HbF and HbA^{T87Q}, respectively. HbF was very low in P1 and heterogeneously distributed in P3 as we measured thanks to the HbF/RBC assay.

To sum up, these results show a global improvement in RBC properties in two SCD patients treated with gene therapy in the HGB-205 study. Extent of HbS polymerization, adherence profile and hemolysis markers were more similar to those observed in healthy donor or sickle cell trait individuals than in non-treated SCD patients. Among the parameters we measured, the presence of dehydrated RBCs, which reduces their deformability at physiologic osmolality, remains after gene therapy procedure.

6. Remaining challenges in gene therapy and future prospects to cure sickle cell disease

Gene therapy to cure SCD presents several remaining challenges. Whereas expressing β-globin gene in transfusion dependent β-thal patients results in improved control of the disease (333), the endogenous β^S-globin is still synthetized in SCD. Both diseases require high levels of transgene expression to be efficient. Therapeutic LV vectors used to treat β-hemoglobinopathies contain human *cis*-regulatory elements that provide erythroid-specific expression of the transgene. However, the 7.5–10 kb packaging limit of LV vectors cannot contain the entire 16 kb human β-LCR, which is required for the high expression of *HBB* gene (316,449). In addition, therapeutic level of globin expression after gene addition in SCD might be difficult to obtain, presumably because of competition with endogenous β^S-globin messenger RNAs. In this context, selecting the best β-LCR elements to allow high transgene expression and considering size limitation might help to develop better LV vectors. Several studies showed that an optimized selection of HS regulatory elements of the β-LCR resulted in increased transgene expression. In addition, some of these studies achieved correction of SCD phenotypes in mouse models, without affecting LV vectors production (330,399,450–452). Moreover, large size LV vectors have also been described to present a negative impact on virus production (453). Therefore, selecting the smallest regulatory elements allowing the best level of transgene production might increase LV vectors-mediated gene therapy in the future (399,454).

In this context, it is possible that reversing the fetal-to-adult Hb switch might represent an easier goal to reach. Indeed, inhibiting *BCL11A* expression via RNA interference may need lower transgene expression than anti-sickling Hb expression to reach sufficient HbF protective amounts in most RBCs.

An additional challenge is that the level of correction of the sickle mutation or the curative induction of anti-sickling Hb is not yet fully and precisely determined. Therefore, one could be encouraged to increase VCN in the infused drug product to achieve better transgene expression and functional correction of the disease. LV vectors are believed to be safer than RT vectors because of their preferential integration into transcribed regions of expressed genes, away from promoters and regulatory elements (455). However, they still present a risk of insertional mutagenesis and oncogenesis (456). Therefore, VCN and the absence of clonal dominance following engraftment are parameters that must be carefully analyzed. The need for an effective engraftment is also a challenge since it will condition the mixed chimerism observed in those patients after gene therapy procedure.

Gene therapy must also face its very expensive production cost. It has been estimated that a sufficient amount of vector needed for one patient is about 300,000 euros (457,458). Today, standard LV vectors are made using a third-generation production system that relies on the transfection of the cell line HEK293T (Human Embryonic Kidney) (459). While this process can generate high-titer of replication-competent lentivirus, it necessitates high amount of handling and consumables costs, mainly because of the adherent nature of the HEK293T cell line. Consequently, healthcare systems will probably not be able to meet the cost for treating large numbers of individuals, even in high-income countries (458).

Gene and genome editing hold great promise as a second-generation approach to gene therapy for β-hemoglobinopathies. In theory, genome-editing approaches may be safer than strategies utilizing LV vectors. Indeed, these approaches are supposed to be “targeted”. However, potentially genotoxic non-specific DNA modifications (off-target) might occur. The CRISPR/Cas9 system may cause more than 50% frequency of off-target activity, leading to the undesired DNA damage and cytotoxicity (460). The generation of double strand breaks to recreates large deletions in the genome might triggers larger deletions than expected,

inversions or translocations (461,462). Such lesions may constitute a first transforming event in stem and progenitors cells, which have a long replicative lifespan. The alternative of currently used gene-editing strategies in the future would be to use the CRISPR/Cas12a-mediated genome editing, which is believed to be more specific than the commonly used Cas9 enzyme (463–465). For DNA targeting, while Cas9 requires both a CRISPR RNAs (crRNAs) as a guide, and a trans-activating crRNA (tracrRNA), which is involved in maturation of the crRNA, Cas12a only requires a single crRNA guide. Moreover, Cas9 possesses two nuclease sites, while Cas12a possesses only one nuclease site (466). For example, CRISPR/Cas12a was applied to correct mutations causing Duchenne muscular dystrophy in patient derived induced pluripotent stem cells and in the corresponding murine model (mdx mice) (467). In addition, the possibility of a non-viral delivery should significantly reduce the overall cost of treatment.

Conclusion

A comprehensive functional analysis of the resulting blood, after a patient has undergone gene-based therapy, is essential for further development of these novel therapies, and verification that a cure has been achieved. Herein we described an assay allowing to assess the Hb quantitative distribution in RBCs which is of interest to, first, determine a protective threshold to reach in order to achieve full correction of the disease, second, to analyze mixed erythrocyte and reticulocyte chimerisms after gene therapy procedure and third, to evaluate selective survival advantage of RBCs expressing high levels of anti-sickling Hb. In addition, the use of functional assays, allowing to determine the biological effects and improvements induced by gene therapy procedures, represent a strategy to validate those new curative approaches for the treatment of SCD.

Bibliography

1. Herrick JB. Peculiar elongated and sickle-shaped red blood corpuscles in a case of severe anemia. 1910. Yale J Biol Med. juin 2001;74(3):179-84.

2. Savitt TL, Goldberg MF. Herrick's 1910 case report of sickle cell anemia. The rest of the story. JAMA. 13 janv 1989;261(2):266-71.

3. Mason VR. Landmark article Oct. 14, 1922: Sickle cell anemia. By V.R. Mason. JAMA. 11 oct 1985;254(14):1955-7.

4. Diggs LW. Pathology of Sickle Cell Disease. JAMA. 25 oct 1971;218(4):600-600.

5. Pauling L, Itano HA. Sickle cell anemia, a molecular disease. Science. 29 avr 1949;109(2835):443.

6. Ingram VM. Gene mutations in human haemoglobin: the chemical difference between normal and sickle cell haemoglobin. Nature. 17 août 1957;180(4581):326-8.

7. Konigsberg W, Goldstein J, Hill RJ. The structure of human hemoglobin. VII. The digestion of the beta chain of human hemoglobin with pepsin. J Biol Chem. juin 1963;238:2028-33.

8. Bunn HF, McDonald MJ. Electrostatic interactions in the assembly of haemoglobin. Nature. 1 déc 1983;306(5942):498-500.

9. Allison AC. Protection afforded by sickle-cell trait against subtertian malareal infection. Br Med J. 6 févr 1954;1(4857):290-4.

10. Taylor SM, Parobek CM, Fairhurst RM. Haemoglobinopathies and the clinical epidemiology of malaria: a systematic review and meta-analysis. Lancet Infect Dis. juin 2012;12(6):457-68.

11. Malaria Genomic Epidemiology Network, Malaria Genomic Epidemiology Network. Reappraisal of known malaria resistance loci in a large multicenter study. Nat Genet. nov 2014;46(11):1197-204.

12. Key NS, Derebail VK. Sickle-cell trait: novel clinical significance. Hematol Am Soc Hematol Educ Program. 2010;2010:418-22.

13. Piel FB, Patil AP, Howes RE, Nyangiri OA, Gething PW, Williams TN, et al. Global distribution of the sickle cell gene and geographical confirmation of the malaria hypothesis. Nat Commun. 2 nov 2010;1:104.

14. Naik RP, Haywood C. Sickle cell trait diagnosis: clinical and social implications. Hematol Am Soc Hematol Educ Program. 2015;2015:160-7.

15. Williams TN, Thein SL. Sickle Cell Anemia and Its Phenotypes. Annu Rev Genomics Hum Genet. 31 2018;19:113-47.

16. Piel FB, Patil AP, Howes RE, Nyangiri OA, Gething PW, Dewi M, et al. Global epidemiology of sickle haemoglobin in neonates: a contemporary geostatistical model-based map and population estimates. Lancet Lond Engl. 12 janv 2013;381(9861):142-51.

17. Wastnedge E, Waters D, Patel S, Morrison K, Goh MY, Adeloye D, et al. The global burden of sickle cell disease in children under five years of age: a systematic review and meta-analysis. J Glob Health. déc 2018;8(2):021103.

18. Piel FB, Hay SI, Gupta S, Weatherall DJ, Williams TN. Global burden of sickle cell anaemia in children under five, 2010-2050: modelling based on demographics, excess mortality, and interventions. PLoS Med. 2013;10(7):e1001484.

19. McGann PT. Time to Invest in Sickle Cell Anemia as a Global Health Priority. Pediatrics. 2016;137(6).

20. Kato GJ, Piel FB, Reid CD, Gaston MH, Ohene-Frempong K, Krishnamurti L, et al. Sickle cell disease. Nat Rev Dis Primer. 15 2018;4:18010.

21. Weed RI, Reed CF, Berg G. Is hemoglobin an essential structural component of human erythrocyte membranes? J Clin Invest. avr 1963;42:581-8.

22. Rhinesmith HS, Schroeder WA, Martin N. The N-Terminal Sequence of the β Chains1 of Normal Adult Human Hemoglobin. J Am Chem Soc. 1 juill 1958;80(13):3358-61.

23. Hill RJ, Konigsberg W, Guidotti G, Craig LC. The structure of human hemoglobin. I. The separation of the alpha and beta chains and their amino acid composition. J Biol Chem. mai 1962;237:1549-54.

24. Thom CS, Dickson CF, Gell DA, Weiss MJ. Hemoglobin variants: biochemical properties and clinical correlates. Cold Spring Harb Perspect Med. 1 mars 2013;3(3):a011858.

25. Bringas M, Petruk AA, Estrin DA, Capece L, Martí MA. Tertiary and quaternary structural basis of oxygen affinity in human hemoglobin as revealed by multiscale simulations. Sci Rep. 07 2017;7(1):10926.

26. Bouzhir-Sima L. Study of the bacterial heme-proteins oxygen-sensors FixL and Dos. 20 nov 2006;

27. Monod J, Wyman J, Changeux JP. ON THE NATURE OF ALLOSTERIC TRANSITIONS: A PLAUSIBLE MODEL. J Mol Biol. mai 1965;12:88-118.

28. Eaton WA, Henry ER, Hofrichter J, Mozzarelli A. Is cooperative oxygen binding by hemoglobin really understood? Nat Struct Biol. avr 1999;6(4):351-8.

29. Henry ER, Bettati S, Hofrichter J, Eaton WA. A tertiary two-state allosteric model for hemoglobin. Biophys Chem. 10 juill 2002;98(1-2):149-64.

30. Viappiani C, Bettati S, Bruno S, Ronda L, Abbruzzetti S, Mozzarelli A, et al. New insights into allosteric mechanisms from trapping unstable protein conformations in silica gels. Proc Natl Acad Sci U S A. 5 oct 2004;101(40):14414-9.

31. Viappiani C, Abbruzzetti S, Ronda L, Bettati S, Henry ER, Mozzarelli A, et al. Experimental basis for a new allosteric model for multisubunit proteins. Proc Natl Acad Sci U S A. 2 sept 2014;111(35):12758-63.

32. Pincez T, Calamy L, Germont Z, Lemoine A, Lopes A-A, Massiot A, et al. [Pulmonary complications of sickle cell disease in children]. Arch Pediatr Organe Off Soc Francaise Pediatr. oct 2016;23(10):1094-106.

33. Rabbitts TH. Bacterial cloning of plasmids carrying copies of rabbit globin messenger RNA. Nature. 18 mars 1976;260(5548):221-5.

34. Frenette PS, Atweh GF. Sickle cell disease: old discoveries, new concepts, and future promise. J Clin Invest. avr 2007;117(4):850-8.

35. Bernet A, Sabatier S, Picketts DJ, Ouazana R, Morlé F, Higgs DR, et al. Targeted inactivation of the major positive regulatory element (HS-40) of the human alpha-globin gene locus. Blood. 1 août 1995;86(3):1202-11.

36. Grosveld F, van Assendelft GB, Greaves DR, Kollias G. Position-independent, high-level expression of the human beta-globin gene in transgenic mice. Cell. 24 déc 1987;51(6):975-85.

37. Sankaran VG, Xu J, Orkin SH. Advances in the understanding of haemoglobin switching. Br J Haematol. avr 2010;149(2):181-94.

38. Sankaran VG, Orkin SH. The switch from fetal to adult hemoglobin. Cold Spring Harb Perspect Med. 1 janv 2013;3(1):a011643.

39. Grosso M, Sessa R, Puzone S, Storino M, Izzo P. Molecular Basis of Thalassemia. In 2012.

40. Smith EC, Orkin SH. Hemoglobin genetics: recent contributions of GWAS and gene editing. Hum Mol Genet. 01 2016;25(R2):R99-105.

41. Martino MD, Sessa R, Storino MR, Giuliano M, Trombetti S, Catapano R, et al. Transcriptional Repressors of Fetal Globin Genes as Novel Therapeutic Targets in Beta-Thalassemia. Beta Thalass [Internet]. 23 janv 2020 [cité 17 sept 2020]; Disponible sur: https://www.intechopen.com/online-first/transcriptional-repressors-of-fetal-globin-genes-as-novel-therapeutic-targets-in-beta-thalassemia

42. Sankaran VG, Menne TF, Xu J, Akie TE, Lettre G, Van Handel B, et al. Human fetal hemoglobin expression is regulated by the developmental stage-specific repressor BCL11A. Science. 19 déc 2008;322(5909):1839-42.

43. Iarovaia OV, Kovina AP, Petrova NV, Razin SV, Ioudinkova ES, Vassetzky YS, et al. Genetic and Epigenetic Mechanisms of β-Globin Gene Switching. Biochem Biokhimiia. avr 2018;83(4):381-92.

44. Deng W, Lee J, Wang H, Miller J, Reik A, Gregory PD, et al. Controlling long-range genomic interactions at a native locus by targeted tethering of a looping factor. Cell. 8 juin 2012;149(6):1233-44.

45. Masuda T, Wang X, Maeda M, Canver MC, Sher F, Funnell APW, et al. Transcription factors LRF and BCL11A independently repress expression of fetal hemoglobin. Science. 15 janv 2016;351(6270):285-9.

46. Norton LJ, Funnell APW, Burdach J, Wienert B, Kurita R, Nakamura Y, et al. KLF1 directly activates expression of the novel fetal globin repressor ZBTB7A/LRF in erythroid cells. Blood Adv. 25 avr 2017;1(11):685-92.

47. Cavazzana M, Antoniani C, Miccio A. Gene Therapy for β-Hemoglobinopathies. Mol Ther J Am Soc Gene Ther. 03 2017;25(5):1142-54.

48. Hardison RC, Chui DH, Riemer C, Giardine B, Lehväslaiho H, Wajcman H, et al. Databases of human hemoglobin variants and other resources at the globin gene server. Hemoglobin. mai 2001;25(2):183-93.

49. Giardine B, Borg J, Viennas E, Pavlidis C, Moradkhani K, Joly P, et al. Updates of the HbVar database of human hemoglobin variants and thalassemia mutations. Nucleic Acids Res. janv 2014;42(Database issue):D1063-1069.

50. Modell B, Darlison M. Global epidemiology of haemoglobin disorders and derived service indicators. Bull World Health Organ. juin 2008;86(6):480-7.

51. Nagel RL, Fabry ME, Steinberg MH. The paradox of hemoglobin SC disease. Blood Rev. sept 2003;17(3):167-78.

52. Pecker LH, Schaefer BA, Luchtman-Jones L. Knowledge Insufficient: The Management of Haemoglobin SC Disease. Br J Haematol. févr 2017;176(4):515-26.

53. Stetson CA. The state of hemoglobin in sickled erythrocytes. J Exp Med. 1 févr 1966;123(2):341-6.

54. White JG, Heagan B. The fine structure of cell-free sickled hemoglobin. Am J Pathol. janv 1970;58(1):1-17.

55. Dykes G, Crepeau RH, Edelstein SJ. Three-dimensional reconstruction of the fibres of sickle cell haemoglobin. Nature. 6 avr 1978;272(5653):506-10.

56. Carragher B, Bluemke DA, Becker M, McDade WA, Potel MJ, Josephs R. Structural analysis of polymers of sickle cell hemoglobin. III. Fibers within fascicles. J Mol Biol. 20 janv 1988;199(2):383-8.

57. Li H, Papageorgiou DP, Chang H-Y, Lu L, Yang J, Deng Y. Synergistic Integration of Laboratory and Numerical Approaches in Studies of the Biomechanics of Diseased Red Blood Cells. Biosensors. 10 août 2018;8(3).

58. Sack JS, Andrews LC, Magnus KA, Hanson JC, Rubin J, Love WE. Location of amino acid residues in human deoxy hemoglobin. Hemoglobin. 1978;2(2):153-69.

59. Ghatge MS, Ahmed MH, Omar ASM, Pagare PP, Rosef S, Kellogg GE, et al. Crystal structure of carbonmonoxy sickle hemoglobin in R-state conformation. J Struct Biol. 2016;194(3):446-50.

60. Noguchi CT, Schechter AN. The intracellular polymerization of sickle hemoglobin and its relevance to sickle cell disease. Blood. déc 1981;58(6):1057-68.

61. Döbler J, Bertles JF. The physical state of hemoglobin in sickle-cell anemia erythrocytes in vivo. J Exp Med. 1 avr 1968;127(4):711-4.

62. Hofrichter J, Ross PD, Eaton WA. Kinetics and mechanism of deoxyhemoglobin S gelation: a new approach to understanding sickle cell disease. Proc Natl Acad Sci U S A. déc 1974;71(12):4864-8.

63. Malfa R, Steinhardt J. A temperature-dependent latent-period in the aggregation of sickle-cell deoxyhemoglobin. Biochem Biophys Res Commun. 5 août 1974;59(3):887-93.

64. Moffat K, Gibson QH. The rates of polymerization and depolymerization of sickle cell hemoglobin. Biochem Biophys Res Commun. 6 nov 1974;61(1):237-42.

65. Eaton WA, Hofrichter J. Hemoglobin S gelation and sickle cell disease. Blood. nov 1987;70(5):1245-66.

66. Henry ER, Cellmer T, Dunkelberger EB, Metaferia B, Hofrichter J, Li Q, et al. Allosteric control of hemoglobin S fiber formation by oxygen and its relation to the pathophysiology of sickle cell disease. Proc Natl Acad Sci U S A. 30 2020;117(26):15018-27.

67. Voet D, Voet JG. Biochimie. De Boeck Superieur; 2016. 1786 p.

68. Ferrone FA, Hofrichter J, Sunshine HR, Eaton WA. Kinetic studies on photolysis-induced gelation of sickle cell hemoglobin suggest a new mechanism. Biophys J. oct 1980;32(1):361-80.

69. Ferrone FA, Hofrichter J, Eaton WA. Kinetics of sickle hemoglobin polymerization. I. Studies using temperature-jump and laser photolysis techniques. J Mol Biol. 25 juin 1985;183(4):591-610.

70. Ferrone FA, Hofrichter J, Eaton WA. Kinetics of sickle hemoglobin polymerization. II. A double nucleation mechanism. J Mol Biol. 25 juin 1985;183(4):611-31.

71. Cohen SIA, Linse S, Luheshi LM, Hellstrand E, White DA, Rajah L, et al. Proliferation of amyloid-β42 aggregates occurs through a secondary nucleation mechanism. Proc Natl Acad Sci. 11 juin 2013;110(24):9758.

72. Ferrone FA. The delay time in sickle cell disease after 40 years: A paradigm assessed. Am J Hematol. mai 2015;90(5):438-45.

73. May A, Huehns ER. The mechanism of the low oxygen affinity of red cells in sickle cell disease. Hamatol Bluttransfus. 1972;10:279-83.

74. Seakins M, Gibbs WN, Milner PF, Bertles JF. Erythrocyte Hb-S concentration. An important factor in the low oxygen affinity of blood in sickle cell anemia. J Clin Invest. févr 1973;52(2):422-32.

75. Sun K, D'Alessandro A, Ahmed MH, Zhang Y, Song A, Ko T-P, et al. Structural and Functional Insight of Sphingosine 1-Phosphate-Mediated Pathogenic Metabolic Reprogramming in Sickle Cell Disease. Sci Rep. 10 2017;7(1):15281.

76. Adebiyi MG, Manalo JM, Xia Y. Metabolomic and molecular insights into sickle cell disease and innovative therapies. Blood Adv. 23 2019;3(8):1347-55.

77. Sunshine HR, Hofrichter J, Ferrone FA, Eaton WA. Oxygen binding by sickle cell hemoglobin polymers. J Mol Biol. 25 juin 1982;158(2):251-73.

78. Kaufman DP, Khattar J, Lappin SL. Physiology, Fetal Hemoglobin. In: StatPearls [Internet]. Treasure Island (FL): StatPearls Publishing; 2020 [cité 17 sept 2020]. Disponible sur: http://www.ncbi.nlm.nih.gov/books/NBK500011/

79. Antwi-Boasiako C, Frimpong E, Ababio GK, Dzudzor B, Ekem I, Gyan B, et al. Sickle Cell Disease: Reappraisal of the Role of Foetal Haemoglobin Levels in the Frequency of Vaso-Occlusive Crisis. Ghana Med J. juin 2015;49(2):102-6.

80. Bookchin RM, Nagel RL. Interactions between human hemoglobins: sickling and related phenomena. Semin Hematol. oct 1974;11(4):577-95.

81. Adachi K, Ozguc M, Asakura T. Nucleation-controlled aggregation of deoxyhemoglobin S. Participation of hemoglobin A in the aggregation of deoxyhemoglobin S in concentrated phosphate buffer. J Biol Chem. 10 avr 1980;255(7):3092-9.

82. Adachi K, Segal R, Asakura T. Nucleation-controlled aggregation of deoxyhemoglobin S. Participation of hemoglobin F in the aggregation of deoxyhemoglobin S in concentrated phosphate buffer. J Biol Chem. 25 août 1980;255(16):7595-603.

83. Eaton WA, Hofrichter J. The biophysics of sickle cell hydroxyurea therapy. Science. 26 mai 1995;268(5214):1142-3.

84. Bunn HF, McDonough M. Asymmetrical hemoglobin hybrids. An approach to the study of subunit interactions. Biochemistry. 26 févr 1974;13(5):988-93.

85. Goldberg MA, Husson MA, Bunn HF. Participation of hemoglobins A and F in polymerization of sickle hemoglobin. J Biol Chem. 25 mai 1977;252(10):3414-21.

86. Benesch RE, Edalji R, Benesch R, Kwong S. Solubilization of hemoglobin S by other hemoglobins. Proc Natl Acad Sci U S A. sept 1980;77(9):5130-4.

87. Adachi K, Konitzer P, Surrey S. Role of gamma 87 Gln in the inhibition of hemoglobin S polymerization by hemoglobin F. J Biol Chem. 1 avr 1994;269(13):9562-7.

88. Nagel RL, Bookchin RM, Johnson J, Labie D, Wajcman H, Isaac-Sodeye WA, et al. Structural bases of the inhibitory effects of hemoglobin F and hemoglobin A2 on the polymerization of hemoglobin S. Proc Natl Acad Sci U S A. févr 1979;76(2):670-2.

89. Eaton WA, Bunn HF. Treating sickle cell disease by targeting HbS polymerization. Blood. 18 2017;129(20):2719-26.

90. Mohandas N, Gallagher PG. Red cell membrane: past, present, and future. Blood. 15 nov 2008;112(10):3939-48.

91. Dzierzak E, Philipsen S. Erythropoiesis: development and differentiation. Cold Spring Harb Perspect Med. 1 avr 2013;3(4):a011601.

92. Barminko J, Reinholt B, Baron MH. Development and differentiation of the erythroid lineage in mammals. Dev Comp Immunol. mai 2016;58:18-29.

93. Zivot A, Lipton JM, Narla A, Blanc L. Erythropoiesis: insights into pathophysiology and treatments in 2017. Mol Med Camb Mass. 23 2018;24(1):11.

94. Bessis M. [Erythroblastic island, functional unity of bone marrow]. Rev Hematol. mars 1958;13(1):8-11.

95. Giger KM, Kalfa TA. Phylogenetic and Ontogenetic View of Erythroblastic Islands. BioMed Res Int. 2015;2015:873628.

96. Centis F, Tabellini L, Lucarelli G, Buffi O, Tonucci P, Persini B, et al. The importance of erythroid expansion in determining the extent of apoptosis in erythroid precursors in patients with beta-thalassemia major. Blood. 15 nov 2000;96(10):3624-9.

97. Mathias LA, Fisher TC, Zeng L, Meiselman HJ, Weinberg KI, Hiti AL, et al. Ineffective erythropoiesis in beta-thalassemia major is due to apoptosis at the polychromatophilic normoblast stage. Exp Hematol. déc 2000;28(12):1343-53.

98. Klei TRL, Meinderts SM, van den Berg TK, van Bruggen R. From the Cradle to the Grave: The Role of Macrophages in Erythropoiesis and Erythrophagocytosis. Front Immunol. 2017;8:73.

99. Manwani D, Bieker JJ. The erythroblastic island. Curr Top Dev Biol. 2008;82:23-53.

100. Broxmeyer HE. Erythropoietin: multiple targets, actions, and modifying influences for biological and clinical consideration. J Exp Med. 11 févr 2013;210(2):205-8.

101. Grebien F, Kerenyi MA, Kovacic B, Kolbe T, Becker V, Dolznig H, et al. Stat5 activation enables erythropoiesis in the absence of EpoR and Jak2. Blood. 1 mai 2008;111(9):4511-22.

102. Moriguchi T, Yamamoto M. A regulatory network governing Gata1 and Gata2 gene transcription orchestrates erythroid lineage differentiation. Int J Hematol. nov 2014;100(5):417-24.

103. Nemeth E, Tuttle MS, Powelson J, Vaughn MB, Donovan A, Ward DM, et al. Hepcidin regulates cellular iron efflux by binding to ferroportin and inducing its internalization. Science. 17 déc 2004;306(5704):2090-3.

104. Johns JL, Christopher MM. Extramedullary hematopoiesis: a new look at the underlying stem cell niche, theories of development, and occurrence in animals. Vet Pathol. mai 2012;49(3):508-23.

105. Paulson RF, Hariharan S, Little JA. Stress erythropoiesis: definitions and models for its study. Exp Hematol. 2 août 2020;

106. Xiang J, Wu D-C, Chen Y, Paulson RF. In vitro culture of stress erythroid progenitors identifies distinct progenitor populations and analogous human progenitors. Blood. 12 mars 2015;125(11):1803-12.

107. Paulson RF, Shi L, Wu D-C. Stress erythropoiesis: new signals and new stress progenitor cells. Curr Opin Hematol. mai 2011;18(3):139-45.

108. Stamatoyannopoulos G, Veith R, Galanello R, Papayannopoulou T. Hb F production in stressed erythropoiesis: observations and kinetic models. Ann N Y Acad Sci. 1985;445:188-97.

109. Luck L, Zeng L, Hiti AL, Weinberg KI, Malik P. Human CD34(+) and CD34(+)CD38(-) hematopoietic progenitors in sickle cell disease differ phenotypically and functionally from normal and suggest distinct subpopulations that generate F cells. Exp Hematol. mai 2004;32(5):483-93.

110. Weinberg RS, Schofield JM, Lenes AL, Brochstein J, Alter BP. Adult « fetal-like » erythropoiesis characterizes recovery from bone marrow transplantation. Br J Haematol. juill 1986;63(3):415-24.

111. Pretini V, Koenen MH, Kaestner L, Fens MHAM, Schiffelers RM, Bartels M, et al. Red Blood Cells: Chasing Interactions. Front Physiol. 2019;10:945.

112. Smith BD, Lambert TN. Molecular ferries: membrane carriers that promote phospholipid flip-flop and chloride transport. Chem Commun Camb Engl. 21 sept 2003;(18):2261-8.

113. Hankins HM, Baldridge RD, Xu P, Graham TR. Role of flippases, scramblases and transfer proteins in phosphatidylserine subcellular distribution. Traffic Cph Den. janv 2015;16(1):35-47.

114. Kobayashi N, Karisola P, Peña-Cruz V, Dorfman DM, Jinushi M, Umetsu SE, et al. TIM-1 and TIM-4 glycoproteins bind phosphatidylserine and mediate uptake of apoptotic cells. Immunity. déc 2007;27(6):927-40.

115. Segawa K, Nagata S. An Apoptotic « Eat Me » Signal: Phosphatidylserine Exposure. Trends Cell Biol. nov 2015;25(11):639-50.

116. McLaughlin S. The electrostatic properties of membranes. Annu Rev Biophys Biophys Chem. 1989;18:113-36.

117. Langner M, Cafiso D, Marcelja S, McLaughlin S. Electrostatics of phosphoinositide bilayer membranes. Theoretical and experimental results. Biophys J. févr 1990;57(2):335-49.

118. Burton NM, Bruce LJ. Modelling the structure of the red cell membrane. Biochem Cell Biol Biochim Biol Cell. avr 2011;89(2):200-15.

119. Lux SE. Anatomy of the red cell membrane skeleton: unanswered questions. Blood. 14 janv 2016;127(2):187-99.

120. Clark MR, Mohandas N, Shohet SB. Osmotic gradient ektacytometry: comprehensive characterization of red cell volume and surface maintenance. Blood. mai 1983;61(5):899-910.

121. Higgins JM. Red blood cell population dynamics. Clin Lab Med. mars 2015;35(1):43-57.

122. Parrow NL, Violet P-C, Tu H, Nichols J, Pittman CA, Fitzhugh C, et al. Measuring Deformability and Red Cell Heterogeneity in Blood by Ektacytometry. J Vis Exp JoVE. 12 2018;(131).

123. Renoux C, Faivre M, Bessaa A, Da Costa L, Joly P, Gauthier A, et al. Impact of surface-area-to-volume ratio, internal viscosity and membrane viscoelasticity on red blood cell deformability measured in isotonic condition. Sci Rep. 01 2019;9(1):6771.

124. Bishop JJ, Popel AS, Intaglietta M, Johnson PC. Effects of erythrocyte aggregation and venous network geometry on red blood cell axial migration. Am J Physiol Heart Circ Physiol. août 2001;281(2):H939-950.

125. Baskurt OK, Meiselman HJ. Red blood cell « aggregability ». Clin Hemorheol Microcirc. 2009;43(4):353-4.

126. Nader E, Skinner S, Romana M, Fort R, Lemonne N, Guillot N, et al. Blood Rheology: Key Parameters, Impact on Blood Flow, Role in Sickle Cell Disease and Effects of Exercise. Front Physiol. 2019;10:1329.

127. Gallagher PG. Disorders of erythrocyte hydration. Blood. 21 2017;130(25):2699-708.

128. Dotsenko OI. In silico study of peculiarities of metabolism of erythrocytes with glucosephosphate isomerase deficiency. Regul Mech Biosyst. 17 juill 2019;10(3):306-13.

129. Joshi A, Palsson BO. Metabolic dynamics in the human red cell. Part IV--Data prediction and some model computations. J Theor Biol. 9 janv 1990;142(1):69-85.

130. Tavazzi D, Taher A, Cappellini MD. Red blood cell enzyme disorders: an overview. Pediatr Ann. 2008;37(5):303-10.

131. Hess JR, Solheim BG. Red blood cell metabolism, preservation, and oxygen delivery. In: Simon TL, McCullough J, Snyder EL, Solheim BG, trauss RGS, éditeurs. Rossi's Principles of Transfusion Medicine [Internet]. Chichester, WestSussex: John Wiley & Sons, Ltd.; 2016 [cité 17 sept 2020]. p. 97-109. Disponible sur: http://doi.wiley.com/10.1002/9781119013020.ch09

132. Ogasawara Y, Funakoshi M, Ishii K. Glucose metabolism is accelerated by exposure to t-butylhydroperoxide during NADH consumption in human erythrocytes. Blood Cells Mol Dis. déc 2008;41(3):237-43.

133. Gallagher P. HEMOLYTIC ANEMIAS : RED BLOOD CELL MEMBRANE AND METABOLIC DEFECTS [Internet]. 2015 [cité 17 sept 2020]. Disponible sur: /paper/HEMOLYTIC-ANEMIAS-%3A-RED-BLOOD-CELL-MEMBRANE-AND-Gallagher/0f01efe030314c2fadd42d007f0683721f854156

134. Rifkind JM, Mohanty JG, Nagababu E. The pathophysiology of extracellular hemoglobin associated with enhanced oxidative reactions. Front Physiol. 2014;5:500.

135. Voskou S, Aslan M, Fanis P, Phylactides M, Kleanthous M. Oxidative stress in β-thalassaemia and sickle cell disease. Redox Biol. déc 2015;6:226-39.

136. Bunn HF, Jandl JH. Exchange of heme among hemoglobins and between hemoglobin and albumin. J Biol Chem. 10 févr 1968;243(3):465-75.

137. Balla J, Jacob HS, Balla G, Nath K, Eaton JW, Vercellotti GM. Endothelial-cell heme uptake from heme proteins: induction of sensitization and desensitization to oxidant damage. Proc Natl Acad Sci U S A. 15 oct 1993;90(20):9285-9.

138. Mohanty JG, Nagababu E, Rifkind JM. Red blood cell oxidative stress impairs oxygen delivery and induces red blood cell aging. Front Physiol. 2014;5:84.

139. Ibrahim HA, Fouda MI, Yahya RS, Abousamra NK, Abd Elazim RA. Erythrocyte phosphatidylserine exposure in β-thalassemia. Lab Hematol Off Publ Int Soc Lab Hematol. juin 2014;20(2):9-14.

140. Mannu F, Arese P, Cappellini MD, Fiorelli G, Cappadoro M, Giribaldi G, et al. Role of hemichrome binding to erythrocyte membrane in the generation of band-3 alterations in beta-thalassemia intermedia erythrocytes. Blood. 1 sept 1995;86(5):2014-20.

141. George A, Pushkaran S, Li L, An X, Zheng Y, Mohandas N, et al. Altered phosphorylation of cytoskeleton proteins in sickle red blood cells: the role of protein kinase C, Rac GTPases, and reactive oxygen species. Blood Cells Mol Dis. 15 juin 2010;45(1):41-5.

142. Percy MJ, Lappin TR. Recessive congenital methaemoglobinaemia: cytochrome b(5) reductase deficiency. Br J Haematol. mai 2008;141(3):298-308.

143. Mannervik B. The enzymes of glutathione metabolism: an overview. Biochem Soc Trans. août 1987;15(4):717-8.

144. van Zwieten R, Verhoeven AJ, Roos D. Inborn defects in the antioxidant systems of human red blood cells. Free Radic Biol Med. févr 2014;67:377-86.

145. Franco RS. The measurement and importance of red cell survival. Am J Hematol. févr 2009;84(2):109-14.

146. Ebaugh FG, Emerson CP, Ross JF. The use of radioactive chromium 51 as an erythrocyte tagging agent for the determination or red cell survival in vivo. J Clin Invest. déc 1953;32(12):1260-76.

147. Bitan ZC, Zhou A, McMahon DJ, Kessler D, Shaz BH, Caccappolo E, et al. Donor Iron Deficiency Study (DIDS): protocol of a study to test whether iron deficiency in blood donors affects red blood cell recovery after transfusion. Blood Transfus Trasfus Sangue. 2019;17(4):274-80.

148. Giarratana M-C, Rouard H, Dumont A, Kiger L, Safeukui I, Le Pennec P-Y, et al. Proof of principle for transfusion of in vitro-generated red blood cells. Blood. 10 nov 2011;118(19):5071-9.

149. Mock DM, Lankford GL, Widness JA, Burmeister LF, Kahn D, Strauss RG. Measurement of red cell survival using biotin-labeled red cells: validation against 51Cr-labeled red cells. Transfusion (Paris). févr 1999;39(2):156-62.

150. Mock DM, Matthews NI, Zhu S, Strauss RG, Schmidt RL, Nalbant D, et al. Red blood cell (RBC) survival determined in humans using RBCs labeled at multiple biotin densities. Transfusion (Paris). mai 2011;51(5):1047-57.

151. Nalbant D, Cancelas JA, Mock DM, Kyosseva SV, Schmidt RL, Cress GA, et al. In premature infants there is no decrease in 24-hour posttransfusion allogeneic red blood cell recovery after 42 days of storage. Transfusion (Paris). 2018;58(2):352-8.

152. Coburn RF, Blakemore WS, Forster RE. Endogenous carbon monoxide production in man. J Clin Invest. juill 1963;42:1172-8.

153. Strocchi A, Schwartz S, Ellefson M, Engel RR, Medina A, Levitt MD. A simple carbon monoxide breath test to estimate erythrocyte turnover. J Lab Clin Med. sept 1992;120(3):392-9.

154. Furne JK, Springfield JR, Ho SB, Levitt MD. Simplification of the end-alveolar carbon monoxide technique to assess erythrocyte survival. J Lab Clin Med. juill 2003;142(1):52-7.

155. Fitzgibbons JF, Koler RD, Jones RT. Red cell age-related changes of hemoglobins AIa+b and AIc in normal and diabetic subjects. J Clin Invest. oct 1976;58(4):820-4.

156. Pfafferott C, Nash GB, Meiselman HJ. Red blood cell deformation in shear flow. Effects of internal and external phase viscosity and of in vivo aging. Biophys J. mai 1985;47(5):695-704.

157. Bosch FH, Werre JM, Roerdinkholder-Stoelwinder B, Huls TH, Willekens FL, Halie MR. Characteristics of red blood cell populations fractionated with a combination of counterflow centrifugation and Percoll separation. Blood. 1 janv 1992;79(1):254-60.

158. Wegner G, Kucera W, Lerche D. Deformability characterization of erythrocytes stored in different resuspension media. Folia Haematol Leipz Ger 1928. 1987;114(4):476-7.

159. Shiga T, Sekiya M, Maeda N, Kon K, Okazaki M. Cell age-dependent changes in deformability and calcium accumulation of human erythrocytes. Biochim Biophys Acta. 11 avr 1985;814(2):289-99.

160. Burger P, Kostova E, Bloem E, Hilarius-Stokman P, Meijer AB, van den Berg TK, et al. Potassium leakage primes stored erythrocytes for phosphatidylserine exposure and shedding of pro-coagulant vesicles. Br J Haematol. févr 2013;160(3):377-86.

161. Sacks DB, Arnold M, Bakris GL, Bruns DE, Horvath AR, Kirkman MS, et al. Guidelines and recommendations for laboratory analysis in the diagnosis and management of diabetes mellitus. Diabetes Care. juin 2011;34(6):e61-99.

162. Nitin S. HbA1c and factors other than diabetes mellitus affecting it. Singapore Med J. août 2010;51(8):616-22.

163. Holmquist WR, Schroeder WA. A new N-terminal blocking group involving a Schiff base in hemoglobin AIc. Biochemistry. août 1966;5(8):2489-503.

164. Bookchin RM, Gallop PM. Structure of hemoglobin AIc: nature of the N-terminal beta chain blocking group. Biochem Biophys Res Commun. 11 juill 1968;32(1):86-93.

165. Bunn HF, Haney DN, Gabbay KH, Gallop PM. Further identification of the nature and linkage of the carbohydrate in hemoglobin A1c. Biochem Biophys Res Commun. 3 nov 1975;67(1):103-9.

166. Haney DN, Bunn HF. Glycosylation of hemoglobin in vitro: affinity labeling of hemoglobin by glucose-6-phosphate. Proc Natl Acad Sci U S A. oct 1976;73(10):3534-8.

167. Bunn HF, Haney DN, Kamin S, Gabbay KH, Gallop PM. The biosynthesis of human hemoglobin A1c. Slow glycosylation of hemoglobin in vivo. J Clin Invest. juin 1976;57(6):1652-9.

168. Mebius RE, Kraal G. Structure and function of the spleen. Nat Rev Immunol. août 2005;5(8):606-16.

169. Duez J, Holleran JP, Ndour PA, Pionneau C, Diakité S, Roussel C, et al. Mechanical clearance of red blood cells by the human spleen: Potential therapeutic applications of a biomimetic RBC filtration method. Transfus Clin Biol J Soc Francaise Transfus Sang. août 2015;22(3):151-7.

170. Safeukui I, Buffet PA, Deplaine G, Perrot S, Brousse V, Sauvanet A, et al. Sensing of red blood cells with decreased membrane deformability by the human spleen. Blood Adv. 23 2018;2(20):2581-7.

171. Sosale NG, Rouhiparkouhi T, Bradshaw AM, Dimova R, Lipowsky R, Discher DE. Cell rigidity and shape override CD47's « self »-signaling in phagocytosis by hyperactivating myosin-II. Blood. 15 janv 2015;125(3):542-52.

172. Lutz HU, Bussolino F, Flepp R, Fasler S, Stammler P, Kazatchkine MD, et al. Naturally occurring anti-band-3 antibodies and complement together mediate phagocytosis of oxidatively stressed human erythrocytes. Proc Natl Acad Sci U S A. nov 1987;84(21):7368-72.

173. Arese P, Turrini F, Schwarzer E. Band 3/complement-mediated recognition and removal of normally senescent and pathological human erythrocytes. Cell Physiol Biochem Int J Exp Cell Physiol Biochem Pharmacol. 2005;16(4-6):133-46.

174. Jandl JH, Greenberg MS, Yonemoto RH, Castle WB. Clinical determination of the sites of red cell sequestration in hemolytic anemias. J Clin Invest. août 1956;35(8):842-67.

175. Theurl I, Hilgendorf I, Nairz M, Tymoszuk P, Haschka D, Asshoff M, et al. On-demand erythrocyte disposal and iron recycling requires transient macrophages in the liver. Nat Med. 2016;22(8):945-51.

176. Buehler PW, Abraham B, Vallelian F, Linnemayr C, Pereira CP, Cipollo JF, et al. Haptoglobin preserves the CD163 hemoglobin scavenger pathway by shielding hemoglobin from peroxidative modification. Blood. 12 mars 2009;113(11):2578-86.

177. Andersen CBF, Torvund-Jensen M, Nielsen MJ, de Oliveira CLP, Hersleth H-P, Andersen NH, et al. Structure of the haptoglobin-haemoglobin complex. Nature. 20 sept 2012;489(7416):456-9.

178. Belcher JD, Marker PH, Geiger P, Girotti AW, Steinberg MH, Hebbel RP, et al. Low-density lipoprotein susceptibility to oxidation and cytotoxicity to endothelium in sickle cell anemia. J Lab Clin Med. juin 1999;133(6):605-12.

179. Kristiansen M, Graversen JH, Jacobsen C, Sonne O, Hoffman HJ, Law SK, et al. Identification of the haemoglobin scavenger receptor. Nature. 11 janv 2001;409(6817):198-201.

180. Smith A, Morgan WT. Haem transport to the liver by haemopexin. Receptor-mediated uptake with recycling of the protein. Biochem J. 15 juill 1979;182(1):47-54.

181. Buehler PW, Humar R, Schaer DJ. Haptoglobin Therapeutics and Compartmentalization of Cell-Free Hemoglobin Toxicity. Trends Mol Med. juill 2020;26(7):683-97.

182. Sundd P, Gladwin MT, Novelli EM. Pathophysiology of Sickle Cell Disease. Annu Rev Pathol. 24 2019;14:263-92.

183. Fabry ME, Nagel RL. Heterogeneity of red cells in the sickler: a characteristic with practical clinical and pathophysiological implications. Blood Cells. 1982;8(1):9-15.

184. Rodgers GP, Schechter AN, Noguchi CT. Cell heterogeneity in sickle cell disease: quantitation of the erythrocyte density profile. J Lab Clin Med. juill 1985;106(1):30-7.

185. Horiuchi K, Stephens MJ, Adachi K, Asakura T, Schwartz E, Ohene-Frempong K. Image analysis studies of the degree of irreversible deformation of sickle cells in relation to cell density and Hb F level. Br J Haematol. oct 1993;85(2):356-64.

186. Bridges KR, Barabino GD, Brugnara C, Cho MR, Christoph GW, Dover G, et al. A multiparameter analysis of sickle erythrocytes in patients undergoing hydroxyurea therapy. Blood. 15 déc 1996;88(12):4701-10.

187. Baudin V, Pagnier J, Labie D, Girot R, Wajcman H. Heterogeneity of sickle cell disease as shown by density profiles: effects of fetal hemoglobin and alpha thalassemia. Haematologia (Budap). 1986;19(3):177-84.

188. Messmann R, Gannon S, Sarnaik S, Johnson RM. Mechanical properties of sickle cell membranes. Blood. 15 avr 1990;75(8):1711-7.

189. Connes P, Lamarre Y, Waltz X, Ballas SK, Lemonne N, Etienne-Julan M, et al. Haemolysis and abnormal haemorheology in sickle cell anaemia. Br J Haematol. mai 2014;165(4):564-72.

190. Bartolucci P, Brugnara C, Teixeira-Pinto A, Pissard S, Moradkhani K, Jouault H, et al. Erythrocyte density in sickle cell syndromes is associated with specific clinical manifestations and hemolysis. Blood. 11 oct 2012;120(15):3136-41.

191. Brugnara C, Bunn HF, Tosteson DC. Regulation of erythrocyte cation and water content in sickle cell anemia. Science. 18 avr 1986;232(4748):388-90.

192. Brugnara C. Sickle cell dehydration: Pathophysiology and therapeutic applications. Clin Hemorheol Microcirc. 2018;68(2-3):187-204.

193. Cox CD, Bae C, Ziegler L, Hartley S, Nikolova-Krstevski V, Rohde PR, et al. Removal of the mechanoprotective influence of the cytoskeleton reveals PIEZO1 is gated by bilayer tension. Nat Commun. 20 janv 2016;7:10366.

194. Joiner CH, Rettig RK, Jiang M, Franco RS. KCl cotransport mediates abnormal sulfhydryl-dependent volume regulation in sickle reticulocytes. Blood. 1 nov 2004;104(9):2954-60.

195. McGoron AJ, Joiner CH, Palascak MB, Claussen WJ, Franco RS. Dehydration of mature and immature sickle red blood cells during fast oxygenation/deoxygenation cycles: role of KCl cotransport and extracellular calcium. Blood. 15 mars 2000;95(6):2164-8.

196. Hannemann A, Rees DC, Tewari S, Gibson JS. Cation Homeostasis in Red Cells From Patients With Sickle Cell Disease Heterologous for HbS and HbC (HbSC Genotype). EBioMedicine. nov 2015;2(11):1669-76.

197. Rees DC, Thein SL, Osei A, Drasar E, Tewari S, Hannemann A, et al. The clinical significance of K-Cl cotransport activity in red cells of patients with HbSC disease. Haematologica. mai 2015;100(5):595-600.

198. Reiss GH, Ranney HM, Shaklai N. Association of hemoglobin C with erythrocyte ghosts. J Clin Invest. nov 1982;70(5):946-52.

199. Bank A, Mears G, Weiss R, O'Donnell JV, Natta C. Preferential binding of beta s globin chains associated with stroma in sickle cell disorders. J Clin Invest. oct 1974;54(4):805-9.

200. Sears DA, Luthra MG. Membrane-bound hemoglobin in the erythrocytes of sickle cell anemia. J Lab Clin Med. nov 1983;102(5):694-8.

201. Clark MR, Mohandas N, Shohet SB. Deformability of oxygenated irreversibly sickled cells. J Clin Invest. janv 1980;65(1):189-96.

202. Smith CM, Kuettner JF, Tukey DP, Burris SM, White JG. Variable deformability of irreversibly sickled erythrocytes. Blood. juill 1981;58(1):71-7.

203. Rab MAE, van Oirschot BA, Bos J, Merkx TH, van Wesel ACW, Abdulmalik O, et al. Rapid and reproducible characterization of sickling during automated deoxygenation in sickle cell disease patients. Am J Hematol. 2019;94(5):575-84.

204. Ballas SK, Smith ED. Red blood cell changes during the evolution of the sickle cell painful crisis. Blood. 15 avr 1992;79(8):2154-63.

205. Renoux C, Romana M, Joly P, Ferdinand S, Faes C, Lemonne N, et al. Effect of Age on Blood Rheology in Sickle Cell Anaemia and Sickle Cell Haemoglobin C Disease: A Cross-Sectional Study. PloS One. 2016;11(6):e0158182.

206. Barabino GA, Platt MO, Kaul DK. Sickle cell biomechanics. Annu Rev Biomed Eng. 15 août 2010;12:345-67.

207. Waltz X, Hedreville M, Sinnapah S, Lamarre Y, Soter V, Lemonne N, et al. Delayed beneficial effect of acute exercise on red blood cell aggregate strength in patients with sickle cell anemia. Clin Hemorheol Microcirc. 2012;52(1):15-26.

208. Connes P, Renoux C, Romana M, Abkarian M, Joly P, Martin C, et al. Blood rheological abnormalities in sickle cell anemia. Clin Hemorheol Microcirc. 2018;68(2-3):165-72.

209. de Jong K, Larkin SK, Styles LA, Bookchin RM, Kuypers FA. Characterization of the phosphatidylserine-exposing subpopulation of sickle cells. Blood. 1 août 2001;98(3):860-7.

210. Blumenfeld N, Zachowski A, Galacteros F, Beuzard Y, Devaux PF. Transmembrane mobility of phospholipids in sickle erythrocytes: effect of deoxygenation on diffusion and asymmetry. Blood. 15 févr 1991;77(4):849-54.

211. Kuypers FA, de Jong K. The role of phosphatidylserine in recognition and removal of erythrocytes. Cell Mol Biol Noisy--Gd Fr. mars 2004;50(2):147-58.

212. Kuypers FA. Membrane lipid alterations in hemoglobinopathies. Hematol Am Soc Hematol Educ Program. 2007;68-73.

213. Stefanovic M, Puchulu-Campanella E, Kodippili G, Low PS. Oxygen regulates the band 3-ankyrin bridge in the human erythrocyte membrane. Biochem J. 1 janv 2013;449(1):143-50.

214. Piccin A, Murphy WG, Smith OP. Circulating microparticles: pathophysiology and clinical implications. Blood Rev. mai 2007;21(3):157-71.

215. Westerman M, Pizzey A, Hirschman J, Cerino M, Weil-Weiner Y, Ramotar P, et al. Microvesicles in haemoglobinopathies offer insights into mechanisms of hypercoagulability, haemolysis and the effects of therapy. Br J Haematol. juill 2008;142(1):126-35.

216. Camus SM, Gausserès B, Bonnin P, Loufrani L, Grimaud L, Charue D, et al. Erythrocyte microparticles can induce kidney vaso-occlusions in a murine model of sickle cell disease. Blood. 13 déc 2012;120(25):5050-8.

217. Romana M, Connes P, Key NS. Microparticles in sickle cell disease. Clin Hemorheol Microcirc. 2018;68(2-3):319-29.

218. Dhaliwal G, Cornett PA, Tierney LM. Hemolytic anemia. Am Fam Physician. 1 juin 2004;69(11):2599-606.

219. Waugh SM, Willardson BM, Kannan R, Labotka RJ, Low PS. Heinz bodies induce clustering of band 3, glycophorin, and ankyrin in sickle cell erythrocytes. J Clin Invest. nov 1986;78(5):1155-60.

220. Poyart C, Wajcman H. Hemolytic anemias due to hemoglobinopathies. Mol Aspects Med. avr 1996;17(2):129-42.

221. Kane I, Nagalli S. Splenic Sequestration Crisis. In: StatPearls [Internet]. Treasure Island (FL): StatPearls Publishing; 2020 [cité 17 sept 2020]. Disponible sur: http://www.ncbi.nlm.nih.gov/books/NBK553164/

222. Liu Y, Jing F, Yi W, Mendelson A, Shi P, Walsh R, et al. HO-1hi patrolling monocytes protect against vaso-occlusion in sickle cell disease. Blood. 5 avr 2018;131(14):1600-10.

223. Liu Y, Zhong H, Bao W, Mendelson A, An X, Shi P, et al. Patrolling monocytes scavenge endothelial-adherent sickle RBCs: a novel mechanism of inhibition of vaso-occlusion in SCD. Blood. 15 2019;134(7):579-90.

224. Hillery CA, Scott JP, Du MC. The carboxy-terminal cell-binding domain of thrombospondin is essential for sickle red blood cell adhesion. Blood. 1 juill 1999;94(1):302-9.

225. Odièvre M-H, Bony V, Benkerrou M, Lapouméroulie C, Alberti C, Ducrocq R, et al. Modulation of erythroid adhesion receptor expression by hydroxyurea in children with sickle cell disease. Haematologica. avr 2008;93(4):502-10.

226. Burger P, Hilarius-Stokman P, de Korte D, van den Berg TK, van Bruggen R. CD47 functions as a molecular switch for erythrocyte phagocytosis. Blood. 7 juin 2012;119(23):5512-21.

227. Kato GJ, Steinberg MH, Gladwin MT. Intravascular hemolysis and the pathophysiology of sickle cell disease. J Clin Invest. 1 mars 2017;127(3):750-60.

228. Santiago RP, Guarda CC, Figueiredo CVB, Fiuza LM, Aleluia MM, Adanho CSA, et al. Serum haptoglobin and hemopexin levels are depleted in pediatric sickle cell disease patients. Blood Cells Mol Dis. 2018;72:34-6.

229. Gladwin MT, Ofori-Acquah SF. Erythroid DAMPs drive inflammation in SCD. Blood. 12 juin 2014;123(24):3689-90.

230. Reiter CD, Wang X, Tanus-Santos JE, Hogg N, Cannon RO, Schechter AN, et al. Cell-free hemoglobin limits nitric oxide bioavailability in sickle-cell disease. Nat Med. déc 2002;8(12):1383-9.

231. Rother RP, Bell L, Hillmen P, Gladwin MT. The clinical sequelae of intravascular hemolysis and extracellular plasma hemoglobin: a novel mechanism of human disease. JAMA. 6 avr 2005;293(13):1653-62.

232. Kato GJ, Gladwin MT, Steinberg MH. Deconstructing sickle cell disease: reappraisal of the role of hemolysis in the development of clinical subphenotypes. Blood Rev. janv 2007;21(1):37-47.

233. Radomski MW, Moncada S. The biological and pharmacological role of nitric oxide in platelet function. Adv Exp Med Biol. 1993;344:251-64.

234. Cardenes N, Corey C, Geary L, Jain S, Zharikov S, Barge S, et al. Platelet bioenergetic screen in sickle cell patients reveals mitochondrial complex V inhibition, which contributes to platelet activation. Blood. 1 mai 2014;123(18):2864-72.

235. Chen G, Zhang D, Fuchs TA, Manwani D, Wagner DD, Frenette PS. Heme-induced neutrophil extracellular traps contribute to the pathogenesis of sickle cell disease. Blood. 12 juin 2014;123(24):3818-27.

236. Pohlman TH, Harlan JM. Adaptive responses of the endothelium to stress. J Surg Res. mars 2000;89(1):85-119.

237. Belcher JD, Chen C, Nguyen J, Milbauer L, Abdulla F, Alayash AI, et al. Heme triggers TLR4 signaling leading to endothelial cell activation and vaso-occlusion in murine sickle cell disease. Blood. 16 janv 2014;123(3):377-90.

238. Pawluczkowycz AW, Lindorfer MA, Waitumbi JN, Taylor RP. Hematin promotes complement alternative pathway-mediated deposition of C3 activation fragments on human erythrocytes: potential implications for the pathogenesis of anemia in malaria. J Immunol Baltim Md 1950. 15 oct 2007;179(8):5543-52.

239. Frimat M, Tabarin F, Dimitrov JD, Poitou C, Halbwachs-Mecarelli L, Fremeaux-Bacchi V, et al. Complement activation by heme as a secondary hit for atypical hemolytic uremic syndrome. Blood. 11 juill 2013;122(2):282-92.

240. Roumenina LT, Chadebech P, Bodivit G, Vieira-Martins P, Grunenwald A, Boudhabhay I, et al. Complement activation in sickle cell disease: Dependence on cell density, hemolysis and modulation by hydroxyurea therapy. Am J Hematol. 2020;95(5):456-64.

241. Kato GJ, McGowan V, Machado RF, Little JA, Taylor J, Morris CR, et al. Lactate dehydrogenase as a biomarker of hemolysis-associated nitric oxide resistance, priapism, leg ulceration, pulmonary hypertension, and death in patients with sickle cell disease. Blood. 15 mars 2006;107(6):2279-85.

242. Olnes M, Chi A, Haney C, May R, Minniti C, Taylor J, et al. Improvement in hemolysis and pulmonary arterial systolic pressure in adult patients with sickle cell disease during treatment with hydroxyurea. Am J Hematol. août 2009;84(8):530-2.

243. Cita K-C, Brureau L, Lemonne N, Billaud M, Connes P, Ferdinand S, et al. Men with Sickle Cell Anemia and Priapism Exhibit Increased Hemolytic Rate, Decreased Red Blood Cell Deformability and Increased Red Blood Cell Aggregate Strength. PloS One. 2016;11(5):e0154866.

244. Manwani D, Frenette PS. Vaso-occlusion in sickle cell disease: pathophysiology and novel targeted therapies. Blood. 5 déc 2013;122(24):3892-8.

245. Hoover R, Rubin R, Wise G, Warren R. Adhesion of normal and sickle erythrocytes to endothelial monolayer cultures. Blood. oct 1979;54(4):872-6.

246. Hebbel RP, Yamada O, Moldow CF, Jacob HS, White JG, Eaton JW. Abnormal adherence of sickle erythrocytes to cultured vascular endothelium: possible mechanism for microvascular occlusion in sickle cell disease. J Clin Invest. janv 1980;65(1):154-60.

247. Barabino GA, McIntire LV, Eskin SG, Sears DA, Udden M. Endothelial cell interactions with sickle cell, sickle trait, mechanically injured, and normal erythrocytes under controlled flow. Blood. juill 1987;70(1):152-7.

248. Zhang D, Xu C, Manwani D, Frenette PS. Neutrophils, platelets, and inflammatory pathways at the nexus of sickle cell disease pathophysiology. Blood. 18 févr 2016;127(7):801-9.

249. Christoph GW, Hofrichter J, Eaton WA. Understanding the shape of sickled red cells. Biophys J. févr 2005;88(2):1371-6.

250. Kaul DK, Finnegan E, Barabino GA. Sickle red cell-endothelium interactions. Microcirc N Y N 1994. janv 2009;16(1):97-111.

251. Gauthier E, Rahuel C, Wautier MP, El Nemer W, Gane P, Wautier JL, et al. Protein kinase A-dependent phosphorylation of Lutheran/basal cell adhesion molecule glycoprotein regulates cell adhesion to laminin alpha5. J Biol Chem. 26 août 2005;280(34):30055-62.

252. Damanhouri GA, Jarullah J, Marouf S, Hindawi SI, Mushtaq G, Kamal MA. Clinical biomarkers in sickle cell disease. Saudi J Biol Sci. janv 2015;22(1):24-31.

253. Brittain HA, Eckman JR, Swerlick RA, Howard RJ, Wick TM. Thrombospondin from activated platelets promotes sickle erythrocyte adherence to human microvascular endothelium under physiologic flow: a potential role for platelet activation in sickle cell vaso-occlusion. Blood. 15 avr 1993;81(8):2137-43.

254. Novelli EM, Little-Ihrig L, Knupp HE, Rogers NM, Yao M, Baust JJ, et al. Vascular TSP1-CD47 signaling promotes sickle cell-associated arterial vasculopathy and pulmonary hypertension in mice. Am J Physiol Lung Cell Mol Physiol. 01 2019;316(6):L1150-64.

255. Polanowska-Grabowska R, Wallace K, Field JJ, Chen L, Marshall MA, Figler R, et al. P-selectin-mediated platelet-neutrophil aggregate formation activates neutrophils in mouse and human sickle cell disease. Arterioscler Thromb Vasc Biol. déc 2010;30(12):2392-9.

256. Curtis SA, Danda N, Etzion Z, Cohen HW, Billett HH. Elevated Steady State WBC and Platelet Counts Are Associated with Frequent Emergency Room Use in Adults with Sickle Cell Anemia. PloS One. 2015;10(8):e0133116.

257. Wongtong N, Jones S, Deng Y, Cai J, Ataga KI. Monocytosis is associated with hemolysis in sickle cell disease. Hematol Amst Neth. déc 2015;20(10):593-7.

258. Steinberg MH. Predicting clinical severity in sickle cell anaemia. Br J Haematol. mai 2005;129(4):465-81.

259. Stuart MJ, Nagel RL. Sickle-cell disease. Lancet Lond Engl. 9 oct 2004;364(9442):1343-60.

260. Tewari S, Brousse V, Piel FB, Menzel S, Rees DC. Environmental determinants of severity in sickle cell disease. Haematologica. sept 2015;100(9):1108-16.

261. Jones S, Duncan ER, Thomas N, Walters J, Dick MC, Height SE, et al. Windy weather and low humidity are associated with an increased number of hospital admissions for acute pain and sickle

cell disease in an urban environment with a maritime temperate climate. Br J Haematol. nov 2005;131(4):530-3.

262. Mekontso Dessap A, Contou D, Dandine-Roulland C, Hemery F, Habibi A, Charles-Nelson A, et al. Environmental influences on daily emergency admissions in sickle-cell disease patients. Medicine (Baltimore). déc 2014;93(29):e280.

263. Fertrin KY, Costa FF. Genomic polymorphisms in sickle cell disease: implications for clinical diversity and treatment. Expert Rev Hematol. août 2010;3(4):443-58.

264. Novelli EM, Gladwin MT. Crises in Sickle Cell Disease. Chest. avr 2016;149(4):1082-93.

265. Maitre B, Habibi A, Roudot-Thoraval F, Bachir D, Belghiti DD, Galacteros F, et al. Acute chest syndrome in adults with sickle cell disease. Chest. mai 2000;117(5):1386-92.

266. Vichinsky EP, Neumayr LD, Earles AN, Williams R, Lennette ET, Dean D, et al. Causes and outcomes of the acute chest syndrome in sickle cell disease. National Acute Chest Syndrome Study Group. N Engl J Med. 22 juin 2000;342(25):1855-65.

267. Gardner K, Douiri A, Drasar E, Allman M, Mwirigi A, Awogbade M, et al. Survival in adults with sickle cell disease in a high-income setting. Blood. 08 2016;128(10):1436-8.

268. Weatherall DJ. The challenge of haemoglobinopathies in resource-poor countries. Br J Haematol. sept 2011;154(6):736-44.

269. DeSimone J, Heller P, Hall L, Zwiers D. 5-Azacytidine stimulates fetal hemoglobin synthesis in anemic baboons. Proc Natl Acad Sci U S A. juill 1982;79(14):4428-31.

270. Charache S, Dover G, Smith K, Talbot CC, Moyer M, Boyer S. Treatment of sickle cell anemia with 5-azacytidine results in increased fetal hemoglobin production and is associated with nonrandom hypomethylation of DNA around the gamma-delta-beta-globin gene complex. Proc Natl Acad Sci U S A. août 1983;80(15):4842-6.

271. Platt OS, Orkin SH, Dover G, Beardsley GP, Miller B, Nathan DG. Hydroxyurea enhances fetal hemoglobin production in sickle cell anemia. J Clin Invest. août 1984;74(2):652-6.

272. Charache S, Dover GJ, Moore RD, Eckert S, Ballas SK, Koshy M, et al. Hydroxyurea: effects on hemoglobin F production in patients with sickle cell anemia. Blood. 15 mai 1992;79(10):2555-65.

273. Ballas SK, Marcolina MJ, Dover GJ, Barton FB. Erythropoietic activity in patients with sickle cell anaemia before and after treatment with hydroxyurea. Br J Haematol. mai 1999;105(2):491-6.

274. Charache S, Terrin ML, Moore RD, Dover GJ, Barton FB, Eckert SV, et al. Effect of hydroxyurea on the frequency of painful crises in sickle cell anemia. Investigators of the Multicenter Study of Hydroxyurea in Sickle Cell Anemia. N Engl J Med. 18 mai 1995;332(20):1317-22.

275. Steinberg MH, Barton F, Castro O, Pegelow CH, Ballas SK, Kutlar A, et al. Effect of hydroxyurea on mortality and morbidity in adult sickle cell anemia: risks and benefits up to 9 years of treatment. JAMA. 2 avr 2003;289(13):1645-51.

276. Claster S, Vichinsky E. First report of reversal of organ dysfunction in sickle cell anemia by the use of hydroxyurea: splenic regeneration. Blood. 15 sept 1996;88(6):1951-3.

277. Ware RE, Zimmerman SA, Schultz WH. Hydroxyurea as an alternative to blood transfusions for the prevention of recurrent stroke in children with sickle cell disease. Blood. 1 nov 1999;94(9):3022-6.

278. Zimmerman SA, Schultz WH, Burgett S, Mortier NA, Ware RE. Hydroxyurea therapy lowers transcranial Doppler flow velocities in children with sickle cell anemia. Blood. 1 août 2007;110(3):1043-7.

279. Bartolucci P, Habibi A, Stehlé T, Di Liberto G, Rakotoson MG, Gellen-Dautremer J, et al. Six Months of Hydroxyurea Reduces Albuminuria in Patients with Sickle Cell Disease. J Am Soc Nephrol JASN. 2016;27(6):1847-53.

280. Voskaridou E, Christoulas D, Bilalis A, Plata E, Varvagiannis K, Stamatopoulos G, et al. The effect of prolonged administration of hydroxyurea on morbidity and mortality in adult patients with sickle cell syndromes: results of a 17-year, single-center trial (LaSHS). Blood. 25 mars 2010;115(12):2354-63.

281. Bartolucci P, Chaar V, Picot J, Bachir D, Habibi A, Fauroux C, et al. Decreased sickle red blood cell adhesion to laminin by hydroxyurea is associated with inhibition of Lu/BCAM protein phosphorylation. Blood. 23 sept 2010;116(12):2152-9.

282. Chaar V, Laurance S, Lapoumeroulie C, Cochet S, De Grandis M, Colin Y, et al. Hydroxycarbamide decreases sickle reticulocyte adhesion to resting endothelium by inhibiting endothelial lutheran/basal cell adhesion molecule (Lu/BCAM) through phosphodiesterase 4A activation. J Biol Chem. 18 avr 2014;289(16):11512-21.

283. Almeida CB, Scheiermann C, Jang J-E, Prophete C, Costa FF, Conran N, et al. Hydroxyurea and a cGMP-amplifying agent have immediate benefits on acute vaso-occlusive events in sickle cell disease mice. Blood. 4 oct 2012;120(14):2879-88.

284. Ballas SK. The Evolving Pharmacotherapeutic Landscape for the Treatment of Sickle Cell Disease. Mediterr J Hematol Infect Dis. 2020;12(1):e2020010.

285. Adragna NC, Fonseca P, Lauf PK. Hydroxyurea affects cell morphology, cation transport, and red blood cell adhesion in cultured vascular endothelial cells. Blood. 15 janv 1994;83(2):553-60.

286. Verger E, Schoëvaërt D, Carrivain P, Victor J-M, Lapouméroulie C, Elion J. Prior exposure of endothelial cells to hydroxycarbamide alters the flow dynamics and adhesion of sickle red blood cells. Clin Hemorheol Microcirc. 2014;57(1):9-22.

287. McGann PT, Niss O, Dong M, Marahatta A, Howard TA, Mizuno T, et al. Robust clinical and laboratory response to hydroxyurea using pharmacokinetically guided dosing for young children with sickle cell anemia. Am J Hematol. 2019;94(8):871-9.

288. Nazon C, Sabo A-N, Becker G, Lessinger J-M, Kemmel V, Paillard C. Optimizing Hydroxyurea Treatment for Sickle Cell Disease Patients: The Pharmacokinetic Approach. J Clin Med. 16 oct 2019;8(10).

289. Telen MJ. Curative vs targeted therapy for SCD: does it make more sense to address the root cause than target downstream events? Blood Adv. 28 juill 2020;4(14):3457-65.

290. Brosnan JT. Interorgan amino acid transport and its regulation. J Nutr. 2003;133(6 Suppl 1):2068S-2072S.

291. Morris CR, Suh JH, Hagar W, Larkin S, Bland DA, Steinberg MH, et al. Erythrocyte glutamine depletion, altered redox environment, and pulmonary hypertension in sickle cell disease. Blood. 1 janv 2008;111(1):402-10.

292. Niihara Y, Miller ST, Kanter J, Lanzkron S, Smith WR, Hsu LL, et al. A Phase 3 Trial of l-Glutamine in Sickle Cell Disease. N Engl J Med. 19 juill 2018;379(3):226-35.

293. Metcalf B, Chuang C, Dufu K, Patel MP, Silva-Garcia A, Johnson C, et al. Discovery of GBT440, an Orally Bioavailable R-State Stabilizer of Sickle Cell Hemoglobin. ACS Med Chem Lett. 9 mars 2017;8(3):321-6.

294. Dufu K, Patel M, Oksenberg D, Cabrales P. GBT440 improves red blood cell deformability and reduces viscosity of sickle cell blood under deoxygenated conditions. Clin Hemorheol Microcirc. 2018;70(1):95-105.

295. Vichinsky E, Hoppe CC, Ataga KI, Ware RE, Nduba V, El-Beshlawy A, et al. A Phase 3 Randomized Trial of Voxelotor in Sickle Cell Disease. N Engl J Med. 08 2019;381(6):509-19.

296. Ataga KI, Kutlar A, Kanter J, Liles D, Cancado R, Friedrisch J, et al. Crizanlizumab for the Prevention of Pain Crises in Sickle Cell Disease. N Engl J Med. 02 2017;376(5):429-39.

297. Kutlar A, Kanter J, Liles DK, Alvarez OA, Cançado RD, Friedrisch JR, et al. Effect of crizanlizumab on pain crises in subgroups of patients with sickle cell disease: A SUSTAIN study analysis. Am J Hematol. 2019;94(1):55-61.

298. Yu L, Myers G, Engel JD. Small molecule therapeutics to treat the β-globinopathies. Curr Opin Hematol. 2020;27(3):129-40.

299. Salinas Cisneros G, Thein SL. Recent Advances in the Treatment of Sickle Cell Disease. Front Physiol. 2020;11:435.

300. Howard J. Sickle cell disease: when and how to transfuse. Hematol Am Soc Hematol Educ Program. 2 déc 2016;2016(1):625-31.

301. Stussi G, Buser A, Holbro A. Red Blood Cells: Exchange, Transfuse, or Deplete. Transfus Med Hemotherapy Off Organ Dtsch Ges Transfusionsmedizin Immunhamatologie. déc 2019;46(6):407-16.

302. Walters MC, Hardy K, Edwards S, Adamkiewicz T, Barkovich J, Bernaudin F, et al. Pulmonary, gonadal, and central nervous system status after bone marrow transplantation for sickle cell disease. Biol Blood Marrow Transplant J Am Soc Blood Marrow Transplant. févr 2010;16(2):263-72.

303. Gluckman E, Cappelli B, Bernaudin F, Labopin M, Volt F, Carreras J, et al. Sickle cell disease: an international survey of results of HLA-identical sibling hematopoietic stem cell transplantation. Blood. 16 2017;129(11):1548-56.

304. Bernaudin F, Dalle J-H, Bories D, de Latour RP, Robin M, Bertrand Y, et al. Long-term event-free survival, chimerism and fertility outcomes in 234 patients with sickle-cell anemia younger than 30 years after myeloablative conditioning and matched-sibling transplantation in France. Haematologica. 2020;105(1):91-101.

305. Hsieh MM, Fitzhugh CD, Weitzel RP, Link ME, Coles WA, Zhao X, et al. Nonmyeloablative HLA-matched sibling allogeneic hematopoietic stem cell transplantation for severe sickle cell phenotype. JAMA. 2 juill 2014;312(1):48-56.

306. Saraf SL, Oh AL, Patel PR, Jalundhwala Y, Sweiss K, Koshy M, et al. Nonmyeloablative Stem Cell Transplantation with Alemtuzumab/Low-Dose Irradiation to Cure and Improve the Quality of Life of Adults with Sickle Cell Disease. Biol Blood Marrow Transplant J Am Soc Blood Marrow Transplant. mars 2016;22(3):441-8.

307. Fitzhugh CD, Cordes S, Taylor T, Coles W, Roskom K, Link M, et al. At least 20% donor myeloid chimerism is necessary to reverse the sickle phenotype after allogeneic HSCT. Blood. 26 2017;130(17):1946-8.

308. Gluckman E. Allogeneic transplantation strategies including haploidentical transplantation in sickle cell disease. Hematol Am Soc Hematol Educ Program. 2013;2013:370-6.

309. High KA, Roncarolo MG. Gene Therapy. N Engl J Med. 01 2019;381(5):455-64.

310. Hacein-Bey-Abina S, Von Kalle C, Schmidt M, McCormack MP, Wulffraat N, Leboulch P, et al. LMO2-associated clonal T cell proliferation in two patients after gene therapy for SCID-X1. Science. 17 oct 2003;302(5644):415-9.

311. Howe SJ, Mansour MR, Schwarzwaelder K, Bartholomae C, Hubank M, Kempski H, et al. Insertional mutagenesis combined with acquired somatic mutations causes leukemogenesis following gene therapy of SCID-X1 patients. J Clin Invest. sept 2008;118(9):3143-50.

312. Naldini L, Blömer U, Gallay P, Ory D, Mulligan R, Gage FH, et al. In vivo gene delivery and stable transduction of nondividing cells by a lentiviral vector. Science. 12 avr 1996;272(5259):263-7.

313. Sakuma T, Barry MA, Ikeda Y. Lentiviral vectors: basic to translational. Biochem J. 1 mai 2012;443(3):603-18.

314. Montini E, Cesana D, Schmidt M, Sanvito F, Bartholomae CC, Ranzani M, et al. The genotoxic potential of retroviral vectors is strongly modulated by vector design and integration site selection in a mouse model of HSC gene therapy. J Clin Invest. avr 2009;119(4):964-75.

315. Schacker M, Seimetz D. From fiction to science: clinical potentials and regulatory considerations of gene editing. Clin Transl Med. 21 oct 2019;8(1):27.

316. Lanigan TM, Kopera HC, Saunders TL. Principles of Genetic Engineering. Genes. 10 2020;11(3).

317. Alagoz M, Kherad N. Advance genome editing technologies in the treatment of human diseases: CRISPR therapy (Review). Int J Mol Med. août 2020;46(2):521-34.

318. Psatha N, Papayanni P-G, Yannaki E. A New Era for Hemoglobinopathies: More Than One Curative Option. Curr Gene Ther. 2017;17(5):364-78.

319. Cone RD, Weber-Benarous A, Baorto D, Mulligan RC. Regulated expression of a complete human beta-globin gene encoded by a transmissible retrovirus vector. Mol Cell Biol. févr 1987;7(2):887-97.

320. Dzierzak EA, Papayannopoulou T, Mulligan RC. Lineage-specific expression of a human beta-globin gene in murine bone marrow transplant recipients reconstituted with retrovirus-transduced stem cells. Nature. 7 janv 1988;331(6151):35-41.

321. Novak U, Harris EA, Forrester W, Groudine M, Gelinas R. High-level beta-globin expression after retroviral transfer of locus activation region-containing human beta-globin gene derivatives into murine erythroleukemia cells. Proc Natl Acad Sci U S A. mai 1990;87(9):3386-90.

322. Talbot D, Collis P, Antoniou M, Vidal M, Grosveld F, Greaves DR. A dominant control region from the human beta-globin locus conferring integration site-independent gene expression. Nature. 23 mars 1989;338(6213):352-5.

323. Tuan DY, Solomon WB, London IM, Lee DP. An erythroid-specific, developmental-stage-independent enhancer far upstream of the human « beta-like globin » genes. Proc Natl Acad Sci U S A. avr 1989;86(8):2554-8.

324. Leboulch P, Huang GM, Humphries RK, Oh YH, Eaves CJ, Tuan DY, et al. Mutagenesis of retroviral vectors transducing human beta-globin gene and beta-globin locus control region derivatives results in stable transmission of an active transcriptional structure. EMBO J. 1 juill 1994;13(13):3065-76.

325. Sadelain M, Wang CH, Antoniou M, Grosveld F, Mulligan RC. Generation of a high-titer retroviral vector capable of expressing high levels of the human beta-globin gene. Proc Natl Acad Sci U S A. 18 juill 1995;92(15):6728-32.

326. May C, Rivella S, Chadburn A, Sadelain M. Successful treatment of murine beta-thalassemia intermedia by transfer of the human beta-globin gene. Blood. 15 mars 2002;99(6):1902-8.

327. Rivella S, May C, Chadburn A, Rivière I, Sadelain M. A novel murine model of Cooley anemia and its rescue by lentiviral-mediated human beta-globin gene transfer. Blood. 15 avr 2003;101(8):2932-9.

328. Pawliuk R, Westerman KA, Fabry ME, Payen E, Tighe R, Bouhassira EE, et al. Correction of sickle cell disease in transgenic mouse models by gene therapy. Science. 14 déc 2001;294(5550):2368-71.

329. Imren S, Payen E, Westerman KA, Pawliuk R, Fabry ME, Eaves CJ, et al. Permanent and panerythroid correction of murine beta thalassemia by multiple lentiviral integration in hematopoietic stem cells. Proc Natl Acad Sci U S A. 29 oct 2002;99(22):14380-5.

330. Miccio A, Cesari R, Lotti F, Rossi C, Sanvito F, Ponzoni M, et al. In vivo selection of genetically modified erythroblastic progenitors leads to long-term correction of beta-thalassemia. Proc Natl Acad Sci U S A. 29 juill 2008;105(30):10547-52.

331. Emery DW, Yannaki E, Tubb J, Stamatoyannopoulos G. A chromatin insulator protects retrovirus vectors from chromosomal position effects. Proc Natl Acad Sci U S A. 1 août 2000;97(16):9150-5.

332. Cavazzana-Calvo M, Payen E, Negre O, Wang G, Hehir K, Fusil F, et al. Transfusion independence and HMGA2 activation after gene therapy of human β-thalassaemia. Nature. 16 sept 2010;467(7313):318-22.

333. Thompson AA, Walters MC, Kwiatkowski J, Rasko JEJ, Ribeil J-A, Hongeng S, et al. Gene Therapy in Patients with Transfusion-Dependent β-Thalassemia. N Engl J Med. 19 2018;378(16):1479-93.

334. McCune SL, Reilly MP, Chomo MJ, Asakura T, Townes TM. Recombinant human hemoglobins designed for gene therapy of sickle cell disease. Proc Natl Acad Sci U S A. 11 oct 1994;91(21):9852-6.

335. Hoban MD, Orkin SH, Bauer DE. Genetic treatment of a molecular disorder: gene therapy approaches to sickle cell disease. Blood. 18 févr 2016;127(7):839-48.

336. Levasseur DN, Ryan TM, Reilly MP, McCune SL, Asakura T, Townes TM. A recombinant human hemoglobin with anti-sickling properties greater than fetal hemoglobin. J Biol Chem. 25 juin 2004;279(26):27518-24.

337. Ribeil J-A, Hacein-Bey-Abina S, Payen E, Magnani A, Semeraro M, Magrin E, et al. Gene Therapy in a Patient with Sickle Cell Disease. N Engl J Med. 02 2017;376(9):848-55.

338. Demirci S, Uchida N, Tisdale JF. Gene therapy for sickle cell disease: An update. Cytotherapy. 2018;20(7):899-910.

339. Persons DA, Hargrove PW, Allay ER, Hanawa H, Nienhuis AW. The degree of phenotypic correction of murine beta -thalassemia intermedia following lentiviral-mediated transfer of a human gamma-globin gene is influenced by chromosomal position effects and vector copy number. Blood. 15 mars 2003;101(6):2175-83.

340. Hanawa H, Hargrove PW, Kepes S, Srivastava DK, Nienhuis AW, Persons DA. Extended beta-globin locus control region elements promote consistent therapeutic expression of a gamma-globin lentiviral vector in murine beta-thalassemia. Blood. 15 oct 2004;104(8):2281-90.

341. Pestina TI, Hargrove PW, Jay D, Gray JT, Boyd KM, Persons DA. Correction of murine sickle cell disease using gamma-globin lentiviral vectors to mediate high-level expression of fetal hemoglobin. Mol Ther J Am Soc Gene Ther. févr 2009;17(2):245-52.

342. Bauer DE, Kamran SC, Orkin SH. Reawakening fetal hemoglobin: prospects for new therapies for the β-globin disorders. Blood. 11 oct 2012;120(15):2945-53.

343. Bauer DE, Orkin SH. Hemoglobin switching's surprise: the versatile transcription factor BCL11A is a master repressor of fetal hemoglobin. Curr Opin Genet Dev. août 2015;33:62-70.

344. Xu J, Peng C, Sankaran VG, Shao Z, Esrick EB, Chong BG, et al. Correction of sickle cell disease in adult mice by interference with fetal hemoglobin silencing. Science. 18 nov 2011;334(6058):993-6.

345. Guda S, Brendel C, Renella R, Du P, Bauer DE, Canver MC, et al. miRNA-embedded shRNAs for Lineage-specific BCL11A Knockdown and Hemoglobin F Induction. Mol Ther J Am Soc Gene Ther. sept 2015;23(9):1465-74.

346. Tsang JCH, Yu Y, Burke S, Buettner F, Wang C, Kolodziejczyk AA, et al. Single-cell transcriptomic reconstruction reveals cell cycle and multi-lineage differentiation defects in Bcl11a-deficient hematopoietic stem cells. Genome Biol. 21 sept 2015;16:178.

347. Chang K-H, Smith SE, Sullivan T, Chen K, Zhou Q, West JA, et al. Long-Term Engraftment and Fetal Globin Induction upon BCL11A Gene Editing in Bone-Marrow-Derived CD34+ Hematopoietic Stem and Progenitor Cells. Mol Ther Methods Clin Dev. 17 mars 2017;4:137-48.

348. Brendel C, Guda S, Renella R, Bauer DE, Canver MC, Kim Y-J, et al. Lineage-specific BCL11A knockdown circumvents toxicities and reverses sickle phenotype. J Clin Invest. 03 2016;126(10):3868-78.

349. Brendel C, Negre O, Rothe M, Guda S, Parsons G, Harris C, et al. Preclinical Evaluation of a Novel Lentiviral Vector Driving Lineage-Specific BCL11A Knockdown for Sickle Cell Gene Therapy. Mol Ther Methods Clin Dev. 12 juin 2020;17:589-600.

350. Deng W, Rupon JW, Krivega I, Breda L, Motta I, Jahn KS, et al. Reactivation of developmentally silenced globin genes by forced chromatin looping. Cell. 14 août 2014;158(4):849-60.

351. Breda L, Motta I, Lourenco S, Gemmo C, Deng W, Rupon JW, et al. Forced chromatin looping raises fetal hemoglobin in adult sickle cells to higher levels than pharmacologic inducers. Blood. 25 2016;128(8):1139-43.

352. Hoban MD, Cost GJ, Mendel MC, Romero Z, Kaufman ML, Joglekar AV, et al. Correction of the sickle cell disease mutation in human hematopoietic stem/progenitor cells. Blood. 23 avr 2015;125(17):2597-604.

353. DeWitt MA, Magis W, Bray NL, Wang T, Berman JR, Urbinati F, et al. Selection-free genome editing of the sickle mutation in human adult hematopoietic stem/progenitor cells. Sci Transl Med. 12 2016;8(360):360ra134.

354. Hoban MD, Lumaquin D, Kuo CY, Romero Z, Long J, Ho M, et al. CRISPR/Cas9-Mediated Correction of the Sickle Mutation in Human CD34+ cells. Mol Ther J Am Soc Gene Ther. 2016;24(9):1561-9.

355. Dever DP, Bak RO, Reinisch A, Camarena J, Washington G, Nicolas CE, et al. CRISPR/Cas9 β-globin gene targeting in human haematopoietic stem cells. Nature. 17 2016;539(7629):384-9.

356. Ye L, Wang J, Tan Y, Beyer AI, Xie F, Muench MO, et al. Genome editing using CRISPR-Cas9 to create the HPFH genotype in HSPCs: An approach for treating sickle cell disease and β-thalassemia. Proc Natl Acad Sci U S A. 20 2016;113(38):10661-5.

357. Traxler EA, Yao Y, Wang Y-D, Woodard KJ, Kurita R, Nakamura Y, et al. A genome-editing strategy to treat β-hemoglobinopathies that recapitulates a mutation associated with a benign genetic condition. Nat Med. 2016;22(9):987-90.

358. Antoniani C, Meneghini V, Lattanzi A, Felix T, Romano O, Magrin E, et al. Induction of fetal hemoglobin synthesis by CRISPR/Cas9-mediated editing of the human β-globin locus. Blood. 26 2018;131(17):1960-73.

359. Lux CT, Pattabhi S, Berger M, Nourigat C, Flowers DA, Negre O, et al. TALEN-Mediated Gene Editing of HBG in Human Hematopoietic Stem Cells Leads to Therapeutic Fetal Hemoglobin Induction. Mol Ther Methods Clin Dev. 15 mars 2019;12:175-83.

360. Métais J-Y, Doerfler PA, Mayuranathan T, Bauer DE, Fowler SC, Hsieh MM, et al. Genome editing of HBG1 and HBG2 to induce fetal hemoglobin. Blood Adv. 12 2019;3(21):3379-92.

361. Weber L, Frati G, Felix T, Hardouin G, Casini A, Wollenschlaeger C, et al. Editing a γ-globin repressor binding site restores fetal hemoglobin synthesis and corrects the sickle cell disease phenotype. Sci Adv. 1 févr 2020;6(7):eaay9392.

362. Canver MC, Smith EC, Sher F, Pinello L, Sanjana NE, Shalem O, et al. BCL11A enhancer dissection by Cas9-mediated in situ saturating mutagenesis. Nature. 12 nov 2015;527(7577):192-7.

363. Platt OS. Hydroxyurea for the treatment of sickle cell anemia. N Engl J Med. 27 mars 2008;358(13):1362-9.

364. Pembrey ME, Wood WG, Weatherall DJ, Perrine RP. Fetal haemoglobin production and the sickle gene in the oases of Eastern Saudi Arabia. Br J Haematol. nov 1978;40(3):415-29.

365. Powars DR, Weiss JN, Chan LS, Schroeder WA. Is there a threshold level of fetal hemoglobin that ameliorates morbidity in sickle cell anemia? Blood. avr 1984;63(4):921-6.

366. Labie D, Pagnier J, Lapoumeroulie C, Rouabhi F, Dunda-Belkhodja O, Chardin P, et al. Common haplotype dependency of high G gamma-globin gene expression and high Hb F levels in beta-thalassemia and sickle cell anemia patients. Proc Natl Acad Sci U S A. avr 1985;82(7):2111-4.

367. Horiuchi K, Osterhout ML, Kamma H, Bekoe NA, Hirokawa KJ. Estimation of fetal hemoglobin levels in individual red cells via fluorescence image cytometry. Cytometry. 1 juill 1995;20(3):261-7.

368. Powars DR, Schroeder WA, Weiss JN, Chan LS, Azen SP. Lack of influence of fetal hemoglobin levels or erythrocyte indices on the severity of sickle cell anemia. J Clin Invest. mars 1980;65(3):732-40.

369. Nagel RL, Erlingsson S, Fabry ME, Croizat H, Susuka SM, Lachman H, et al. The Senegal DNA haplotype is associated with the amelioration of anemia in African-American sickle cell anemia patients. Blood. 15 mars 1991;77(6):1371-5.

370. Alsultan A, Alabdulaali MK, Griffin PJ, Alsuliman AM, Ghabbour HA, Sebastiani P, et al. Sickle cell disease in Saudi Arabia: the phenotype in adults with the Arab-Indian haplotype is not benign. Br J Haematol. févr 2014;164(4):597-604.

371. Steinberg MH, Chui DHK, Dover GJ, Sebastiani P, Alsultan A. Fetal hemoglobin in sickle cell anemia: a glass half full? Blood. 23 janv 2014;123(4):481-5.

372. Wilson JB, Headlee ME, Huisman TH. A new high-performance liquid chromatographic procedure for the separation and quantitation of various hemoglobin variants in adults and newborn babies. J Lab Clin Med. août 1983;102(2):174-86.

373. Tomoda Y. DEMONSTRATION OF FOETAL ERYTHROCYTE BY IMMUNOFLUORESCENT STAINING. Nature. 30 mai 1964;202:910-1.

374. Hosoi T. STUDIES ON HEMOGLOBIN F WITHIN SINGLE ERYTHROCYTE BY FLUORESCENT ANTIBODY TECHNIQUE. Exp Cell Res. mars 1965;37:680-3.

375. Gitlin D, Sasaki T, Vuopio P. Immunochemical quantitation of proteins in single cells. I. Carbon anhydrase B, beta-chain hemoglobin and gamma-chain hemoglobin in some normal and abnormal erythrocytes. Blood. nov 1968;32(5):796-810.

376. Boyer SH, Belding TK, Margolet L, Noyes AN. Fetal hemoglobin restriction to a few erythrocytes (F cells) in normal human adults. Science. 25 avr 1975;188(4186):361-3.

377. Wood WG, Stamatoyannopoulos G, Lim G, Nute PE. F-cells in the adult: normal values and levels in individuals with hereditary and acquired elevations of Hb F. Blood. nov 1975;46(5):671-82.

378. Dover GJ, Boyer SH, Bell WR. Microscopic method for assaying F cell production: illustrative changes during infancy and in aplastic anemia. Blood. oct 1978;52(4):664-72.

379. Dover GJ, Boyer SH. Quantitation of hemoglobins within individual red cells: asynchronous biosynthesis of fetal and adult hemoglobin during erythroid maturation in normal subjects. Blood. déc 1980;56(6):1082-91.

380. Navenot JM, Merghoub T, Ducrocq R, Muller JY, Krishnamoorthy R, Blanchard D. New method for quantitative determination of fetal hemoglobin-containing red blood cells by flow cytometry: application to sickle-cell disease. Cytometry. 1 juill 1998;32(3):186-90.

381. Chen JC, Bigelow N, Davis BH. Proposed flow cytometric reference method for the determination of erythroid F-cell counts. Cytometry. 15 août 2000;42(4):239-46.

382. Rakotoson MG. Déterminants de la réponse à l'Hydroxyurée au cours du traitement de la drépanocytose [Internet] [These de doctorat]. Paris Est; 2016 [cité 18 sept 2020]. Disponible sur: http://www.theses.fr/2016PESC0092

383. Franco RS, Lohmann J, Silberstein EB, Mayfield-Pratt G, Palascak M, Nemeth TA, et al. Time-dependent changes in the density and hemoglobin F content of biotin-labeled sickle cells. J Clin Invest. 15 juin 1998;101(12):2730-40.

384. Pannu KK, Joe ET, Iyer SB. Performance evaluation of QuantiBRITE phycoerythrin beads. Cytometry. 1 déc 2001;45(4):250-8.

385. Abbyad P, Tharaux P-L, Martin J-L, Baroud CN, Alexandrou A. Sickling of red blood cells through rapid oxygen exchange in microfluidic drops. Lab Chip. 7 oct 2010;10(19):2505-12.

386. Esrick EB, Achebe M, Armant M, Bartolucci P, Ciuculescu MF, Daley H, et al. Validation of BCL11A As Therapeutic Target in Sickle Cell Disease: Results from the Adult Cohort of a Pilot/Feasibility Gene Therapy Trial Inducing Sustained Expression of Fetal Hemoglobin Using Post-Transcriptional Gene Silencing. Blood. 21 nov 2019;134(Supplement_2):LBA-5-LBA-5.

387. Magrin E, Semeraro M, Magnani A, Puy H, Miccio A, Hebert N, et al. Results from the Completed Hgb-205 Trial of Lentiglobin for β-Thalassemia and Lentiglobin for Sickle Cell Disease Gene Therapy. Blood. 13 nov 2019;134(Supplement_1):3358-3358.

388. Eaton WA, Hofrichter J, Ross PD. Editorial: Delay time of gelation: a possible determinant of clinical severity in sickle cell disease. Blood. avr 1976;47(4):621-7.

389. Di Liberto G, Kiger L, Marden MC, Boyer L, Poitrine FC, Conti M, et al. Dense red blood cell and oxygen desaturation in sickle-cell disease. Am J Hematol. 2016;91(10):1008-13.

390. Uyoga S, Macharia AW, Mochamah G, Ndila CM, Nyutu G, Makale J, et al. The epidemiology of sickle cell disease in children recruited in infancy in Kilifi, Kenya: a prospective cohort study. Lancet Glob Health. 2019;7(10):e1458-66.

391. Kauf TL, Coates TD, Huazhi L, Mody-Patel N, Hartzema AG. The cost of health care for children and adults with sickle cell disease. Am J Hematol. juin 2009;84(6):323-7.

392. Campbell A, Cong Z, Agodoa I, Song X, Martinez DJ, Black D, et al. The Economic Burden of End-Organ Damage Among Medicaid Patients with Sickle Cell Disease in the United States: A Population-Based Longitudinal Claims Study. J Manag Care Spec Pharm. sept 2020;26(9):1121-9.

393. Abraham A, Hsieh M, Eapen M, Fitzhugh C, Carreras J, Keesler D, et al. Relationship between Mixed Donor-Recipient Chimerism and Disease Recurrence after Hematopoietic Cell Transplantation for Sickle Cell Disease. Biol Blood Marrow Transplant J Am Soc Blood Marrow Transplant. déc 2017;23(12):2178-83.

394. Walters MC, Patience M, Leisenring W, Rogers ZR, Aquino VM, Buchanan GR, et al. Stable mixed hematopoietic chimerism after bone marrow transplantation for sickle cell anemia. Biol Blood Marrow Transplant J Am Soc Blood Marrow Transplant. 2001;7(12):665-73.

395. Wu CJ, Gladwin M, Tisdale J, Hsieh M, Law T, Biernacki M, et al. Mixed haematopoietic chimerism for sickle cell disease prevents intravascular haemolysis. Br J Haematol. nov 2007;139(3):504-7.

396. Andreani M, Testi M, Battarra M, Lucarelli G. Split chimerism between nucleated and red blood cells after bone marrow transplantation for haemoglobinopathies. Chimerism. janv 2011;2(1):21-2.

397. Andreani M, Testi M, Gaziev J, Condello R, Bontadini A, Tazzari PL, et al. Quantitatively different red cell/nucleated cell chimerism in patients with long-term, persistent hematopoietic mixed chimerism after bone marrow transplantation for thalassemia major or sickle cell disease. Haematologica. janv 2011;96(1):128-33.

398. Romero Z, Urbinati F, Geiger S, Cooper AR, Wherley J, Kaufman ML, et al. β-globin gene transfer to human bone marrow for sickle cell disease. J Clin Invest. 1 juill 2013;

399. Weber L, Poletti V, Magrin E, Antoniani C, Martin S, Bayard C, et al. An Optimized Lentiviral Vector Efficiently Corrects the Human Sickle Cell Disease Phenotype. Mol Ther Methods Clin Dev. 21 sept 2018;10:268-80.

400. Magnani A, Pondarré C, Bouazza N, Magalon J, Miccio A, Six E, et al. Extensive multilineage analysis in patients with mixed chimerism after allogeneic transplantation for sickle cell disease: insight into hematopoiesis and engraftment thresholds for gene therapy. Haematologica. mai 2020;105(5):1240-7.

401. de Almeida Santiago M, de Paula Fonseca E Fonseca B, da Silva Marques C de F, Domingos da Silva E, Bertho AL, Nogueira ACM de A. Flow Cytometry as a Tool for Quality Control of Fluorescent Conjugates Used in Immunoassays. PloS One. 2016;11(12):e0167669.

402. Rodgers GP, Dover GJ, Noguchi CT, Schechter AN, Nienhuis AW. Hematologic responses of patients with sickle cell disease to treatment with hydroxyurea. N Engl J Med. 12 avr 1990;322(15):1037-45.

403. Goldberg MA, Brugnara C, Dover GJ, Schapira L, Charache S, Bunn HF. Treatment of sickle cell anemia with hydroxyurea and erythropoietin. N Engl J Med. 9 août 1990;323(6):366-72.

404. Steinberg MH, Lu ZH, Barton FB, Terrin ML, Charache S, Dover GJ. Fetal hemoglobin in sickle cell anemia: determinants of response to hydroxyurea. Multicenter Study of Hydroxyurea. Blood. 1 févr 1997;89(3):1078-88.

405. Pule GD, Mowla S, Novitzky N, Wiysonge CS, Wonkam A. A systematic review of known mechanisms of hydroxyurea-induced fetal hemoglobin for treatment of sickle cell disease. Expert Rev Hematol. oct 2015;8(5):669-79.

406. Steinberg MH, Voskaridou E, Kutlar A, Loukopoulos D, Koshy M, Ballas SK, et al. Concordant fetal hemoglobin response to hydroxyurea in siblings with sickle cell disease. Am J Hematol. févr 2003;72(2):121-6.

407. Ma Q, Wyszynski DF, Farrell JJ, Kutlar A, Farrer LA, Baldwin CT, et al. Fetal hemoglobin in sickle cell anemia: genetic determinants of response to hydroxyurea. Pharmacogenomics J. déc 2007;7(6):386-94.

408. Poillon WN, Kim BC, Rodgers GP, Noguchi CT, Schechter AN. Sparing effect of hemoglobin F and hemoglobin A2 on the polymerization of hemoglobin S at physiologic ligand saturations. Proc Natl Acad Sci U S A. 1 juin 1993;90(11):5039-43.

409. Quinn CT, Smith EP, Arbabi S, Khera PK, Lindsell CJ, Niss O, et al. Biochemical surrogate markers of hemolysis do not correlate with directly measured erythrocyte survival in sickle cell anemia. Am J Hematol. 2016;91(12):1195-201.

410. Platt OS, Brambilla DJ, Rosse WF, Milner PF, Castro O, Steinberg MH, et al. Mortality in sickle cell disease. Life expectancy and risk factors for early death. N Engl J Med. 9 juin 1994;330(23):1639-44.

411. Darbari DS, Wang Z, Kwak M, Hildesheim M, Nichols J, Allen D, et al. Severe painful vaso-occlusive crises and mortality in a contemporary adult sickle cell anemia cohort study. PloS One. 2013;8(11):e79923.

412. Elmariah H, Garrett ME, De Castro LM, Jonassaint JC, Ataga KI, Eckman JR, et al. Factors associated with survival in a contemporary adult sickle cell disease cohort. Am J Hematol. mai 2014;89(5):530-5.

413. Tolu SS, Reyes-Gil M, Ogu UO, Thomas M, Bouhassira EE, Minniti CP. Hemoglobin F mitigation of sickle cell complications decreases with aging. Am J Hematol. 2020;95(5):E122-5.

414. Zhu X, Hu T, Ho MH, Wang Y, Yu M, Patel N, et al. Hydroxyurea differentially modulates activator and repressors of γ-globin gene in erythroblasts of responsive and non-responsive patients with sickle cell disease in correlation with Index of Hydroxyurea Responsiveness. Haematologica. 2017;102(12):1995-2004.

415. Yahouédéhou SCMA, Carvalho MOS, Oliveira RM, Santiago RP, da Guarda CC, Carvalho SP, et al. Sickle Cell Anemia Patients in Use of Hydroxyurea: Association between Polymorphisms in Genes Encoding Metabolizing Drug Enzymes and Laboratory Parameters. Dis Markers. 2018;2018:6105691.

416. van Beers EJ, Samsel L, Mendelsohn L, Saiyed R, Fertrin KY, Brantner CA, et al. Imaging flow cytometry for automated detection of hypoxia-induced erythrocyte shape change in sickle cell disease. Am J Hematol. juin 2014;89(6):598-603.

417. Dover GJ, Boyer SH, Charache S, Heintzelman K. Individual variation in the production and survival of F cells in sickle-cell disease. N Engl J Med. 28 déc 1978;299(26):1428-35.

418. Nagel RL, Vichinsky E, Shah M, Johnson R, Spadacino E, Fabry ME, et al. F reticulocyte response in sickle cell anemia treated with recombinant human erythropoietin: a double-blind study. Blood. 1 janv 1993;81(1):9-14.

419. Franco RS, Barker-Gear R, Miller MA, Williams SM, Joiner CH, Rucknagel DL. Fetal hemoglobin and potassium in isolated transferrin receptor-positive dense sickle reticulocytes. Blood. 15 sept 1994;84(6):2013-20.

420. Horiuchi K, Osterhout ML, Ohene-Frempong K. Survival of F-reticulocytes in sickle cell disease. Biochem Biophys Res Commun. 26 déc 1995;217(3):924-30.

421. Mundee Y, Bigelow NC, Davis BH, Porter JB. Flow cytometric method for simultaneous assay of foetal haemoglobin containing red cells, reticulocytes and foetal haemoglobin containing reticulocytes. Clin Lab Haematol. juin 2001;23(3):149-54.

422. Franco RS, Yasin Z, Palascak MB, Ciraolo P, Joiner CH, Rucknagel DL. The effect of fetal hemoglobin on the survival characteristics of sickle cells. Blood. 1 août 2006;108(3):1073-6.

423. Meier ER, Wright EC, Miller JL. Reticulocytosis and anemia are associated with an increased risk of death and stroke in the newborn cohort of the Cooperative Study of Sickle Cell Disease. Am J Hematol. sept 2014;89(9):904-6.

424. Onyike AE, Ohene-Frempong K, Horiuchi K. Sickling in vitro at venous and arterial oxygen tensions of reticulocytes from patients with sickle cell disease. Biochem Biophys Res Commun. 15 juin 1995;211(2):504-10.

425. Bookchin RM, Ortiz OE, Lew VL. Evidence for a direct reticulocyte origin of dense red cells in sickle cell anemia. J Clin Invest. janv 1991;87(1):113-24.

426. Chasis JA, Prenant M, Leung A, Mohandas N. Membrane assembly and remodeling during reticulocyte maturation. Blood. 15 août 1989;74(3):1112-20.

427. Mankelow TJ, Griffiths RE, Trompeter S, Flatt JF, Cogan NM, Massey EJ, et al. Autophagic vesicles on mature human reticulocytes explain phosphatidylserine-positive red cells in sickle cell disease. Blood. 8 oct 2015;126(15):1831-4.

428. Sugihara K, Sugihara T, Mohandas N, Hebbel RP. Thrombospondin mediates adherence of CD36+ sickle reticulocytes to endothelial cells. Blood. 15 nov 1992;80(10):2634-42.

429. Swerlick RA, Eckman JR, Kumar A, Jeitler M, Wick TM. Alpha 4 beta 1-integrin expression on sickle reticulocytes: vascular cell adhesion molecule-1-dependent binding to endothelium. Blood. 15 sept 1993;82(6):1891-9.

430. Setty BN, Kulkarni S, Dampier CD, Stuart MJ. Fetal hemoglobin in sickle cell anemia: relationship to erythrocyte adhesion markers and adhesion. Blood. 1 mai 2001;97(9):2568-73.

431. Lee K, Gane P, Roudot-Thoraval F, Godeau B, Bachir D, Bernaudin F, et al. The nonexpression of CD36 on reticulocytes and mature red blood cells does not modify the clinical course of patients with sickle cell anemia. Blood. 15 août 2001;98(4):966-71.

432. Ataga KI, Cappellini MD, Rachmilewitz EA. Beta-thalassaemia and sickle cell anaemia as paradigms of hypercoagulability. Br J Haematol. oct 2007;139(1):3-13.

433. Hsieh MM, Kang EM, Fitzhugh CD, Link MB, Bolan CD, Kurlander R, et al. Allogeneic hematopoietic stem-cell transplantation for sickle cell disease. N Engl J Med. 10 déc 2009;361(24):2309-17.

434. Arlet J-B, Ribeil J-A, Guillem F, Negre O, Hazoume A, Marcion G, et al. HSP70 sequestration by free α-globin promotes ineffective erythropoiesis in β-thalassaemia. Nature. 9 oct 2014;514(7521):242-6.

435. Arlet J-B, Dussiot M, Moura IC, Hermine O, Courtois G. Novel players in β-thalassemia dyserythropoiesis and new therapeutic strategies. Curr Opin Hematol. mai 2016;23(3):181-8.

436. Wu CJ, Krishnamurti L, Kutok JL, Biernacki M, Rogers S, Zhang W, et al. Evidence for ineffective erythropoiesis in severe sickle cell disease. Blood. 15 nov 2005;106(10):3639-45.

437. Hasegawa S, Rodgers GP, Dwyer N, Noguchi CT, Blanchette-Mackie EJ, Uyesaka N, et al. Sickling of nucleated erythroid precursors from patients with sickle cell anemia. Exp Hematol. avr 1998;26(4):314-9.

438. Blouin MJ, De Paepe ME, Trudel M. Altered hematopoiesis in murine sickle cell disease. Blood. 15 août 1999;94(4):1451-9.

439. Park S-Y, Matte A, Jung Y, Ryu J, Anand WB, Han E-Y, et al. Pathologic angiogenesis in the bone marrow of humanized sickle cell mice is reversed by blood transfusion. Blood. 4 juin 2020;135(23):2071-84.

440. El Hoss S, Cochet S, Godard A, Yan H, Dussiot M, Frati G, et al. Fetal hemoglobin rescues ineffective erythropoiesis in sickle cell disease. Haematologica. 27 août 2020;

441. Novelli EM, Kato GJ, Ragni MV, Zhang Y, Hildesheim ME, Nouraie M, et al. Plasma thrombospondin-1 is increased during acute sickle cell vaso-occlusive events and associated with acute chest syndrome, hydroxyurea therapy, and lower hemolytic rates. Am J Hematol. mars 2012;87(3):326-30.

442. Novelli EM, Kato GJ, Hildesheim ME, Barge S, Meyer MP, Lozier J, et al. Thrombospondin-1 inhibits ADAMTS13 activity in sickle cell disease. Haematologica. nov 2013;98(11):e132-134.

443. Rogers NM, Sharifi-Sanjani M, Yao M, Ghimire K, Bienes-Martinez R, Mutchler SM, et al. TSP1-CD47 signaling is upregulated in clinical pulmonary hypertension and contributes to pulmonary arterial vasculopathy and dysfunction. Cardiovasc Res. 2017;113(1):15-29.

444. Fendel R, Mordmüller B, Kreidenweiss A, Rudat A, Steur C, Ambrosch C, et al. New method to quantify erythrophagocytosis by autologous monocytes. Cytom Part J Int Soc Anal Cytol. avr 2007;71(4):258-64.

445. Gallo V, Skorokhod OA, Schwarzer E, Arese P. Simultaneous determination of phagocytosis of Plasmodium falciparum-parasitized and non-parasitized red blood cells by flow cytometry. Malar J. 21 déc 2012;11:428.

446. Groner W, Mohandas N, Bessis M. New optical technique for measuring erythrocyte deformability with the ektacytometer. Clin Chem. sept 1980;26(10):1435-42.

447. Parrow NL, Tu H, Nichols J, Violet P-C, Pittman CA, Fitzhugh C, et al. Measurements of red cell deformability and hydration reflect HbF and HbA2 in blood from patients with sickle cell anemia. Blood Cells Mol Dis. 2017;65:41-50.

448. Ballas SK, Connes P, Investigators of the Multicenter Study of Hydroxyurea in Sickle Cell Anemia. Rheological properties of sickle erythrocytes in patients with sickle-cell anemia: The effect of hydroxyurea, fetal hemoglobin, and α-thalassemia. Eur J Haematol. déc 2018;101(6):798-803.

449. Kim A, Dean A. Chromatin loop formation in the β-globin locus and its role in globin gene transcription. Mol Cells. juill 2012;34(1):1-5.

450. Lisowski L, Sadelain M. Locus control region elements HS1 and HS4 enhance the therapeutic efficacy of globin gene transfer in beta-thalassemic mice. Blood. 15 déc 2007;110(13):4175-8.

451. Morianos I, Siapati EK, Pongas G, Vassilopoulos G. Comparative analysis of FV vectors with human α- or β-globin gene regulatory elements for the correction of β-thalassemia. Gene Ther. mars 2012;19(3):303-11.

452. Morgan RA, Ma F, Unti MJ, Brown D, Ayoub PG, Tam C, et al. Creating New β-Globin-Expressing Lentiviral Vectors by High-Resolution Mapping of Locus Control Region Enhancer Sequences. Mol Ther Methods Clin Dev. 12 juin 2020;17:999-1013.

453. May C, Rivella S, Callegari J, Heller G, Gaensler KM, Luzzatto L, et al. Therapeutic haemoglobin synthesis in beta-thalassaemic mice expressing lentivirus-encoded human beta-globin. Nature. 6 juill 2000;406(6791):82-6.

454. Morgan RA, Unti MJ, Aleshe B, Brown D, Osborne KS, Koziol C, et al. Improved Titer and Gene Transfer by Lentiviral Vectors Using Novel, Small β-Globin Locus Control Region Elements. Mol Ther J Am Soc Gene Ther. 08 2020;28(1):328-40.

455. Cattoglio C, Pellin D, Rizzi E, Maruggi G, Corti G, Miselli F, et al. High-definition mapping of retroviral integration sites identifies active regulatory elements in human multipotent hematopoietic progenitors. Blood. 16 déc 2010;116(25):5507-17.

456. Cesana D, Ranzani M, Volpin M, Bartholomae C, Duros C, Artus A, et al. Uncovering and dissecting the genotoxicity of self-inactivating lentiviral vectors in vivo. Mol Ther J Am Soc Gene Ther. avr 2014;22(4):774-85.

457. Coquerelle S, Ghardallou M, Rais S, Taupin P, Touzot F, Boquet L, et al. Innovative Curative Treatment of Beta Thalassemia: Cost-Efficacy Analysis of Gene Therapy Versus Allogenic Hematopoietic Stem-Cell Transplantation. Hum Gene Ther. 2019;30(6):753-61.

458. Magrin E, Miccio A, Cavazzana M. Lentiviral and genome-editing strategies for the treatment of β-hemoglobinopathies. Blood. 10 2019;134(15):1203-13.

459. Dull T, Zufferey R, Kelly M, Mandel RJ, Nguyen M, Trono D, et al. A third-generation lentivirus vector with a conditional packaging system. J Virol. nov 1998;72(11):8463-71.

460. Zheng N, Li L, Wang X. Molecular mechanisms, off-target activities, and clinical potentials of genome editing systems. Clin Transl Med. janv 2020;10(1):412-26.

461. Kosicki M, Tomberg K, Bradley A. Repair of double-strand breaks induced by CRISPR-Cas9 leads to large deletions and complex rearrangements. Nat Biotechnol. 2018;36(8):765-71.

462. Song Y, Liu Z, Zhang Y, Chen M, Sui T, Lai L, et al. Large-Fragment Deletions Induced by Cas9 Cleavage while Not in the BEs System. Mol Ther Nucleic Acids. 4 sept 2020;21:523-6.

463. Zetsche B, Gootenberg JS, Abudayyeh OO, Slaymaker IM, Makarova KS, Essletzbichler P, et al. Cpf1 is a single RNA-guided endonuclease of a class 2 CRISPR-Cas system. Cell. 22 oct 2015;163(3):759-71.

464. Shmakov S, Abudayyeh OO, Makarova KS, Wolf YI, Gootenberg JS, Semenova E, et al. Discovery and Functional Characterization of Diverse Class 2 CRISPR-Cas Systems. Mol Cell. 5 nov 2015;60(3):385-97.

465. Swarts DC, van der Oost J, Jinek M. Structural Basis for Guide RNA Processing and Seed-Dependent DNA Targeting by CRISPR-Cas12a. Mol Cell. 20 avr 2017;66(2):221-233.e4.

466. Paul B, Montoya G. CRISPR-Cas12a: Functional overview and applications. Biomed J. 2020;43(1):8-17.

467. Zhang Y, Long C, Li H, McAnally JR, Baskin KK, Shelton JM, et al. CRISPR-Cpf1 correction of muscular dystrophy mutations in human cardiomyocytes and mice. Sci Adv. avr 2017;3(4):e1602814.

Annex

Received: 7 January 2020 | Revised: 6 July 2020 | Accepted: 10 July 2020

DOI: 10.1002/ajh.25937

RESEARCH ARTICLE

Individual red blood cell fetal hemoglobin quantification allows to determine protective thresholds in sickle cell disease

Nicolas Hebert[1,2,3] | Marie Georgine Rakotoson[1] | Gwellaouen Bodivit[1,2] | Etienne Audureau[3] | Laura Bencheikh[1,3] | Laurent Kiger[1,3] | Nadia Oubaya[4] | Sadaf Pakdaman[1,2] | Mehdi Sakka[4] | Gaetana Di Liberto[1,2] | Philippe Chadebech[1,2] | Benoit Vingert[1,2] | France Pirenne[1,2] | Frédéric Galactéros[1,3] | Marie Cambot[5] | Pablo Bartolucci[1,3]

[1]Institut Mondor de Recherche Biomédicale, Unité 955, team Pirenne, INSERM, EFS, UPEC, Laboratory of excellence LABEX GRex, Créteil, France

[2]Etablissement Français du Sang, Île-de-France, Hôpital Henri Mondor, Créteil, France

[3]Sickle cell referral center, UMGGR, Plateforme d'expertise Maladies Rares Grand Paris Est, UPEC Hôpitaux Universitaires Henri Mondor, APHP, Créteil, France

[4]Hôpital Henri Mondor, Assistance Publique-Hôpitaux De Paris (APHP), Université Paris-Est Créteil, Créteil, France

[5]UMR_S1134, Université Sorbonne Paris Cité, Université Paris Diderot, Inserm, INTS, Unité Biologie Intégrée du Globule Rouge, Laboratory of excellence LABEX GRex, Paris, France

Correspondence
Pablo Bartolucci, Sickle Cell Referral Center, UMGGR, Service de Médecine Interne, Hôpital Henri Mondor; 51, avenue du Maréchal de Lattre-de-Tassigny, 94010 Créteil Cedex, France
Email: pablo.bartolucci@aphp.fr

Abstract

Polymerization of the sickle hemoglobin (HbS) is a key determinant of sickle cell disease (SCD), an inherited blood disorder. Fetal hemoglobin (HbF) is a major modulator of the disease severity by both decreasing HbS intracellular concentration and inhibiting its polymerization. However, heterocellular distribution of HbF is common in SCD. For HbS polymerization inhibition, the hypothesis of an "HbF per red blood cell (HbF/RBC) threshold" requires accurate measurement of HbF in individual RBC. To date, HbF detection methods are limited to a qualitative measurement of RBC populations containing HbF - the F cells, which are variable. We developed an accurate method for HbF quantification in individual RBC. A linear association between mean HbF content and mean RBC fluorescence by flow cytometry, using an anti-Human-HbF antibody, was obtained from non-SCD subjects presenting homogeneous HbF distribution. This correlation was then used to measure HbF/RBC. Hydroxyurea (HU) improves SCD clinical manifestations, mainly through its ability to induce HbF synthesis. The HbF distribution was analyzed in 14 SCD patients before and during HU treatment. A significant decrease in RBC population containing less than 2 pg of HbF/RBC was observed. Therefore, we tested associations for %RBC above different HbF/RBC thresholds and showed a decrease in the pathognomonic vaso-occlusive crisis incidence from the threshold of 4 pg. This quantity was also correlated with the level of sickle RBC after in vitro deoxygenation. This new method allows the comparison of HbF/RBC distributions and could be a useful tool to characterize baseline patients HbF distribution and therapeutic response to HbF inducers.

1 | INTRODUCTION

Sickle cell disease (SCD) is one of the most common monogenic disorder in the world and is due to a single amino acid substitution in the beta-globin chain of the hemoglobin (Glu6Val). Sickle hemoglobin (HbS) has the unique property of forming polymers within red blood cells (RBCs) under a deoxygenated state, distorting their normal shape and altering their properties and ability to carry oxygen throughout the body. Acute chest syndromes (ACS), vaso-occlusive crisis (VOC) and chronic organ damages are the major causes of death in SCD patients.

Nicolas Hebert and Marie Georgine Rakotoson contributed equally to this work.

Fetal hemoglobin (HbF) is known to be the most protective independent factor in SCD by inhibiting HbS polymerization, decreasing clinical manifestation and mortality.[1,2] The HbS content and the percentage of HbF are the two main modulators of clinical severity. However, the association between the HbF percentage of total Hb (%HbF) and chronic SCD complications is variable; conversely a low incidence of VOC has been observed in patients with low %HbF, not explained by other protective factors.[3,4] These observations suggested that rather than the %HbF, a threshold of HbF content in individual RBCs could be a critical determinant of the HbF effect.[5] The protective effects of HbF can be easily rationalized when there is a homogeneous HbF distribution, as seen in most HbS/beta thalassemia and HbS/HPFH (hereditary persistence of fetal hemoglobin) patients, while the heterocellular distribution of HbF observed in homozygous patients presents a challenge.[6]

In the last decades, several techniques have been developed to detect HbF in RBCs. High performance liquid chromatography (HPLC), routinely used, provides the percentage of HbF in a hemolysate.[7] Chemical[8] or immunological methods estimate the percentage of RBCs containing variable amounts of HbF, named F cells.[9-16] Although widely used in maternal/fetal incompatibility diagnosis or hemoglobinopathies, these methods are limited to a qualitative measurement of HbF. In addition, the lack of a standardized HbF level in F cells does not allow comparison between patients from different centers or over time for a same patient.

Herein, we developed a new and easy to implement method to accurately measure HbF amount per RBC (HbF/RBC) providing a quantitative HbF distribution. This method is based on the correlation between the mean corpuscular HbF (MCHbF) and the fluorescence intensity by flow cytometry using an anti-Human-HbF monoclonal antibody coupled with phycoerythrin (PE). This relationship is linear in patients with homogeneous HbF distribution, as for beta thalassemia and HPFH patients. The HbF fluorescence intensity is normalized from standardized beads allowing the analysis on any flow cytometer.

We show that this quantitative approach has the potential of being a novel tool in the treatment of SCD patients and could provide an in-depth assessment of any HbF inducers. As a proof of concept, we used this new method to study and analyze changes in the cellular HbF distribution in SCD patients, following 6 months of treatment by the well-known HbF inducer hydroxyurea (HU).[17] Multiple studies have shown that HU increases %HbF mainly by increasing the fraction of both F cells and F reticulocytes,[18-20] but none of them analyzed the cellular HbF content distribution. Our results strengthen the hypothesis that the number of RBCs above a threshold of HbF is likely more protective than a heterocellular distribution,[21] both from a biologic and a clinical point of view, and suggest that this threshold might be low.

2 | METHODS

2.1 | Patients

Eligible patients were selected from the SICLOPEDIE cohort monitored in our referral center (Henri Mondor Hospital, Creteil, France). This protocol was approved by the local ethics committee (CPP-Île-de-France IV Saint-Louis Hospital, IRB 00003835). In accordance with the Declaration of Helsinki, all patients gave their signed informed consent. All data were rendered anonymous to protect patients' privacy and confidentiality.

Two groups of patients, all ≥18 years, were recruited: group A was used for method development and group B was used to assess changes produced by HU treatment.

2.1.1 | Inclusion criteria in group A

Patients carrying HPFH, β or δβ Thalassemia or genetic hemochromatosis (as controls with very low HbF). Homogeneous HbF distribution was confirmed by flow cytometry. Exclusion criteria were SCD (HbSS, Sβ-thalassemia or SC) or sickle cell trait (AS), blood transfusion within 3 months preceding the enrolment and pregnancy.

2.1.2 | Inclusion criteria in group B

Patients SS or S-β^0 thalassemia at steady state (>1 month from a VOC and > 3 months from a transfusion) and undergoing a treatment with hydroxyurea (HU). Exclusion criteria were SC or S-β^+ thalassemia genotype, chronic transfusion program, erythropoietin treatment and pregnancy. We collected samples and biologic parameter values before treatment (D0), between 15 days and 1 month (D15-M1), 3 and 4 months (M3-4) and ≥ 6 months (≥M6) on HU.

2.2 | HbF assays

The HbF level was determined in RBCs using three techniques: HPLC of total hemoglobin, complete blood count and flow cytometry.

2.2.1 | Percentage HbF determination on HPLC

The HbF dosage was performed through ion exclusion liquid chromatography using a Variant II Hemoglobin Testing System (Bio-Rad). The different Hbs were eluted from column based on ionic interaction with carboxyl group, and then introduced in a photometer detector using two different wavelengths of 690 nm and 415 nm for baseline and sample detection, respectively. The chromatography system run time was 6 minutes and HbF was eluted up to 0.5 minute. Results were acquired with CDM 5.2 software.

2.2.2 | Complete blood count

The RBC count, mean corpuscular volume (MCV) and mean corpuscular hemoglobin (MCH) were determined using a Horiba ABX Micros ES 60 counter (HORIBA Medical).

Mean Corpuscular HbF (MCHbF in pg) was calculated using the following equation[22]:

$$\text{MCHbF} = \frac{(\%HbF \times MCH)}{100}$$

2.2.3 | HbF detection by flow cytometry

The HbF fluorescence in RBCs was measured using a eight-color BD FACSCanto II flow cytometer (BD Biosciences). Acquired data on flow cytometer were analyzed using FlowJo v10 software (BD Biosciences).

2.2.4 | RBC fixation and permeabilization

Prior to intracellular staining, the RBC membrane was fixed and permeabilized using Fetal Cell Count kit reagents (Cat IQP-363, IQ Products) according to the manufacturer's instructions using 5 μL of packed RBC.

2.2.5 | HbF immunofluorescent staining

Mouse monoclonal anti-human HbF antibody conjugated with R-phycoerythrin (R-PE) (reagent F, Fetal Cell Count kit, IQ Products) was used for immunologically based HbF detection, and 20 μL of a PE mouse IgG1 Kappa (BD Pharmingen) used as a negative isotypic control. The RBCs were incubated for 15 minutes, shielded from light at room temperature. Thereafter, RBCs were washed with phosphate buffer saline (PBS) and centrifuged at 300*g* for 3 minutes. Stained RBCs were immediately analyzed on a flow cytometer. The anti-carbonic anhydrase (CA), presents in the fetal cell count kit, was never used, first, to avoid fluorescence interference on the measured signal from the anti-HbF because of spectral overlap of FITC and R-PE emission spectra and second, because all the quantifications were performed on adult RBCs (not from a fetus).

2.2.6 | Flow cytometry acquisition

For each experiment, a negative isotypic control and a positive control (patient two from group A with HPFH and presenting 100% HbF - as confirmed by HPLC - Figure S1) were processed. Light scatter thresholds were used to select RBC population and exclude cellular debris. Every PE fluorescence intensity (FL-2) was monitored with a photomultiplier tube (PMT) voltage set at 400 V. 1×10^5 cells were gated on FSC-A vs SSC-A plot and recorded. Doublet exclusion was performed based on selecting single cells on FSC-H (FSC-Height) plotted against FSC-W (FSC-Width) and then on SSC-H vs SSC-W. In parallel, quantitation beads (Becton Dickinson QuantiBRITE PE, BD Biosciences)[23] were analyzed on the same flow cytometer using the same settings as used for RBCs. A minimum of 1×10^4 beads was recorded allowing four fluorescence levels corresponding to a number of PE molecules per bead which is batch specific. A linear regression involving bead fluorescence intensity and number of PE molecules per bead was then obtained (Figure S3A).

2.3 | HbF determination method in individual RBC

A method for HbF quantification in single RBC was developed from samples collected from patients assigned in group A. Mathematically, we applied a correction factor to the measured PE fluorescence intensities to consider the variability of the degree of coupling of the antibody, which can differ from one batch to another. Fluorescence: protein ratios were 1.2, 1.04 and 0.66 for batches number 1, 2 and 3, respectively. Fluorescence values of each RBC were converted into PE molecules per RBC giving a normalized HbF fluorescence by using the quantitation beads. Normalized HbF fluorescence per RBC was then determined by replacing bead fluorescence intensity by RBC fluorescence. Because MCHbF corresponds to an average HbF content per RBC when homogeneous HbF distribution is observed, a linear regression associating the normalized HbF fluorescence and MCHbF was obtained. This linear regression was used to assess the HbF/RBC for group B patients.

2.4 | F cell detection methods

The F cell percentages were assessed by using two different methods as previously described.[16,24] Briefly, cells were analyzed by flow cytometry as above. The F cell percentage was calculated as the fraction of positive cells when incubated with the anti-HbF antibody, compared to a threshold set up according to the fluorescence intensity of unstained cells (method 1) or cells incubated with the isotypic control (method 2). (See F cell detection strategy - Figure S2).

2.5 | Analysis of the HbF distribution normality

To assess the log-normal distribution of HbF in RBCs from group A patients D'Agostino & Pearson normality tests were performed. HbF/RBC was measured by flow cytometry as described. The R-PE fluorescence of each RBC was extracted using FlowJo software and 500 events were randomly selected to test the normality. A homogeneous HbF distribution was considered when the *P* value was > .05.

2.6 | Association between HbF/RBC and vaso-occlusive crisis occurrence

Number of vaso-occlusive crisis (VOC) was collected from computerized patient's file from Henri Mondor Hospital for each group B patient. The VOC incidence during the 3 years period before the

beginning of HU treatment was compared to HbF/RBC measured at D0, and the VOC incidence during the 3 years period after 6 months of HU treatment at stable dose was compared to HbF/RBC measured at ≥M6. The VOC was defined as pain or tenderness, affecting at least one part of the body, including limbs, ribs, sternum, head (skull), spine, and/or pelvis, that required opioids, was associated with a hospitalization and was not attributable to other causes.

2.7 | In vitro sickling assay

Blood samples were collected from 46 SCD patients from the SICLOPEDIE cohort and not included in group B. Total blood was washed as described and RBCs were diluted 400-fold in PBS pH = 7.4 containing 5 mM glucose (Sigma-Aldrich). The oxygen was enzymatically depleted by adding glucose oxidase and catalase (Sigma-Aldrich) to diluted blood to final concentrations of 0.625 mg/mL and 0.01 mg/mL, respectively. Samples were rested for at least 2 minutes at room temperature and then observed under an inverted microscope (Zeiss AxioObserver).[25] Pictures were analyzed using ImageJ 1.52a software (NIH). Results were expressed as the ratio of sickle RBCs on total RBCs.

2.8 | Statistical analysis

For group A patients, association between MCHbF and normalized HbF fluorescence was assessed by a Pearson correlation. The log-normal distribution of HbF was assessed by the D'Agostino & Pearson normality test.

For group B patients, comparisons of biologic parameters between D0 and ≥ M6 were performed using Wilcoxon matched-pairs signed rank tests. Comparisons of HbF/RBC at D0, D15-M1, M3-M4 and ≥ M6 were performed using Friedman tests. Correlations between %RBC above HbF thresholds and biologic parameters or number of VOC before and after HU treatment were performed using Spearman correlation tests. The ROC (receiver operating characteristics) analysis were performed by applying a cut-off for VOC incidence of ≤1 over 3 years.

Statistical analyeses were performed using Prism 8 software (GraphPad) or STATA 15.1 software (Statacorp). All tests were 2-tailed using a significance level set at .05.

3 | RESULTS

3.1 | Determination of HbF per RBC

The distribution of HbF content per RBC was assessed by flow cytometry (Figure 1A) for the 18 group A patients (Table S1). A log-normal distribution, as verified by D'Agostino & Pearson normality tests, indicates a homogeneous HbF content among the RBC population (Table S2). Patients A-1 to A-6 and A-8 to A-12 were selected for further study while A-7 and A-13 to A-18 were excluded because of a non-log-normal distribution. To consider a variability introduced by the fetal cell count kit batch, linear regressions were independently determined as the relationship between the mean corpuscular HbF (MCHbF) and the mean normalized HbF fluorescence for each patient, using three different batches (n°1; 2 and 3) (Figure 1B). The linear regressions obtained were similar for the three batches (r = 0.9911 and P = .001; r = 0.9930 and P < .001; r = 0.9978 and P < .001 for batches n°1, 2 and 3 respectively). We thus calculated a mean linear regression including all the data measured with the three batches (r = 0.9984; P < .001). This mean linear regression which functions as a standard curve, allows the determination of the HbF/RBC according to the corrected fluorescence intensity and was used for all the quantifications of the study. The inclusion of the group A patients presenting a heterogeneous HbF distribution (patients A-7 and A-13 to A-18) modified both r parameters (0.9979 and 0.9559) and linearity (R^2 = 0.9958 and 0.9137) between mean HbF and fluorescence intensity and was then discarded (Figure S3B).

3.2 | Repeatability and reproducibility of the HbF/RBC measurement

To further validate the quantification of HbF/RBC using our method, several samples from patients or healthy donors have been analyzed at different times. To simplify, percentages of RBC classified in ranges of more than 10 pg of HbF/RBC were analyzed together. First, freezing of the RBCs does not alter the quantification as we observed similar distributions between fresh and frozen samples (Figure S4). Second, slight differences were obtained when the same samples were acquired using two different flow cytometers with highest coefficients of variation (CV) obtained for the less represented ranges (containing less than 5% of total RBC) (Figure S5). Third, repeatability (Figure S6) and reproducibility (Figure S7) experiments gave good precision results with highest CV (> 20%) only observed for ranges containing less than 1% of total RBC. This is expected to be due to the low mean %RBC in the corresponding ranges (as the coefficient of variation is a ratio of the SD to the mean).

3.3 | Quantitative measurements of HbF/RBC upon HU treatment

Fourteen adult SCD patients (11 women and 3 men; mean age [± SD] = 34.9 ± 8 years) were included in group B. Hydroxyurea was administered at an average and stable dose of 15 mg/kg/day. Table 1 provides the biologic parameters assessed before and after ≥6 months of HU.

The HbF distributions were assessed by flow cytometry before and during HU treatment showing different types of response (Figure S8). The R-PE fluorescence intensity was collected for each RBC, normalized and referred to the mean linear regression to calculate the corresponding amount of HbF/RBC in picograms. Percentages of RBC were classified according different ranges of HbF/RBC which were compared during HU treatment for the 14 group B patients.

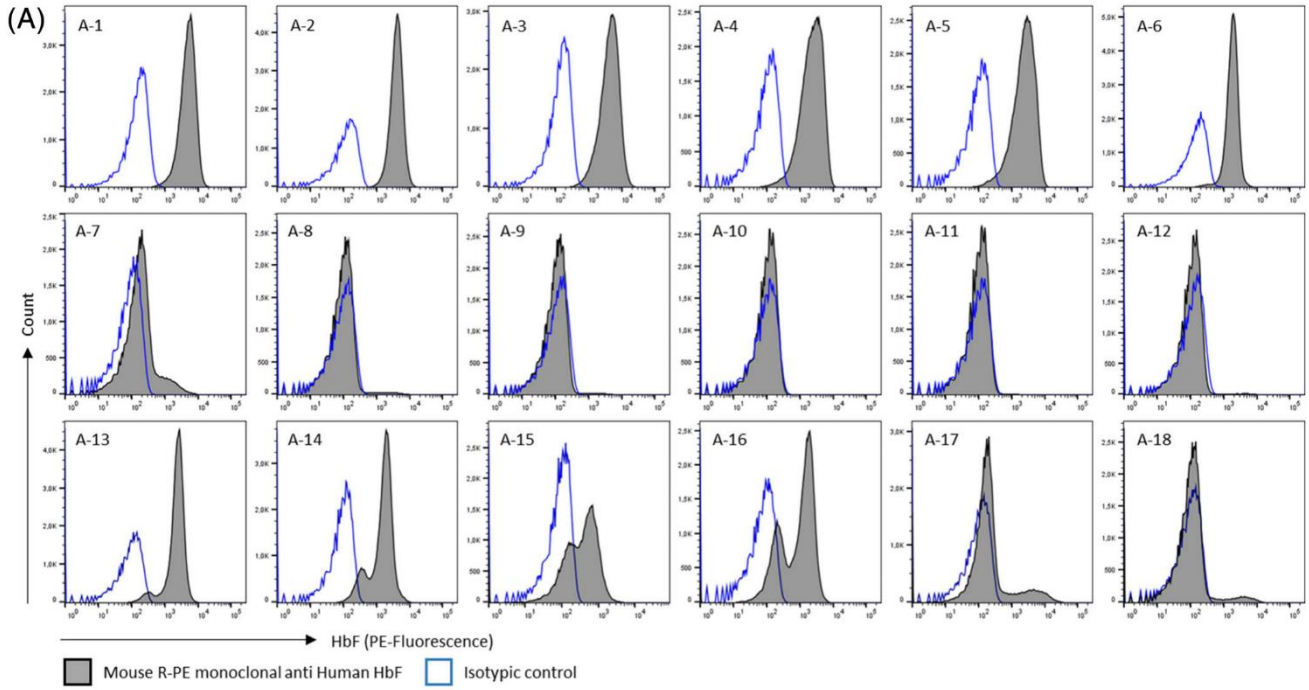

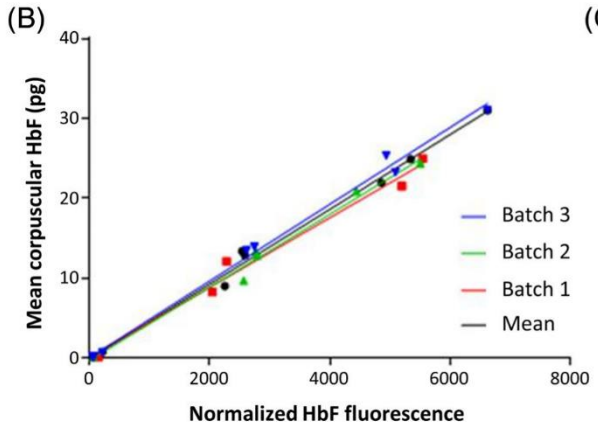

(C)

HU follow up

HbF/RBC (pg)	D0	D15-M4	≥M6	P	n
[0;2[	75.21	65.10	62.69	.001	14
[2;4[	10.36	14.88	17.72	< .001	14
[4;6[	5.46	7.37	6.52	.223	14
[6;8[	2.97	4.06	3.01	.223	14
[8;10[	1.77	2.38	1.79	.145	14
[10;15[	0.88	1.23	1.42	.257	14
[15;20[	2.11	2.88	2.52	.135	14
≥20	1.24	2.11	4.34	.135	14
Mean HbF	6.2%	7.9%	15.2%		

Colorimetric scale (% of RBC):

1 5 10 15 20 30 40 50 60 70 80 90 100

FIGURE 1 HbF quantification per RBC assessed by flow cytometry. A, Individual histograms of the 18 group A patients. A log-normal distribution of fluorescence (gray histograms) indicates a homogeneous distribution of HbF (patients A-1 to A-6 and A-8 to A-12) (one representative experiment). Blue lines represent the isotypic control. The horizontal axis shows the R-PE fluorescence (log scale); the vertical axis shows the RBC count. B, Linear regressions between the mean corpuscular HbF (assessed by HPLC) and the mean normalized HbF fluorescence. Three different batches (batch n°1, 5 patients, $n = 3$; batch n°2, 6 patients, $n = 4$; and batch n°3, 11 patients, $n = 4$) were independently used (Pearson correlations). C, Percentages of RBC classified by HbF/RBC ranges before and under HU. Data represents mean % of RBCs in each range of HbF/RBC for the 14 group B patients at D0, between D15 and M4, and at ≥M6 of HU (Friedman test). Mean %HbF was assessed by HPLC. The color scale shows the %RBC by range

Statistically significant variations were only found in low ranges of HbF/RBC (HbF <2 pg, $P = .001$ and 2 ≤ HbF <4 pg, $P < .001$; Friedman test) (Figure 1C) with a 16.6% decrease between D0 and ≥ M6 in RBCs containing less than 2 pg, and a 1.7-fold increase in RBCs containing between 2 and 4 pg. Interestingly, the increase in cells containing 2-4 pg HbF (+7.36%) accounted for almost 40% of the sum of the increase of cells containing more than 2 pg HbF (+15.69%). Concomitantly, RBC population with HbF/RBC >20 pg increased up to 3.5-fold but this change was not statistically significant ($P = .135$; Friedman test). Supplemental Figure 9 displays HbF quantification obtained for patients B-1 and B-8 presenting a similar response to HU in term of mean %HbF increasement but with different HbF distributions at ≥ 6 months (Figure S9).

3.4 | Correlations between biologic parameters and HbF/RBC thresholds

As we observed that HU mainly decreases RBCs with low HbF content (Figure 1C), the thresholds of HbF/RBC ≥2, 4, 6, 8, 10 and 20 pg were analyzed (Figure S10). Upon HU treatment, an increase in mean

TABLE 1 Changes in biological parameters during hydroxyurea treatment for group B patients (Median [first quartile - third quartile]) (Wilcoxon matched-pairs signed rank test)

	D0	≥M6	P	mv
%HbF	6.2 [2.8-8.4]	14.2 [7.7-21.1]	**.001**	2
Total hemoglobin (g/L)	84 [73-94]	95 [83-105]	**.006**	3
Red blood cells (10^{12}/L)	2.6 [2.2-3.4]	2.8 [2.4-3.4]	.865	3
Reticulocytes (10^9/L)	245.5 [190.5-260.0]	120 [78.5-211.0]	**.008**	4
MCV (fL)	89.5 [83.0-94.5]	100.5 [91.2-115.2]	**.002**	2
MCHC (g/L)	340 [330-350]	330 [320-340]	**.016**	3
MCH (pg)	30 [28.0-32.9]	34.5 [32-40.7]	**.001**	2
Leucocytes (10^9/L)	10.3 [9.7-12.1]	6.5 [5.4-8.5]	**.002**	3
Platelets (10^9/L)	432.5 [329.0-529.2]	354.5 [269.0-468.5]	**.005**	2
*LDH (μkat/L)	6.0 [3.7-8.5]	5.5 [3.6-6.4]	.067	3
Total bilirubin (μmol/L)	42 [34.2-53.7]	33.5 [24.2-46.2]	**.005**	2
ASAT (μkat/L)	0.6 [0.4-0.9]	0.5 [0.4-0.8]	.060	2
F cells (%) method 1	40.3 [20.6-48.2]	54.6 [41.1-73.3]	**.001**	0
F cells (%) method 2	35.6 [18.3-42.7]	52.8 [31.8-70.2]	**.001**	0

Note: All statistically significant values ($P < .05$) are provided in bold.
Abbreviations: ASAT, aspartate aminotransferase; LDH, lactate dehydrogenase; MCH, mean corpuscular hemoglobin; MCHC, mean corpuscular hemoglobin concentration; MCV, mean corpuscular volume; mv, missing value.

%RBC for every threshold was observed, statistically significant for the amount of RBCs containing at least 2 pg of HbF ($P = .001$; Friedman test).

Correlations were evaluated between percentages of RBC by each HbF/RBC threshold and biologic parameters, independently of the duration of HU treatment (Figure 2). Increase in mean %HbF, MCV and MCH and decrease in RBC count were significantly associated with the number of RBC containing at least 2 pg of HbF ($P < .001$; $< .001$; $< .001$; and $< .001$, respectively). Interestingly, LDH, total bilirubin and ASAT were statistically not correlated with a HbF/RBC threshold.

Moreover, when looking at the change between day 0 and ≥ 6 months, the median increase in %RBC with more than 2 pg of HbF/RBC (+12.06% [4.09-22.0]; median [interquartile range]) was correlated with the median increase in %HbF (+7.8% [2.2-14.1]) ($r = 0.7426$; $P = 0.007$), and correlated with the median decrease in total bilirubin (−8.0 μmol/L [13.5-0.7]) ($r = -0.5860$; $P = 0.037$) and decrease in reticulocytes (−78.0 10^9/L [159.5-3.5]) ($r = -0.7133$; $P = 0.012$) (Spearman correlations).

3.5 | Associations between HbF/RBC thresholds and VOC incidence

The VOC incidence for the 14 group B patients was collected for the 3 years preceding D0 and the 3 following years after 6 months of HU at stable dose. The VOC number/3 years before and after HU was not statistically different ($P = 0.441$; Wilcoxon test). Among the 14 patients, six decreased their VOC incidence after HU treatment (B-2; B-6; B-10; B-11; B-12 and B-14), four did not change (B-1; B-4; B-8 and B-13) and four increased (B-3; B-5; B-7 and B-9). When looking at the HbF distribution, 66.6% of patients with decreased

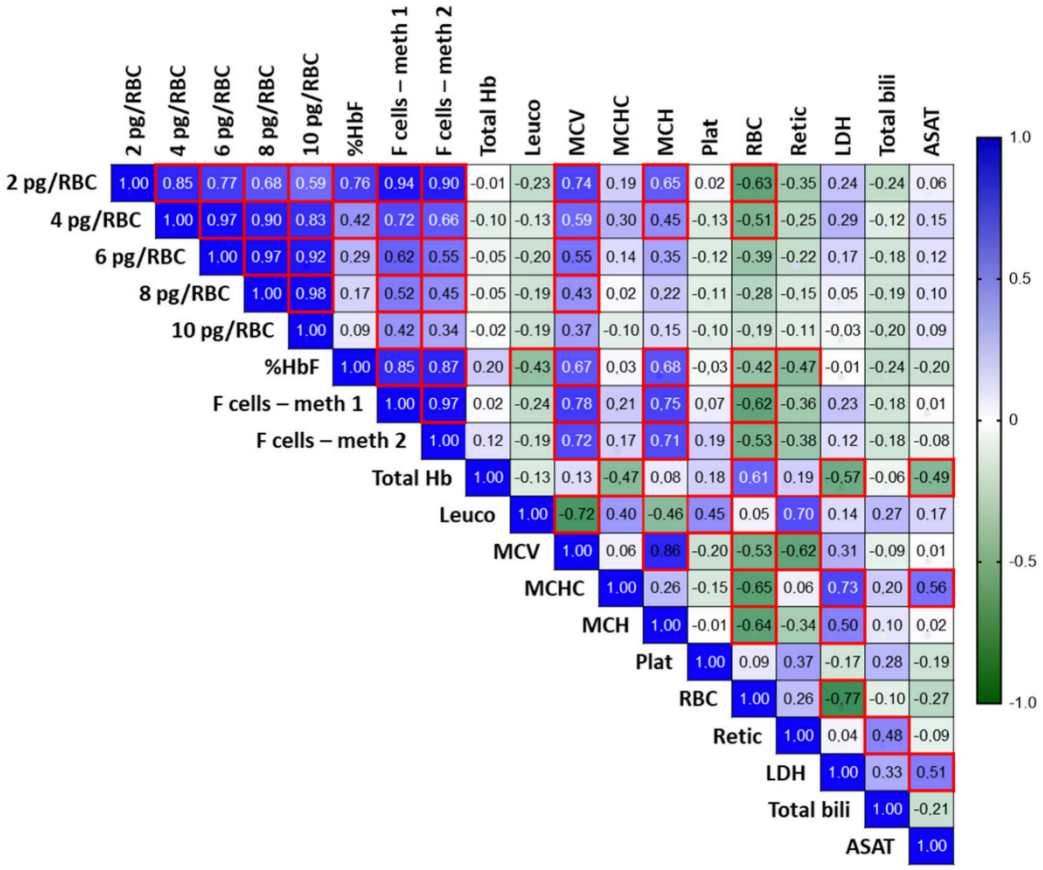

FIGURE 2 Triangular heat map representing the pairwise correlation coefficients between biologic parameters and %RBC containing at least the indicated quantity of HbF (2, 4, 6, 8 and 10 pg) at day 0 and ≥ 6 months. The color scale shows the value of the Spearman correlation coefficient (r). Blue values represent positive correlations and green values represent negative correlations. Values in red frame correspond to statistically significant correlations ($P < .05$). ASAT: aspartate aminotransferase; LDH: lactate dehydrogenase; Leuko: leukocytes; MCH: mean corpuscular hemoglobin; MCHC: mean corpuscular hemoglobin concentration; MCV: mean corpuscular volume; Plat: platelets; RBC: red blood cells; Retic: reticulocytes; Total bili: total bilirubin; Total Hb: total hemoglobin

VOC incidence (4/6) had pancellular distribution while 75% of patients with increased VOC (3/4) had heterocellular distribution after HU (Figure S8).

Percentage of HbF determined by HPLC, and F cell frequency assessed by methods 1 and 2, were not significantly related to VOC incidence (r = −0.036; $P = .856$, r = −0.203; $P = .299$, r = −0.287; $P = .139$, respectively - Spearman correlation) (Figure S11A).

Hypothesizing that a threshold of HbF/RBC could impact the VOC incidence, we analyzed hospitalizations for VOC for the two 3-year periods (before and after HU treatment) with corresponding HbF/RBC thresholds. The association of VOC incidence during 3 years was statistically significant with the percentage of RBC above HbF/RBC thresholds of 4, 6, 8 and 10 pg, with a trend toward association with threshold of 2 pg (Figure S11B).

The ROC analyzes were performed to compare %HbF, F cell frequency and HbF/RBC thresholds as a predictive value of the VOC incidence with a threshold of ≤1 VOC over a period of 3 years (Figure 3A). For each threshold area under curve (AUC) were higher than %HbF (AUC = 0.549; $P = .659$) or F cells frequency (AUC = 0.734; $P = .139$ and AUC = 0.693; $P = .086$, for methods 1 and 2, respectively). Moreover, only ROC curves performed with %RBC above the different thresholds of HbF/RBC were statistically significant as compared to global %HbF and F cell frequency.

3.6 | HbF detection level in F cells is variable

To assess the minimal quantity of HbF/RBC corresponding to the level of detection of F cells by flow cytometry, we performed HbF/RBC quantification on SCD patients and applied the two described methods (Figure S2). The lowest value of fluorescence intensity was extracted and then converted into pg of HbF. We measured a variable HbF positivity threshold of 1.86 pg ± 0.47 (mean ± SD) (ranging from 0.91 to 2.80 pg) and 3.21 pg ± 1.26 (ranging from 0.87 to 6.04 pg) for methods 1 and 2, respectively ($n = 71$) (Figure 3B), inducing higher values of F cell frequencies measured by method 1 for group B patients (Table 1).

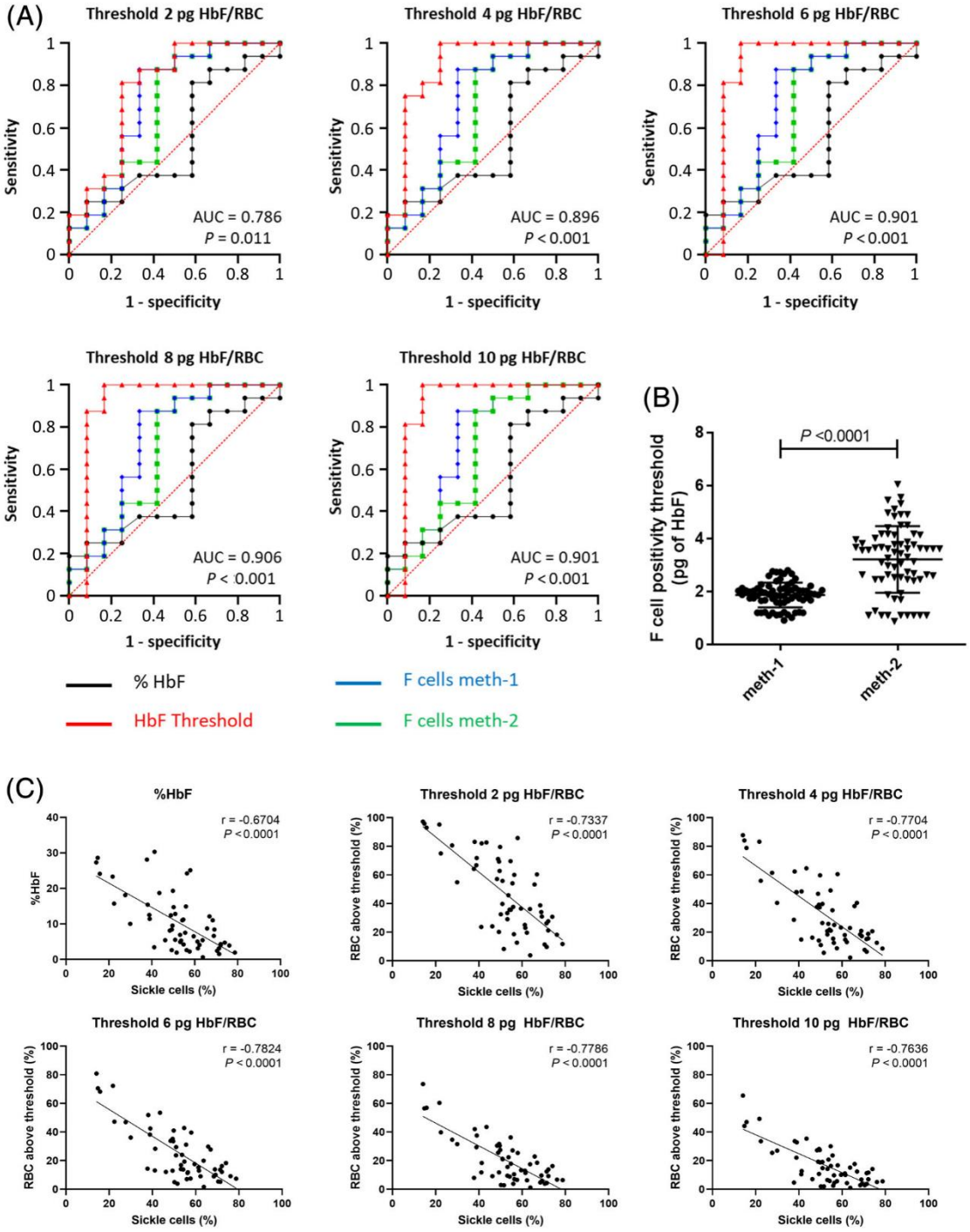

FIGURE 3 Protective effects according to HbF content per RBC. A, ROC curves of %HbF, F cell frequency (by method 1 and 2) and %RBC containing at least the indicated threshold of HbF for a VOC incidence cut-off of ≤1 over 3 years. B, Variability of F cell detection threshold measured by flow cytometry for methods 1 (meth 1) and 2 (meth 2) (n = 71) showing discrepancy according to the method used - Wilcoxon test. C, Association between global %HbF of %RBC containing at least the indicated threshold of HbF/RBC and percentage of sickle cells counted after enzymatic deoxygenation (n = 46) (Spearman correlations)

3.7 | Associations between HbF/RBC thresholds and in vitro RBC sickling

To confirm our results, in vitro sickling assays by enzymatic deoxygenation were performed on RBCs from 56 SCD patients treated by HU or not (n = 13 and n = 43, respectively) and healthy donors as control (n = 4) (Figure S12). Mean %HbF and mean percentage of sickle cells were 15.3% ± 10.2 and 36.5% ± 18.0 for treated patients and 8.9% ± 6.8 and 57.2% ± 11.6 for untreated patients. Percentage of sickle cells was inversely correlated with global %

HbF and HbF/RBC thresholds of 2, 4, 6, 8 and 10 pg (Spearman correlations) (Figure 3C).

4 | DISCUSSION

The new method developed here allows the precise and direct measurement of HbF content distribution in RBCs at the single cell level. The development of this technique has been possible by using samples from non-SCD subjects presenting a homogeneous distribution of HbF for whom the mean HbF fluorescence can be directly related to the MCHbF. Despite the choice of an accurate monoclonal antibody, the slight variability we observed came from the batch.[26] The integration of the variability of the degree of coupling of PE molecules per antibody, by applying a correction factor to the measured fluorescence intensities, allows greater accuracy of the assay with good reproducibility and repeatability. In a clinical context, it would be necessary to re-perform the linear regression obtained from patients with homogeneous HbF distribution for every new batch. Using flow cytometry allows analysis of thousands of RBCs and subpopulations of interest such as reticulocytes or patients' RBCs in the case of a chronic transfusion program.

To our knowledge, only one attempt to precisely quantify HbF/RBC has been done using a fluorescent antibody.[27] The method developed by Horiuchi et al., consisted of HbF content measurement in F cells assessed by fluorescence microscopy. While this method showed a good correlation between total fluorescence intensity and %HbF, it is time-consuming and requires technical expertise for reproducible smear preparation. Contrary to flow cytometry assay, RBCs size, in terms of MCV, could also affect the fluorescence density quantification because of the variation of the inner hemoglobin concentration, making correlation with standards unreliable.

This method could be applied to other hemoglobins with appropriate antibodies. Moreover, combining quantitative measurements of different hemoglobins and the total hemoglobin per RBC, would inform about their relative amount and concentration, which is of interest for an anti-polymerization effect, using the corpuscular Hb concentration (MCHC) per RBC.[21,28] However, the latter requires an individual volume measurement which is difficult to obtain when the shape is not regular as in SCD. To this purpose, imaging flow cytometry, which has already been used to analyze SCD erythrocytes morphology,[29] could be coupled to the quantitative Hb measurement.

As a proof of concept, we applied this method to measure HbF content in SCD patients during hydroxyurea treatment. Hydroxyurea has been shown to prevent VOC and ACS,[30,31] improve splenic function regeneration,[32] cerebrovascular involvement in children,[33-35] or to treat early adult glomerular disease,[36] reflecting its broad clinical effects. Importantly HU decreases the rate of mortality, mainly, but not exclusively, in a HbF dependent way.[2,31] During the longitudinal follow-up, a significant decrease in %RBC containing a very low HbF level (<2 pg) as well as a significant increase in %RBC containing between 2 and 4 pg of HbF were observed. These results are consistent with published data showing an increase in both %HbF and F cell frequency.[18-20]

Improvements in biologic parameters were associated with F cell frequency, assessed by the two most commonly used methods. By comparing them, we show that using a positivity threshold corresponding to the fluorescence intensity of unstained cells gave statistically significant fewer variable, but higher results than using an isotypic control. Whatever the method, F cell frequency was not statistically associated with VOC incidence over 3 years in this study. This result might be explained by the fact that F cells corresponds to only one threshold of HbF content and methods used can induce, as we showed, the setting of either a too variable or a too low positivity threshold, resulting in no clinical significance.

Steinberg et al. hypothesized that if HbF content was 10 pg in each RBC, there would be no disease events.[21] Here we show that assessing the distribution of HbF/RBC allows analyzing any possible protective threshold against SCD phenotypes. The number of RBC containing at least 2 pg of HbF was significantly associated with an increase in mean %HbF, MCV and MCH and a decrease in RBC count. Moreover, we provide results showing that %RBC above thresholds of HbF/RBC, even from 2 pg of HbF could have a clinical significance according to VOC incidence. As expected, the effect on VOC is more pronounced in case of %RBC reaching higher levels of HbF/RBC. These results were strengthened by performing in vitro sickling assays using samples from other patients, which was also correlated with the threshold of 4, 6, 8 and 10 pg of HbF/RBC in a stronger way than % HbF and F cell frequency as observed by ROC analysis. While studied on a small cohort, the distribution of HbF (ie, pancellular or heterocellular), which is of interest from a biological point of view, seems to be associated with the VOC incidence, with heterocellular distribution having a negative effect, as reported.[37]

Hemolytic markers LDH, bilirubin and ASAT were not correlated with a HbF threshold, whereas we observed a decrease in bilirubin and reticulocytes count between D0 and ≥ M6, which were correlated with an increase in the %RBC with HbF/RBC higher than 2 pg. These results are consistent with published data showing that hemolytic markers did not correlate with RBC survival, improved by HbF level.[38] Interestingly, the HbF threshold could explain the discrepancy between some studies showing a positive effect of the % HbF on survival,[2,31,39,40] and those without a close relationship.[41,42] All together our results show that HU effect on hemolysis is probably more complex. A study in larger cohorts of patients including their clinical manifestations, treatments and genetic analysis could be considered to evaluate the best threshold of HbF/RBC and the proportion of cells above it and to study clinical and genetic associations. Indeed, genetic factors have been hypothesized as an explanation of a differential response of patients to HU,[43,44] suggesting that a personalized HU dose according to pharmacokinetic,[45] coupled with the study of the thresholds, might attenuate these differences.

Finally, the effect of HU on HbF distribution was undertaken as a proof of concept of a new method for HbF measurement in each RBC. This method opens up interesting prospects for analysis of new therapeutic approaches, including epigenetic and gene therapy HbF inducers.[46-50]

ACKNOWLEDGEMENTS

The authors would thank Wassim El Nemer and the French institute CNRGS (Centre National de Référence pour les Groupes Sanguins) for providing samples analyzed in this study. They also thank Cécile Fligny for editorial assistance and Michael Marden for manuscript correction.

AUTHOR CONTRIBUTIONS

P. B. designed research; N. H., M. G. R., G. B., L.B., L.K., and G. D. L. performed research; N. H., M. G. R., L.B., G. D. L., F. G., M. C., and P. B. analyzed data; E. A., and N. O. performed statistical analysis; S. P., and F. G. monitored and selected patients for the study; M. S., P. C., B. V., F. P., F. G., and M. C. critically reviewed the manuscript; and N. H., M. G. R., and P. B. wrote the manuscript.

CONFLICT OF INTERESTS

M. G. R., G. D. L., F. P., F. G., M. C., and P. B. are co-inventors of the patent number WO2018083426A1. P. B. declares being member on a standing advisory council or committee consultancy for Addmedica, Roche, Bluebird bio, Emmaus, Agios, Global Blood Therapeutics, Novartis and Hemanext. M.C. and P.B. declare being co-founders of Innovhem. The other authors declare no competing financial interests.

ORCID

Nicolas Hebert https://orcid.org/0000-0003-0232-831X
Philippe Chadebech https://orcid.org/0000-0003-0757-4309
Benoit Vingert https://orcid.org/0000-0003-4156-2504
France Pirenne https://orcid.org/0000-0003-3547-3994

REFERENCES

1. Platt OS. Hydroxyurea for the treatment of sickle cell anemia. *N Engl J Med*. 2008;358(13):1362-1369.
2. Voskaridou E, Christoulas D, Bilalis A, et al. The effect of prolonged administration of hydroxyurea on morbidity and mortality in adult patients with sickle cell syndromes: results of a 17-year, single-center trial (LaSHS). *Blood*. 2010;115(12):2354-2363.
3. Powars DR, Schroeder WA, Weiss JN, Chan LS, Azen SP. Lack of influence of fetal hemoglobin levels or erythrocyte indices on the severity of sickle cell anemia. *J Clin Invest*. 1980;65(3):732-740.
4. Nagel RL, Erlingsson S, Fabry ME, et al. The Senegal DNA haplotype is associated with the amelioration of anemia in African-American sickle cell anemia patients. *Blood*. 1991;77(6):1371-1375.
5. Powars DR, Weiss JN, Chan LS, Schroeder WA. Is there a threshold level of fetal hemoglobin that ameliorates morbidity in sickle cell anemia? *Blood*. 1984;63(4):921-926.
6. Eaton WA, Bunn HF. Treating sickle cell disease by targeting HbS polymerization. *Blood*. 2017;129(20):2719-2726.
7. Wilson JB, Headlee ME, Huisman TH. A new high-performance liquid chromatographic procedure for the separation and quantitation of various hemoglobin variants in adults and newborn babies. *J Lab Clin Med*. 1983;102(2):174-186.
8. Betke K, Marti HR, Schlicht I. Estimation of small percentages of foetal haemoglobin. *Nature*. 1959;184(Suppl 24):1877-1878.
9. Tomoda Y. Demonstration of foetal erythrocyte by immunofluorescent staining. *Nature*. 1964;202:910-911.
10. Hosoi T. Studies on Hemoglobin F within single erythrocyte by fluorescent antibody technique. *Exp Cell Res*. 1965;37:680-683.
11. Gitlin D, Sasaki T, Vuopio P. Immunochemical quantitation of proteins in single cells. I. Carbon anhydrase B, beta-chain hemoglobin and gamma-chain hemoglobin in some normal and abnormal erythrocytes. *Blood*. 1968;32(5):796-810.
12. Boyer SH, Belding TK, Margolet L, Noyes AN. Fetal hemoglobin restriction to a few erythrocytes (F cells) in normal human adults. *Science*. 1975;188(4186):361-363.
13. Wood WG, Stamatoyannopoulos G, Lim G, Nute PE. F-cells in the adult: normal values and levels in individuals with hereditary and acquired elevations of Hb F. *Blood*. 1975;46(5):671-682.
14. Dover GJ, Boyer SH, Bell WR. Microscopic method for assaying F cell production: illustrative changes during infancy and in aplastic anemia. *Blood*. 1978;52(4):664-672.
15. Dover GJ, Boyer SH. Quantitation of hemoglobins within individual red cells: asynchronous biosynthesis of fetal and adult hemoglobin during erythroid maturation in normal subjects. *Blood*. 1980;56(6):1082-1091.
16. Navenot JM, Merghoub T, Ducrocq R, Muller JY, Krishnamoorthy R, Blanchard D. New method for quantitative determination of fetal hemoglobin-containing red blood cells by flow cytometry: application to sickle-cell disease. *Cytometry*. 1998;32(3):186-190.
17. Platt OS, Orkin SH, Dover G, Beardsley GP, Miller B, Nathan DG. Hydroxyurea enhances fetal hemoglobin production in sickle cell anemia. *J Clin Invest*. 1984;74(2):652-656.
18. Bridges KR, Barabino GD, Brugnara C, et al. A multiparameter analysis of sickle erythrocytes in patients undergoing hydroxyurea therapy. *Blood*. 1996;88(12):4701-4710.
19. Rodgers GP, Dover GJ, Noguchi CT, Schechter AN, Nienhuis AW. Hematologic responses of patients with sickle cell disease to treatment with hydroxyurea. *N Engl J Med*. 1990;322(15):1037-1045.
20. Goldberg MA, Brugnara C, Dover GJ, Schapira L, Charache S, Bunn HF. Treatment of sickle cell anemia with hydroxyurea and erythropoietin. *N Engl J Med*. 1990;323(6):366-372.
21. Steinberg MH, Chui DHK, Dover GJ, Sebastiani P, Alsultan A. Fetal hemoglobin in sickle cell anemia: a glass half full? *Blood*. 2014;123(4):481-485.
22. Franco RS, Lohmann J, Silberstein EB, et al. Time-dependent changes in the density and hemoglobin F content of biotin-labeled sickle cells. *J Clin Invest*. 1998;101(12):2730-2740.
23. Pannu KK, Joe ET, Iyer SB. Performance evaluation of QuantiBRITE phycoerythrin beads. *Cytometry*. 2001;45(4):250-258.
24. Chen JC, Bigelow N, Davis BH. Proposed flow cytometric reference method for the determination of erythroid F-cell counts. *Cytometry*. 2000;42(4):239-246.
25. Abbyad P, Tharaux P-L, Martin J-L, Baroud CN, Alexandrou A. Sickling of red blood cells through rapid oxygen exchange in microfluidic drops. *Lab Chip*. 2010;10(19):2505-2512.
26. de Almeida Santiago M, de Paula Fonseca E, Fonseca B, et al. Flow cytometry as a tool for quality control of fluorescent conjugates used in immunoassays. *PloS One*. 2016;11(12):e0167669.
27. Horiuchi K, Osterhout ML, Kamma H, Bekoe NA, Hirokawa KJ. Estimation of fetal hemoglobin levels in individual red cells via fluorescence image cytometry. *Cytometry*. 1995;20(3):261-267.
28. Fertrin KY, van Beers EJ, Samsel L, et al. Imaging flow cytometry documents incomplete resistance of human sickle F-cells to ex vivo hypoxia-induced sickling. *Blood*. 2014;124(4):658-660.
29. van Beers EJ, Samsel L, Mendelsohn L, et al. Imaging flow cytometry for automated detection of hypoxia-induced erythrocyte shape change in sickle cell disease. *Am J Hematol*. 2014;89(6):598-603.
30. Charache S, Terrin ML, Moore RD, et al. Effect of hydroxyurea on the frequency of painful crises in sickle cell anemia. Investigators of the Multicenter Study of Hydroxyurea in Sickle Cell Anemia. *N Engl J Med*. 1995;332(20):1317-1322.
31. Steinberg MH, Barton F, Castro O, et al. Effect of hydroxyurea on mortality and morbidity in adult sickle cell anemia: risks and benefits up to 9 years of treatment. *JAMA*. 2003;289(13):1645-1651.

32. Claster S, Vichinsky E. First report of reversal of organ dysfunction in sickle cell anemia by the use of hydroxyurea: splenic regeneration. *Blood*. 1996;88(6):1951-1953.
33. Wiles N, Howard J. Role of hydroxycarbamide in prevention of complications in patients with sickle cell disease. *Ther Clin Risk Manag*. 2009;5:745-755.
34. Zimmerman SA, Schultz WH, Burgett S, Mortier NA, Ware RE. Hydroxyurea therapy lowers transcranial Doppler flow velocities in children with sickle cell anemia. *Blood*. 2007;110(3):1043-1047.
35. Ware RE, Zimmerman SA, Schultz WH. Hydroxyurea as an alternative to blood transfusions for the prevention of recurrent stroke in children with sickle cell disease. *Blood*. 1999;94(9):3022-3026.
36. Bartolucci P, Habibi A, Stehlé T, et al. Six months of hydroxyurea reduces albuminuria in patients with sickle cell disease. *J Am Soc Nephrol*. 2016;27(6):1847-1853.
37. Tolu SS, Reyes-Gil M, Ogu UO, Thomas M, Bouhassira EE, Minniti CP. Hemoglobin F mitigation of sickle cell complications decreases with aging. *Am J Hematol* Published online. 2020;95:E122-E125.
38. Quinn CT, Smith EP, Arbabi S, et al. Biochemical surrogate markers of hemolysis do not correlate with directly measured erythrocyte survival in sickle cell anemia. *Am J Hematol*. 2016;91(12):1195-1201.
39. Platt OS, Brambilla DJ, Rosse WF, et al. Mortality in sickle cell disease. Life expectancy and risk factors for early death. *N Engl J Med*. 1994;330(23):1639-1644.
40. Gardner K, Douiri A, Drasar E, et al. Survival in adults with sickle cell disease in a high-income setting. *Blood*. 2016;128(10):1436-1438.
41. Darbari DS, Wang Z, Kwak M, et al. Severe painful vaso-occlusive crises and mortality in a contemporary adult sickle cell anemia cohort study. *PloS One*. 2013;8(11):e79923.
42. Elmariah H, Garrett ME, De Castro LM, et al. Factors associated with survival in a contemporary adult sickle cell disease cohort. *Am J Hematol*. 2014;89(5):530-535.
43. Steinberg MH, Voskaridou E, Kutlar A, et al. Concordant fetal hemoglobin response to hydroxyurea in siblings with sickle cell disease. *Am J Hematol*. 2003;72(2):121-126.
44. Ma Q, Wyszynski DF, Farrell JJ, et al. Fetal hemoglobin in sickle cell anemia: genetic determinants of response to hydroxyurea. *Pharmacogenomics J*. 2007;7(6):386-394.
45. McGann PT, Niss O, Dong M, et al. Robust clinical and laboratory response to hydroxyurea using pharmacokinetically guided dosing for young children with sickle cell anemia. *Am J Hematol*. 2019;94(8):871-879.
46. Brendel C, Guda S, Renella R, et al. Lineage-specific BCL11A knockdown circumvents toxicities and reverses sickle phenotype. *J Clin Invest*. 2016;126(10):3868-3878.
47. Hoban MD, Orkin SH, Bauer DE. Genetic treatment of a molecular disorder: gene therapy approaches to sickle cell disease. *Blood*. 2016;127(7):839-848.
48. Ribeil J-A, Hacein-Bey-Abina S, Payen E, et al. Gene Therapy in a Patient with Sickle Cell Disease. *N Engl J Med*. 2017;376(9):848-855.
49. Thompson AA, Walters MC, Kwiatkowski J, et al. Gene Therapy in Patients with Transfusion-Dependent β-Thalassemia. *N Engl J Med*. 2018;378(16):1479-1493.
50. Esrick EB, Achebe M, Armant M, et al. Validation of BCL11A As therapeutic target in sickle cell disease: Results from the adult cohort of a pilot/feasibility gene therapy trial inducing sustained expression of fetal hemoglobin using post-transcriptional gene silencing. *Blood*. 2019;134(Suppl. 2):LBA-5.

SUPPORTING INFORMATION

Additional supporting information may be found online in the Supporting Information section at the end of this article.

How to cite this article: Hebert N, Rakotoson MG, Bodivit G, et al. Individual red blood cell fetal hemoglobin quantification allows to determine protective thresholds in sickle cell disease. *Am J Hematol*. 2020;1–11. https://doi.org/10.1002/ajh.25937